

**Growth and Productivity
of a Recombinant Chinese Hamster Ovary
Cell Line in Batch Culture**

by

Roshni Lynne Dutton

A thesis
presented to the University of Waterloo
in fulfilment of the
thesis requirement for the degree of
Doctor of Philosophy
in
Chemical Engineering

Waterloo, Ontario, Canada, 1998

© Roshni L. Dutton 1998



**National Library
of Canada**

**Acquisitions and
Bibliographic Services**

**395 Wellington Street
Ottawa ON K1A 0N4
Canada**

**Bibliothèque nationale
du Canada**

**Acquisitions et
services bibliographiques**

**395, rue Wellington
Ottawa ON K1A 0N4
Canada**

Your file Votre référence

Our file Notre référence

The author has granted a non-exclusive licence allowing the National Library of Canada to reproduce, loan, distribute or sell copies of this thesis in microform, paper or electronic formats.

The author retains ownership of the copyright in this thesis. Neither the thesis nor substantial extracts from it may be printed or otherwise reproduced without the author's permission.

L'auteur a accordé une licence non exclusive permettant à la Bibliothèque nationale du Canada de reproduire, prêter, distribuer ou vendre des copies de cette thèse sous la forme de microfiche/film, de reproduction sur papier ou sur format électronique.

L'auteur conserve la propriété du droit d'auteur qui protège cette thèse. Ni la thèse ni des extraits substantiels de celle-ci ne doivent être imprimés ou autrement reproduits sans son autorisation.

0-612-32827-9

The University of Waterloo requires the signatures of all persons using or photocopying this thesis. Please sign below, and give address and date.

ABSTRACT

A Chinese Hamster Ovary cell line (CHO1-5₅₀₀) co-transfected with *h-tPA* and *dhfr* was studied in batch culture mode. The concept of the cell-hour (the biological capacity for production) was developed, placing evaluation of cell population and protein production on the same cumulative basis, within the epigenetic time domain. The specific productivity of human tissue type plasminogen activator (h-tPA) was found to be growth-phase-associated, with maxima in the lag (0.065 pg c-h⁻¹) and early decline (0.040 pg c-h⁻¹) growth phases. The product titer was found to have a maximum (10.5 mg L⁻¹) in batch culture under many different conditions. The h-tPA production was also evaluated as a function of the physiological state of the cells, by population segregation on the basis of cell cycle phase. Appearance of extracellular h-tPA was found to directly correlate to the G1 cell cycle phase (0.080 pg G1c-h⁻¹), while DHFR content per cell was greatest during the S cell cycle phase.

Morphological type (substratum adherent, aggregate suspension, and dispersed suspension) could be induced by agitation rate and serum concentration. Aggregates, which were seen to have large void volumes stabilized by cytoplasmic bridging, had a medium growth rate ($\mu_{\max} = 0.016 \text{ h}^{-1}$), but a short exponential growth phase and low batch averaged specific productivity ($q_{\text{tPA}} = 0.021 \text{ pg c-h}^{-1}$). Simple dispersed suspension systems with serum-free medium (DS) attained the same product titer as microcarrier-attached systems with 10% FBS (MS), while the h-tPA concentration as a percent of total extracellular protein was greater by a factor of 8. Slow growing DS ($\mu_{\max} = 0.012 \text{ h}^{-1}$), had a higher specific productivity ($q_{\text{tPA}} = 0.045 \text{ pg c-h}^{-1}$) than the MS ($\mu_{\max} = 0.026 \text{ h}^{-1}$, $q_{\text{tPA}} = 0.037 \text{ pg c-h}^{-1}$).

Three metabolic phases were identified during batch culture, supporting the view that phase I gluconeogenesis and DHFR mediated glycine production are used by CHO1-5₅₀₀ cells. Production of h-tPA coincided with the first metabolic phase so that strategies to lengthen this phase should extend the productive portion of a batch culture.

A partially structured model for hybridomas was adapted to the more complex metabolism of CHO1-5₅₀₀. The model, which contained 15 equations and 24 parameters, provided a good fit to the three metabolic phases. Metabolic switches were assumed to coincide with depletion of glucose and glutamine to constant levels of 0.5 mmol L⁻¹.

ACKNOWLEDGEMENTS

'Science is above all a cooperative enterprise'
Hermann Bondi, Nature 1977

No body of work is created in isolation. There are people who contributed in tangible and intangible ways, directly and indirectly. I thank you all.

In the Department of Chemical Engineering, I wish to extend sincere appreciation to my two supervisors, Professor Murray Moo-Young who provided opportunity, guidance, and financial support, and Professor Jenö Scharer, mentor and friend, who provided encouragement, enthusiasm, expression of confidence, editorial skills, humor and counsel. Thank you, also, Jenö, for the opportunity to teach. Murray is to be commended for maintaining a diverse and dynamic research group who collectively expand the savvy and surmise of each individual: Thanks to all you members of the Biochemical Engineering group, past and present. I would like particularly to thank my friend Professor Gordon Hayward, who is always ready and willing to assist., with 'child-in-a-playroom' fascination and innovation. Animal cell culture is a finicky and labourious thing. I couldn't have collected the data without the help of technicians, summer students, and undergraduate research assistants: Jana, Qui-Ping, Qian, Christine, and Elizabeth. And finally, I would like to thank my committee members: Professor Michael Butler, Professor Neils Bols, Professor Gordon Hayward (yes, your getting thanked again, because you're wearing a different hat), and Professor Ray Legge for their time commitments, advise, and editorial comments. Thank you also, Ray, for your friendship and advise over the years.

No vocation is unaffected by homelife, and most people can't be grad students without some familial input. My husband Michael said it all in the acknowledgements of his thesis, which he completed just a few months ago. So here it is again, verbatim: *The decision for me and my wife Roshni to go to graduate school, have a child, train horses, play hockey, and renovate a crack house could simply not have been undertaken without considerable and ongoing family help, love, and encouragement (and cash!). Gifts (tools, dishwashers, money), labour, and loans were gratefully accepted from my parents (Vernon Dutton and Viviane Dutton), my brother Gil, Rosh's family (John (brother) and Corinne Packer, Nan (sister) and Al Bennett, and Cliff (dad) and Ellen (mom) Packer). Without your assistance, I don't think I'd be here now. Thank you all!*

To my son Drew, who is my avocation: now I can play that video game. And to Michael, who is my life mentor, my guru, my prime example, my inspiration, my soul-mate: Your unstinting advise, help, understanding, interest, and devotion will always pull me through.

'Research is to see what everybody has seen and think what nobody has thought.'

Albert Szent-Gyorgyi

'The essence of knowledge is, having it, to use it.'

Confucius

'Some times you just have to go with what you've got.'

Neils Bols

TABLE OF CONTENTS

Abstract	iv
List of Tables	x
List of Figures	
CHAPTER 1 - INTRODUCTION	1
1.1 Animal Cell Culture: History and Current Status	1
1.1.1 Cell Lines	2
1.2 Biopharmaceuticals from Genetically Engineered Mammalian Cells	4
1.2.1 Research and Development	6
1.3 Scope and Objectives	10
CHAPTER 2 - LITERATURE REVIEW	13
2.1 Mammalian Cell Culture	13
Population Growth Dynamics	13
The Mammalian Cell Cycle	21
Substratum Adherence	31
Time Domains	34
2.2 Chinese Hamster Ovary Cells	37
Major Substrate Concentrations and Growth and Productivity	39
Morphological Types	42
Cell Cycle Kinetics	44
Recombinant Protein Products and the DHFR Amplification System	45
2.3 Modeling Growth and Production Kinetics	50
A Partially Structured Metabolic Model	53

CHAPTER 3 - MATERIALS AND METHODS	59
3.1 Cell Lines and Maintenance	59
3.2 Medium Preparaton	60
3.3 Culture Systems	61
3.4 Assays	63
CHAPTER 4 - RESULTS AND DISCUSSION	69
4.1 Population Growth and Recombinant tPA Production	69
4.1.1 The Biological Capacity for Production	69
Apparent Population Growth Rate	71
Specific Productivity	73
Cell Hours, Cumulative Production, and Specific Productivity	74
Association of Productivity to Population Growth Phase	77
Concluding Remarks	81
4.1.2 Productivity and the Segregated Population	84
Population Growth Dynamics	87
Population Segregation on the Basis of DNA Content	93
Estimating Concentrations in the Dead Cell and Lysed Cell	102
Recombinant Protein Productivity	103
The Role of Dihydrofolate Reductase Expression	106
The Role of Native Plasminogen Activators	110
Concluding Remarks	111
4.2 Morphological Type	112
Microcarrier Suspension Culture	113
Aggregate Suspension Culture	118
Dispersed Suspension Culture	126
Concluding Remarks	128

4.3 Metabolism of rCHO in Batch Culture	129
4.3.1 Population-Averaged Metabolism of rCHO Cells	129
Major Substrates and Metabolites	129
DHFR and the Production of Glycine	137
Glucogenic Compound Metabolism in Animal Cells	140
Metabolism of <i>dhfr</i> -System Recombinant Chinese Hamster Ovary	151
Concluding Remarks	153
4.3.2 Preliminary Modeling of Growth and rProtein Production	156
CHAPTER 5 - CONCLUSIONS AND RECOMMENDATIONS	177
5.1 Conclusions	177
5.2 Recommendations	180
APPENDICES	181
A: Experimental Data	181
B: Model Computer Code and Simulation Results	207
Model Computer Code	208
Simulation Graphs	215
C: Preliminary Experiments and Reproducibility	223
Preliminary Experiments and Reproducibility	224
Reproducibility of Morphological Types Experimental Set	233
Initial Substrate Concentrations Factorial Experiment	234
D. Standard Curves	244
Typical Glucose Standard Curve	245
Typical Lactate Standard Curve	246

Typical Set of Amino Acid Standards HPLC Peaks	247
Typical Set of Amino Acids Standard Curves	253
Typical tPA Standard Curve	263
Typical ELISA Monoclonal Antibody Standard Curve	264
List of Symbols	265
REFERENCES	269

List of Tables

Table 1.1	Some pharmaceuticals produced from cultured animal cells.	3
Table 1.2	Post-translational modifications most frequently encountered in mammalian proteins.	5
Table 1.3	Current progress in key areas in production of animal cell-based biopharmaceuticals.	7
Table 1.4	Commercially available tPA assays.	11
Table 2.1	Some parameters used in describing batch mammalian cell growth and protein production.	14
Table 2.2	Some observed rCHO growth parameters and requirements.	38
Table 2.3	A selection of serum-free media for CHO cell culture.	37
Table 2.4	Some rCHO cell lines used to produce various glycoproteins.	46
Table 3.1	Basal medium formulation for initial substrate concentration experiments	62
Table 4.1.1	Population growth and production batch culture parameters	72
Table 4.1.2	Metabolic batch culture parameters	78
Table 4.2.1	Conditions employed for batch culture in the three morphological types	114
Table 4.2.2	Substratum adherent population kinetics in static and stirred bioreactors	117
Table 4.2.3	Growth of CHO 1-5 ₅₀₀ in microcarrier suspension, aggregate suspension, and dispersed suspension systems.	124
Table 4.2.4	Production of tPA from CHO 1-5 ₅₀₀ in microcarrier suspension, aggregate suspension, and dispersed suspension systems.	125

Table 4.3.1	Growth, protein production, and metabolism kinetics of CHO1-5 ₅₀₀ in dispersed suspension batch culture.	138
Table 4.3.2	Glucogenic amino acids	145
Table 4.3.3	Occurrence of gluconeogenesis and/or glucogenic compound catabolism in animal cell culture.	147
Table 4.3.4	Chemical factors affecting gluconeogenesis and/or glucogenic compound metabolism.	148
Table 4.3.5	Model parameters and initial conditions	162
Table 4.3.6	Initial substrate concentrations in dispersed suspension	171
Table 4.3.7	Population growth parameters of initial substrate concentration experiment.	172
Table 4.3.8	Production parameters of initial substrate concentration experiment	173
Table 4.3.9	Substrate and ammonia concentrations at metabolic switches of initial substrate concentration experiment.	174
Table 4.3.10	Specific substrate consumption rates during the metabolic phases of initial substrate concentration experiment.	175
Table 4.3.11	Yields of byproducts on substrates during the metabolic phases of initial substrate concentration experiment	176

List of Figures

Figure 1.1	Aspects of interactive manufacturing and regulatory steps in the production of a biopharmaceutical.	9
Figure 2.1	A simplified representation of metabolic pathways in mammalian cells.	19
Figure 2.2	Overall reaction system of mammalian cell culture.	22
Figure 2.3	Specific events of the mammalian cell cycle.	24
Figure 2.4	Relationship of quiescent and senescent cells to the cell cycle.	26
Figure 2.5	Sites of action of antimetabolites on DNA synthesis pathways.	47
Figure 2.6	Schematic drawing of plasmid constructed for expression of tPA in CHO cells using DHFR as an amplifiable marker.	49
Figure 4.1.1	Batch culture population and protein titer curves.	70
Figure 4.1.2	Protein productivity for M4-1 hybridomas and rCHO cells in batch culture: use of cumulative cell hours (CH_{vol}).	75
Figure 4.1.3	Cumulative protein product concentration (Mab or tPA) in relation to volumetric cell hours.	80
Figure 4.1.4	Theoretical examples of the basic types of protein production kinetics	82
Figure 4.1.5	Flow cytometric analyses of CHO cells in cell cycle phases	85
Figure 4.1.6	Cell cycle fractions of rCHO cells in dispersed suspension batch culture: temporal changes.	88
Figure 4.1.7	LDH as an indicator of leaky membranes (dead, dying, lysed cells)	90
Figure 4.1.8	Semi-synchrony of batch rCHO culture	92
Figure 4.1.9	Flow cytometric profiles of rCHO cells in batch culture	94

Figure 4.1.10	Subpopulation compartments based on cell cycle theory	102
Figure 4.1.11	The viable population presented as cell-hours	104
Figure 4.1.12	The specific productivity is partially-growth-phase-associated	105
Figure 4.1.13	The appearance of tPA in the medium is a linear function of the time spent in the G1/G0 phase	107
Figure 4.1.14	Relative specific DHFR content and relative DNA content during cell cycle phases.	108
Figure 4.2.1	Polystyrene microcarrier attached cells (SEM micrographs)	115
Figure 4.2.2	An aggregate formed in static T-flask culture (SEM micrographs)	120
Figure 4.2.3	An aggregate formed in a spinner flask at 60 rpm (SEM micrographs)	121
Figure 4.2.4	Morphological features of aggregated cells (SEM micrographs)	123
Figure 4.3.1	Dispersed suspension in stirred tank: lactate, glucose, and pH	130
Figure 4.3.2	Total and viable cell density profiles in stirred tank batch culture	132
Figure 4.3.3	Dispersed suspension in stirred tank: alanine, glutamine, ammonia	133
Figure 4.3.4	Dispersed suspension in stirred tank: amino acid profiles	135
Figure 4.3.5	Glycine synthesis and the role of tetrahydrofolate	139
Figure 4.3.6	Precursors of phosphoenolpyruvate and gluconeogenesis	142
Figure 4.3.7	The opposing pathways of glycolysis and gluconeogenesis	143
Figure 4.3.8	Metabolic pathways of the CHO1-5 ₅₀₀ cell line	152
Figure 4.3.9	Summary of overall pathways for the consumption of major substrates by rCHO	154
Figure 4.3.10	Model simulations of rCHO growth, production, and metabolism	163

1. INTRODUCTION

1.1 Animal Cell Culture: History and Current Status

Animal cell culture had its beginnings more than 100 years ago (1885), when Roux maintained embryonic chick cells in a saline solution (Butler, 1991). Over the next half century, the techniques necessary for the culturing of animal cells *in vitro* were developed, but animal cell culture was not widely used, primarily because of the high probability of bacterial contamination. The discovery and production development of antibiotics such as penicillin and streptomycin in the 1940s resulted in the widespread use of animal cell culture as a laboratory technique. Long term animal cell culture was still hampered by the mortality of normal cells, until continuous cell lines began to be available such as the chemically transformed mouse L cells and the tumor-derived HeLa (human carcinoma) cell line. In the 1950s Earle and Eagle developed chemically defined basal media to replace the undefined biological extracts previously used (Butler, 1996). This had the advantage of consistency between batches, ease of sterilization and reduced risk of contamination.

The basis for the development of commercial products from animal cell cultures was established by the work of Enders' group, when they reported in 1949 that the poliomyelitis virus could be grown in cultures of human embryonic cells (Butler, 1996). The polio vaccine was produced for mass vaccination in the 1950s, becoming one of the first major commercial products from cultured animal cells. From that time on, until the mid-1970s, the biologicals that were developed were primarily human and veterinary vaccines (Butler, 1996). In 1975, Kohler and Milstein established monoclonal antibody production from hybridomas, while the first recombinant cell line was developed in 1979. Human tissue plasminogen activator became the first recombinant protein therapeutic to be produced commercially by mammalian cell culture (Watson *et al.*, 1992). Over the past 20 years, an ever increasing range of products from animal cell culture have found, and continue to find, commercial application. Hence, the study of the optimization of animal cell culture to maintain consistently high specific productivities and product titers is of increasing importance.

1.1.1 Cell Lines

Animal cell cultures can be divided into three main categories: primary cell cultures, finite cell lines, and continuous cell lines (Schaeffer, 1990).

Cells taken directly from an animal are used to form a primary culture *in vitro*. The cells of primary culture can be detached from the culture vessel by serine proteases such as trypsin, or by chelating agents such as EDTA. These cells can then be used to initiate a secondary culture, by reseeding them into fresh medium at high density. Cells originating from a primary culture can often be transferred serially several times, as a secondary culture.

Primary animal cultures are usually prepared from relatively large tissue masses, and so will contain a variety of more and less differentiated cells. The cells from a primary culture can be manipulated so as to isolate a single cell type. Cells that divide best in culture are of embryonic origin, or have the spindle shape and growth rate of fibroblasts, both of which are relatively non-differentiated. These cells can outgrow other cell types in a primary culture. Cell types can be separated on the basis of size or density. A single cell type isolated from a primary or secondary culture can be used to form a cell line. Primary and secondary cultures are known as diploid or normal cell cultures, while cultures of a single cell type are known as 'finite' cell lines, because normal cells are characterized by a finite life span. Cells derived from human embryonic tissue have been shown to have a growth capacity of approximately 50 generations (Hayflick and Moorhead, 1961), while cells derived from an adult animal have a proportionately lesser growth capacity. Normal cells can be stored in liquid nitrogen, arresting the natural aging of the cell population, and thus allowing finite cell lines to be available for culture indefinitely.

Normal cells can become transformed to 'immortality', which is defined as a capacity for infinite number of divisions. Such a population of cells is termed a 'continuous' cell line. Transformation causes the cells to lose their sensitivity to one or more of the stimuli normally associated with growth control. Transformation is sometimes associated with altered chromosomal patterns such as aneuploid chromosomal complements of the individual cells, resulting in a heteroploid culture. Transformation can occur spontaneously, especially as a normal cell line ages, or it can be brought about by the fusion of normal cells with immortal cells, or by the use of oncogenic chemicals or viruses.

Continuous cell lines offer obvious advantages over normal cell lines for the large-scale formation of commercially valuable bioproducts, which are termed biologicals. The origins of these cells has been the cause of concern over the possibility of contamination of their products with tumorigenic agents, particularly with respect to biologicals for human consumption. However, stringent monitoring, control of the recognized dangers, and improved analysis of the final product have led to a relaxation of the restrictions on the use of these cells in the last decade.

Well-characterized animal cell lines are usually chosen in the development of production processes for biologicals. Known growth characteristics can be used to monitor and control reproducibility between batches, while known genetic characteristics can be used to monitor genetic drift. Biologicals produced from well-characterized animal cell lines are generally more readily acceptable to regulatory and licensing bodies. Some commonly used cell lines are listed in Table 1.1.

Table 1.1: Some pharmaceuticals produced from cultured animal cells (Genetic Engineering News, 1997)

Product	Clinical Use	Animal Cell	Production System
Alpha-Interferon	cancer, viral infection	Namalwa	stirred tank
Beta-Interferon	cancer, viral infection	CHO	various
Erythropoietin	anemia	CHO	roller bottles
tPA	thrombolysis	CHO	stirred tank
Factor VIII	hemophilia	CHO	various
Hepatitis B surface antigen	vaccine	CHO	??
Human growth hormone	dwarfism	C127	??
Granulocyte colony stimulating factor	chemotherapy rescue	CHO	stirred tank
Monoclonal Antibodies: various	diagnostics	Hybridomas	various
Orthoclone OKT3	kidney transplant	Hybridomas	stirred tank
Centoxin	septic shock	Hybridomas	perfused suspension

1.2 Biopharmaceuticals from Genetically Engineered Mammalian Cells

Animal cell lines, particularly mammalian cell lines, are an important source of protein products, especially protein therapeutics and (medical) diagnostics. Extreme selectivity is frequently a requirement of proteins used for diagnostic purposes. Therapeutic proteins must be not only highly specific, but also essentially free of undesirable side effects, such as the elicitation of an immune response. For these reasons, the protein product must be identical or nearly identical to the naturally occurring protein. That is, the protein must be produced, purified and formulated with high fidelity.

Genetically engineered proteins represent a new generation of drugs. Such drugs must be precise copies of the proteins in the human body that they are intended to replace. Because of their complexity, these molecules can only be made by biotechnological methods, and the only systems able to produce completely accurate copies of the most complex proteins are cultures of animal cells (Cartwright, 1994). The source cell producing the natural protein may not be a good candidate for cell line development and culture (eg. the native cell may be difficult and/or dangerous to culture *in vitro*). The advent of recombinant DNA technology has enabled the production of mammalian protein products, which are virtually identical to the natural proteins, in well-established mammalian cell lines.

In the late 1970's, when production of heterologous protein in bacteria was demonstrated, it was confidently predicted that cell culture methods would eventually be completely superseded by recombinant DNA technology using microbial host systems (Cartwright, 1994). By the early 1990s, however, animal cell culture for recombinant proteins represents over half of the revenue generated by the new biotechnology (Spier, 1992). The higher absolute protein yield in yeast or bacteria is offset by product losses in purification and lack of fidelity in the protein product. In contrast, the lower absolute yield from mammalian cells is more than offset by the relative ease of downstream processing and the fidelity of protein synthesis. In fact, the main reason why bacterial and yeast systems have not proved satisfactory for the production of all proteins is their incapacity to reproduce mammalian proteins with complete fidelity. Even after accurate translation of the relevant mRNA, many proteins produced in animal cells undergo a number of post-translational chemical modifications or processing steps before the mature protein is secreted (Table 1.2). These modifications, including the secretion itself, cannot all be accurately reproduced by microbial systems (Cartwright, 1994).

Table 1.2: The post-translational modifications most frequently encountered in mammalian proteins.
(Cartwright, 1994)

Post-Translational Modifications
glycosylation
γ -carboxylation of glutamic acid
β -hydroxylation of aspartic acid
phosphorylation and sulphatations
proteolytic processing
amidations

The relaxation of the previous regulations which limited production to strictly diploid cells opened the way to the use of cells of unlimited life span which can be cultivated on a large scale using new bioreactor configurations that are not well adapted to the growth of diploid cells. It also opened the way to the use in production of newly created types of cells such as hybridomas and cells transfected with exogenous genes placed under the control of powerful promoters and enhancers capable of driving levels of protein expression unobtainable in normal diploid cells. For example, the maximum level of beta interferon obtainable in diploid fibroblasts was of the order of 4×10^4 U/mL compared with levels of 10^7 U/mL obtained in recombinant CHO cells. Also, the yield of tPA was 0.2 mg/L in the highest producing naturally occurring cells (Bowes melanoma) compared with 50 mg/L and higher in engineered myeloma or CHO cells (Cartwright, 1994). In practice, several high-performance cell types now have an established track record in biopharmaceutical production, including CHO cells, BHK 21 cells, and various hybridomas, myelomas, and lymphoblastoid cells.

1.2.1 Research and Development

Animal cell biotechnology as a means of producing pure protein products can be roughly divided into six key areas, which are all actively evolving (Table 1.3). Cartwright (1994) summarizes the status of some aspects of these areas:

1. Expression of heterologous proteins in animal cells

Many systems exist which successfully obtain high levels of transcription of heterologous genes in animal cells. A need remains for the development of more efficient transfection procedures, better amplification methods and methods for directing the required gene to the regions of the genome which are most efficiently transcribed. The influence of post-translational events on the eventual secretion of recombinant proteins is being actively studied. While this work is still in its infancy, investigation indicates that the processing and secretory mechanisms may be limiting in cells which produce very high levels of heterologous mRNA. Overall, knowledge of processing pathways and how they can be manipulated are topics which require in depth investigation in the future.

2. Medium design

Medium design has advanced greatly over the last few years. Defined media are now available for most cell types, and it is not usually necessary to supplement cultures with animal serum. It is clear that any new processes should be designed to operate using serum-free or (even) protein-free medium. One phenomenon which requires further investigation is that of programmed cell death or apoptosis. It appears that continuous stimulation by specific growth factors via cell-surface receptors may be essential to prevent activation of a preprogrammed 'suicide' sequence.

3. Large-scale growth of animal cells (bioreactor design)

Advances in this area have been considerable. A wide range of different types of bioreactors have now been operated successfully and the previously held dogmas of the fragility of animal cells and their nonsuitability for the application of mass-culture techniques have been largely laid to rest. Much attention is currently focused on how to deliver adequate oxygen supply without damage to the cells caused by their contact with gas bubbles.

Diagnostic and therapeutic proteins are low volume, high value products. For example, microgram quantities per test or per dose are frequently sufficient. Mammalian cell bioreactor volumes of 100 liters or less are commonly sufficient for commercial production of protein products. Therefore, scale-up constraints and/or strategies of bioreactor designs are not a crucial issue of commercial mammalian cell culture in comparison to commercial microbial culture such as the production of antibiotics.

Table 1.3: Current progress in key areas in the production of animal cell based biopharmaceuticals.
(Cartwright, 1994)

Technical Area	Resolved Issues	Unresolved Issues
Expression of heterologous protein	<ul style="list-style-type: none"> - High transcription levels are achieved in several systems. 	<ul style="list-style-type: none"> - Control of transcription - Adequate and correct post-translational processing and secretion - Better knowledge of insect cells
Medium Design	<ul style="list-style-type: none"> - Serum-free media exist for many cell types - Completely protein-free media exist for some cells 	<ul style="list-style-type: none"> - Optimization of media for specific cell types in specific production systems
Bioreactor Design	<ul style="list-style-type: none"> - A wide variety of bioreactor configurations are established permitting large scale culture of most cell types 	<ul style="list-style-type: none"> - More efficient oxygenation without cell damage - Improved monitoring - Control of cell cultures based on the physiological state of the cells - Better homogeneity in high density systems
Cell physiology		<ul style="list-style-type: none"> - Control of differentiation and of switches in physiological state - Limitation of toxic product production - Ideal nutrient feed programs - Role of physiological state in protein production
Downstream processing	<ul style="list-style-type: none"> - Very effective purification procedures exist - Very effective characterization procedures exist 	<ul style="list-style-type: none"> - Development of more and better specific synthetic ligands - Improved stability of membranes and column support material for better CIP - Higher capacity, higher flux systems
Regulatory	<ul style="list-style-type: none"> - Approval framework for the use of high yield continuous cell lines - Adaptation of the batch concept to incorporate production from fed batch culture systems 	<ul style="list-style-type: none"> - Rationalization of some aspects of the required procedures - Development of simpler validated tests for DNA, virus, etc. - Integration of continuous cell culture processes into the regulatory framework.

The control and monitoring of cell growth, viability and product generation is one of the key areas requiring further study. No satisfactory way exists at present of following many of the important culture parameters in real time. This is important both for the reproducibility of production runs and for early detection of deviations occurring from the established process norms. Recent studies have shown that post-translational modifications of protein may be very sensitive to changes in the culture environment and therefore accurate process control can have a direct effect on product authenticity as well as on product yield. Process control is being approached both by the design of new, near on-line monitoring instrumentation and by the development and validation of appropriate mathematical models. However, much remains to be accomplished in both of these areas.

4. Physiology of cultured cells

Although it is known that many external factors and reagents influence the productivity of cells, little is known regarding the mechanisms by which this occurs and optimization of such factors is still essentially empirical. Recently, cell cycle theory is beginning to be applied to observed population dynamics. However, for the most part, the cell remains a 'black box' with few inputs being monitored and their effects on the outputs being poorly understood. Thus, cellular physiology is also an area where substantial research is required. The relationship between the study of cellular physiology and the ability to monitor and model cell responses is clear, as is the relationship between these elements and the design of a fully optimized and defined medium. Integrated studies in these areas are likely to be particularly fruitful in tuning the cells for maximum production of authentic product.

5. Product purification and characterization (Downstream processing)

Advances in efficient protein purification methods and in the analytical procedures required to demonstrate the purity of the product and the absence of proscribed contaminants have been central in permitting exploitation of the animal cell production systems now available. Effective, validated purification is one of the main struts supporting the regulatory position which permits the use of continuous cell lines. Protein chemistry techniques are particularly important for the verification of product authenticity, such as the identification of the correct glycoform of the protein. Successful downstream processing is directly dependent on the upstream processes.

6. Regulatory considerations

Each phase of the production process has to satisfy the relevant regulatory requirements. The parallel existence between the successive manufacturing steps and associated regulatory concerns is illustrated in Figure 1.1.

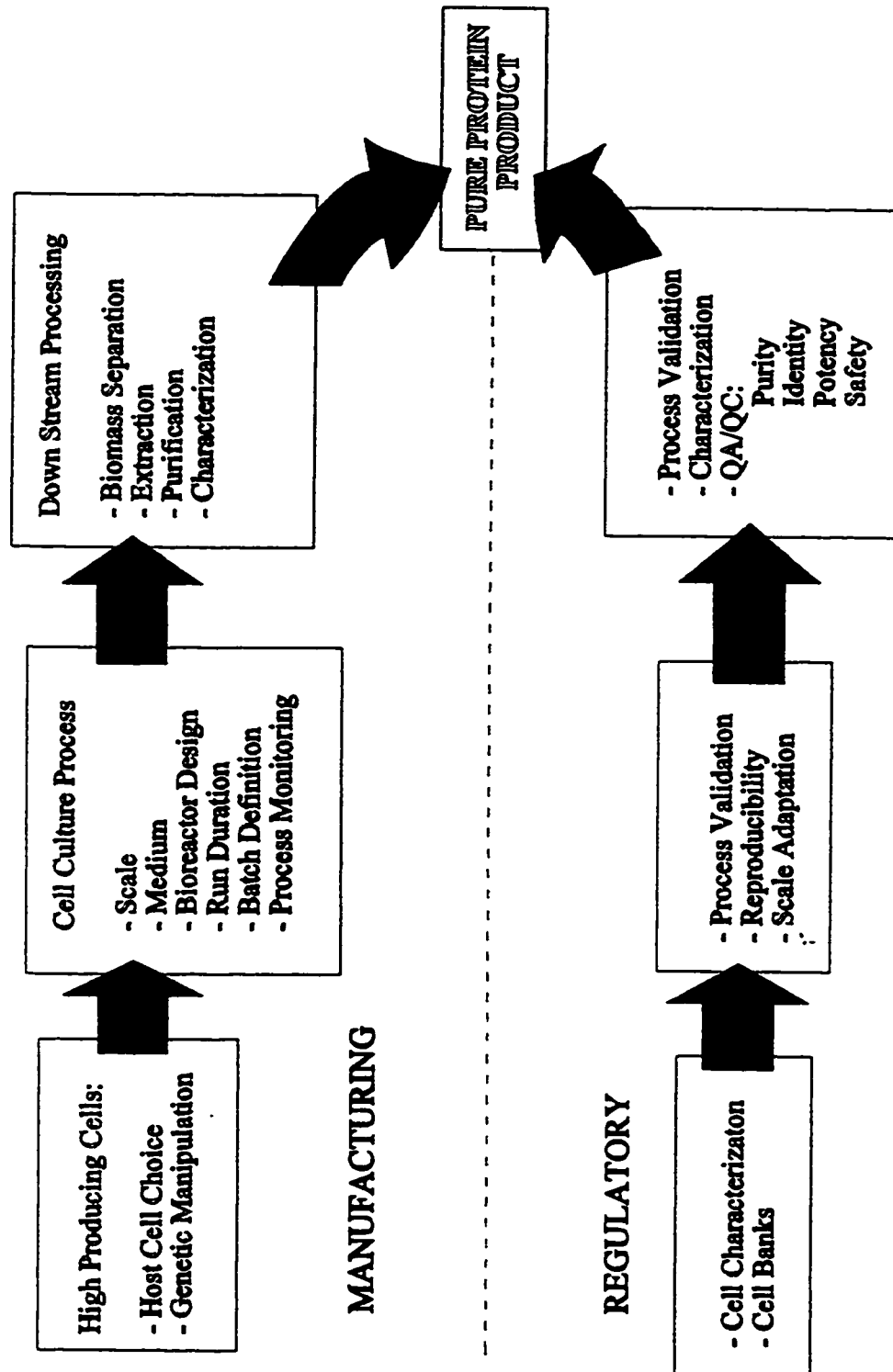


Figure 1.1: Aspects of interactive manufacturing and regulatory steps in the production of a biopharmaceutical

1.3 Scope and Objectives

The overall objective of this work was to further the understanding of the metabolism of rCHO cells, and to apply the resulting information to the optimization of the culture system for the production of a recombinant protein. The study involved two key areas for comparison:

i) morphological type; and ii) major substrate concentrations.

All studies were carried out on a relatively small scale, ranging from 10 mL to 1000 mL working volumes. Bioreactor configurations were restricted to static T-flasks and Spinner Flasks. The spinner flasks fall within the stirred tank category of bioreactors, which is the most commonly employed bioreactor configuration. The batch mode was utilized in these studies, as this mode is used almost exclusively in the production of therapeutic proteins.

The growth and productivity of the cells were compared in three different morphological types:

a) substratum attached (on T-flask surface or on microcarriers); b) aggregated suspension; and c) dispersed (single cell) suspension.

The effects on growth and productivity of the initial concentrations of serum, glucose, glutamine, and lactate were evaluated.

Finally, mathematical modeling was attempted in order to predict recombinant protein productivity as a function of major substrate initial concentrations, and of the biological capacity for production. A partially structured, non-segregated metabolic model which was developed in this laboratory (Phillips, 1991) for a hybridoma cell line, was modified for this recombinant Chinese Hamster Ovary cell line. Population growth phase association of production was evaluated, and assessed as a function of the physiological state of the cells (cell cycle phase).

This study focused on the second and fourth key areas of animal cell biopharmaceutical technology for the production of pure (secretory) protein products, as described above. Specifically, the work centered on cellular physiology and metabolism in batch culture and the impact of initial substrate concentrations.

As mentioned above, Chinese Hamster Ovary (CHO) cells, are one of the cell types with established records in biopharmaceutical production. As such, serum-free media are commercially available that will support many CHO cell lines. A number of CHO cell lines expressing recombinant secretory proteins are available to the researcher,

through (for example) the American Type Culture Collection (ATCC). In choosing a representative cell line, it is of primary importance that the secretory protein product can be assayed accurately and (relatively) easily. With these constraints in mind, a CHO cell line expressing recombinant human tissue plasminogen activator (h-tPA) was chosen from ATCC (accession # CRL 9606). A body of knowledge exists with respect to the culturing of Chinese Hamster Ovary cell lines. Human tissue plasminogen activator is a secretory glycoprotein, and is therefore representative of this class of biopharmaceuticals. Human tissue plasminogen activator has been purified and produced for at least the last 15 years (Section 2). Therefore, a number of assay procedures have been developed (Table 1.4).

Table 1.4: Commercially available tPA assays (e-tPA = extracellular tPA; i-tPA = intracellular tPA)

Detection Format	Assay Type	Reference/Manufacturer
e-tPA concentration	spectrophotometric: cleavage reaction	Boehringer Mannheim
e-tPA activity	spectrophotometric: cleavage reaction	Boehringer Mannheim
e-tPA concentration	sandwich ELISA	COELIZA, KabiVitrum
e-tPA activity	spectrophotometric: fibrinolysis	Verheijen <i>et al.</i> , 1982
i-tPA concentration	enhanced sonication/chemiluminescent blot	Lin <i>et al.</i> , 1993

In summary, the specific goals of the research were:

- to more fully characterize growth and productivity of a commercially important recombinant mammalian continuous cell line in batch mode, with the aid of improved analytical techniques such as those currently available with flow cytometry.
- to compare growth and productivity of this cell line in static and stirred tank bioreactor configurations; adherent on reactor surface or suspended microcarriers, as an aggregated suspension, or as a single cell suspension.
- to adapt an existing partially structured model for simulating batch growth and productivity of this cell line, by utilizing metabolic information obtained experimentally.

2. LITERATURE REVIEW

2.1 Mammalian Cell Culture

The growth characteristics of mammalian cells differ considerably from those of bacteria and fungi, the traditional workhorses of biotechnology. All three cell types exhibit similar growth profiles, the classical lag, exponential, stationary, and decline phases of batch cell culture. Mammalian cells are distinct among these cell types in that the growth phases are longer (days) relative to those of bacteria and fungi, which are on the order of hours. Also, relative to the entire mammalian cell growth curve, its stationary phase is short. Typically, data collected on a daily or twice daily basis suggests a disappearingly short or non-existent stationary phase. Secretory proteins, which may be thought of as secondary metabolites, are typically produced over the entire span of the growth curve in mammalian culture, and are therefore not completely growth-phase-associated. Again, this is not typical of secondary metabolite productivity in microbial systems, which tends towards a strong growth-phase-association.

Population Growth Dynamics

Parameters commonly used in describing batch mammalian cell culture are summarized in Table 2.1. Population growth (cell proliferation) is conventionally assessed in terms of the concentration of cells per unit volume of medium (X), frequently termed the cell density (Xie and Wang, 1996; Merten, 1988; Takahashi *et al.*, 1994; Suzuki and Ollis, 1990). In addition, the maximum viable cell concentration attained ($X_{v_{max}}$), the specific growth rate (μ), the percent viability (%V), and the average viable cell concentration ($X_{v_{avg}}$) are all employed as measures of the state of the population (Xie and Wang, 1996; Merten, 1988; Takahashi *et al.*, 1994; Suzuki and Ollis, 1990).

Production of secreted (extracellular) proteins is commonly measured as the concentration of protein in the medium (Xie and Wang, 1996; Merten, 1988). Hence, production is the end point of synthesis, post-translational modifications, intracellular transport, and secretion (Suzuki and Ollis, 1990). Productivity may be represented by one or more of three parameters: 1) the specific productivity (q_p) (Xie and Wang, 1996; Merten, 1988, Suzuki and Ollis, 1990; Luan *et al.*, 1987) which is the amount of protein product produced per cell per unit time; 2) the protein product accumulation rate (dP/dt) (Xie and Wang, 1996; Merten, 1988), also termed the volumetric productivity (P_{vol}); and 3) the maximum protein product concentration (P_{max}) (Xie and Wang, 1996; Merten, 1988). The latter two are often expressed as functions of the specific growth rate (Takahashi *et al.*, 1994; Gaertner and Dhurjati,

Table 2.1: Some parameters used in describing batch mammalian cell growth and protein production.

Parameter	Symbol	Formula	Reference
viable cell density	X_v	$\frac{\text{viable cell number}}{\text{volume of medium}}$	
maximum cell density	$X_{v(\max)}$		
average cell density	$X_{v(\text{ave})}$	$\frac{\sum_{j=1}^n X_{v_j}}{n}$	
specific population growth rate	$\mu_{(\text{ave})}$	$\frac{\sum_{j=1}^n \frac{\ln(X_{v_{j+1}} / X_{v_j})}{(t_{j+1} - t_j)}}{n}$	Dutton (1992)
	μ	$\mu_{\max} \frac{GLC}{K_{GLC} + GLC} \frac{GLN}{K_{GLN} + GLN}$	Müller <i>et al.</i> (1988), de Tremblay <i>et al.</i> (1992)
	μ	$\mu_{\min} + \frac{(\mu_{\max} - \mu_{\min})(GLC - GLC_s)}{K_{GLC} + (GLC - GLC_s)}$	Frame & Hu (1991a)
percent viability	%V	$(X_v X_i^{-1})100\%$	
protein product accumulation rate	dP/dt	$\mu_a X_v + b X_v$	Xie & Wang (1996), Shirai <i>et al.</i> (1994)
or volumetric productivity	P_{vol}	$\frac{(c_2 - c_1)}{(t_2 - t_1)}$	Merten (1988)
product titre	[Protein]	$\frac{\text{mass or moles Protein}}{\text{volume of medium}}$	
maximum product titre	P_{\max}		
viability index	VI	<i>integral of X_v</i>	Luan <i>et al.</i> (1987)
cumulative volumetric cell-hours	CH_{tot}	$\sum_{j=1}^n \frac{(X_{v_{j+1}} - X_{v_j})}{\ln(X_{v_{j+1}}/X_{v_j})} (t_{j+1} - t_j)$	Dutton <i>et al.</i> (1998)

Table 2.1: Some parameters used in describing batch mammalian cell growth and protein production. (continued)

Parameter	Symbol	Formula	Reference
specific productivity	q _{p-I}	$\frac{P_{max}}{(Xv_{max})(t_f)}$	
	q _{p-II}	$\left(\sum_{j=g}^h \left(\frac{(P_{j+1} - P_j)}{(Xv_{j+1} - Xv_j)} \right) \right) \left(\frac{\mu_{max}}{n} \right)$	Merten (1988)
	q _{p-II}	$\left(\sum_{j=i}^f \left(\frac{(P_{j+1} - P_j)}{(Xv_{j+1} - Xv_j)} \right) \right) \left(\frac{\mu_v}{n} \right)$	Hayter <i>et al.</i> (1992), Goergen <i>et al.</i> (1992)
	q _{p-III}	$\frac{[Protein]}{VT}$	Luan <i>et al.</i> (1987)
	q _{p-III}	$\frac{[Protein]}{CHvol}$	Dutton <i>et al.</i> (1998)
yield of cells on substrate	Y _{x,s}	$\frac{Xf_{max}}{(S_f - S_i)}$	
specific consumption of substrate	q _s or q _{CON} eg: q _{GLC}	$\frac{GLC}{CHvol}$	Xie & Wang (1996), Dutton <i>et al.</i> (1998)
	q _s	$\frac{\mu}{Y_{x,s}} + \frac{aS}{b+S}$	de Tremblay <i>et al.</i> (1992)
	q _s	$\frac{\mu}{Y_{x,s}} + m$	Miller <i>et al.</i> (1988)
	q _s	$\mu \left(\frac{1}{Y_{x,s}} - \frac{\beta}{Y_{p,s}} \right) + \frac{\alpha}{Y_{p,s}} - \frac{\mu_{min}}{Y_{x,s}}$	Frame & Hu (1991b)
specific production of metabolites	q _{PROD} eg: q _{LAC}	$\frac{LAC}{CHvol}$	Xie & Wang (1996), Dutton <i>et al.</i> (1998)
yield of metabolite on substrate	eg: Y _{LAC,GLC}	$\frac{q_{LAC}}{q_{GLC}}$	Dutton <i>et al.</i> (1998)

X_t: total cell concentration; a,b,α,β: constants; c_p: Product concentration; S: substrate concentration; f: final; i: initial; g: start exponential growth phase; h: end exponential growth phase; n: number of observations; GLC: glucose concentration; LAC: lactate concentration; GLN: glutamine concentration; m: maintenance coefficient; t: culture time; μ_v: variable specific growth rate

1993a,b) or the viable cell concentration (Xie and Wang, 1996; Takahashi *et al.*, 1994; Suzuki and Ollis, 1990), respectively.

The specific productivity, q_p , has been calculated in at least three different ways. For example, a method for evaluating the specific productivity was developed by Luan and co-workers (1987). In their technique, the volumetric cumulative product concentration measurements over the course of a batch culture were linearly regressed against the integral of the cell density measurements (which the authors called the “Viability Index”) over the same time interval.

Employing apparent kinetic parameters, the kinetics of mammalian cell population growth and secretory protein productivity have been investigated in batch and continuous operating modes for the dispersed suspension morphological type. Similarities to the growth kinetics of microbial suspension systems have enabled the fitting of primary data (total cell concentrations and viable cell fraction) in simple, unstructured models to describe growth kinetics (Phillips, 1991):

$$\frac{dX_T}{dt} = \mu_{app} f_V X_T \quad (2.1)$$

where X_T is the measured total cell concentration (cells/mL)
 f_V is the measured fractional viability
 and μ_{app} is the apparent specific growth rate (h^{-1})

and where:

$$\mu_{app} = \mu - k_d \quad (2.2)$$

where μ is the specific growth rate (h^{-1})
 and k_d is the specific death rate

Descriptive parameters, such as the population doubling time ($t_d = \ln 2 / \mu_{app}$), have been derived from these simple expressions. The apparent growth rate has been assumed to be approximately constant within a growth phase, so that doubling times can be calculated which are characteristic of each growth phase.

Not all of the viable cells in a population of mammalian cells are actively dividing. Descriptions of mammalian cell population growth kinetics can be modified to include variables for growth fraction and for cell cycle length (Dutton, 1992):

$$\frac{dX_V}{dt} = (\mu f_g - k_d) X_V \quad (2.3)$$

where X_V is the viable cell concentration (cells/mL)
 μ is the *average* cell cycle rate (h^{-1})
 f_g is the growth (actively dividing) fraction
 and k_d is the specific death rate (h^{-1})

The apparent population growth rate then becomes:

$$\mu_{app} = \mu f_g - k_d \quad (2.4)$$

where each of the variables is a function of culture time.

Similarly, productivity has been fitted to a simple unstructured kinetic model from primary data consisting of total cell concentration, viable cell fraction and extracellular secretory protein concentration in the bulk medium (Dalili and Ollis, 1989):

$$\frac{dP_{vol}}{dt} = q_p X_V \quad (2.5)$$

where q_p is the apparent specific production rate (mg/million cells/h)

This model assumes that none of the secretory protein is cell-associated (cytosolic and/or membrane bound), and that productivity is non-growth-associated. If the apparent specific production rate is assumed to be constant over the course of a culture, then it can be calculated as the slope of the measured cumulative secretory protein concentration against the integral of the viable cell concentration. Several researchers have found q_p to be a function of μ_{app} . It has been suggested that this growth association is complete such that (Merten *et al.*, 1985):

$$q_p = \alpha\mu \quad (2.6)$$

where α is the proportionality constant (mg/million cells)

Other researchers have found evidence that secretory protein production is partially-growth-associated, and have modified the descriptive unstructured model for secretory protein production to include a term for growth association and a term for non-growth association (Miller *et al.*, 1988), generally referred to as the Luedeking-Piret model in microbial systems (Bailey and Ollis, 1986):

$$q_p = \alpha\mu - \beta \quad (2.7)$$

where β is the constant portion of q_p which is independent of μ (mg/million cells/h)

Mammalian cells have been shown to utilize two main substrates, glucose and glutamine, as a carbon and energy source (Phillips, 1991) (Figure 2.1). Substrate consumption includes a growth rate dependent term and a population dependent term. Therefore, the rate expression for the consumption of each substrate is (Phillips, 1991):

$$\frac{ds}{dt} = -\frac{\mu X_V}{Y_s} - mX_V \quad (2.8)$$

where s is the substrate concentration (g/L)
 Y_s is the cell yield on substrate (number cells produced / gram substrate consumed)
 m is the maintenance coefficient (g substrate/d/cell)
 μ is the specific growth rate (h^{-1})

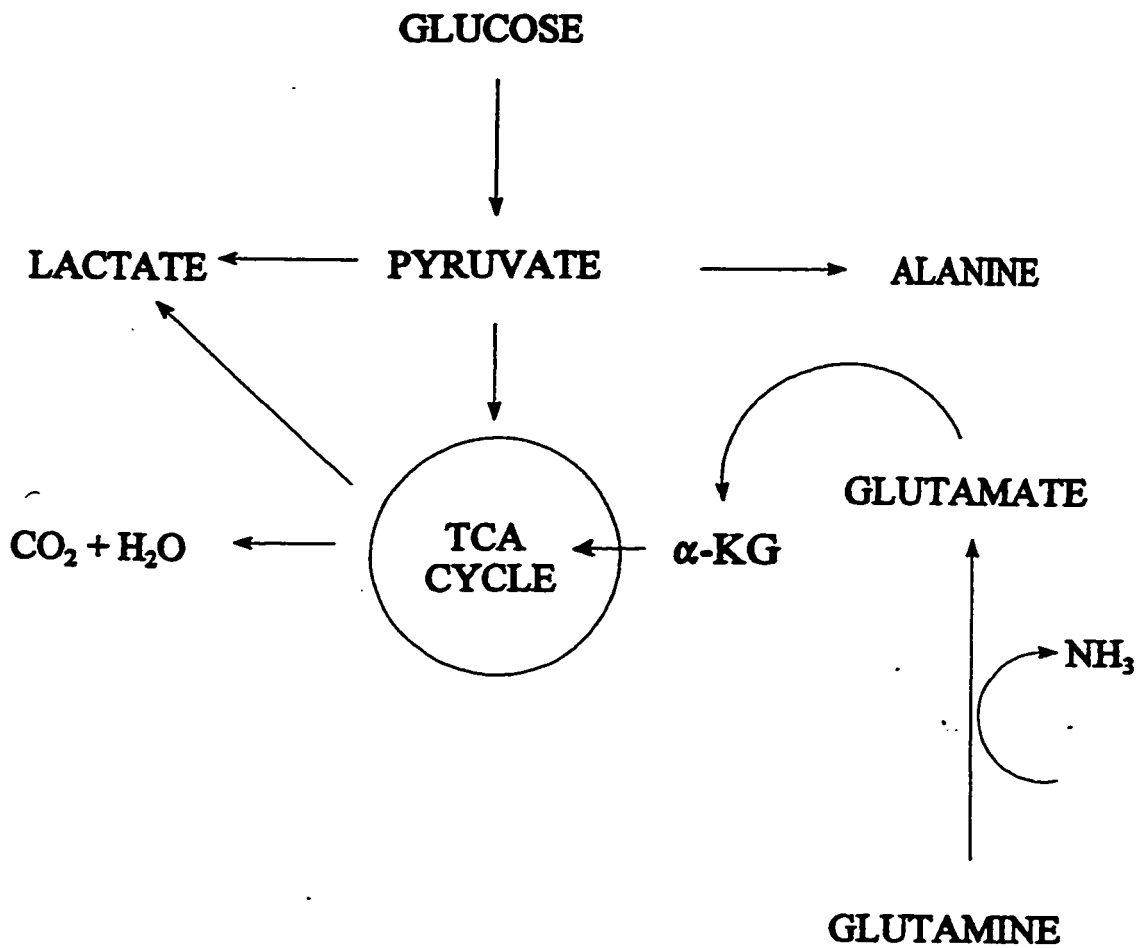


Figure 2.1 Simplified representation of the major metabolic pathways in cultured mammalian cells

Adenosine triphosphate, ATP, is the energy carrier of the cell, and is produced by the catabolic processes of metabolism, including glycolysis and the TCA cycle. It is consumed in the anabolic processes of metabolism, including biosynthesis and maintenance processes. The specific rate of ATP utilization may be expressed as (Pirt, 1975):

$$q_{ATP} = \frac{\mu}{Y_{ATP}} + m_{ATP} \quad (2.9)$$

where Y_{ATP} is the yield of cells from ATP (cells/ mol ATP)
and m_{ATP} is the maintenance energy requirement (mol ATP/cell/h)

Mammalian cells have a substantial maintenance energy requirement, which may even exceed utilization of energy for biosynthesis (Miller *et al.*, 1989). Thus, even non-dividing viable cells consume significant quantities of substrate. In contrast, microbial cells have a very low maintenance energy requirement.

Expressions for yield have been based on primary data consisting of the two major substrates, glucose and glutamine, and their associated major waste metabolites, lactate and ammonia. Glucose, which is normally provided in excess, is catabolized via glycolysis to lactate, with a molar lactate yield on glucose ranging from 1.0:1.0 to 1.8:1.0. Lactate concentrations as high as 33 mmol/L have been shown not to affect growth or secretory protein production (Adamson *et al.*, 1987).

Glutamine is utilized as a carbon source, a nitrogen source, an energy source and is also incorporated directly into proteins (Ozturk and Palsson, 1990a). Glutamine is subject to chemical decomposition, with a half-life, in culture medium at 37 °C, of 6.7 days (Ozturk and Palsson, 1990). This decomposition also occurs at lower temperatures, such as when basal medium is stored at 8 °C, although at a slower rate. Accumulation of 3 to 4 mmol/L of ammonium, which is an end product of glutamine catabolism and chemical decomposition, has been shown to have no effect on cell growth (McQueen and Bailey, 1990; Glacken *et al.*, 1986). Both glucose depletion and glutamine depletion are sufficient, but not necessary to cause hybridoma cell death (Phillips, 1991). Glutamine depletion can also end secretory protein production by hybridomas. The accumulation of ammonium and lactate yield a net decrease in pH which can also trigger cell death, once the buffering capacity of the medium has been exceeded. Phillips (1991) and Luan *et al.* (1987) have shown that the glucose to glutamine mole ratio affects cell growth and secretory protein production.

Mammalian cells also require essential amino acids and trace nutrients such as vitamins and minerals. A group of apparently essential components, required by most mammalian cell lines, includes insulin, transferrin, ethanolamine, and selenium (referred to as ITES). Some cell lines apparently require phospholipids in addition to ITES. Serum albumin is normally included in medium formulations, both as a protein and for its 'protective' properties. Many cell lines exhibit impaired growth and productivity in defined medium (serum-free medium), which is overcome at high cell densities. This suggests that 'growth factors' may be autocrine factors. This theory is the basis for utilization of 'conditioned medium' (Dutton *et al.*, 1998) and of feeder cells in cloning.

In addition, of course, mammalian cells require approximately 0.06 to 0.6 mmol of oxygen per billion cells per hour (1.9 to $19.2 \text{ mg} \cdot 10^9 \text{ cells} \cdot \text{h}^{-1}$) (Butler, 1996), and (an as yet undetermined concentration of) carbon dioxide. Mammalian cells require neutral pH, in the range of 6.5 to 7.5 pH units, and a narrow temperature range (eg. approximately 37°C for human cells and most other mammalian cells *in vitro*).

The population kinetics may be described in terms of three overall reactions (Figure 2.2) (Dutton, 1992). The second reaction, which is unique to viable reaction systems, complicates the catalytic reaction kinetics (see below). Productivity may be maximized through optimization of this reaction system. The convergence of maximization of the first and second reactions with minimization of the third reaction should maximize secretory protein yield. Maximization of the rate of productivity is less clear (Dutton, 1992).

The Mammalian Cell Cycle

The cell theory was first proposed by Theodor Schleiden and Jacob Schwann in 1838 (Murray and Hunt, 1993). Their proposal had two main tenets: that every living organism is composed of one or more cells and that new cells can arise only by the division of pre-existing cells. Cell division is the only path to immortality. Nondividing cells can live for as long as a hundred years, but they always eventually die.

Cell growth and division is a cornerstone of biology (Murray and Hunt, 1993), and is critical to the understanding of the dynamics of cell populations. Without understanding the checks and balances that direct orderly cell division, we cannot devise effective strategies to manipulate the dynamics of a population of cells.

The cell cycle, a term coined by Howard and Pelc in 1953 (Lloyd *et al.*, 1982), is conceptualized as a clock that measures the time it takes for a single cell to replicate (Martin, 1994). The four phases of the cell cycle were initially defined by the events in cell replication. The synthesis of DNA and mitosis itself were measurable in the early years of cell biology, and these provided the basis for 2 of the cell cycle phases, S (for DNA synthesis), and M (for

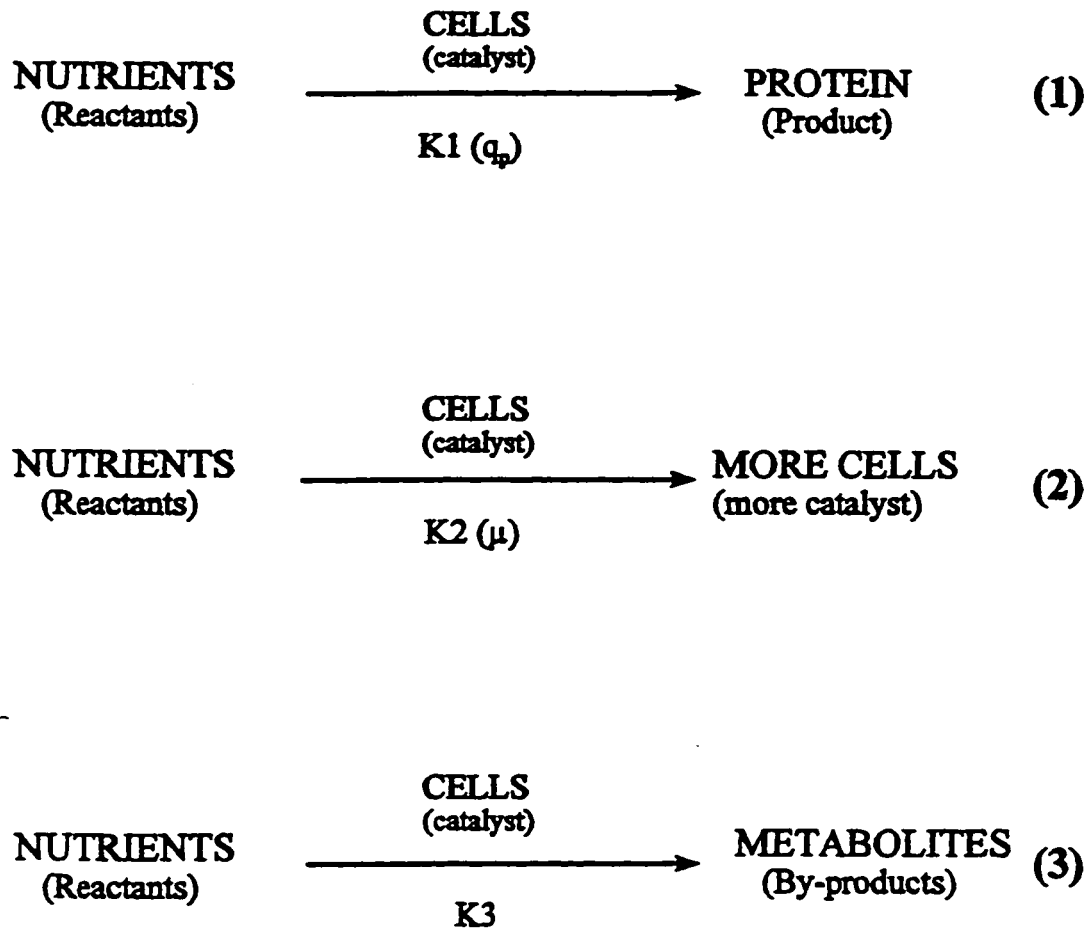


Figure 2.2 Overall reaction system of mammalian cell culture.

mitosis). Other events between the S and M phases were not easily measured, and were assigned the somewhat arbitrary names G1 and G2, for the Gaps between M and S, and S and M phases, respectively (Martin, 1994).

The following gives a brief summary of the mammalian cell cycle as described by Baserga (1976). The cell cycle of continuously dividing cells is represented in Figure 2.3.

Following cell division, or mitosis (M phase), there is a period (G1 phase) during which the cell is preparing for DNA synthesis, but no DNA synthesis occurs. The G1 phase is followed by the S phase, during which DNA is replicated. After completion of DNA replication, the cell enters the G2 phase, in which it prepares for mitosis. The average mammalian cell cycle is approximately 24 hours in duration, but the length of the cell cycle as a whole and of its component phases vary greatly from one cell population to another and even among individual cells within a population. The cell size (volume and mass) alters throughout the cell cycle corresponding to DNA synthetic activity and cellular division.

The main event during the S phase is the replication of genetic material: DNA, histones, and nonhistone chromosomal proteins. Secretion of certain specific proteins occurs during the early part of the S phase. The G1 phase is characterized by synthesis of various proteins (including microtubular proteins) and RNA required for mitosis. In mitosis, the tetraploid DNA splits into the normal diploid complement and is pulled apart along with the cell itself (*i.e.* the cell divides). The M phase is characterized by a marked decrease in protein and RNA synthesis, which ceases completely during metaphase and anaphase. By virtue of the very specific events of the M phase and the lack of synthetic activity, the length of the M phase is relatively short and is non-variable. The bulk of RNA and protein synthesis occurs during the G1 phase, including the synthesis of specific and secretory proteins. The accumulation and/or synthesis of components required for DNA replication occurs in the latter part of the G1 phase and the S phase.

Cells which are not actively dividing are either senescent (terminally differentiated, or in the process of dying) or quiescent ('resting' with respect to proliferative activity). The life span of a cycling mammalian cell in culture has been shown to be typically 2.0 to 2.2 days, at which time the cell drops out of the cell cycle permanently and enters senescence (de la Broise *et al.*, 1991). This type of senescence is termed apoptosis, or programmed cell death. Life span varies both from cell line to cell line and within cell populations (de la Broise *et al.*, 1991). Populations of normal cells (non-transformed) have a finite existence. Human embryonic cells have been shown to undergo a maximum of about 50 to 60 doublings, after which the final generation enters apoptosis (Butler, 1996). Hence, the generation number of the inoculum will impact on the maximum duration of culture propagation. It is likely that

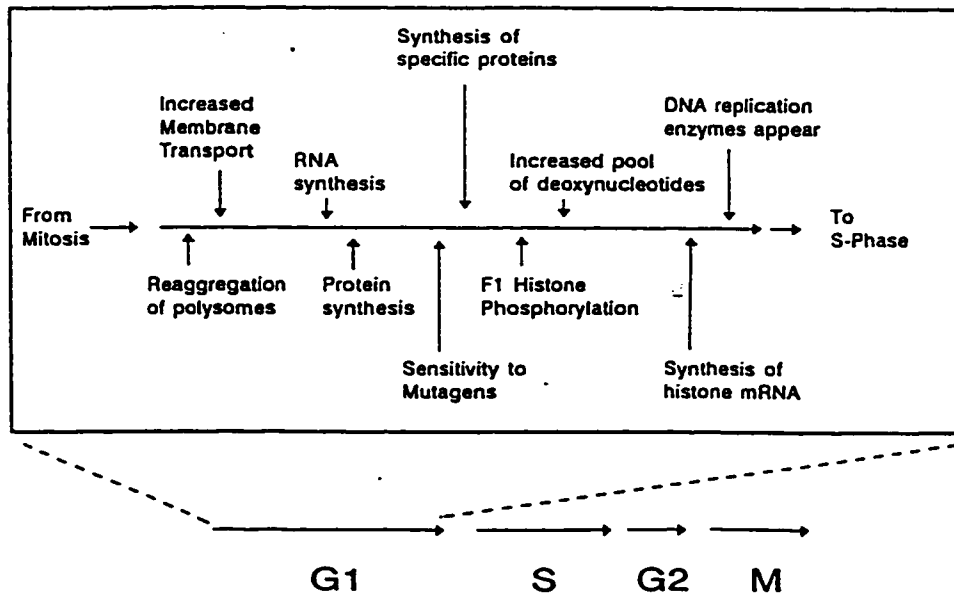
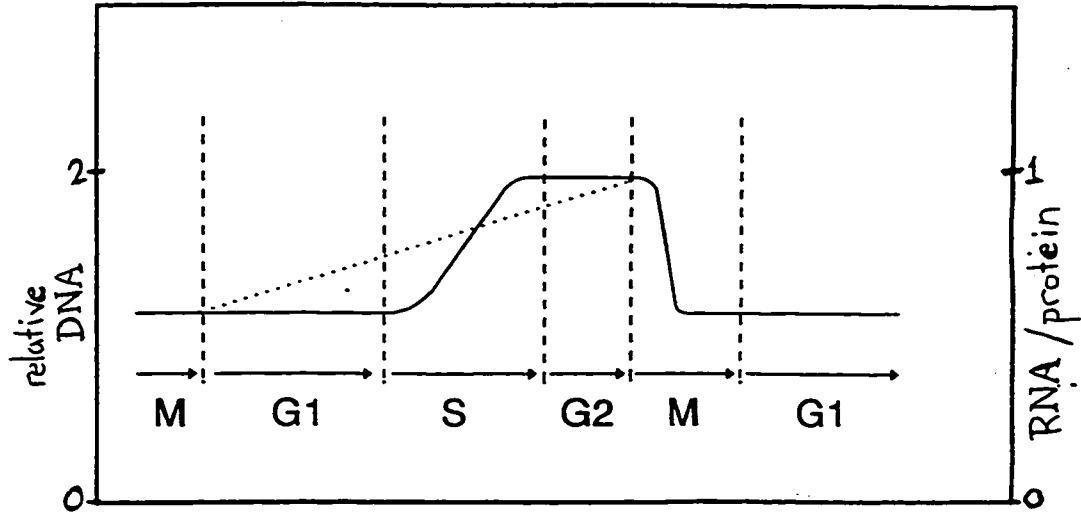


Figure 2.3 a). The mammalian cell cycle: S = phase of DNA synthesis; G1 and G2 = phases before and after DNA synthesis; M = phase of cell division; solid line = DNA concentration; dotted line = RNA and protein synthesis. b) Specific events of the G1 phase of the mammalian cell cycle.

environmental conditions may affect the life span of individual cells. Numerous stimuli (eg. viral infection, slow starvation, and deprivation of cell growth factors) can induce apoptosis of cells grown in culture (Mastrangelo and Betenbaugh, 1995). This natural process of dying is distinct, both in time span and in physiological state, from the general degenerative, traumatic cell death termed necrosis (Cartwright, 1994). Necrosis is a catastrophic event which is brought about by hostile changes in the culture environment, such as acidic pH levels. Cells enter necrosis from any quiescent or proliferative phase, while entry into apoptosis apparently occurs from the early G1 phase, before the restriction point.

A few of the characteristics that define apoptotic cells are 1) high levels of transglutaminase activity, 2) high cytoplasmic calcium ion concentrations, 3) shrunken cell size and accompanying increased buoyant density and rippled or ruffled membrane, 4) nuclear condensation and accompanying double-strand endonuclease cleavage of cellular DNA at linker regions between nucleosomes, 5) the formation of pseudopodia-like extensions, or blebs, of the membrane, 6) increased membrane permeability, 7) increased RNA and protein syntheses, and 8) increased rigidity (decreased membrane fluidity) (Mercille and Massie, 1994; Franek, 1995; Singh *et al.*, 1994). In contrast, necrotic cells are characterized by increased cell size; increased membrane fluidity; and a marked decrease or cessation of RNA and protein syntheses (Mercille and Massie, 1994; Franek, 1995; Singh *et al.*, 1994).

Apoptotic and necrotic cells have a number of defining characteristics pertinent to protein production from a cell population. In contrast to necrotic cells which exhibit a marked decrease in RNA and protein syntheses (Mercille and Massie, 1994; Franek, 1995; Singh *et al.*, 1994), apoptotic cells exhibit increases in the synthesis of some types of RNA and protein syntheses. Increases in the specific productivity during the decline phase of batch cultures could be explained if the protein product is preferentially synthesized by the increasing number of apoptotic cells. It has also been suggested that apoptotic cells exhibit increased secretion of accumulated protein (Al-Rubeai *et al.*, 1992). In contrast, where protein productivity is associated with proliferation, it has been assumed that retarding the transition of a cell population into apoptosis will increase protein titre (Mercille and Massie, 1994; Mastrangelo and Betenbaugh, 1995; Franek, 1995).

Cells can also exit the proliferative cycle reversibly, by entering a quiescent (with respect to cellular division) state. 'Resting' cells are arrested in some stage of the cell cycle, but with the correct stimulation, may re-enter the proliferative state. Cells can be arrested in the G2 phase, the early part of the G1 phase, or the S phase (Figure 2.4). Cells arrested in G2 are termed R2 and are characterized by a tetraploid DNA complement. Most commonly, cells are arrested in G1, and are termed G0. The G0 phase differs from the G1 phase in that none of the prerequisite material for DNA replication is assembled or synthesized, but synthesis of certain specific proteins continues. Cells arrested in G0 have as much as a 30% lower complement of RNA (particularly ribosomal RNA) and total cellular proteins, when compared to cells in G1 phase. Once cycling cells have commenced the assemblage and/or synthesis

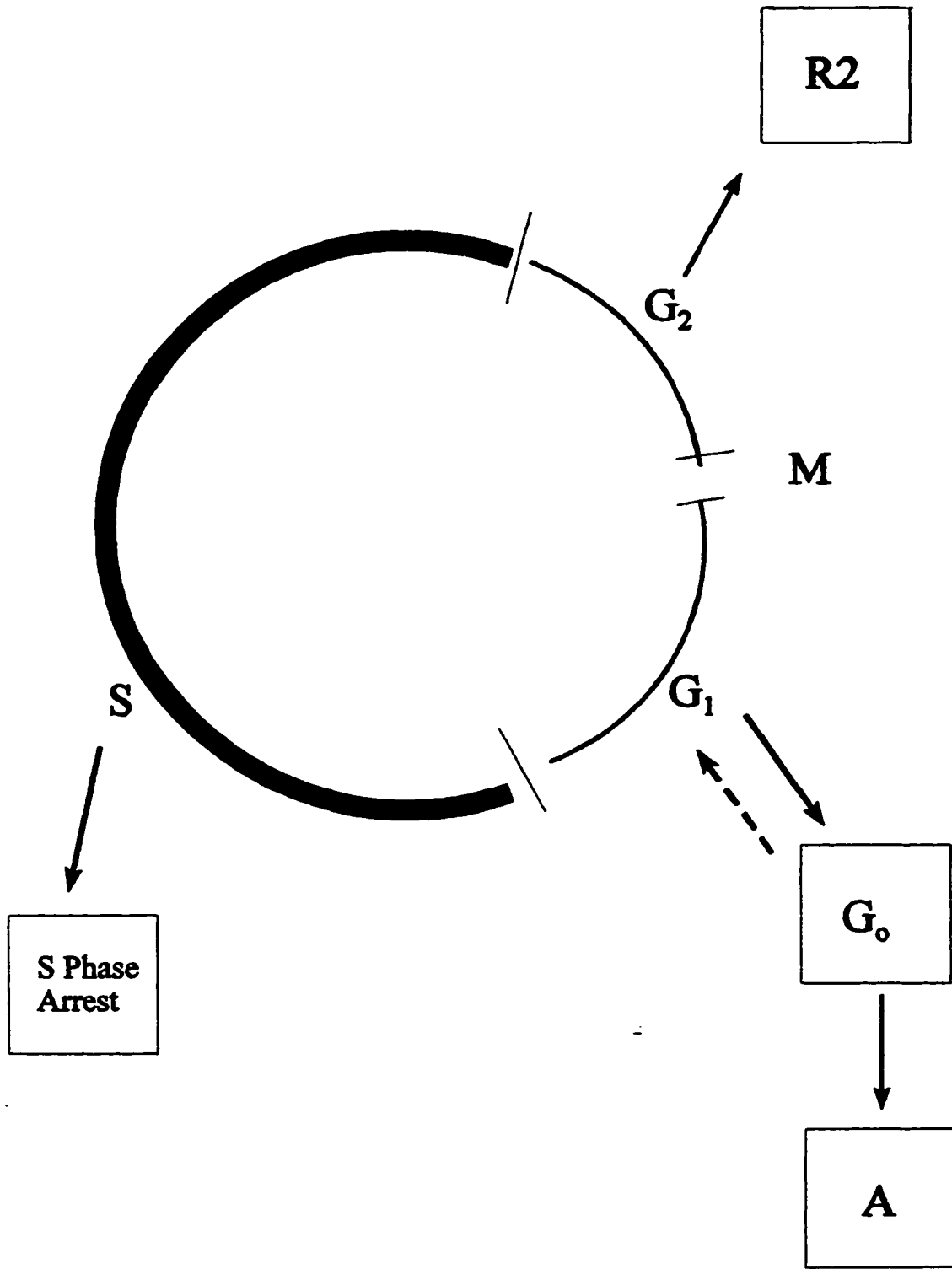


Figure 2.4 Relationship of quiescent and senescent cells to the cell cycle. (A= apoptosis)

of materials prerequisite for DNA replication, they are committed to enter the S phase. The point of commitment to proceed around the cell cycle is termed the restriction point, R. Cells that have passed the restriction point cannot exit the cell cycle to enter a resting phase until after the completion of DNA replication, except when induced to do so artificially (S phase arrest). It is controversial as to whether the resting state exists, or is merely a greatly extended G1 or G2 phase, but this distinction is immaterial to the impact of variable cell cycle length on population kinetics.

Nearly all cells (» 99%) in the exponential growth phase are maximally proliferative, such that the doubling time (of the growth, or cycling, fraction) is equal to the minimum length of the cell cycle (Baserga, 1985), the growth fraction is maximal and the death rate is negligible. This is one of the measures of balanced growth. In all other phases of the growth curve, the population is a mixture of nondividing cells, dying cells and dividing cells at various cell cycle lengths, such that the doubling time is a complex function of cell cycle time, growth fraction and rates of cell death and lysis (Baserga, 1985). Cell lysis is included here, as it may in itself affect the apparent growth rate. It is clear that conditions which affect any or all of these variables will impact on the apparent growth rate of the population.

An inoculum taken from an exponential population growth phase will frequently exhibit a lag phase, with physiological factors such as amino acid uptake temporarily decreasing upon inoculation into fresh medium (Baserga, 1976). Cells may exhibit an extended G1 phase, or temporarily enter the G0 phase. In general, the post-inoculation lag phase can be attributed to the orders of magnitude reduction in growth factors associated with the medium dilution attendant upon inoculation. The growth lag occurs while new enzymes and cofactors (required for nutrient assimilation) and growth factors (required for cell division) are synthesized (Baserga, 1985). In contrast, inoculating at high cell densities of exponential phase cells can prevent the population entering a lag phase (Dutton *et al.*, 1998a). This supports the view that the use of low density inocula dilutes autocrine growth factors below some critical value required for continued exponential phase growth.

While much of the investigative effort continues to be placed on the proliferative events of the cell cycle phases, there is some focus on RNA and protein synthetic activity also, as this is pertinent to protein productivity of a cell population (Suzuki and Ollis, 1990; Cartwright, 1994; Kromenaker and Srienc, 1994). For example, it has been reported that many 'secondary metabolites', such as MAbs, are preferentially synthesized during the G1 cell cycle phase (Kromenaker and Srienc, 1994; Tziampazis and Sambanis, 1994; Martens *et al.*, 1993; Singh *et al.*, 1994), while an absence of translation during G2 and M cell cycle phases has been observed (Suzuki and Ollis, 1990). Bibila and Flickinger (1992a) observed whole population averaged specific productivity of a secretory macromolecule (monoclonal antibody) to go through a rapid maximum at 15 to 20 hours, followed by steady decline throughout the exponential phase and then a slow increase in the stationary phase and early decline phase. They found that DNA and protein synthetic activity peaked by the early exponential phase and decreased rapidly during middle to late exponential phase. Synthesis of DNA is restricted to the S phase, while synthesis and secretion of specific proteins by

several different cell lines have been reported to be restricted to the G1 and early S phases of the cell cycle (Rubeai and Emery, 1990).

Cell size (mass and volume) closely correlates to the progression of the cell through the cell cycle: the cell size is at a minimum by the end of M phase, increases throughout late G1 phase and S phase, and remains at a constant maximum throughout the G2 phase (Ramirez and Mutharasan, 1990). Leno *et al.* (1992) found that the average specific cell mass and the average specific cell volume as well as total DNA synthesis increased with increasing growth rate, and postulated that fewer cells are in the G1 or G0 cell cycle phase per unit time at high growth rates. The average cell volume of batch cultures is constant and at a maximum during the exponential phase and decreases through the stationary and decline phases (Ozturk and Palsson, 1991; Dalili and Ollis, 1990). This finding correlates to a maximum growth rate during the exponential phase.

In order for the specific growth rate of the cycling fraction to increase, the total length of the cell cycle must decrease. It is unlikely that the rate of DNA synthesis (S phase) and the rate of cell division (M phase) are widely variable within the cycle of the individual cell. Therefore, it is most likely that the overall rate of the cell cycle depends upon the length of the G1 and G2 phases and on movement into and out of the resting states. As stated above, many investigators have found that variation of the length of cell cycle phases is limited to the G1 phase.

The synthesis and secretion of specific proteins (collectively referred to as specific protein production) proceeds in a highly orderly fashion from transcription through post-transcriptional modification, translation, post-translational modification, and interorganelle transportation, to exocytotic release of vesicle contents (Rubeai and Emery, 1990). Little is known about the post-transcriptional regulation of specific protein synthesis (Bibila and Flickinger, 1992b). Investigation of the biosynthesis of multi-chain secretory proteins such as immunoglobulins, suggest that these complex pathways may be regulated, with the rate of individual steps capable of being affected by manipulation of growth rates, nutrients and/or autocrine factors that may also stimulate proliferation (Bibila and Flickinger, 1992b).

Transcription through to transportation to the Golgi apparatus appears to be restricted to the G1 phase of the cell cycle for many secretory proteins (Ramirez and Mutharason, 1990). Specific protein synthesis is a positive linear function of its mRNA concentration (Leno *et al.*, 1992). Leno and co-workers (1992) found that the fraction of specific protein mRNA in the total RNA pool increased with increasing growth rate, and showed that this was due to an increase in the half-life of the mRNA rather than an increase in synthesis of the mRNA. In batch cultivation, the levels of cytoplasmic mRNA specifying the heavy and light chains of an immunoglobulin, as well as the levels of total RNA, peak during the exponential phase and decrease significantly during the decline phase (Leno *et al.*, 1992). This variation parallels the rate of DNA synthesis and the total cytoplasmic RNA. That is, transcription is not affected by growth rate, or by RNA concentration.

Bibila and Flickinger (1992b) found specific antibody production to be controlled by the time scale of post-transcriptional events, and established a set of ranges: complete assembly, 10 to 20 minutes; half-time for endoplasmic reticulum to Golgi apparatus transport, 30 to 60 minutes; and half-time for Golgi apparatus to medium transport, 5 to 20 minutes. Assuming that the G1 phase comprises transcription, translation and a portion of transportation, and assuming that the overall length of the G1 phase is controlled by the growth rate; interactions of the post-transcriptional events and the growth rate will affect specific antibody production (Bibila and Flickinger, 1992b). Accordingly, in their model the length of the G1 phase can vary by up to approximately 2 hours.

Bibila and Flickinger (1992b) assumed amino acid assembly (translation) to be the rate limiting step. They simulated the effect of the magnitude of the assembly rate constant, which they termed k_A , on the response of specific protein production rate to changing growth rate. Presumably, the driving force for specific productivity of cell lines having a low k_A is length, and not the number, of the G1 phases per unit time. Conversely, the length of time available for assembly may be limited at high growth rates. This is in agreement with Leno *et al.* (1992) who observed a 7- to 10-fold increase in the intracellular levels of immunoglobulin mRNA during the exponential population growth phase (*i.e.* during the maximum apparent population growth rate), implying that antibody assembly (translation) is limited at high growth rates. According to the model of Bibila and Flickinger (1992b), a cell line having a medium k_A of $\approx 1.0 \times 10^{10}$ (molecules/cell-hour)⁻¹ would have a specific production rate that is independent of exponential phase growth rate, while a high k_A would yield a positive correlation between growth rate and specific production rate.

Leno *et al.* (1992) observed a 15- to 20-fold decrease in the levels of cytoplasmic and membrane-bound monoclonal antibody as the population passes from the exponential into the decline phase of growth. Meilhoc *et al.* (1989) found that the fraction of the cell population with high membrane bound, or membrane associated, immunoglobulin G decreases throughout a batch cultivation, in parallel with the variation of the apparent population growth rate. The fraction of viable cells in the S phase is maximal in early exponential phase and the fraction of viable cells in G1 and/or G0 phase increases significantly during the decline phase (Leno *et al.*, 1992). This suggests that as the cell division rate slows down, the time and energy available for interorganelle transport and post-translational modifications increases such that an increasing fraction of synthesized secretory protein is shifted to the Golgi apparatus. Conversely, interorganelle transportation of secretory proteins may be interrupted by the onset of DNA synthesis and cell division, such that membrane bound secretory protein concentration increases with increasing growth rate.

Suzuki and Ollis (1990) developed a simple structured model for monoclonal antibody (MAb) production kinetics by combining the cell cycle theory with the population growth rate. They assumed that (some) rate-controlling step is first order in MAb transcription, and that the growth rate variation does not alter the (overall) MAb synthesis rate (translation), but only changes the relative time length of the individual cell cycle and sub-cell cycle phases. They

found a 50 to 130% MAb production rate enhancement for growth slowed up to 50%, but that further decreases in the growth rate also decreased the MAb production rate. This suggests that 1) a minimum secretory protein synthesis constant exists per cell cycle; or 2) decreased secretory protein productivity at very low growth rates is an artifact of nutritional and/or environmental inhibition or limitation.

Phillips (1991) and Dalili and Ollis (1990) both found negligible release of monoclonal antibody from sonically disrupted hybridomas. However, the population growth phase of the disrupted cells was not reported by either of these investigators. Leno *et al.* (1992) observed total cytosolic immunoglobulin to be at a minimum when cell cycle length is at a maximum. Hence, cells in the decline phase would have negligible cytosolic immunoglobulin concentrations. Following cessation of the exponential phase, MAb secretion is maintained at a high level for a limited period of time (48 to 72 hours) even though mRNA levels are decreasing (Bibila and Flickinger, 1992a). This implies that accumulated mRNA is being utilized and cell associated antibody is completing interorganelle transport, post-translational modifications, and secretion; while synthesis of mRNA is declining as the fraction of non-cycling (non-proliferative) viable cells increases. Detergent extraction of cell lysates from particular population growth phases (associated with absolute or relative population growth rates) would better elucidate the pattern of intracellular secretory protein accumulation.

Flickinger *et al.* (1992) attributed the apparent rapid increase of specific antibody secretion rates during late decline phase to the increase of membrane degradatory agents (enzymes) released into the medium from lysing cells, which in turn release membrane bound antibody from dead and dying cells and cell fragments into the medium. They postulated that this cell-associated immunoglobulin accumulated as a result of insufficient time to complete secretion during each cell cycle.

Increasing specific production rates during the decline phase may result from a specific increase of synthesis of monoclonal antibody, in response to an increased pool of necessary nutrients released into the medium from dead and dying cells. Flickinger *et al.* (1992) found that a pulse of amino acids (including L-glutamine) stimulated the rate of antibody release and that the effect of these amino acids was not attributable to release of previously synthesized and transiently stored MAb from the endoplasmic reticulum, Golgi apparatus, or post-Golgi vesicles.

Bibila and Flickinger (1992b) calculated that hybridomas synthesize enough immunoglobulin mRNA to support (translate) a gene dosage of 60 (*i.e.* enough mRNA to simultaneously translate 60 copies of the protein). Thus rDNA technology could markedly increase the specific productivity.

In summary, the apparently baffling inconsistencies of superficial, non-segregated population dynamics indicate that a more detailed examination is required in order to elucidate growth and productivity patterns. The single units

comprising the population are the individual cells. An understanding of the mechanisms and environmental interactions of the individual cell must be established in order to extrapolate to population dynamics. Much work remains to be done in this area, but the current body of knowledge concerning cell cycle dynamics may be applied to better clarify observed population dynamics.

Much of the above research was conducted with hybridoma cells. This is probably because: 1) hybridomas are non-adherent, and can therefore be grown in single cell suspension culture, which lends itself easily to analytical techniques such as flow cytometry; 2) hybridomas are commercially important; and 3) there is not a large body of biological research on hybridoma culture available for exploitation by the engineering research community (biological research on cell culture tends to be the purview of medical research, particularly cancer research.).

Substratum Adherence

Cell transformation has been known for many years to result in loss of the normal requirement for attachment and spreading before cell division can occur, and the ability to grow in suspension is observed in many malignant cells (Winterbourne *et al.*, 1993). Growth of cells as aggregates in static culture has been used as a criterion of transformation (Tolbert *et al.*, 1980). Transformed cells differ morphologically from normal cells, which is a reflection of alterations in the structure of the cytoskeleton (Barritt, 1992). Transformed cells exhibit constitutive proliferation, which is thought to result from the presence of an oncogene which encodes an abnormal growth factor, an abnormal plasma-membrane receptor for a growth factor, or an altered component of one of the pathways of intracellular signaling (Barritt, 1992). These factors coupled with an alteration in the composition of the extracellular matrix permit the anchorage-independent growth of transformed cells, although often at reduced specific growth rates (Smith and Wood, 1996). To optimize growth kinetics, it is therefore advantageous promote the substratum adherent morphological type.

Stable adhesion of anchorage-independent transformed cells to substratum (such as microcarriers) under the influence of hydrodynamic shear in a bioreactor is often difficult to achieve. This can be explained by a combination of two theories: 1. the consecutive mechanisms of stable cell-substratum attachment; and 2. the model of consecutive replacement of substratum adsorbed proteins by surface-active attachment proteins.

Stable Cell-Substratum Attachment

Cell adhesion to a surface is a very complex process involving an initial interaction between the cell and the substratum, followed by interaction between cell surface-binding sites and adhesive ligands, and finally reorganization of membrane components and cytoskeletal elements with accompanying spreading of the cell on the substratum (Cheung and Juliano, 1984). Adhesive ligands of more than one type may be involved, with interactions occurring sequentially.

A pericellular matrix, or glycocalyx, composed of glycoproteins, proteoglycans, and carbohydrates forms around animal cells (Foa *et al.*, 1994). Both integral and peripheral proteins contribute to the glycocalyx (Smith and Wood, 1996). The peripheral proteins are bound to the surface of membranes by weak ionic interactions, and are easily removed in aqueous solutions (Smith and Wood, 1996). In cell culture, peripheral glycoproteins and proteoglycans can be contributed to the glycocalyx from serum in the medium. Conversely, when operating in serum-free conditions the peripheral components of the glycocalyx are easily lost to the medium. The addition to and preservation of the peripheral components in the glycocalyx is likely the aspect of serum which confers its well known 'protective role' in animal cell culture.

One carbohydrate component of the glycocalyx is sialic acid, a highly charged acid-sugar molecule which contributes much of a cell's negative surface charge, and is thus a determining factor in electrophoretic mobility (McQuiddy and Lilien, 1974). The surface charge of cells is the instrument of initial interaction with substrata (Varani *et al.*, 1996). The electrostatic attachment of cells to negatively charged glass surfaces is dependent upon the involvement of cations such as Ca^{-2} and Mg^{-2} . Electrostatic interactions of cells with plastic surfaces may be direct (positively charged plastic surfaces) or cation dependent. These electrostatic interactions are weak and can be easily broken. Cell surface attachment must be stabilized chemically with ligand to cell surface receptor binding followed by intramolecular disulfide bond rearrangements to form strong intermolecular covalently bonded aggregates of adhesion ligands connecting the cell to the substratum (Smith and Woods, 1996). Lastly, adherence is stabilized biologically through membrane component and cytoskeletal rearrangements.

The glycocalyx may also contain extracellular matrix components such as fibronectin, collagen types I and III, and laminin (Wierzbza *et al.*, 1995), depending upon their availability in the medium. (When these components are not included in the medium formulation (eg. serum-free medium), the concentration gradient between the surface of cells in suspension and the medium ensures their absence from the glycocalyx.) These attachment factors can adsorb strongly to glass and plastic surfaces. In addition, growth factors present in the glycocalyx rapidly stimulate actin polymerization at the plasma membrane, to produce lamellipodia and edge ruffles (Konstantopoulos and Clark, 1996). The lamellipodia are connected with integrins to form focal adhesion sites

(Konstantopoulos and Clark, 1996). Hence, integrins, which are the receptors for attachment proteins, provide a physical link to the cytoskeleton, which leads to the cytoskeletal rearrangements necessary for the morphological changes associated with spreading of the cell the substratum surface. Bonds form between substratum-attached proteins and integrins, and the pericellular matrix expands at the substratum-cell interface to become continuous with the extracellular matrix. The attachment factor ligand between the cell and the substratum results in cytoskeletal rearrangement, which in turn results in further attachments and the spreading of the cell on the substratum. Crouch and co-workers (1985) have reported that the shear forces causing the detachment of cells are of the order of 1000-fold greater than those permitting cell attachment. This reflects the chemical and biological stabilization of cell-substratum attachment, and the relatively weak electrostatic interactions associated with initial attachment.

Once cells have adhered, autocrine attachment factors are secreted into the space between the cells and the substratum, creating a locally elevated concentration. It has been shown that as CHO cells reach confluence they secrete procollagen type I in addition to fibronectin and procollagen type III (Aggeler *et al.*, 1982). Collagen type I bonds tightly to attachment receptors and to substrata, so that the confluent population is securely anchored (see Section 4.1.2).

Substratum Adsorbed Proteins

The direct interaction of cells with substratum primarily involves electrostatic phenomena, perhaps with some adsorption of membrane surface proteins. These interactions are not stable. The stable attachment of cells to substratum requires the deposit of extracellular matrix proteins on the surface of the substratum and subsequent bonding between extracellular matrix components and their membrane bound receptors.

Serum contains extracellular matrix proteins, as well as nonadhesive proteins such as bovine serum albumin (BSA). Neither fibronectin nor BSA in solution interact with cell surface receptors. Most proteins adsorb to substrata and upon adsorption undergo changes in their conformations to activated forms (Smith and Woods, 1996). Fibronectin undergoes a change upon adsorption which permits its interaction with appropriate cell surface receptors.

Kim and co-workers (1992) have developed a theory which can explain the failure of cells to stick stably to surfaces, even in serum containing medium. When a solid surface is in contact with mixed proteins solution such as serum, the composition of the adsorbate changes with time. This is due to a consecutive replacement of adsorbed proteins by more surface-active proteins that are present in lower concentrations. In this process, abundant, low molecular weight proteins are replaced by high molecular weight proteins present at low

concentrations. The proteins apparently displace each other in the following order: albumin, immunoglobulins, fibrinogen and fibronectin, and finally high molecular weight kininogen and factor XII. The exchange behavior is influenced by overall concentration of protein in solution and the type of surface.

When substrata are contacted with pure serum, fibronectin, present at a concentration of approximately 20 to 30 mg L⁻¹, can displace albumin to form an approximately continuous attachment surface for cells. Once cells have attached, they can cement the attachment through secretion of autocrine extracellular matrix proteins into the space between the cell membrane and the substratum surface.

When non-serum precoated microcarriers are exposed at the time of inoculation to medium containing 10% serum, albumin adsorption prevents initial attachment of cells. The concentration of fibronectin (2 to 3 mg L⁻¹) is not sufficient to form a continuous coating once it has displaced albumin. Coupled with hydrodynamic shear in agitated vessels, stable cell attachments are strongly inhibited.

When serum-free medium is used, the probability of cell to substratum attachment is greatly diminished. The major component in the 'supplement' of most commercially available serum-free media is BSA (ca. 300 mg L⁻¹), while fibronectin is not normally found in serum-free media.

Serum precoating of substrata can permit initial cell attachment in both serum-containing and serum-free media, without the addition of costly attachment factors. If the cells are then provided with an environment free of hydrodynamic shear for a few hours, their attachment can be stabilized through cytoskeletal rearrangement and spreading, with associated increase in the number of bonds between receptors and extracellular matrix proteins.

Time Domains

An integrated view of the multiplicity of biochemical reactions involved in biological systems is not possible without an explicit awareness of the various levels of organization occurring over time (Lloyd, D. *et al.*, 1982). Biological reactions can be grouped and arranged from fast reactions proceeding independently of diffusion, through 'metabolic time' and 'epigenetic time' to the cell division cycle (genetic) time domain, which can, in turn, overlap with the circadian time domain.

The Metabolic Time Domain

The Metabolic Time Domain includes rapid reactions and slower reactions. The most rapidly-occurring biological reactions that have been measured occur on a picosecond (10^{-12} s) time scale. Current limits of measurement capabilities, such as fluorescence lifetime measurements, provide information in the nanosecond (10^{-9} s) range, the time required for a small metabolite such as glucose over a distance of 1 nm by diffusion. In 100 ps, the small metabolite would diffuse over a distance smaller than the molecular radius of the macromolecule. Therefore, resolution of time to 0.1 ns is sufficient to appreciate the elementary molecular dynamics in the macromolecular environment accompanying any physiologically significant change.

The 'slower' reactions in the metabolic time domain include enzyme-substrate interactions. Relevant time frames for these reactions are much longer than for the rapid reactions, with turnover rates for these molecules occurring in the millisecond to microsecond range.

The Epigenetic Time Domain

The epigenetic time domain encompasses the consequences of gene expression and altered activities of genes (including biosynthesis, processing, transport, and interaction of macromolecules). The epigenetic system may be regarded as having relaxation times within the range $10^2 - 10^4$ seconds (1.5 minutes to 3 hours). The production of specific secretory proteins of concern to bioengineering fall into this time domain.

The Genetic Time Domain

Generation times for cultured mammalian cells lie mostly within the range 7.7 to 30 hours, over which time the recurrent sequence of discrete events of the cell cycle (DNA replication and cell growth) occur. The time domain of the cell cycle subsumes the metabolic and the epigenetic domains.

Circadian Time Domain

Many daily rhythms of biological activity persist for long periods even when organisms are placed in conditions of constant temperature and constant light (or darkness). These circadian rhythms are driven by an endogenous oscillation in cellular controls and play the key role of time-measuring for the organism. All eukaryotic cells (but probably not prokaryotes) possess a light-entrainable cellular pacemaker (circadian clock). Circadian clocks are characterized by a persistent free-running period of about 25 hours; and by entrainability and phase-responsiveness to single or multiple externally-applied signals which include light, temperature, nutrients, oxygen, electrolytes, etc.

Populations of cells operate within the circadian time domain, as do the human beings that study them.

Time Domain Summary

Living organisms may be considered as hierarchical systems in both space and time; spatial organization has been explored more thoroughly than temporal aspects. The levels of organization within the temporal hierarchy range from ultrafast reactions on a subpicosecond time scale, through rapid reactions, metabolic, epigenetic, cell division cycle and circadian domains. A network of controls operates within and between time domains. A temperature-compensated period may represent a fundamental unit of time, which may explain interactions between different time domains.

The hazards of overlooking cellular time-structure cannot be over-stressed; it is evident that many of the dogmas currently dominating biochemistry, microbiology, cell biology, and biotechnology have become established from studies of exponentially growing (asynchronous) cell populations. Measurements made on heterogeneous populations of this kind are time-averaged ones. Particularly suspect in this respect are claims that metabolite pools are present at "stabilized" levels, or that the accumulation of a constituent occurs "continuously". In other words, observations made on biological processes always have a kinetic component, and it is imperative to avoid deriving from them "time-independent" conclusions. This is a danger associated with data gathered from periodic sampling, or "snap shots in time", particularly if the sampling is set at a constant time period.

An analogous situation is that of deciding whether a mountain is a rigid or a flexible structure. Evidently over a period of a human lifetime, of the order of tens of years, the mountain would not change appreciably its shape, but this conclusion could not be extended as valid over periods of geological time, of the order of 10^8 years.

Conversely, in cell culture studies, the investigator is likened to the geological time while the study subject is likened to the human life span time. The danger of loss of resolution exists in this context: details tend to merge, and discrete entities appear indistinguishable. Hence, a cell population is labelled "homogeneous", while details of the epigenetic and metabolic time domains are considered "continuous".

2.2 Chinese Hamster Ovary Cells

Chinese Hamster Ovary cells are one of the cell line workhorses of animal cell based biotechnological processes (Croughan and Wang, 1990). As such, they have been studied extensively and many of their population growth parameters and requirements are well documented (Table 2.2). Observed parameters are typical of mammalian cells in culture (Section 2.1). Culture morphological types of CHO cell lines include single cell suspension, anchorage dependent (surface adherent), and aggregate suspension. Serum-free, low protein, medium formulations are commercially available for CHO cell lines (Table 2.3).

The effects of a number of environmental conditions on growth and productivity of rCHO cells have been investigated. Lin and coworkers (1993) found that mild hypoxia could induce a specific oxygen consumption rate decrease of at least 50%, without affecting the cell growth rate, maximum cell concentration, recombinant tPA production rate, or recombinant tPA activity.

Table 2.3: List of serum-free media for Chinese Hamster Ovary cell culture.

Product (protein content (mg/L))	Supplier
Ultra-Chow (< 300)	Bio-Whittaker Inc.
CHO-SFM (400)	Gibco
CCM5 (< 400)	Hyclone Laboratories
Ex-cell 301 (100)	JRH Biosciences (Seralab)
SoftCell - CHO (300)	TCS Biologicals Ltd.
HB-CHO (320)	Immucor Inc.

Table 2.2: Some observed rCHO growth parameters and requirements

Parameter	Requirement	Reference
extracellular pH	-decreased glycosylation of recombinant protein outside $6.9 < \text{pH}_e < 8.2$ -optimal growth at $7.0 < \text{pH}_e < 7.6$	Borys <i>et al.</i> , 1993
agitation rate	- growth, viability, DNA synthesis good at 80 rpm - inhibited at 250 rpm	Lakhotia <i>et al.</i> , 1992
doubling times (0.5% serum, aggregate suspension)	- 20 to 30 h in T-flasks (0.2 to 1.2×10^6 c/mL) - 35 h in spinner perfusion (1.2 to 12×10^6 c/mL) - > 69 h ($> 12 \times 10^6$ c/mL)	Avgerinos <i>et al.</i> , 1990
q_{GLC} q_{Oxygen} $Y_{\text{LAC,GLC}}$	- 1.0 to 1.5 mmol/ 10^{10} cells/h - 1.25 to 1.50 mmol/ 10^{10} cells/h - 1.1 to 1.2 mol/mol	Lin <i>et al.</i> , 1993
aggregate cell density	2×10^6 c/mL (suspensions in spinners)	Tolbert <i>et al.</i> , 1980
aggregate suspension microcarrier suspension	- μ_{max} 0.025 h^{-1} , $Y_{\text{LAC,GLC}}$ 1.2, $Y_{\text{NH}_4,\text{GLN}}$ 1.0, q_{rP} $3.5 \text{ U}/10^8$ cells/h - μ_{max} 0.040 h^{-1} , $Y_{\text{LAC,GLC}}$ 1.2, $Y_{\text{NH}_4,\text{GLN}}$ 0.60, q_{rP} $20 \text{ U}/10^8$ cells/h	Chevalot <i>et al.</i> , 1994
aggregate growth adherent growth	-correctly folded and glycosylated rProtein - incorrectly folded and glycosylated rProtein	Watson <i>et al.</i> , 1994

Jenkins and Hovey (1993) studied the effects of temperature induced growth arrest on rCHO cells. They found that the cells arrested in the G1/G0 cell cycle phase, and that these arrested cells exhibited increased specific recombinant protein production, and decreased specific glucose uptake and lactate production. These findings indicate that glucose consumption is linked to proliferation and that the recombinant protein production is correlated to the G1 cell cycle phase.

Borys *et al.* (1993) showed that an optimum pH range maximizes specific production rates of two recombinant proteins in CHO cells. They also showed that pH affected glycosylation patterns of the proteins.

Major Substrate Concentrations and Growth and Productivity

In the current work, the effects on batch growth and productivity of the initial concentrations of major substrates are evaluated. The substrates investigated included glucose, glutamine, and serum. The impact of initial concentrations of lactate was also assessed. Some relevant information on each of these chemical species or groups of chemical species (serum) has been reported in the literature:

Glucose

Glucose is one of the two major carbon substrates utilized by mammalian cells in culture (Section 2.1). Glucose can be catabolized anaerobically, via glycolysis, or aerobically. Investigators report metabolic glucose quotients of 1 to 1.5 mmol/10¹⁰ cells/h for CHO cells growing under normal operating conditions (eg. 20 to 21 % oxygen in gas phase; 10 to 30 mmol L⁻¹ initial glucose concentration; 2 to 6 mmol L⁻¹ initial glutamine concentration; 37 ° C; 5 % CO₂ in gas phase; etc.) (Lin *et al.*, 1993; Lin and Miller, 1992). Hayter and coworkers (1992, 1993) report glucose levels of at least 8.5 mmol/10⁶ cells to be growth limiting for CHO cells. While their calculations indicate that there is no maintenance requirement for glucose, the maintenance requirement for glucose-catabolism-derived intermediates suggests a minimum glucose requirement of 80 mmol/10¹² cells/h .

The metabolic endproduct of glycolysis is lactate, with a theoretical maximum yield of 2 lactate molecules from each glucose molecule. Although glutamine, which is the other major substrate utilized by mammalian cells in culture, can also be catabolized to lactate, the glutamine contribution to the lactate pool is usually assumed to be negligible (Phillips, 1991). Hence, the yield of lactate on glucose, $Y_{LAC,GLC}$, can be used as a measure of the percentage of glucose which is catabolized via glycolysis. Typically, hybridoma cells exhibit $Y_{LAC,GLC}$ of approximately 2, implying that close to 100% of the glucose is incompletely oxidized to lactate. In contrast, several investigators report $Y_{LAC,GLC}$ for CHO cell lines of only 1.1 to 1.4 under normal (usual) operating conditions (Lin *et al.*, 1993; Lin and Miller, 1992; Hayter *et al.*, 1993), implying that upto 45 % of the glucose is completely (aerobically) oxidized to carbon dioxide and water. Under glucose-limited conditions, $Y_{LAC,GLC}$ decreases significantly: Hayter's group (1993) observed yields of lactate on glucose of as low as 0.49 mol/mol, which implies that more than 75 % of the glucose consumed is completely oxidized. In support, Lin *et al.* (1993) report an increasing apparent $Y_{LAC,GLC}$ with decreasing levels of dissolved oxygen in the culture medium.

Hayter *et al.* (1993) demonstrated a decreasing glucose metabolic quotient with decreasing specific growth rate, and they calculate a Monod-type saturation constant for glucose of $59.6 \mu\text{mol L}^{-1}$. Similarly, in perfusion mode, the glucose metabolic quotient (specific uptake rate) has been shown to decrease with decreasing dilution rate (Konstantinov *et al.*, 1996). These studies support the hypothesis that glucose is utilized more efficiently as its availability is decreased.

Hayter's group (1992) observed that while limited glucose conditions did not affect the production of recombinant human interferon- γ from CHO cells, the proportion of fully glycosylated recombinant protein was decreased. Conversely, at high glucose concentrations, the specific rate of recombinant protein production was decreased, while the apparent population specific growth rate increased. Similarly, operating in perfusion mode, the overall production of a recombinant protein from CHO cells was observed to decrease with increasing glucose concentrations (Konstantinov *et al.*, 1996). This suggests that synthesis of the recombinant proteins is proportional to the length of the G1 cell cycle phase, and that post-translational modifications are negatively impacted by limited glucose concentrations.

In a further study, Hayter and co-investigators (1993) found that dilution rate in glucose limited chemostat culture varied directly with specific recombinant protein production. This would seem counter to their previous findings. However, the proportion of the population in the G1 cell cycle phase also increased with increasing dilution rate.

Ammonia

Ammonia is known to be a toxic byproduct of metabolism, as discussed above (Section 2.1). A few investigators report on the inhibition of CHO cell growth in response to elevated levels of ammonia, during batch culture. Hayter *et al.* (1991) found that growth was not inhibited by initial ammonium chloride concentrations of up to 2 mmol L⁻¹, but inhibition did occur at an initial ammonium concentration of 4.5 mmol L⁻¹. Schlaeger and Shumpp (1989) found that CHO cells are relatively insensitive to growth inhibition by ammonium, with 8 to 10 mmol L⁻¹ eliciting only a 50 % inhibitory response. Similarly, Kurano *et al.* (1990) found a 50 % reduction in the early exponential specific growth rate at an ammonium level of 8 mmol L⁻¹, which they express as a Monod-type inhibition constant. Hansen and Emborg (1994) found no effect on the cell density by ammonium levels upto 8 mmol L⁻¹. They did, however, find that the ammonium metabolic quotient, expressed as a function of the specific growth rate and the viable cell density, decreased at elevated ammonium levels in the culture medium, with a corresponding increase in the alanine metabolic quotient. They postulate that the CHO cells have a mechanism that changes the metabolism, so that less ammonium is generated during growth under high ammonium concentrations. Miller *et al.* (1988) observed the same phenomenon for a hybridoma cell line. They explain this phenomenon as a metabolic shift from use of the glutamate dehydrogenase pathway to use of the alanine aminotransferase pathway in the conversion of glutamate to 2-oxoglutarate (Miller *et al.*, 1988).

In addition to its growth inhibitory action, ammonia has been shown to play a role in the degree of glycosylation of secretory proteins. Structural changes in the oligosaccharide chain can potentially affect glycoprotein folding, solubility, biological activity, antigenicity, circulatory lifetime, and the susceptibility of glycoproteins to denaturing agents and protease attack (Borys *et al.*, 1994).

Ammonium ion concentrations in the range from 0 to 45 mmol L⁻¹ have been shown to affect *O*-linked sialylation of granulocyte colony-stimulating factor, produced in recombinant CHO cells, in a manner that was not caused by extracellular degradation of the oligosaccharides (Andersen and Goochee, 1995). Ammonia, which is a natural product of glutamine metabolism and chemical degradation, may rise upto 10 mmol L⁻¹ during a batch culture. The *O*-linked sialylation has been observed to be reduced at extracellular ammonia levels as low as 2 mmol L⁻¹ (Anderson and Goochee, 1995). This effect of ammonia on glycosylation was found to be rapid and sustained, but did not affect the secretion rate of the recombinant protein. The authors linked the effect to ammonia-induced increase in the *trans*-Golgi pH from the normal 6.5 to 6.75, upto about 7.0. The reduction in

glycosylation of recombinant proteins produced by CHO cells has been shown to be inversely correlated to the extracellular pH, over the range of 7.2 to 8.0 (Borys *et al.*, 1994), and directly correlated to the extracellular pH over the range of 6.5 to 7.0 (Borys *et al.*, 1993), when ammonia was present in the culture medium. Other weak bases mimic the impact of ammonia on the degree of glycosylation (Anderson and Goochee, 1995).

It is postulated that the unprotonated ammonia species, NH_3 , is responsible for the inhibitory effects of ammonia on animal cells. This is because the uncharged base can freely diffuse across plasma membranes, where it can impact on the intracellular pH, while the ammonium ion, NH_4^+ , can only enter the cell through ion-transport systems (Borys *et al.*, 1994). A direct linear correlation was found between the extracellular NH_3 concentration and the extracellular-pH-dependent inhibition of glycosylation (Borys *et al.*, 1994), while the extracellular pH alone was not found to correlate with the degree of glycosylation. Hence, extracellular pH can only be utilized as an indicator of potential intracellular pH levels. The measurement of extracellular ammonia concentrations is a more direct means of assessing the impact of culture medium conditions on intracellular pH levels.

In contrast to the findings of Anderson and Goochee (1995), Hansen and Emborg (1994) observed a decrease of approximately 50 % in the concentration of a recombinant protein secreted into the culture medium, at an ammonium level of 7.5 mmol L^{-1} . Hansen and Emborg suggest that the decrease in recombinant protein production could be due to a limitation of medium components, such as amino acids, rather than to a negative ammonium influence. It should be noted that the ELISA assay used to determine the concentration of the protein may be impeded by its potential structural/functional differences resulting from reduced glycosylation associated with elevated levels of ammonia.

Morphological Types

The three morphological types exhibited by CHO cells have also been the subject of a number of studies. These studies range from observational analyses of the effect of single cell suspension, anchorage dependent, and aggregate suspension morphological types on population growth and productivity; to physical and chemical methodologies of altering the morphological types.

Ruaan's group (1993) showed that population growth of anchorage dependent CHO cells was directly dependent on the size of the exposed surface area of the individual cells, and was only secondarily affected by the degree of confluence. They correlated growth factor/exposed surface area interaction to cell proliferation. They concluded that the shape that cells assume, which is dependent on the type of surface to which they adhere, influences proliferation. These findings are in agreement with Nikolai and Hu (1992), who enhanced maximum cell concentration by employing macroporous microcarrier beads as the surface for adherence.

Grinnell (1980) explored the interaction of cold insoluble globulin (CIG) (plasma fibronectin) and cell adhesion to surfaces. He utilized serum free medium in order to isolate the roles of fibronectin and bovine serum albumin (BSA) in cell adhesion to surfaces. Cells bound CIG coated 0.76 mm uncharged latex beads, but did not interact with the same beads coated with BSA instead of CIG. Adhesion occurred over a temperature range of 4 to 37 °C, and was accompanied by endocytosis of the beads at 37 °C. Grinnell also showed that CIG receptors were not detectable on the exposed surface of cells spread (attached) on a flat surface, and that CIG receptors were lost after trypsinization. The former observation suggests that CIG receptors migrate across the cell membrane to the site of interaction with surfaces. Cheung and Juliano (1984) induced surface adherence of non-adhering cells by coating beads with fibronectin, poly-L-lysine, ConA, and/or extracellular matrix. This work clearly demonstrates the role of protein ligands, as well as the cytoskeletal rearrangements involved in surface adherence of cells.

Several investigations have indicated that divalent cations, such as calcium and magnesium, play a role in cell-surface adhesion and in cell-cell adhesion. Takeichi (1974) explored the role of divalent cations in cell-surface adhesion in serum free medium. Madhusudan *et al.* (1992) demonstrated positive correlations between extracellular calcium concentration and aggregate formation rate, size, and cell packing. Packer (1990) found that retinoids, such as retinoic acid (RA) increases both the ability of cells to attach to a surface, as well as the strength of that attachment, as measured by EDTA and/or serine protease (eg. trypsin) mediated detachment.

Borys and Papoutsakis (1992) explored the phenomenon of microcarrier aggregation via cell-cell adhesion of microcarrier-adherent cells. They found that microcarrier aggregation occurred only during periods of rapid cell growth; decreased with increasing agitation intensity; decreased in the presence of 1% (v/v) serum; and decreased in the presence of 1% (v/v) dimethyl sulfoxide (DMSO). O'Connor and Papoutsakis (1992) compared agitation effects on microcarrier adherent cells CHO cells to agitation effects on (single cell?) suspension CHO cells. They attributed intense agitation damage to bulk-fluid turbulence for attachment

dependent cells, and to bubble breakup associated with vortex formation for attachment independent cells. They were also able to demonstrate that intrinsic changes in DNA synthesis accompanied cell damage.

Renner and coworkers (1993) investigated cell aggregate formation induced at sub-optimal growth conditions. Under such conditions, aggregates form around dead cell clusters. Renner's group showed that DNA released from the dead cells mediated the cell-cell adhesion, which could be prevented in the presence of DNase I. In comparison to cells in free suspension, cells within aggregates showed a strongly reduced specific proliferation rate and a greater sensitivity to shear forces, as measured by an increased specific death rate.

Chevalot *et al.* (1994) compared all three morphological types of a line of rCHO cells. In their study, microcarrier adherent cells exhibited the highest levels of proliferation rate and specific productivity of the recombinant protein (an enzyme), as well as attaining the highest maximum cell concentration. Cell aggregates and cells in free suspension had similar growth and productivity patterns, with an increased yield of ammonia on glutamine in comparison to the microcarrier adherent cells. The activity of the enzyme was not affected by the morphological type.

Cell Cycle Kinetics

Cell cycle kinetics of CHO cell populations have not been studied to a great extent. In one paper, the effect of damaging agitation rates on cell cycle phase distributions of a CHO cell population was reported (Lakhotia *et al.*, 1992). Although the viable cell fraction decreased at high agitation rates (increased cell death), the fraction of the viable cells in S phase was enhanced by as much as 50%, and the DNA synthesis rate per viable S phase cell was increased.

The relationship between foreign gene expression (recombinant protein production) and the cell cycle of the host CHO cells is beginning to be investigated. In a 1993 paper, Gu and coworkers describe the G1 cell cycle phase dependent synthesis of a recombinant protein in CHO cells. Their work shows that the physiological state associated with the G1 cell cycle phase is necessary and sufficient for synthesis of the recombinant protein: traverse around the cell cycle (proliferation) is not required for recombinant protein synthesis.

Recombinant Protein Products and the DHFR Amplification System

Currently, there are many recombinant DNA, secretory proteins produced from CHO cells in culture (Table 2.4). Even when foreign genes packaged in the most efficient transcription units, including powerful promoter and enhancer sequences, are integrated into productive regions of the genome of the chosen host, they are still rarely capable of producing useful quantities of protein (Cartwright, 1994). This is partly because the number of copies of the vector in the host genome typically remains low. Higher levels of expression can be achieved if the number of copies can be effectively increased. It has been shown that one mechanism by which animal cells acquire resistance to certain toxic substances is by increasing the copy number of (or amplifying) genes whose products tend to nullify the effects of the toxic agent (Cartwright, 1994). The rCHO cell line used in this study utilizes the dihydrofolate reductase (DHFR) amplification system.

This type of amplification uses the antimetabolic agent methotrexate (MTX) which functions by competitive inhibition of DHFR. MTX is a folic acid antagonist that binds to the active catalytic site of DHFR, interfering with the synthesis of the reduced form that accepts one-carbon units (Salmon and Sartorelli, 1985). Lack of this cofactor interrupts the synthesis of thymidylate, purine nucleotides, and the amino acids serine and methionine, thereby interfering with the formation of DNA, RNA, and protein (Figure 2.5). DHFR binds MTX extremely tightly, so that an increase in the concentration of DHFR can overcome inhibition by MTX (Salmon and Sartorelli, 1985).

This amplification system is described by Cartwright (1994) as follows: Resistance to MTX is achieved by amplification of the *dhfr* structural gene. Increasing concentrations of MTX can result in amplification of up to 1000-fold of the *dhfr* gene and, importantly, of segments of DNA exceeding 1000 bp adjacent to the *dhfr* gene which are usually amplified at the same time. Thus, great amplification of the required (product) gene can be obtained when expression vectors are used which place the gene of interest in the correct context for co-amplification with DHFR, and when selective pressure is applied.

It is particularly useful to be able to perform amplification procedures in cell lines which lack the amplifiable gene. In the presence of endogenous enzyme activity, higher levels of inhibitor are required to achieve effective amplification. There is also the possibility that amplification of the endogenous enzyme gene may occur, thereby reducing the effective amplification of the product gene.

Table 2.4: Some rCHO cell lines used to produce various glycoproteins

Cell Line Promoter Selection Vector Selection Promoter	Recombinant Protein	References
??	- human tissue kallikrein	Watson <i>et al.</i> , 1994
CHO-K1 CMV promoter neomycin resistance ??	- human gamma-glutamyl transferase	Chevalot <i>et al.</i> , 1994
CHO-K1 ?? neomycin resistance ??	- human chorionic gonadotropin B subunit	Bedows <i>et al.</i> , 1992
CHO-K1 ?? ?? ??	- mouse placental lactogen I	Borys & Papoutsakis, 1992, 1993
CHO-K1 (ATCC CCL61)	??	Papoutsakis <i>et al.</i> , 1990, 1992
CHO-K1, <i>dhfr</i> ⁻ ?? DHFR SV40 promoter	- human tissue type plasminogen activator	Lin <i>et al.</i> , 1993
CHO, <i>dhfr</i> ⁻ ?? DHFR SV40 promoter	- human gamma interferon	Croughan & Wang, 1990
??	- urinary type plasminogen activator	Avgerinos <i>et al.</i> , 1990
CHO, <i>dhfr</i> ⁻ CMV promoter DHFR SV40 promoter	- β -galactosidase	Gu <i>et al.</i> , 1993
CHO, <i>dhfr</i> ⁻ SV40 promoter DHFR SV40 promoter	- human interferon-A	Hayter <i>et al.</i> , 1993

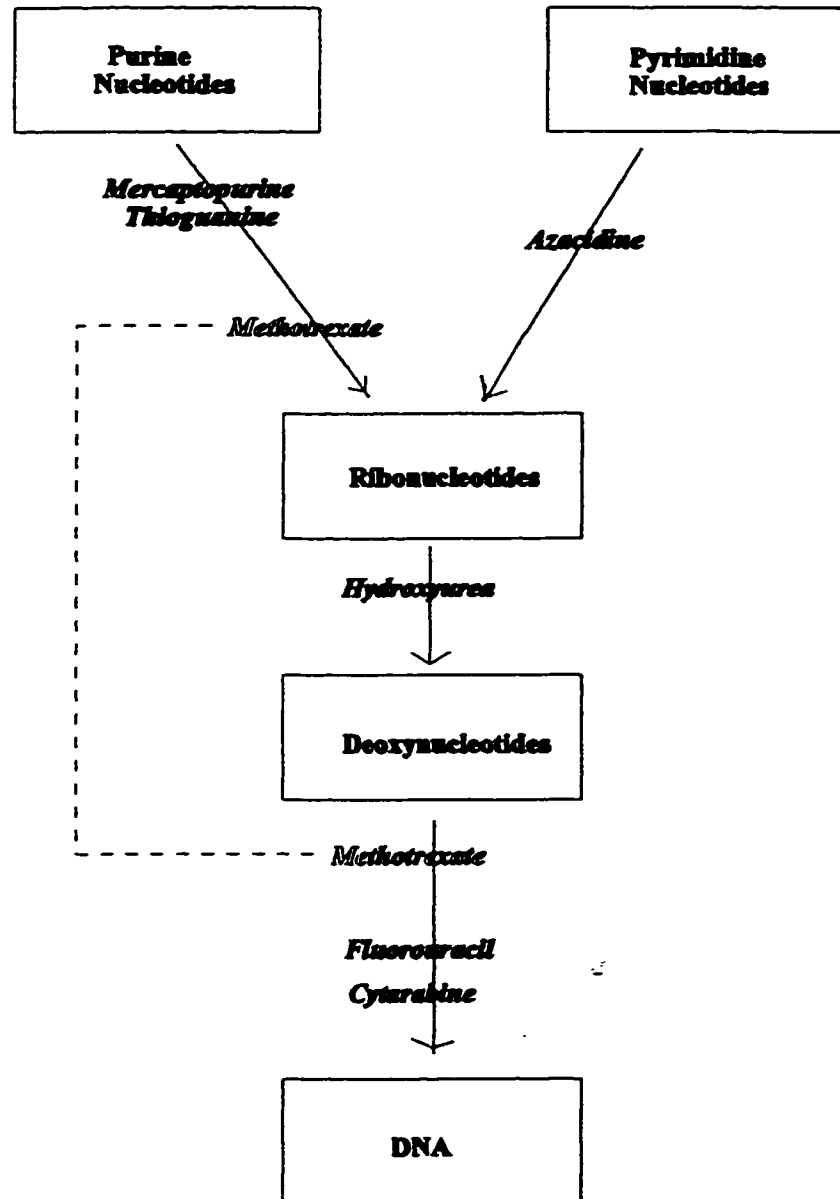


Figure 2.5: Sites of action of antimetabolites on DNA synthetic pathways.

DHFR⁻ mutants of CHO cells have been used in most systems employing DHFR amplification, including the cell line to be used in this study. An h-tPA encoding, amplifiable vector designed for use with the DHFR/MTX system is shown in Figure 2.6. The use of the DHFR⁻ mutant confers an additional benefit: *dhfr*⁻ cells will not proliferate under normal circumstances (in normal media formulations), so that continuous selection pressure ensures that only cells containing the expression vector are stable in the culture.

Intracellular content of DHFR in cultured cells in concert with the phases of the cell cycle has been investigated by several groups, who have drawn varied conclusions.

Kubbies *et al.* (1996) found that both the concentration and absolute amount of recombinant DHFR was highest in G1 phase cells. They showed that a critical threshold cell size and DHFR amount (not concentration) was required for entry into the S phase, and that although this amount of DHFR is slightly increased over the mean of the DHFR distribution in G1-phase cells, it is significantly lower than the maximum DHFR content of G1-phase cells. In agreement, it was found that after mitogen-stimulation of quiescent murine cells, endogenous *dhfr* mRNA levels increased approximately 4-fold, which closely correlated with DHFR levels, two to six hours before DNA synthesis began (Denhardt *et al.*, 1986).

In contrast, Matherly *et al.* (1989) found no cell cycle dependency of recombinant DHFR synthesis, while Mariani *et al.* (1981) demonstrated an S phase association. Endogenous *dhfr* expression was linked to the S phase in L1210 cells by Matherly's group (1989) and in CHO cells by Mariani and co-workers (1981), but was found to be independent of cell cycle phase in both a rodent (CHO) and a human cell line by Feder *et al.* (1989). Cycling-dependent accumulation of *dhfr* mRNA, with cycling cells containing 10-fold more mRNA than quiescent cells, was found in transformants that utilized either the *dhfr* or SV40 late polyadenylation signals, but not in transformants that utilized the CHO or the early SV40 signal (Denhardt *et al.*, 1986). These authors report that in contrast to the close association between continued DNA synthesis and histone mRNA transcription, *dhfr* mRNA transcription was unaffected by inhibitors of DNA synthesis (Denhardt *et al.*, 1986).

In an excellent review of the expression of DHFR and thymidylate synthase genes in mammalian cells, Johnson (1984) points out that DHFR hnRNA is present at approximately constant levels throughout the cell cycle. The levels of mRNA increase from the G1 phase throughout the S phase, with accompanying increases in the levels of the DHFR protein. This implies that *dhfr* is transcribed constitutively, but that post-transcriptional modifications are regulated. It is notable that more than 95% of the DHFR hnRNA molecule is removed during the splicing reactions leading to mature-sized DHFR mRNA. The increase in the rate of DHFR synthesis is due to an increase in the content of mature DHFR mRNA and perhaps an increase in the efficiency of translation of the message, but not due to a change in the rate of transcription (Johnson, 1984). Even assuming that

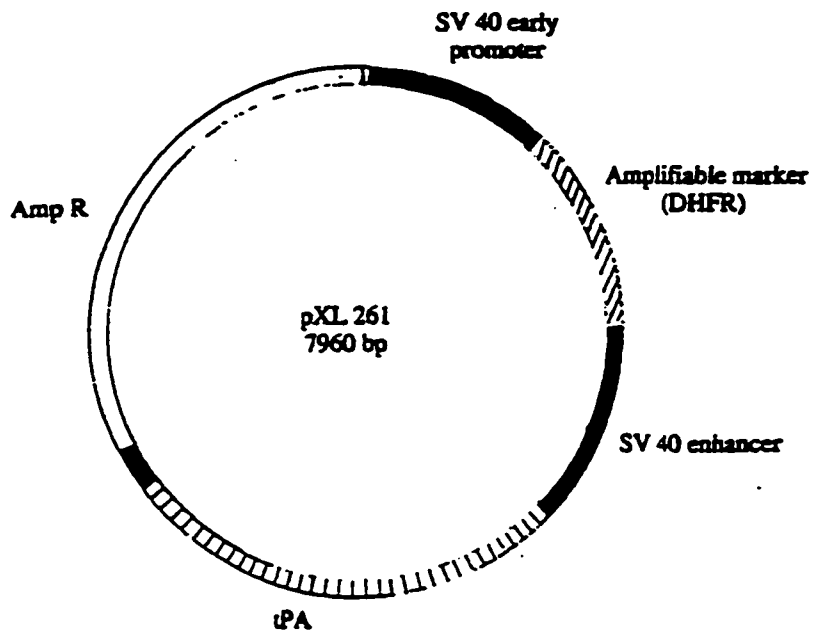


Figure 2.6 Schematic drawing of plasmid pXL 261 constructed for expression of tPA in CHO cells using DHFR as an amplifiable marker. The black segments are SV40 sequences including the SV40 early promoter, enhancer and polyadenylation sequence.

transcription of *tPA* occurs coincidentally with transcription of *dhfr*, there is no reason to suppose post-transcriptional modifications of the two hnRNA molecules are under the same control mechanisms; let alone subsequent translation of the mature mRNA molecules.

When the gene of a protein such as tPA is co-transfected with *dhfr* into a DHFR-negative host, and methotrexate selective pressure is applied, both genes are inserted as stable constructs into various chromosomal regions (Kubbies and Stockinger, 1990). In a study involving recombinant *dhfr* and *tPA*, under control of the AMLP promoter and the SV40 promoter, respectively, these authors found that CHO cells increase their cellular DHFR levels maximally prior to S phase, in accordance with the normal regulation during the cell cycle, and that DHFR levels continue to increase in the cell throughout the S phase (Kubbies and Stockinger, 1990). In contrast, it was found that the rate of increase of tPA titer in the culture supernatant rose continuously from G1 to early S, reaching a maximum during late S and decreasing in G2/M. The authors point out that two different cellular events were measured during the study: DHFR synthesis and intracellular accumulation; and tPA secretion. The exit of correctly folded and assembled proteins from the endoplasmic reticulum is the rate limiting step in the appearance of secreted proteins outside of the cell (Freedman *et al.*, 1995). Moreover, secretion itself may be a cell cycle dependent process (Gu *et al.*, 1993). It is therefore quite possible that tPA is co-synthesized with DHFR, primarily during the G1 phase.

2.3 Modeling Growth and Production Kinetics

A model is any representation of a real system, and may deal with the structure and/or function of the real system. Because no model can totally represent the real system in every detail, it must always involve varying degrees of simplification or abstraction. Models and other analogies have always played an important role in the thinking of scientists. The use of models is such a fundamental part of human thinking that we are usually unconscious of the important difference between models and the real systems. The difference becomes quite clear if we become lost in the woods or in a city, for then we are faced bluntly with the failure of our conceptual model of location and its lack of conformity with the real system.

Currently, biology has a greater potential for mathematical development than other sciences (Keen and Spain, 1992). Living systems are made up of interacting chemical and physical processes, all of which can be described in mathematical terms. However, these systems are so immensely complex that they have resisted mathematical analysis by the classical methods successfully used by chemists, physicists, and engineers. Only within the last four decades have analysts of biological systems had the benefit of digital computers to begin to deal with these complex systems.

The first step to the modeling of any system is the development of a concept of the system. This conceptual model is a representation of the system in words or pictures. It may involve how a structure or function arises (mechanistic), or merely the structure or function itself (phenomonologic) (Karim and Stephanopoulos, 1992). Conceptual models, by themselves, are generally lacking in rigor. They can be imprecise and open to interpretation. Hence, the conceptual model should be given a more precise form that is unambiguous and can be evaluated and validated. One form of model that provides these advantages is the mathematical model.

A mathematical model of a biological system may be as simple as a single equation relating one variable to another, or it may be a multicomponent model involving the interaction of many equations having several mutually dependent variables (Keen and Spain, 1992). A mathematical model results from a formalization of the conceptual model in quantitative terms, usually as equations describing the response of a system to some variable such as time or temperature. The thinking required to formulate the mathematical model generally improves the conceptual model.

Most mathematical models are can be derived in a straightforward way from conceptual models, or can be obtained empirically from statistical analysis of experimental data. Hall and Day (1977) refer to these two approaches as "mechanistic" and "descriptive". Purely descriptive empirical models (unstructured models) disregard intracellular processes, while completely detailed structured models are based on a thorough comprehension of cell metabolism (Portner and Schafer, 1996). The latter is, by its nature, applicable to a large range of different growth conditions while the former can only be employed for the very process conditions and data range it was derived from (Portner and Schafer, 1996). Many of the mammalian cell models that have been developed lie between these two extremes, and are partially structured in terms of the major inputs and outputs of the metabolite pool, so that the system is seen as a 'gray' box.

Currently, mammalian cell modeling is frustrated by the limited understanding of cell metabolism and its response to varying growth conditions. The majority of correlations for growth kinetics are based on Monod-type equations, with glucose and/or glutamine taking the role of limiting substrates. Some Monod-type models have been extended to include ammonia and lactate as inhibiting species (Miller *et al.*, 1988; Frame and Hu, 1991a,b; Glacken *et al.*, 1988). Attempts have been made to set up structured kinetic frameworks (Batt and Kompalla, 1989; Barford *et al.*, 1992),

but the majority of the parameters must be estimated via recourse to the limited body of knowledge of metabolism. Thus the majority of mammalian cell models are unstructured (Portner and Schafer, 1996). In addition to structure, mammalian cell models can be segregated into subsets of the viable population. To date, such partitioning has been attempted on the basis of the different physiological states associated with the phases of the cell cycle and quiescence and senescence (apoptosis and necrosis) (Lakhotia *et al.*, 1992). Such models are highly complex, with multiple equations and parameters. Frequently, many of the parameters for these models are not measured experimentally, or are deduced from abnormal culture conditions such as chemically synchronized cell populations. The sheer magnitude of complexity of these models coupled with a limited understanding of the metabolic, epigenetic and genetic processes of transformed and genetically engineered populations of mammalian cells limits their usefulness. Compared to chemical and mechanical systems, the intricate biological ones are capable of compensating for minor changes in environment, for instance by adaptation of metabolism (Portner and Schafer, 1996). This may work to confound highly detailed structured and segregated models which have been developed from an imperfect understanding of the system.

The non-segregated, unstructured or partially structured models usually follow the kinetics of substrates and metabolites, population growth, and protein product accumulation. Correlations for specific substrate uptake rates usually follow the maintenance energy model of Pirt (1975):

$$q_s = \frac{1}{Y_{x,s}} \mu + m \quad (2.10)$$

where: $Y_{x,s}$ is the yield of cells on substrate
 μ is the specific growth rate
 and m is the maintenance term

Population growth is normally depicted as proportional to the apparent growth rate, with terms sometimes added for cell death and cell lysis in order to follow the entire growth curve of a batch culture.

Specific productivity, which is often partially-growth-associated, is frequently given the same general form as substrate utilization, with a term for growth-association and a term for non-growth-association:

$$\frac{dP}{dt} = \alpha \mu X_v + \beta X_v \quad (2.11)$$

where α is the extent of growth-association (mass Protein/cell)
 β is the extent of non-growth-association (mass Protein/cell/time⁻¹)
 and X_v is the viable cell concentration

In cases where protein production is non-growth-phase-associated, and therefore non-growth-associated (Dutton *et al.*, 1998), the equation reduces to a single term which can then be expressed in units compatible with the epigenetic time domain.

The third step in model development is validation. The process of simulation expands the power of the quantitative research loop by using the mathematical model to generate simulation data which may be compared to real data to evaluate the differences. The fine tuning of a simulation can produce further improvements in both the conceptual model and the mathematical model. Simulation provides another important benefit: it allows "experiments" on system models that lie outside the range of normal possibility. This is especially valuable to the engineer, who is interested in the manipulation of the biological system: It allows us to ask questions about "what would happen to the system if ..." (Keen and Spain, 1992).

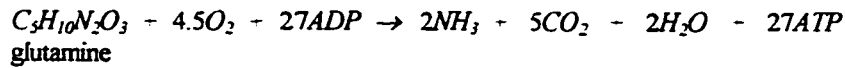
The degree of complexity/detail incorporated into a model depends upon its intended use, and how closely it must approximate the real system. While a correlation involving only one or two parameters may be unable to yield more than a general correspondence with the behavior of the real system, it is also possible to make a simulation so complex that it contributes little or nothing to the understanding of the system being modeled: The major factors that control the system may be hidden if the model is overly complex (Keen and Spain, 1992). It must be understood that any biological system must always remain to some extent a "black box" (Keen and Spain, 1992). No matter how much information we have about a particular biological entity, we must always remain on the outside looking in.

A Partially Structured, Metabolic Model

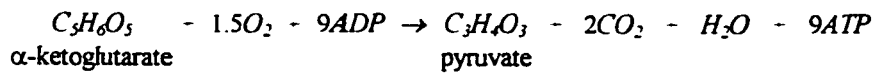
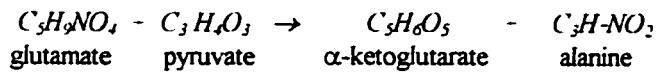
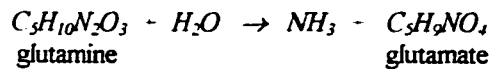
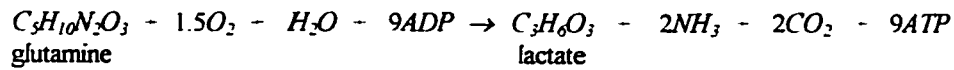
A partially structured, metabolic model for hybridoma growth and MAb production which was developed in this laboratory (Phillips, 1991), was used to form the basis of rCHO model development in this study. The Phillip's model (PM) is partially structured with respect to the substrate utilization kinetics, according to the simplified mammalian cell metabolism depicted in Figure 2.1. The model assumes glutamine and glucose are the only major substrates used by the hybridoma population. The substrate utilization is balanced by population growth and MAb production, with incidental metabolite byproduct. The metabolites represented in the model include lactate, ammonia, and alanine. Thus, the modeling of substrate utilization is based on the main tenet of metabolism: catabolic processes are exactly energetically balanced by anabolic processes. The balance is made on the basis of ATP equivalents (abbreviated as ATP) from the following stoichiometric equations:

1. Glutamine Catabolism:

1.1 Complete Oxidation:



1.2 Partial Oxidation:



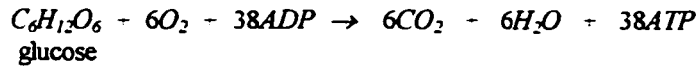
1.3 Rate of ATP formation from glutamine:

The rate of ATP formation depends on the fraction of glutamine which follows each of the pathways depicted above. If f_1 is the fraction of glutamine completely oxidized to carbon dioxide and water, then $(1 - f_1)$ is the fraction of glutamine catabolized via partially oxidative pathways to alanine or lactate:

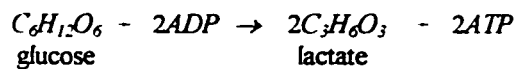
$$\frac{d[ATP]_{GLN}}{dt} = -(9 + 18f_1) \frac{dGLN}{dt} \quad (2.12)$$

2. Glucose Catabolism:

2.1 Complete Oxidation:



2.2 Reduction:



2.3 Rate of ATP formation from glucose:

If f_2 is the fraction of glucose catabolized aerobically to carbon dioxide and water, then $(1 - f_2)$ is the fraction of glucose catabolized anaerobically to lactate:

$$\frac{d[ATP]_{GLC}}{dt} = -(2 + 36f_1) \frac{dGLC}{dt} \quad (2.13)$$

3. ATP demand (Anabolic Pathways):

The ATP demand is represented in the model by a variation of Pirt's (1975) unstructured expression (equation 2.9, see page 20), as developed by Kilburn *et al.* (1969):

$$\frac{d[ATP]_{TOT}}{dt} = A\mu X_t + BX_v \quad (2.14)$$

where

- A is the specific biosynthetic energy rate (moles ATP/cell)
- B is the specific maintenance energy rate (moles ATP/cell/time)
- μ is the specific growth rate (time^{-1})
- X_t is the total cell concentration (cells/volume)

and

- X_v is the viable cell concentration (cells/volume)

The specific maintenance energy rate is a lumped parameter, inclusive of energy utilization for growth, protein production, and all other cellular processes.

The ATP consumption and production balance is completed by combining equations 2.12, 2.13, and 2.14:

$$A\mu X_v + BX_v = -(9 + 18f_1) \frac{dGLN}{dt} - (2 + 36f_2) \frac{dGLC}{dt} \quad (2.15)$$

Phillip's model accounts for the interaction between glucose and glutamine metabolism (mutual competition between the two substrates) by defining a preferential utilization term:

$$\frac{dGLN}{dt} = G_s \frac{GLC}{GLN} \frac{dGLC}{dt} \quad (2.16)$$

where G_s is the substrate preference index
 and GLC is the concentration of glucose (mmol/volume)
 GLN is the concentration of glutamine (mmol/volume)

Substitution of equation 2.16 into equation 2.15 yields the final form of the partially structured equation describing substrate utilization:

$$-(A\mu(X_v + X_d) + BX_v) = (9 + 18f_1) \frac{dGLN}{dt} + \frac{1}{G_s} \frac{GLC}{GLN} (2 + 36f_2) \frac{dGLN}{dt} \quad (2.17)$$

Phillip's model consists of a conservative six equations and eight parameters. Population growth is expressed by the following two equations:

Accumulation of Viable Population:

$$\frac{dX_v}{dt} = (\mu - k_d) X_v \quad (PM-1)$$

where k_d is the apparent specific death rate (time⁻¹)

Accumulation of Dead Population:

$$\frac{dX_d}{dt} = k_d X_v - k_l X_d \quad (\text{PM-2})$$

where k_l is the specific rate of cell lysis (time^{-1})
and X_d is the dead cell population

The simple kinetic unstructured model developed by Miller *et al.* (1988) was employed to describe the accumulation of partially-growth-associated secretory protein:

Accumulation of Protein Product:

$$\frac{dP}{dt} = \alpha X_v + \beta \mu X_v \quad (\text{PM-3})$$

where α is the extent of non-growth-association (mass protein/cell)
and β is the extent of growth-association (mass protein / time/cell)

The values of the non-growth-association term and the growth-association term are determined from the slopes of a plot of the cumulative product concentration against the viability index (VI), as formulated by Luan *et al.* (1987):

$$\Delta P = (\alpha + \beta \mu) VI ; \quad (\text{PM-4})$$

$$\text{where } VI = \int_0^t X_v dt \quad (2.18)$$

where t is the culture time

The consumption of glutamine and glucose are followed explicitly from rearrangements of equation 2.17, and including the chemical degradation of glutamine:

Glutamine Consumption:

$$\frac{dGLN}{dt} = - \left[\frac{G_s GLN X_v (A\mu + B)}{G_s GLN(9 + 18f_1) + GLC(2 + 36f_2)} \right] - k_{GLN} GLN \quad (\text{PM-5})$$

where k_{GLN} is the glutamine chemical degradation constant (time^{-1})

Glucose Consumption:

$$\frac{dGLC}{dt} = -\frac{1}{G_S} \frac{GLC}{GLN} \left[\frac{G_S GLN X_V (A\mu + B)}{G_S GLN(9 + 18f_1) + GLC(2 + 36f_2)} \right] \quad \text{(PM-6)}$$

Phillip's model is a good compromise between the unwieldy complexity of multiple equations and parameters, and the overly simplistic purely phenomenological models. It was used successfully to simulate hybridoma batch growth, substrate, and production kinetics with six of the eight parameters either measured experimentally or calculated from direct measurements and only two of the parameters estimated from published data (Phillips 1991). In the current study, observed population averaged metabolic patterns were used to adapt the Phillip's model for the description of the growth, metabolism, and production kinetics of a recombinant Chinese Hamster Ovary cell line.

3. MATERIALS AND METHODS

3.1 Cell Lines and Maintenance

The cell line used in this investigation was a Chinese Hamster Ovary (CHO) cell producing recombinant human tissue type plasminogen activator (tPA), via the DHFR vector and amplification system, developed by Genentech Inc. (US patent 4,766,075 1988). Briefly, a p342E 3500 bp vector was ligated with three tPA encoding fragments comprising approximately 2160 bp. A plasmid containing all of the base pairs in the correct sequence was isolated, characterized, and designated pE342-tPA. The plasmid pEHER, which expresses mutant dihydrofolate reductase (DHFR) was digested with SacII, and a resulting approximately 1700 bp fragment coding for DHFR and for DHFR expression control sequences, was ligated into the pE342-tPA plasmid to create pETPAER400. This plasmid is analogous to pEHER except that the HBsAg coding region has been replaced by the cDNA sequences from human tPA. The pETPAER400 plasmid was transfected into *dhfr*⁻ CHO-DUX B11 cells. Transfected *dhfr*⁺ cells were selected by growth in glycine, hypoxanthine, and thymidine deficient medium. The cell line was then amplified initially in 50 nM MTX, and then further amplified in 500 nM MTX, to yield a stable cell line that produces amounts of t-PA greater than 1 µg/million cells/d.

This rCHO cell line was named CHO1-5₅₀₀ and deposited with the American Tissue Culture Collection (ATCC # CRL 9606). Genentech currently produces tPA from a cell line resulting from further amplification with MTX, yielding tPA production levels approaching 100 µg/million cells/d, but a trade off exists between tPA productivity and cell culture parameters, including increased doubling time and increased fragility (which may prevent efficient cell growth in stirred fermentors). The h-tPA produced from these cell lines exhibits no detectable immunogenicity, and is therefore surmised to be identical in structure to naturally occurring h-tPA.

For comparative purposes (see Section 4.1.1), the robust M4-1 hybridoma cell line (courtesy of Center for Infectious Diseases, Ottawa) was also used in this study. This hybridoma produces low levels of an IgG₁ type antibody against bovine light chain IgG.

The rCHO cell line was propagated as an adherent monolayer on 225 cm² T-flasks, in Ham's F12 basal medium containing 10% FBS and 50 IU/L penicillin and 50 mg/L streptomycin, and under 5% CO₂, at 37 °C, for 14 days (approximately 20 population doublings). The M4-1 hybridoma cell line was propagated as a static suspension in 175 cm² T-Flasks, in MEM supplemented with 1.5 g L⁻¹ glucose to make an initial glucose concentration of 2.5 g L⁻¹, 10% horse serum, 4.77 g L⁻¹ HEPES buffer, 0.5 g L⁻¹ sodium bicarbonate, 50 mg L⁻¹ pyruvate, and 50 IU/L penicillin and 50 mg/L streptomycin. Both propagated cell populations were then frozen down as aliquots of 1.0 X 10⁶ cells, in serum containing 7% (CHO cells) to 10% (hybridoma cells) DMSO. Aliquots of both cell lines were stored in the vapour phase of a liquid nitrogen dewar for use as the seed culture for the experiments.

Inocula for experiments were prepared from seed culture in T-flasks as described above, and were propagated for between 10 and 20 population doublings.

3.2 Medium Preparation

HAM's F12 medium (Sigma Chemical Co., St. Louis MO) was used as the basal medium for preparation of rCHO inocula. This basal medium was supplemented with glutamine (ICN Biomedicals Inc., Costa Mesa CA), HEPES buffer (Sigma Chemical Co., St. Louis, MO); and sodium bicarbonate (Sigma Chemical Co., St. Louis, MO). The combined dry chemicals were dissolved in distilled and deionized, 18 MOhm-cm, water, pH adjusted to 7.2 - 7.4 with saturated NaOH, sterilised by means of filtration through a 0.22 µm membrane, and stored for up to 2 weeks at 4 °C. The basal medium was further supplemented for propagation of inocula with 50 IU/L penicillin and 50 mg/L streptomycin (ICN Biomedicals, Costa Mesa CA), and 10% (v/v) foetal bovine serum (Flow Laboratories, Virginia).

HB-CHO serum free medium (Irvine Scientific, Santa Ana CA; Immucor, Edmonton AB) was used as the growth medium for the majority of the rCHO experiments. This basal medium was supplemented with HEPES buffer (Sigma Chemical Co., St. Louis, MO), and sodium bicarbonate (Sigma Chemical Co., St. Louis, MO). The combined dry chemicals were dissolved in distilled and deionized, 18 MOhm-cm, water, pH adjusted to 7.2 - 7.4 with saturated NaOH, sterilised by means of filtration through a 0.22 µm membrane, and stored for up to 2 weeks at 4 °C. The basal

medium was further supplemented for propagation of cells with 50 IU/L penicillin and 50 mg/L streptomycin, various concentrations of glutamine, and 10 mL/L HB-CHO supplement.

MEM basal medium (Flow Laboratories Inc., Virginia) was used in the M4-1 hybridoma experiments. It was supplemented as described above using the same preparation procedure as described for Ham's F12 medium. The horse serum was obtained Whittaker BioProducts Inc. (Walkersville MD). Glucose and pyruvate were obtained from Sigma Chemical Co. (St. Louis MO).

For the studies of medium component initial concentration effects, glucose free DMEM (Sigma Chemical Co., St. Louis MO) was supplemented with amino acids and other components as listed in Table 3.1. Glucose, glutamine, asparagine, lactate (Sigma Chemical Co., St. Louis MO), and serum (Flow Laboratories, Virginia) were added at various concentrations for experimental purposes.

3.3 Culture Systems

Cells were propagated as aggregate suspensions, adherent on bioreactor surface or on microcarriers, and as dispersed suspensions in two bioreactor configurations. Static cultures were performed in 25 cm², 175 cm², and 225 cm² T-flasks. Mechanically agitated bioreactors were represented by 250 mL (100 mL working volume) and 2000 mL (1000 mL working volume) spinner flasks operating at 60 rpm, 100 rpm, or 150 rpm. T-flasks and spinner flasks were housed in a 37 °C, 95% humidity incubator, supplied with 5% CO₂ in air. An adequate supply of oxygen was introduced to the system by headspace aeration, as determined by Glacken and his colleagues (1983). The stirred bioreactors have a height to diameter aspect ratio of 1.5. Sample ports are located at the top of the bioreactors.

The inoculum concentration ranged from 0.1 E6 cells/mL to 0.4 E6 cells/mL, and was charged into 100% fresh pre-warmed and gassed medium. In order to reduce foaming, caused by the presence of BSA and other proteins in the medium, 20% silicone antifoam emulsion AF72 in sterile water (General Electric Silicone Products Division, Waterford, NY) was added dropwise as required. Bioreactors were sterilised in an autoclave at 121 °C for 1 hour, prior to use. Apart from the HEPES and bicarbonate-CO₂ buffering systems, no additional pH control was employed.

Table 3.1: Basal medium formulation for initial substrate concentration experiments

Component	g/L (or mL, as indicated)
Basal Medium:	
glucose free DMEM basal powder	8.3000
calcium chloride	0.0200
magnesium chloride · 6H ₂ O	0.0300
sodium phosphate dibasic	0.0400
L-arginine · HCl	0.1000
L-cysteine · HCl	0.0250
L-proline	0.0200
pyruvic acid	0.1100
HEPES buffer	4.0000
sodium bicarbonate	2.0000
RSNM - 100X	10 (mL)
RFNM - 1000X	1 (mL)
MEM - 100X*	10 (mL)
RSNM - 100X:	
vitamin B ₁₂	0.1360
hypoxanthine	0.4080
phenol red · Na	0.1300
putrescine dihydrochloride	0.0161
RFNM - 1000X:	
cupric sulfate · 5H ₂ O	0.0025
ferrous sulfate · 7H ₂ O	0.7000
zinc sulfate · 7H ₂ O	0.8630
D - biotin	0.0073
linoleic acid	0.0840
thioctic acid	0.2100
thymidine	0.7300

* MEM - 100X : non-essential amino acids for MEM Eagle (ICN Biomedicals Inc., Costa Mesa CA)

3.4 Assays

Cell Number

Protein ligands adhering cells onto substrata were degraded with 25 mg/mL of the serine protease porcine trypsin in PBS (Sigma Chemical Co., St. Louis MO). Aggregated cells were disrupted with a citric acid/TritonX-100 mixture, to form a whole nuclei suspension.

Suspended cell numbers were then determined by haemocytometer or using an electronic particle counter (Electrozone/Celloscope, Particle Data Inc.), having a 100 μ m aperture. A 0.5 mL sample was diluted with 9.5 mL of isotone and counted four times. The resulting counts were averaged and multiplied by 40 to correct for the dilution as well as the sample size counted. Particle counter results were repeatable to \pm 3%.

Alternatively and/or additionally, a whole nuclei suspension was prepared from culture broths. Culture broths were centrifuged at 2000 xg for 10 minutes. Cell pellets were then resuspended in 1 M citric acid in 1% Tween 20 containing 0.1% crystal violet and 0.1% TritonX-100, and this suspension was incubated at 37 °C for 30 minutes. All chemicals were obtained from Sigma Chemical Co. (St. Louis MO). Whole nuclei released from the lysed cells were then counted on a haemocytometer. It was not possible to determine viability of whole nuclei suspensions. Whole nuclei counts were repeatable to \pm 12%.

Viability

Cell viability was determined using the Trypan Blue Exclusion Test (Phillips, 1973). The cells were counted on five fields of a haemocytometer. The counts were carried out within one minute of dye addition to ensure that only the dead cells stained blue. Only dark staining cells were considered nonviable. It was noted that the suspended viable CHO cells were highly luminescent when viewed under the light microscope. Counts of luminescent to non-luminescent cells correlated precisely to non-stained to darkly stained cells (Trypan Blue Exclusion Test). This method of determination of viability was used in conjunction with the Trypan Blue Exclusion Test. Haemocytometer percent viability determinations were repeatable to \pm 2%.

Cell Number per Bead

Adherent cells were separated from beads via incubation in trypsin. The number of beads per unit volume and the number of cells per unit volume were then counted on a haemocytometer. Haemocytometer counts were repeatable to \pm 10%.

Medium pH

Medium pH was determined on culture broth which was isolated from the atmosphere and within 10 minutes of sampling, using an Orion Research digital pH/millivolt meter 611 (Orion Research Co., Boston, MA) with a combination pH electrode. pH measurements were repeatable to ± 0.03 pH units.

Glucose

Glucose was determined using a hexokinase assay, Sigma Cat. No. 115-5 (Sigma Chemical Co., St. Louis, MO). This is based on using hexokinase and glucose-6-phosphate dehydrogenase in a coupled reaction with the reduction of iodinitrotetrazolium to produce a coloured compound which is read spectrophotometrically at 520 nm (Spectronic Genesys 5, Milton Roy Co., Rochester NY). Sample concentrations are determined against a standard curve which was made by serial dilution of pure glucose (Sigma Chemical Co., St. Louis MO), using the standard curve application of the Spectronic Genesys 5 (Application II SoftCard, Milton Roy Co., Rochester NY). The assay is accurate to within 4% over the range of 0.025 g/L to 5 g/L glucose. A typical standard curve is illustrated in Appendix D.

Lactate

Lactic acid was determined using a Lactate Dehydrogenase assay Sigma Cat. No. 826 UV (Sigma Chemical Co., St. Louis, MO). This test is based on the conversion of L-lactate to pyruvate by lactate dehydrogenase, resulting in the reduction of an equivalent amount of NAD. The lactate concentration is proportional to an increase in the absorbance reading at 340 nm (Spectronic Genesys 5, Milton Roy Co., Rochester NY). Sample concentrations are determined against a standard curve which was made by serial dilution of pure glucose (Sigma Chemical Co., St. Louis MO), using the standard curve application of the Spectronic Genesys 5 (Application II SoftCard, Milton Roy Co., Rochester NY). The assay is accurate to within 4% over the range of 0.02 g/L to 3 g/L lactate. A typical standard curve is illustrated in Appendix D.

Ammonia

Ammonia was measured using a quantitative enzymatic determination at 340 nm: Sigma Procedure 170-UV (Sigma Chemical Co., St. Louis, MO). This test is based on reductive amination of 2-oxoglutarate using glutamate dehydrogenase and reduced NAD(NADH). The decrease in absorbance at 340 nm due to the oxidation of NADH is proportional to the ammonia concentration.

Amino Acids

Glutamine and alanine were measured using an OPA-precursor derivatization method (Ashman and Bosserhoff, 1985) and separation on a 3.9 mm by 30 cm C18-reversed phase HPLC (Waters, Millipore Corporation, Milford, MA), as described in detail by Berne *et al.* (1994). Samples were diluted in HPLC grade water saturated with chloroform, and 25 μ L aliquots of the derivitized amino acid mixtures (samples) were automatically injected onto the C18 column (Waters 717plus AutoSampler, Waters, Millipore Corporation, Milford MA). The derivitized amino acids were then separated via gradient elution from the C18 column with 75% methanol containing 3% tetrahydrofuran (Waters 600E System Controller Multisolvent Delivery System, Waters, Millipore Corporation, Milford MA). The blue fluorescence of the eluted peaks was detected (Waters 470 Scanning Fluorescence Detector, Waters, Millipore Corporation, Milford MA), and compared with standard peaks from glutamine, alanine, and amino acid mixtures, using the Millennium 2010 Chromatography Manager Software package (Waters, Millipore Corporation, Milford MA). The pure amino acids for standard curves were obtained from Sigma Chemical Co. (St. Louis MO). Glutamine and alanine are quantified as the integral of their respective peaks. Critical parameters for integration optimization are threshold and peak width. Eight other amino acids were measured incidentally, as they are eluted before alanine: aspartic acid, glutamic acid, asparagine, serine, arginine, glycine, threonine, and tyrosine. The detection limit was 1 picomole. A typical set of calibration data is shown in Appendix D.

Extracellular tPA

Single chain tPA concentration was measured via a modified Chromozym t-PA spectrophometric assay (Boehringer Mannheim). The assay has been modified to a micro assay. Chromozym-tPA (trademark) is cleaved by tPA to yield the chromophore 4-nitraniline which is detected at 405 nm (Microplate EL308 Reader, Bio-Tek Instruments). The absorbance is calibrated to a standard curve using pure tPA (Sigma Chemical Co., St. Louis) (Appendix D). Results for serum-free samples were accurate to $\pm 5\%$, while serum-containing samples were less accurate at $\pm 12\%$.

The activity of tPA was confirmed by the ability to dissolve a standard fibrin clot containing plasminogen, as monitored by a piezoelectric based method (Hayward *et al.*, 1998).

Monoclonal Antibody

The anti bovine light chain IgG was quantitated using a competitive ELISA (Enzyme Linked ImmunoSorbent Assay). A modified version of the competitive ELISA assay originally described by Bosworth *et al.* (1983) was used. Absorbance values were converted to antibody concentrations from a calibration curve generated by a multivariable least squares procedure as developed and described by Hayward *et al.* (1991). A typical calibration curve is presented in Appendix D. Replicates were within $\pm 5\%$.

LDH

Extracellular lactate dehydrogenase was quantitated using a Lactate Dehydrogenase assay Sigma Kit. Based on the same test as for the determination of lactate, the rate of oxidation of NADH is directly proportional to lactate dehydrogenase activity in the sample. In this case, the pyruvate substrate and the coenzyme NADH are added to the sample, but no LDH. In the determination of lactate, on the other hand, NAD and LDH, but no substrate, are added to the sample. Accuracy was approximately $\pm 10\%$.

Extracellular Total Protein

Extracellular total protein concentrations were determined by the Bradford dye-binding method (Bradford, 1976). The dye reagent was made by dissolving 0.1 g of Coomassie blue dye (Pierce Chemical Co.) in 50 mL of ethanol and adding 100 mL of concentrated phosphoric acid (Fisher Chemical, Fair Lawn NJ). This concentrate was made up to 1000 mL with deionized water and filtered through a Whatman #1 filter.

Samples were analyzed as follows: 100 μL of sample was combined with 1 mL of dye reagent and mixed by gentle vortexing. After 5 minutes, absorbance was measured at 595 nm (Spectronic Genesys 5, Milton Roy Co., Rochester NY). Protein concentration was estimated from a haemoglobin (Sigma Chemical Co., St. Louis MO) standard curve. Samples were diluted as necessary with water to ensure that absorbance was always in the linear portion of the standard curve (0.025 to 0.250 mg/mL haemoglobin).

Relative Cell Size and Relative Cell Density

Relative individual cell size and relative individual cell density were measured as the degree of forward scatter and side scatter, respectively, on a tri-filter channel flow cytometer (EPICS XL-MCL, with System II Software, Coulter Corporation, Miami FL). Samples prepared for measurement of DNA content (see below) were injected into the flow cytometer within 45 minutes of sampling.

Relative Specific DNA and RNA Content (Cell Cycle Phase)

DNA and RNA content per cell was determined from an Acridine Orange staining method (Darzynkiewicz, 1994). Samples of dispersed suspension cells were enriched by centrifugation at 2000 xg and decantation of supernatant, or diluted with basal medium as necessary to attain a concentration of approximately 1.0×10^6 cells/mL, and then placed on ice. Cell and nuclear membranes were permeabilized by adding 0.4 mL of ice cold 0.1% (v/v) Triton X-100 solution to 0.2 aliquots of sample and incubating on ice for 30 seconds. The DNA and RNA was then stained immediately by adding 1.2 mL of ice-cold 20 μ M Acridine Orange solution. Acridine orange was excited with the 488 nm line from a 5 W argon ion laser (Coherent, Palo Alto CA) at 400 mW, within 2 to 10 minutes of staining. Fluorescence emission at 520 nm from DNA, and at 640 nm from RNA, was detected by passing the excited samples through the bandpass filters of a tri-channel flow cytometer (EPICS XL-MCL, with System II Software, Coulter Corporation, Miami FL). Mean fluorescence intensities were calculated from 256 channel integrated linear fluorescence histograms. The percentage of the population within each of the G1/G0, S, G2/M, and A phases was calculated from the proportion of the sample having relative DNA associated fluorescence (emission at 520 nm) of 1, > 1 but < 2 , 2, and < 1 , respectively (Milner *et al.*, 1996). The data was fitted to Gaussian distributions for the A, G1/G0, and G2/M phases, and to an extended polynomial for the S phase (Multicycle DNA analysis Software, Coulter Corporation, Miami FL).

Intracellular DHFR Content

DHFR content of individual cells was measured by an adaptation of the methods of Kaufman *et al.* (1978) and Assaraf *et al.* (1989). Samples of dispersed suspension cells were enriched by centrifugation at 2000 xg and decantation of supernatant, or diluted with basal medium as necessary to attain a concentration of approximately 1.0×10^6 cells/mL, and then placed on ice. Cell and nuclear membranes were permeabilized by adding 0.4 mL of ice cold 0.1% (v/v) Triton X-100 solution to 0.2 aliquots of sample, and incubating on ice for 30 seconds. The DHFR was then stained immediately by adding MTX ligated to the fluorochrome fluorescein (F-MTX) (Molecular Probes Inc., Eugene OR), and incubating on ice for 2 minutes. The cells were washed three times with basal medium to remove unbound F-MTX via centrifugation at 2000 xg and decanting the supernatant, then adding the same volume of basal medium and mixing by gentle vortexing. F-MTX was excited with the 488 nm line from a 5 W argon ion laser (Coherent, Palo Alto CA) at 400 mW, within 20 to 30 minutes of staining. Fluorescence emission at 520 nm was detected by passing the excited samples through the bandpass filters of a tri-channel flow cytometer (EPICS XL-MCL, with System II Software, Coulter Corporation, Miami FL). Mean fluorescence intensities were calculated from 256 channel integrated linear fluorescence histograms. Relative DHFR content was assessed qualitatively from fluorescence peak heights and widths.

SEM Sample Preparation

Samples were prepared for scanning electron microscopy as follows. Cell pellets were obtained by centrifugation at 2000 xg. Cells were washed three times with PBS and were then fixed with 2.5% glutaraldehyde for 3 hours. Cells were then washed three times with PBS and incubated in PBS at 4 °C for 1 hour. Cells were then dehydrated sequentially in acetone: 20% acetone for 5 minutes, 50% acetone for 5 minutes, 70% acetone for 10 minutes, and 100% acetone for 10 minutes. Fixed and dehydrated samples were mounted on stubs and coated with gold and were then observed and photographed on the scanning electron microscope.

4. Results and Discussion

4.1 Population Growth and Recombinant tPA Production

4.1.1 The Biological Capacity for Production

Growth and productivity patterns in batch culture are usually represented in graphical form by the viable cell concentration and product titer plotted as functions of the culture time. As discussed in Section 2.1, the majority of published animal cell culture data pertains to hybridomas. Methodologies for depicting growth and productivity were therefore assessed initially for the M4-1 hybridoma cell line producing α -bovine-light-chain-IgG monoclonal antibody. This cell line was propagated as a dispersed suspension static batch culture (100 mL T-flask), with MEM medium containing 10 % horse serum. The rCHO cell line was then assessed, and compared with the typical non-growth-associated M4-1 hybridoma cell line. The rCHO cell line was propagated as a free dispersed suspension agitated static batch culture in 1000 mL spinner flasks, with serum free HB-CHO medium. The reproducibility of four batch runs operated at different times was acceptable (Appendix C). One representative culture is presented here.

The conventional representation of batch mammalian cell culture is shown in Figure 4.1.1 for the rCHO cell line and also for the M4-1 hybridoma cell line for purposes of comparison. This method of presentation has inherent conceptual problems. For example, the production of protein (tPA and MAb) is an obvious function of the concentration of viable cells, apparently varying with the population growth phase. Although this seems to suggest that productivity is at least partially-growth-phase-associated, the exact relationship is difficult to assess quantitatively. While the viable cell curve and protein titer curve of the hybridoma cell line are smooth, that of the rCHO cell line exhibits an extended decline phase with decreasing concentration of protein product. The early decline phase of the rCHO cell line is characterized by an approximately constant viable cell concentration. The onset of the decrease in the tPA protein titer coincides with the onset of the decreasing viable cell concentration of the late decline phase. This is probably the result of tPA degradation by proteases released from dead, dying, and lysing cells coupled with the cessation of the production of tPA. The tPA production and degradation are discussed further in Section 4.1.2.

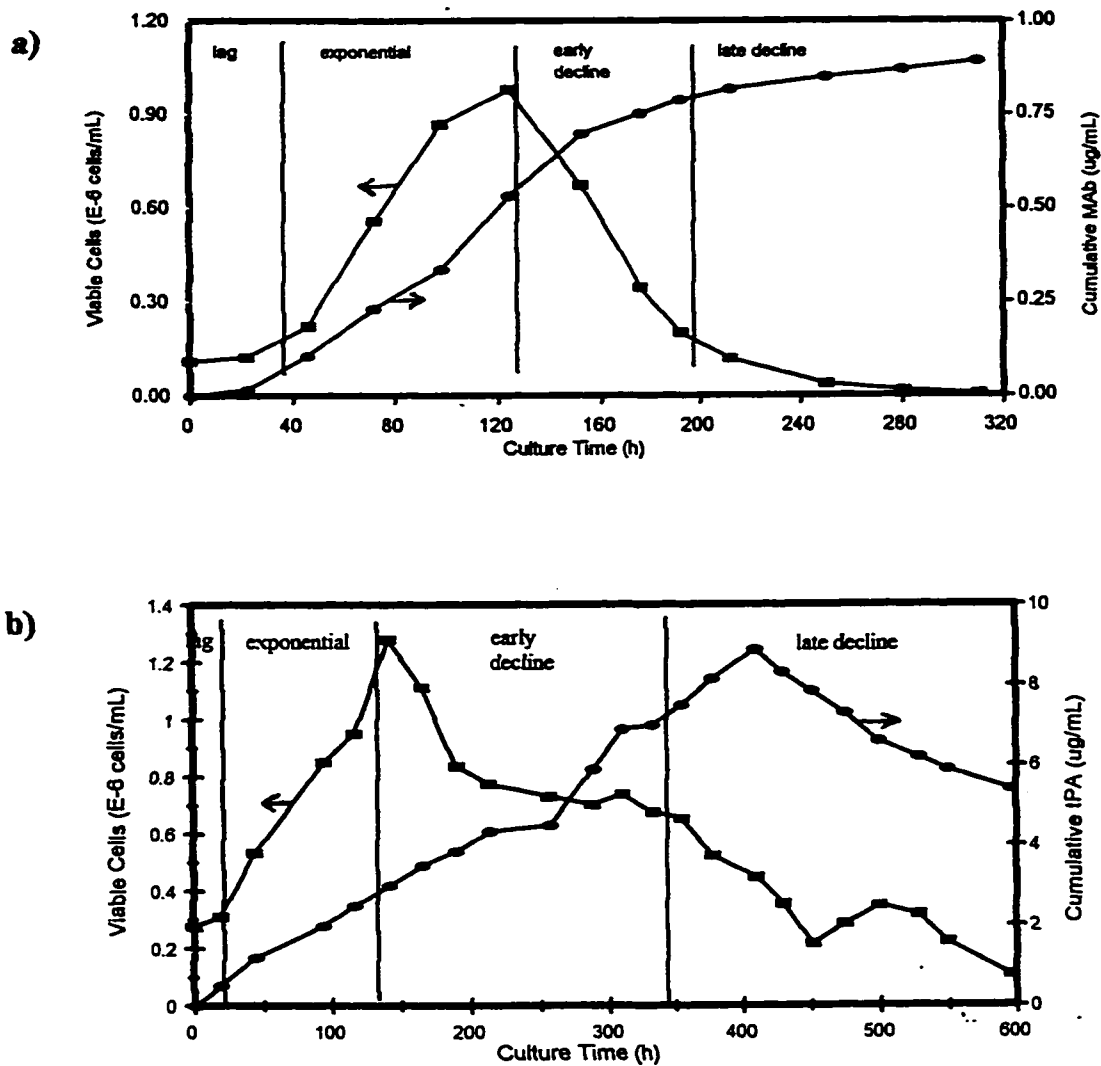


Figure 4.1.1: Conventional representation of batch culture viable population curve and protein product titer curve. Clearly, the production of protein is a function of the viable cell concentration, but the exact relationship is difficult to assess from this representation of the data. squares: X_v ; circles: protein concentration.

a) M4-1 hybridomas and associated α -bovine-light-chain-IgG monoclonal antibody. Cells were propagated as free suspension static batch cultures in 100 mL working volume T-flask.

b) CHO1-5₅₀₀ cells and associated tPA serine protease. Cells were propagated as free dispersed suspension agitated batch cultures in 1000 mL working volume spinner flask.

A second frequently used technique for assessing population growth is the maximum viable cell concentration (X_{Vmax}) attained, which is thought to indicate the success of population growth (Xie and Wang, 1996) and, by extension, the biological capacity for production of the system (Table 4.1.1). While a large number of cells will invariably produce a larger amount of protein product than will a small number of cells in the same time span, the single measurement of the instantaneous viable cell concentration has not been found to correlate with the maximum product titer (P_{max}) achieved in batch culture (Bushell *et al.*, 1993; Suzuki and Ollis, 1990; Xie and Wang, 1994a; Merten, 1988). The average number of viable cells over the course of the batch culture (X_{Vavg}) (Table 4.1.1) is probably a better indicator of both the biological capacity for production and the success of population growth or maintenance. The maximum product concentration can be assessed as a function of the average viable cell concentration ($P_{max} X_{Vavg}^{-1}$) (Table 4.1.1).

Apparent Population Growth Rate

The specific growth rate, μ , is derived from the instantaneous viable cell concentration, as the number of cells produced per cell per hour (usually expressed as h^{-1}). The specific growth rate changes continuously over the course of the batch process, as shown in Figure 4.1.1, particularly for the rCHO cell line. In spite of this obvious variability, μ is generally utilized as a constant, frequently with μ_{max} taken to be the value of this parameter (Table 2.1) (Hayter *et al.*, 1992; Goergen *et al.*, 1992; Xie and Wang, 1994a).

In recent years, the effect of μ on the rate of productivity and on the maximum product titer has become a topic of intense investigation (Hayter *et al.*, 1992; Bushell *et al.*, 1993; Goergen *et al.*, 1992; Takahashi *et al.*, 1994; Suzuki and Ollis, 1990). In particular, the protein product has frequently been shown to be at least partially growth phase associated, and is therefore sensitive to changes in the apparent population growth rate. While an obvious indicator of population growth, μ is only superficially connected to protein productivity. Underlying population growth are the life and proliferative cycles of the individual cells comprising the population. The proliferative cycle of the individual cells is known as the cell cycle. The relationship of the cell cycle to population parameters is discussed in Section 4.1.2.

Table 4.1.1: Population growth and production batch culture parameters of free suspension M4-1 hybridoma and CHO1-5₅₀₀ cells.

Parameter	M4-1	CHO1-5 ₅₀₀
$X_{v_{max}}$ (E-6 c/mL)	0.980	1.280
$t(X_{v_{max}})$ (h)	124	142
$X_{v_{avg}}$ (E-6 c/mL)	0.328	0.578
μ_{max} (h ⁻¹)	0.026	0.012
P_{max} (mg/L)	0.902	8.88
$t(P_{max})$ (h)	310	409
$P_{max} X_{v^{-1}}$ (pg/c)	2.75	19.75
q_{P-I} (pg/c/h)	0.009	0.033
q_{P-II} (pg/c/h)	0.014	0.017
$q_{P-III-lag}$ (pg/c-h)	0.008	0.076
$q_{P-III-exp}$ (pg/c-h)	0.008	0.018
$q_{P-III-ed}$ (pg/c-h)	0.008	0.042
$q_{P-III-ld}$ (pg/c-h)	0.008	-0.069

c: cell; c-h: cell-hour; ed: early decline; ld: late decline

Specific Productivity

A descriptor of the specific productivity, q_p ($\mu\text{g}/\text{cell}/\text{hour}$), can be calculated from the maximum product concentration per culture hour and normalized with respect to the average cell concentration. Such a way of expressing q_p , here labeled q_{p-I} (Table 4.1.1), is based on an assumption that all cells are in an identical physiological state throughout the batch culture (*i.e.* a homogeneous, time-invariant cell population), although this is biologically unreasonable. For example, growing cells are obviously physiologically distinct from dying cells. This parameter (q_{p-I}) can serve as a good estimation of productivity, but is not useful in formulating fine optimization strategies, as it has been found to vary from batch run to batch run (run dependent) (Bushell *et al.*, 1993), suggesting that it changes as the physiological make-up of the cell population changes.

In batch culture, a second form of the specific productivity (q_{p-II}), which is the protein product concentration divided by the viable cell concentration (Hayter *et al.*, 1992), indicates that MAb productivity of the M4-1 hybridoma cell line is increasing throughout the decline phase when the viable cell number is very low and decreasing (Figure 4.1.1). While cells undergoing apoptotic senescence have been shown to increase the production of some proteins (Mercille and Massie, 1994; Singh *et al.*, 1994), and while all senescent cells may also be increasing the rate of secretion or release of accumulated intracellular MAb (Leno *et al.*, 1992; Flickinger *et al.*, 1992; Al-Rubeai *et al.*, 1992), there is no biological justification for this apparently very high rate of production from so few cells which are in a dying state. In the case of the rCHO cell line, this methodology returns a specific productivity of $0.0170 \text{ pg}\cdot\text{c}^{-1}\cdot\text{h}^{-1}$, when assessed up to the point of maximum product titer (midway through the decline phase) (Table 4.1.1). This at best serves as an estimate of the averaged specific productivity, and is an underestimate here.

These apparent phenomena are artifacts which arise from comparing cumulative protein production (which the MAb concentration in the medium is a measure of) with the instantaneous measure of the biological capacity for production (*i.e.* the cell number). This is effectively comparing a time integral to a derivative function. In part, this contradiction has been recognized by constraining the use of q_{p-II} to the exponential growth phase (Goergen *et al.*, 1992; Gaertner and Dhurjati, 1993a,b), where the specific growth rate is approximately constant, and, therefore, the trace of the cumulative protein production approximately parallels the trace of the cell number for the M4-1 hybridoma cell line (Figure 4.1.1). When the slopes of these two traces are compared, q_{p-II} is presented as a specific protein production rate with respect to culture time. Merten's method of calculating this parameter is presented in Table 2.1 (Merten, 1988). It is clear that in the case of the rCHO cell line, the viable cell concentration curve and the product titer curve are not parallel, even during the exponential phase. When the measurement of the specific productivity is restricted to the exponential phase for the rCHO cell line, it returns an even lower estimated value of $0.0167 \text{ pg}\cdot\text{c}^{-1}\cdot\text{h}^{-1}$. Ideally,

such a parameter should be applicable over the entire course of the culture, therefore, the validity of q_p -II, calculated in this way, is questionable. Attempts to apply this method of calculating the specific productivity over the entire batch run by utilizing a variable μ , results in complex curves which are difficult to interpret (Hayter *et al.*, 1992; Goergen *et al.*, 1992; Al-Rubeai *et al.*, 1992).

A third representation of this parameter, which is gaining acceptance, expresses the protein concentration as a function of the so-called Viability Index (VI) (Luan *et al.*, 1987). This parameter is also called the specific productivity, and has been given the same symbol (q_p), leading to confusion. Here, this form of the specific productivity is labeled q_p -III. Luan and co-workers defined the Viability Index as “the number of viable cells at each count integrated over the duration of the experiment”. Their data illustrated “a very good direct correlation between the Viability Index and the cumulative MAb concentration over the entire course of a batch hybridoma culture”, suggestive of a physical basis which would substantiate the validity of this parameter, VI, and of calculating q_p as a function of VI.

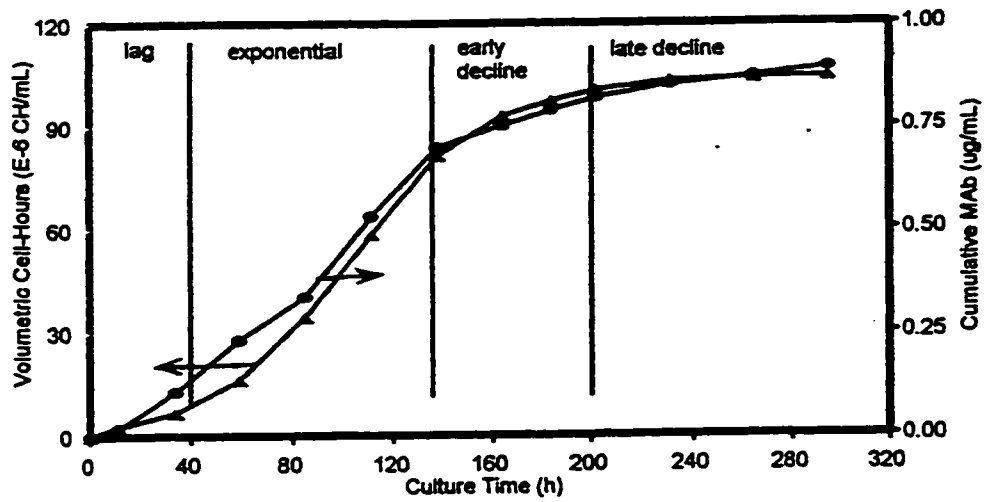
Cell Hours, Cumulative Production, and Specific Productivity

The calculation of the Viability Index transposes the instantaneous measurement of the biological capacity into a cumulative measurement of the biological capacity for production on a unit volume of medium. Since protein synthesis and secretion is a spatio-temporal property of living cells, expressing production as the integral of viable cells (*i.e.* the cumulative length of time that live cells have been present in the batch run) per unit volume is a useful approach. However, Viability Index is a vague term, which is therefore proposed to be replaced by the term “cumulative volumetric cell hours”, CH_{vol} , defined as the cumulative number of hours spent in the medium by all viable cells. With respect to productivity, CH_{vol} represents the cumulative productive (*eg.* protein producing) life span of cells in the medium (bioreactor). It is important to recognize that one cell has the potential to produce as much protein in ten hours as ten cells can produce in one hour. In both cases, the total number of production hours is identical. The use of the CH_{vol} parameter allows for the assessment of productivity and of the biological capacity for production on the same (cumulative) basis (Figure 4.1.2). The volumetric cell-hours, CH_{vol} , is defined as:

$$CH_{vol} = \int_0^t X_V dt \quad (4.1)$$

where X_V is the viable cell concentration

a)



b)

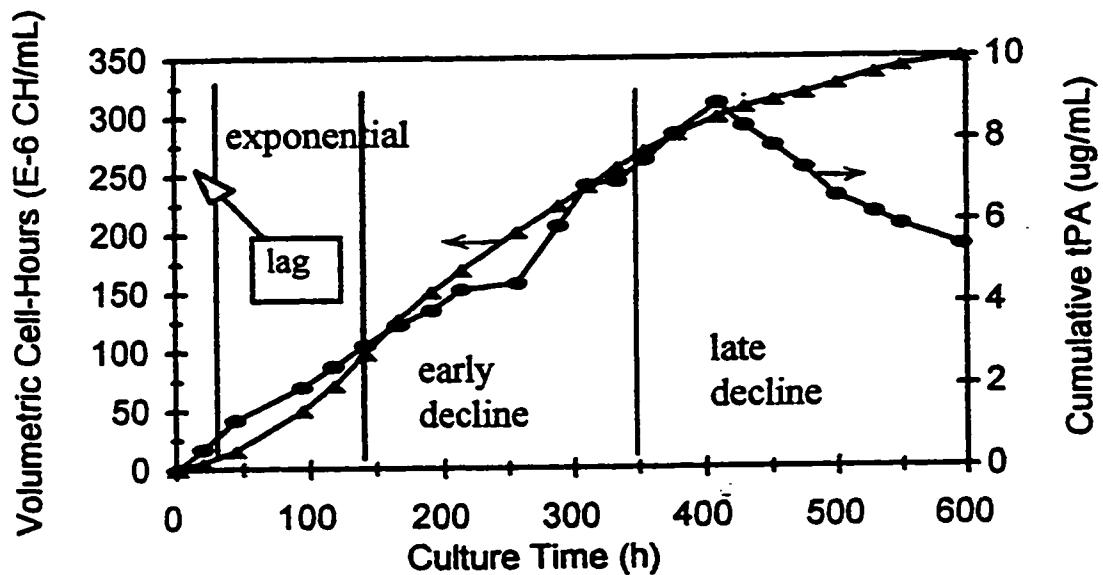


Figure 4.1.2: Free dispersed suspension batch cultures represented as the cumulative biological capacity for production (cell-hours) and associated cumulative product titer. Recalculated from the data in Figure 4.1.1. Clearly, protein productivity is closely correlated to cell-hours. Here, it is possible to discern that Mab productivity by M4-1 hybridomas does not appear to vary with growth rate, while tPA productivity by rCHO cells closely parallels the cell-hour curve until product degradation begins in the late decline phase. triangles: volumetric cell-hours; circles: protein concentration

a) M4-1 hybridomas

b) CHO1-5₉₀ cells.

The volumetric cell-hours can be calculated by a simple numerical integration technique, using the log average of the cell density between data points, as it is a more accurate estimate of the average of a curved function than is the arithmetic average:

$$CH_{vol} = \sum_0^t \frac{(Xv_{t+\Delta t} - Xv_t)}{\ln\left(\frac{Xv_{t+\Delta t}}{Xv_t}\right)} (\Delta t) \quad (4.2)$$

where t is the culture time

Alternatively, cumulative protein concentration data can be manipulated to yield the instantaneous antibody production, and compared with the measured viable cell concentration. Mathematically, this would involve finding the derivative of the function representing the cumulative protein concentration data over the entire course of the culture. However, this may prove problematic, in that the specific productivity does not necessarily remain constant over the entire course of the culture. That is, the cumulative protein product data trace may be composed of the combination of more than one function, as the number of cells in various subpopulations (physiological states, such as different cell cycle phases) changes over time.

The volumetric productivity (P_{vol} or dP/dt), which is frequently calculated as a function of the specific growth rate and the viable cell concentration (Xie and Wang, 1994a; Shirai *et al.*, 1994), is an estimated measure of the instantaneous protein production. The deviation of dP/dt from direct proportionality to μ has been accommodated by the inclusion of a second, non- μ dependent, term. This term is referred to as the non-growth-associated term.

The maximum volumetric productivity has been found to correlate directly with μ_{max} (Hayter *et al.*, 1992; Goergen *et al.*, 1992). In contrast, μ_{max} , which is often cited as a measure of the success of the propagation system, does not correlate with the maximum titer. The average volumetric productivity has no obvious connection to the viable cell concentration curve. This is not surprising when the length of the proliferative cycle of animal cells is compared with the length of the epigenetic time domain (Section 2.1). In contrast to microorganisms, where genetic and epigenetic activities are contained within approximately the same time domain (measured in hours), the length of the animal cell cycle is measured on the order of days, while protein production proceeds on the order of hours (Lloyd *et al.*, 1982).

Cells that are apparently not growing may yet produce significant quantities of protein. (In this regard, protein production in mammalian cells would be equivalent to secondary metabolite synthesis in bacteria.) Hence, protein productivity from animal cells is more closely correlated to the length of time spent in the reactor by all viable cells, than it is correlated to the frequency of division (growth rate) of that viable cell population. It should be noted that the cell-hour parameter, CH_{vol} , is inclusive of all non-growth-associated metabolic activity. In this context, it is apparent that the yield of cells on a particular substrate ($Y_{X,S}$) has limited interpretive value with respect to optimization of productivity.

The method of evaluating the specific productivity as a function of cumulative volumetric cell hours can and should be extended to the evaluation of metabolic parameters. The metabolic time domain (for ATP synthesis) which is measured on the order of minutes, is even further removed from the time frame of cell division than is protein productivity. Specific glucose consumption rate, specific glutamine consumption rate, specific lactate production rate, specific ammonia production rate, *etc.*, expressed in this way are inclusive of growth-, maintenance-, and protein-product-associated metabolic activities. Yields of metabolic byproducts on substrates, such as the yield of lactate on glucose ($Y_{LAC,GLC}$), can then be calculated from the specific rates. These metabolic parameters are presented in Table 4.1.2 for the rCHO cell line batch culture presented in Figure 4.1.1. The metabolism of the rCHO line is discussed in Section 4.3.

Association of Productivity to Population Growth Phase and to Specific Growth Rate

CH_{vol} is a direct quantification of the “load” on the medium, while the maximum volumetric cell hours attained (*i.e.* the maximum of CH_{vol}) is a quantification of the success both of population growth and/or maintenance and of medium utilization for the support of the population. The rCHO cell line attains approximately three times the cell-hours of the M4-1 hybridoma cell line, while the maximum viable cell concentrations attained differ by less than a factor of 1.25. A break in the CH_{vol} curve of the rCHO cell line (Figure 4.1.2b) coincides with the onset of the early decline phase. The cell-hours continue to increase rapidly through this portion of the batch run, coinciding with the approximately constant viable cell concentration. Remarkably, approximately 60% of the total cell-hours are accumulated during the decline phase. In contrast, the M4-1 hybridoma cell line yields a rapidly decelerating increase in cell-hours throughout the decline phase, with an accumulation of only about 15% of the total cell-hours of the batch run.

Table 4.1.2: Metabolic batch culture parameters of dispersed suspension CHO1-S₅₀₀ cells.

Metabolite	Q _{con} ($\mu\text{mol c-h}^{-1}$)
First Metabolic Phase:	
Glucose	0.143
Glutamine	0.06
Lactate	-0.185
Alanine	-0.0135
Ammonia	-0.0411
Serine	0.0015
Glycine	-0.00092
Second Metabolic Phase:	
Glucose	0.0012
Glutamine	0.01
Lactate	0.00035
Alanine	-0.0135
Ammonia	-0.01115
Serine	0
Glycine	-0.00092
Third Metabolic Phase:	
Glucose	0
Glutamine	0
Lactate	0.030
Alanine	0.005
Ammonia	-0.01115
Serine	0
Glycine	-0.00092

By simply re-plotting cell population and product data on the same (cumulative) basis (Figure 4.1.2), growth-phase-associated, non-growth-phase-associated, or partially-growth-phase-associated productivity is qualitatively obvious graphically, and simple to analyze quantitatively. When cumulative volumetric product concentration is linearly regressed against cumulative volumetric cell hours, as proposed by Luan *et al.* (1987), the nature of the association between these two parameters is immediately, and quantifiably apparent. The dependence of the cumulative protein product concentration on the volumetric cell hours is shown in Figure 4.1.3. The applicability of this approach for both the rCHO cell line and the hybridoma cell line is evident.

As is the case for the M4-1 hybridomas (Figure 4.1.3a and Table 4.1.1), a single line of constant slope (constant q_p -III) over the entire course of the batch culture, indicates non-growth-phase-associated productivity, suggesting that the protein is produced at approximately the same rate during all phases of the cell cycle as well as during periods of quiescence and during senescence. The slight hint of increase in the specific productivity during the late decline population growth phase suggests that apoptotic cells may exhibit a marginal increase in the production of this MAb.

In contrast, the rCHO cell line exhibits growth-phase-association of productivity (Figure 4.1.3b and Table 4.1.1) as indicated by four distinct straight lines that are of constant slope within each growth phase. Productivity is greatest in the lag and early decline phases, and becomes negative in the late decline phase as discussed above. It is difficult to determine whether the actual productivity has become zero in the late decline phase, as this possibility is obscured by tPA degradation.

The two cell lines examined in this study represent two different productivity patterns, namely non-growth-phase-associated and growth-phase-associated. A third type of productivity pattern is possible. Were the protein productivity partially-growth-phase-associated, it would be variable even within each of the growth phases.

In addition to productivity patterns based on correlations to population growth phases, it is possible to distinguish productivity patterns based on correlations to specific growth rates of the population. The two cell lines examined in this study represent two of the four possible relationships between the specific productivity and the specific growth rate. Excluding the late decline phase from consideration, the specific productivity is inversely related to the specific growth rate (negatively growth-associated) in the rCHO cell line, suggesting that protein may be preferentially produced during the G1 and/or G0 cell cycle phases. In the M4-1 cell line, the specific productivity remains constant as the specific growth rate changes (non-growth-associated), as is the case with all cell lines exhibiting non-growth-phase-associated productivity.

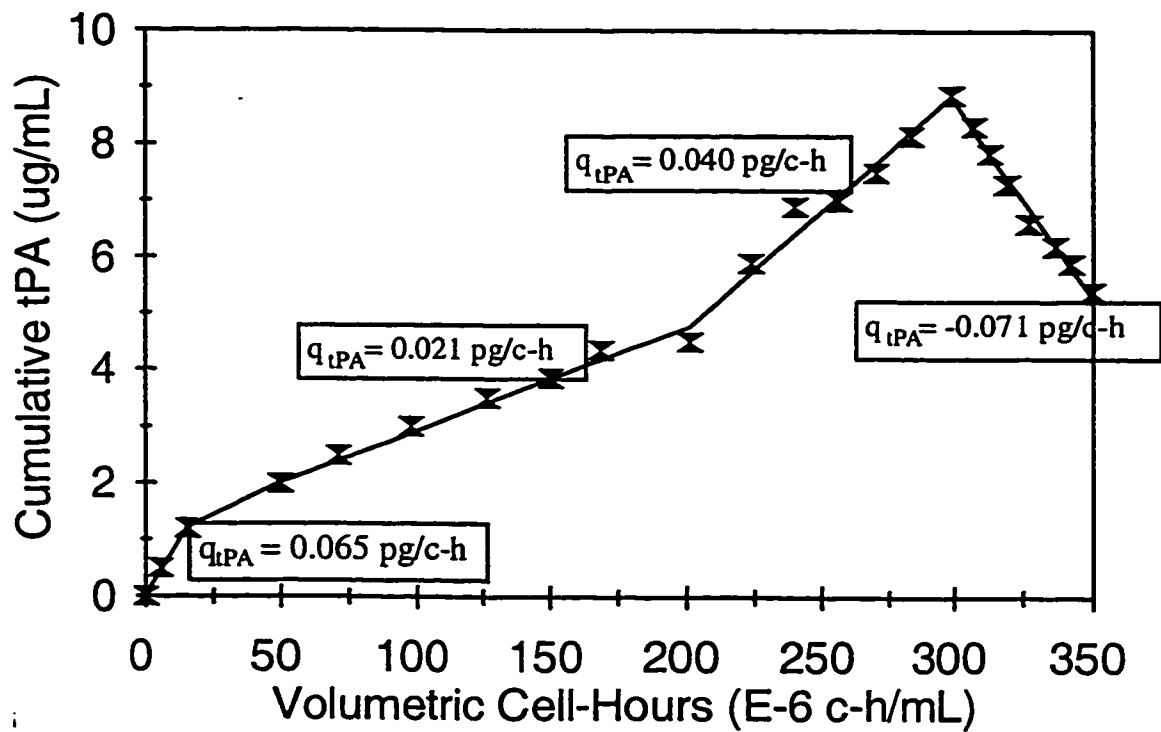
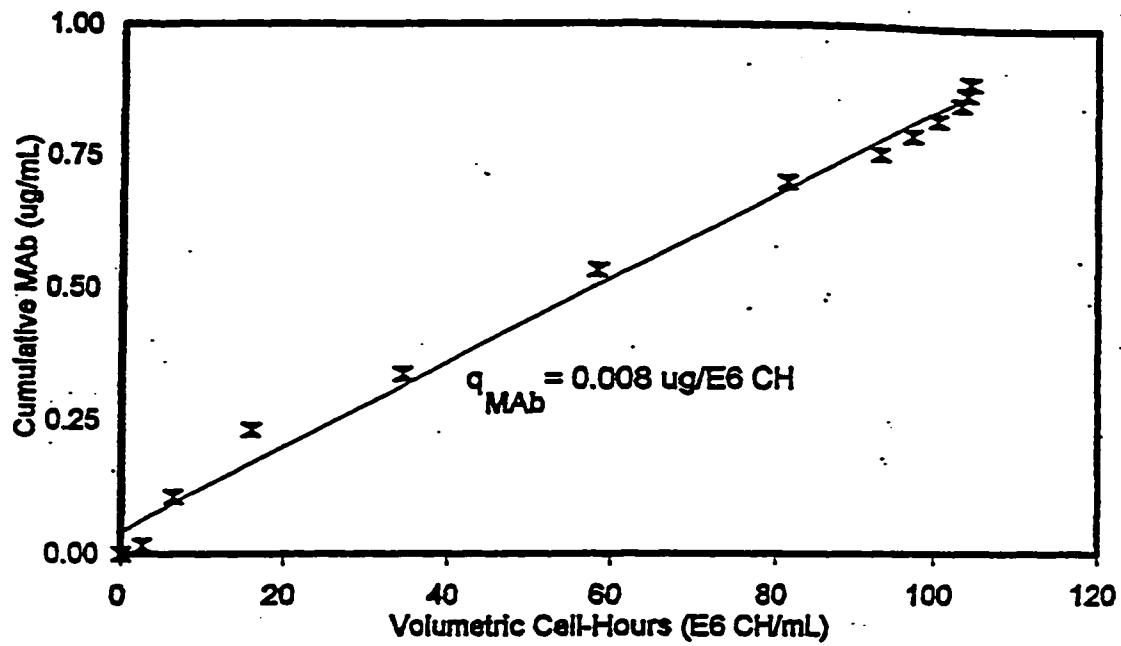


Figure 4.1.3: Cumulative protein concentration as a function of the cumulative volumetric cell-hours. The specific productivity can be calculated from the slope of the curve.

a) M4-1 hybridomas

b) CHO1-500 cells.

A third type of cell line, which exhibits increasing specific productivity with increasing specific growth rate (growth-associated), suggests that product is produced preferentially or exclusively during the S, M, and G₂ phases of the cell cycle. Conditions which extend exponential growth (perhaps including continuous culture mode) should therefore optimize productivity of this type of cell line.

In a fourth type of cell line, the relationship of productivity to growth rate is less clear, and may exhibit several different regions of association-types (negatively growth-associated, growth-associated, and non-growth-associated regions). This type of association is termed partially-growth-associated. The rCHO cell line falls into this category when the entire growth curve is included in the assessment. When the regions of association-type vary rapidly, a plot of the specific productivity against the specific growth rate results in complex curves. When the specific productivity changes with the physiological state of the population (growth phase), these complex curves may loop as the batch run proceeds. As discussed above, the relationship of productivity to specific growth rate is, at best, loose, so that many cell lines fall into this category. Optimization strategies based on the specific growth rate for such cell lines are difficult to formulate. Here, such is the case for the rCHO cell line.

Concluding Remarks

Analyses of the parameters associated with the evaluation of batch cultures of mammalian cells must be performed on the same basis. Measured concentrations of substrates, metabolic byproducts, and protein products represent cumulative values. A simple numerical integration technique can be employed to convert the instantaneous viable cell number to cumulative cell-hours. Specific productivity and consumption parameters can then be calculated on the basis of volumetric cell-hours. Specific productivity is evaluated in this way (labeled q_p -III in this Section) throughout the remainder of this thesis, and labeled simply q_p . Using this approach, three basic patterns of protein production as a function of the non-segregated cell population emerge. Theoretical examples of these patterns are illustrated in Figure 4.1.4a.

For comparison, the possible correlations of the specific productivity to the specific growth rate are presented in Figure 4.1.4b. Partial-growth-association results in complex patterns, suggesting that correlations of specific productivity to specific growth rate may not have a clear-cut biological basis. Particularly, the non-linear patterns shown in Figure 4.1.4b can be more readily interpreted by analysis within the epigenetic time domain (Figure 4.1.4a).

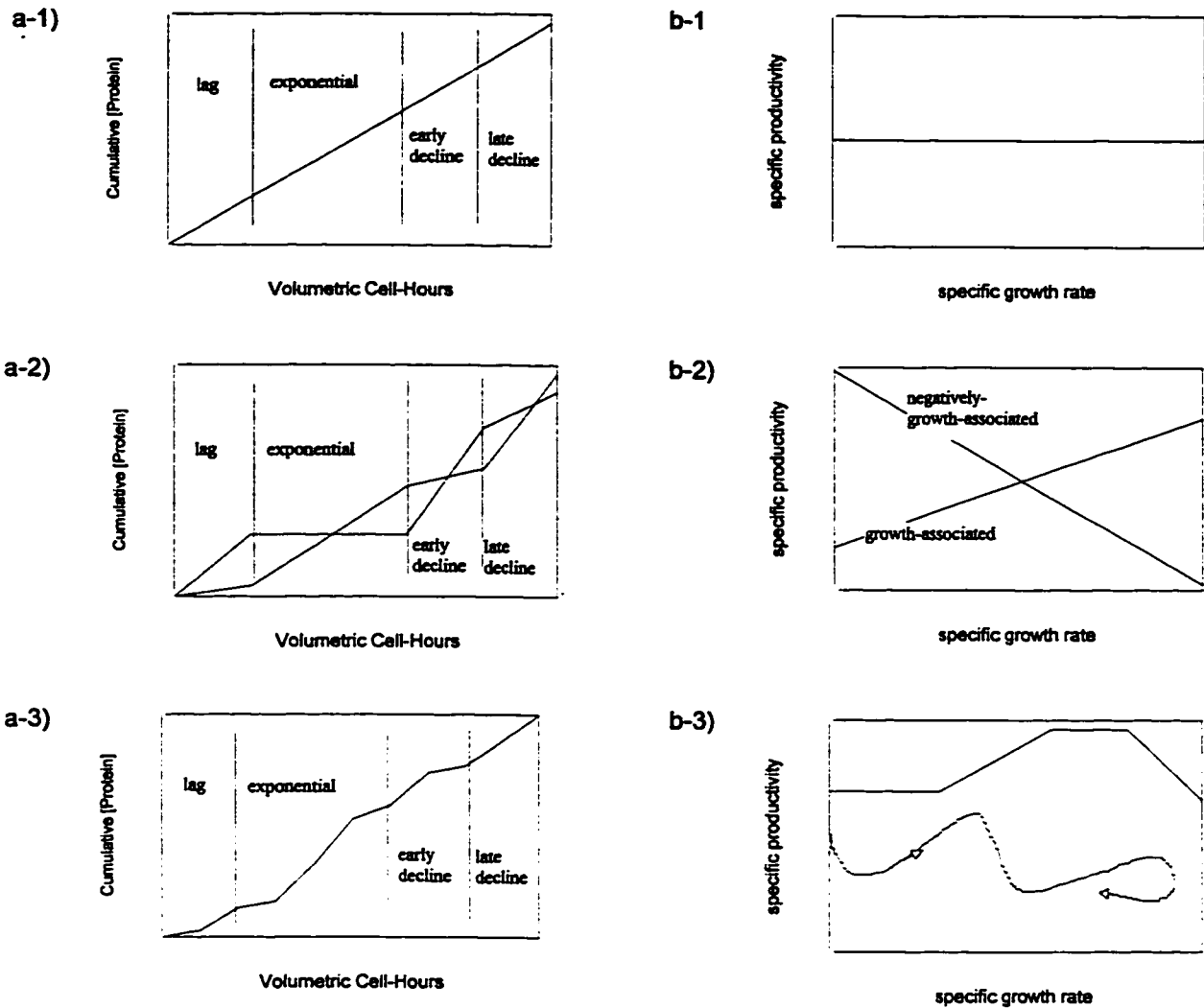


Figure 4.1.4: Theoretical examples of the basic types of protein production kinetics.

a) Protein titer as a function of the biological capacity for production (volumetric cell-hours) during the different population growth phases. The slopes of the lines are the specific productivities. 1 non-growth-phase-associated (constant slope); 2 growth-phase-associated (variable slope, but constant within each growth phase); 3 partially-growth-phase-associated (variable slope, no distinct correlation to growth phase).

b) Specific productivity as a function of the specific growth rate. This correlation's biological basis is ambiguous. 1 non-growth-associated (constant zero slope); 2 growth-associated, negatively-growth-associated (constant positive, or negative, slope); 3 partially-growth-associated (at least partially non-linear).

Simplicity, both in measurement techniques and in data analysis, is a highly desirable attribute of evaluation techniques. Evaluation of the physiological make-up of the population, or detailed cell cycle analyses, may not be necessary to the development of a successful optimization strategy. For example, conditions which maintain viability but retard growth rates for the rCHO cell line should serve to enhance the product titer. Conversely, the rate of transit through the population growth phases should have no impact on the productivity of the M4-1 cell line, and therefore, for a given number of cell-hours, the faster the growth rate, the faster product will accumulate. Hence, evaluation techniques at the whole population (macro or non-segregated) level may be sufficient for optimization purposes. Thus it may be unnecessary to evaluate the system at the individual cell (micro or segregated) level.

4.1.2 Productivity and the Segregated Population

Underlying the growth of populations are the proliferative cycles of the individual cells comprising the population (see Section 2.1). To investigate the relationship between the production of the recombinant protein during batch culture and the physiological state of the cells, the population was segregated into four subpopulations on the basis of relative DNA content per cell. The experimental work considered here differed in a number of conditions from the experiment evaluated in Section 4.1.1, so that these two experiments are not compared. The impact of these conditions on growth and productivity is considered in Sections 4.2 and 4.3. In this experiment the cells were grown as a dispersed suspension in a 100 milliliter working volume spinner flask, agitated at 150 rpm, with serum free HB-CHO medium containing 40 mmol·L⁻¹ glucose.

In spite of the probability of a certain degree of aneuploidy in this rCHO continuous cell line, it was assumed that cells in the G2 and M phases would have approximately twice as much DNA as cells in the G1 and G0 phases. Cells traversing the S phase would have a DNA content between that found in the G1 phase and that found in the G2 phase, while viable apoptotic cells would have a DNA content less than that found in the G1 phase (hypodiploid). Typical relative DNA content profiles for populations of this rCHO cell line are shown in Figure 4.1.5. Scatter graphs of DNA to RNA content per cell and for forward light scatter (relative size, FS) and side light scatter (relative density, SS) of individual cells are also presented in this figure. The light scatter graph illustrates the gate employed in the flowcytometric analyses, which was set to include particles from 8 to 20 μm in diameter. Particles with a diameter greater than 20 μm are likely 2 to 5 cell aggregates or clumped cells.

The sample illustrated in Figure 4.1.5a is after one day of culture in an environment similar to the environment from which the inoculum was taken. The inoculum used in this experiment was taken from a mid-exponential asynchronous culture in balanced growth, and contained an insignificant subpopulation of apoptotic cells. The DNA to RNA scatter reveals a subpopulation in G1/G0 phase with diploid DNA content and a range of RNA content, an S phase subpopulation with an increasing DNA content coupled to an increasing RNA content, a G2/M phases subpopulation with a tetraploid DNA content and rich RNA content, and an A phase subpopulation with hypodiploid DNA content and low RNA content, suggesting that cells exit the cycling fraction in early G1. A few cells with hypodiploid DNA content and higher RNA content have perhaps entered apoptosis from late G1, but no hypodiploid cells appear to have the rich RNA content associated with the S and G2/M phases. The few cells exhibiting hypertetraploid DNA content may be due to aneuploidy or aggregation of these rCHO transformed cells. It is also noteworthy that cells are apparently capable of existing in the S phase with a relatively low RNA content.

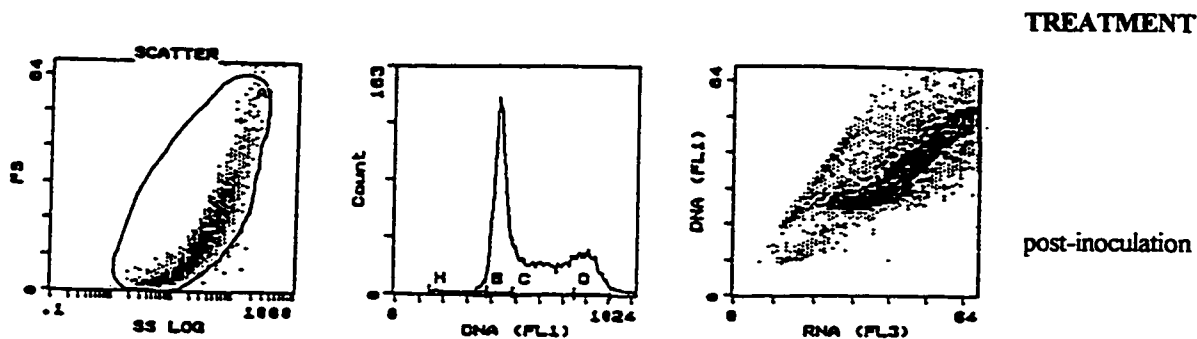


Figure 4.1.5a: Flow cytometric plots of CHO1-5₀₀ cells in cell cycle phases in conditions shortly after inoculation. The population is in balanced growth, with only a small portion in apoptosis.

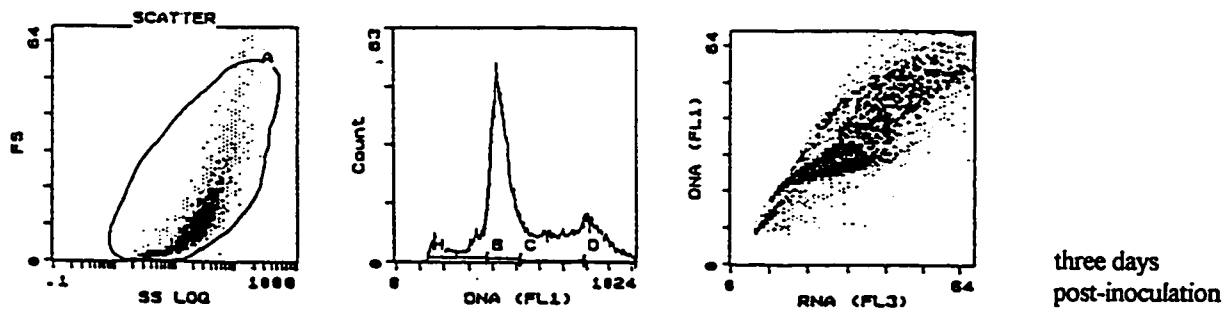
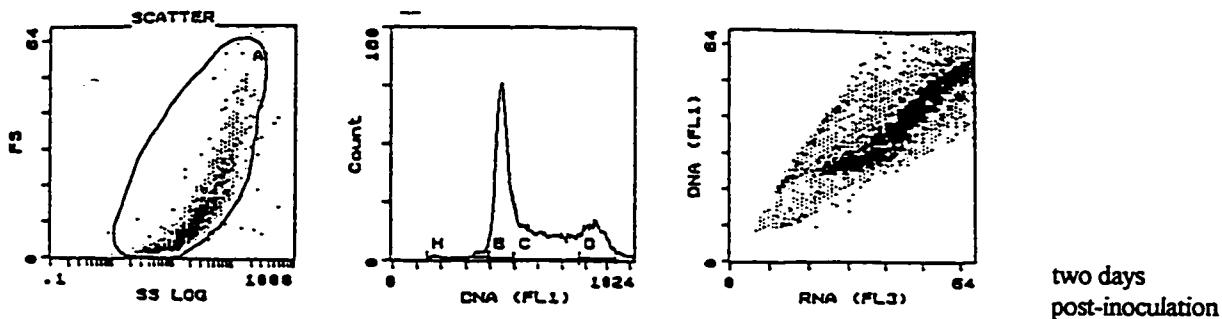
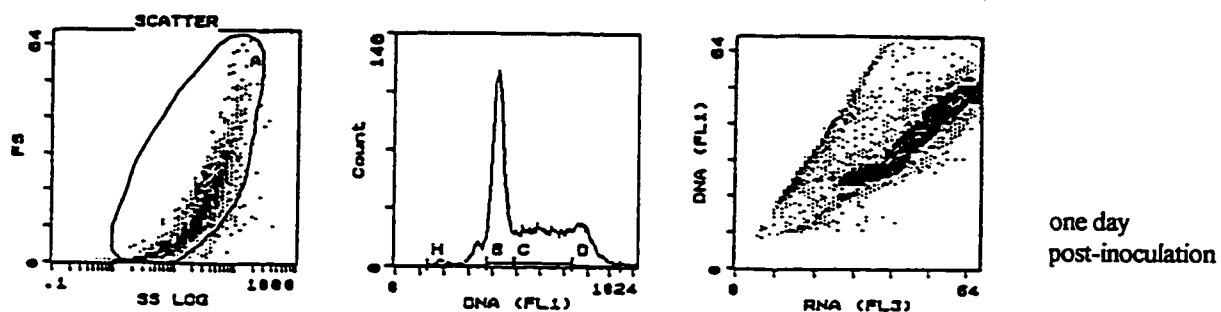


Figure 4.1.5b: Cell cycle distribution of the population moving through the exponential growth phase.

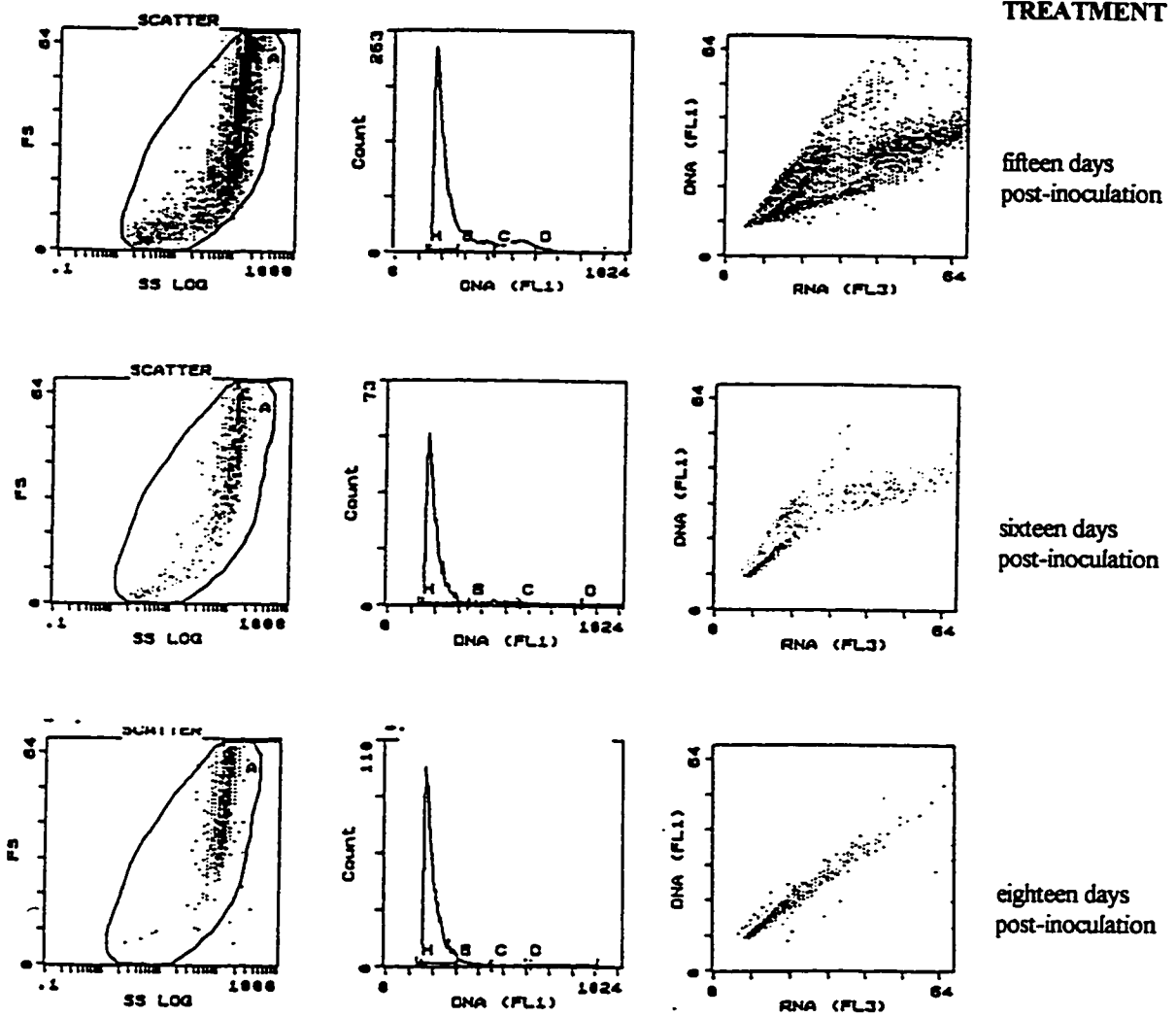


Figure 4.1.5c: The population accumulates in the apoptotic sub-compartment during the late decline phase.

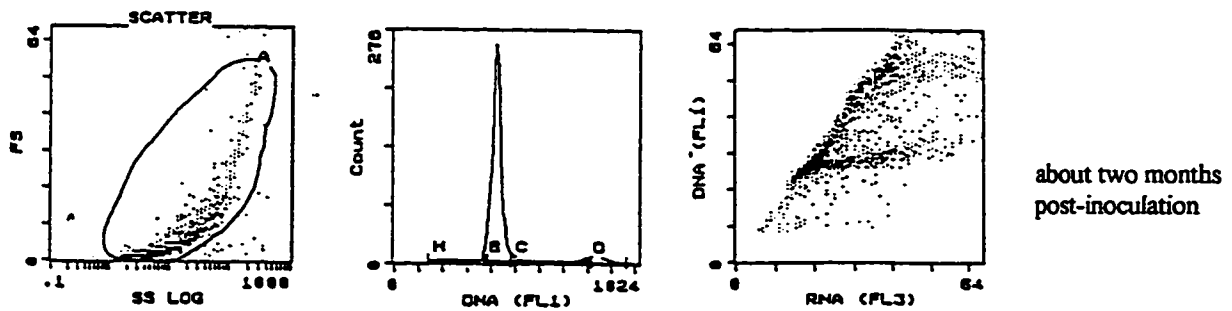


Figure 4.1.5d: Density arrested CHO1-5₀₀ cells accumulate in the G1/G0 cell cycle phase.

When the culture environment is similar to the environment from which the inoculum is derived, inclusive of an adequately large inoculation cell density, the population continues in balanced growth as is the case in the samples illustrated in Figure 4.1.5b. As the batch culture proceeds, the proportion of the population traversing the cell cycle with a relatively low RNA content diminishes. By 72 hours of culture time, a significant apoptotic subpopulation is accumulating, and the proportion of the population in G1/G0 is increasing, so that the population is falling out of balanced growth although the exponential phase continues for another 72 hours.

Figure 4.1.5c depicts a population in the late decline phase, with a rapidly increasing percentage of the gated population in apoptosis. Very few cells with a DNA complement greater than diploid are seen during the late decline phase. Interestingly, these cells are both large and dense, in contrast to the expectation of small cell size associated with apoptosis. Further evidence of the apoptotic nature of cell death, as opposed to necrotic cell death, is presented in Section 4.2.

The cells in the sample in Figure 4.1.5d, taken from a density arrested population, reside primarily in the G1/G0 phase. This population of cells was maintained as an adherent confluent monolayer for a period of two months. Daily replacement of medium ensured that nutrient limitation and biowaste toxicity were not factors in the behavior of this culture. Cell to cell contact and cell signaling had apparently resulted in contact inhibition and the population was arrested in G1. From the analysis of the DNA profile, less than 4% of the population has been assigned to the apoptotic compartment.

Population Growth Dynamics

Commencing with an inoculum of 0.25×10^6 viable cells per milliliter, there is apparently no population lag phase (Figure 4.1.6: see total viable cell density curve). However, when the segregated population pools are considered, it can be seen that cells are accumulating in the G1/G0 phase during the first three days of the batch culture (Figure 4.1.6). This is consistent with G1 arrest (entry into G0 phase) associated with population lag phase, in response to the step change in environment associated with inoculation: the mid-exponential phase inoculum was grown as a static culture in medium containing 5% serum, while the experimental conditions involved agitation in serum-free medium. Presumably, cells are temporarily arrested in G1 phase while cell constituents necessary for continued or alternate metabolic pathways are synthesized.

Following the lag phase, some of the cells fall out of G1/G0 phase into A phase, while the majority of the cells re-enter the cycling fraction of the population, as can be seen with the increase of the S phase subpopulation from 100 hours to 200 hours of batch culture. In this serum-free medium, the maximum specific growth rate is only 0.0115 h^{-1} which

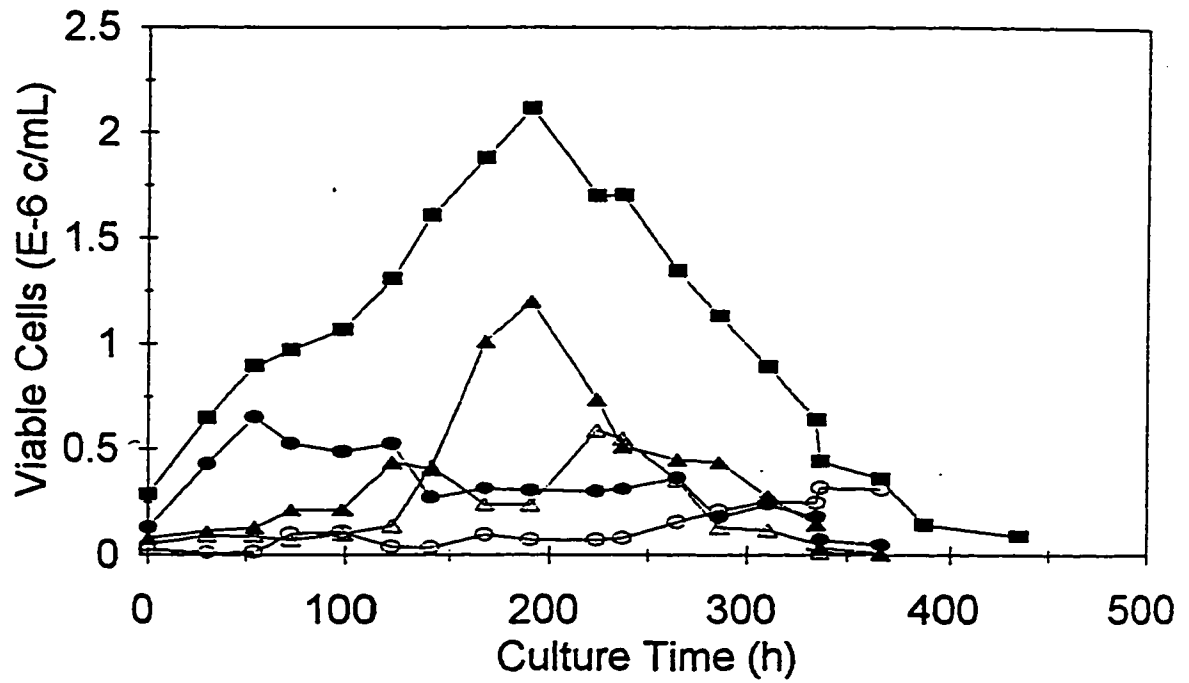


Figure 4.1.6: Population growth dynamics of CHO1-5₃₀₀ cells of dispersed suspension batch culture using serum-free medium, from an inoculum grown in serum containing medium. The population initially accumulates in G1/G0 and then traverses the cell cycle in semi-synchrony.

solid squares: viable population; solid triangles: S phase; open triangles: G2/M; solid circles: G1/G0; open circles: A phase.

corresponds to a doubling time of approximately 60 h, so that daily sampling results in 2 to 3 sampling points per complete cell cycle period. Hence, it can be seen that the population exits the lag phase in partial synchrony with peaks in the subpopulations corresponding to traverse through the S phase, G2/M phases, and G1 phase.

After three population doublings, the cells enter the decline phase. Under the conditions of this experiment, the viable cell concentration decreases smoothly, at a constant rate of 0.01 h^{-1} , throughout most of the decline phase. By the late decline phase, most of the viable population is senescing through apoptosis, and the rate of decline diminishes.

A population of cells in culture does not contain the housekeeping phagocytes which engulf and destroy apoptotic bodies *in vivo*. Thus, as the individual cells complete the physiological process of apoptosis, they enter secondary necrosis, in which membrane integrity is lost and cytoplasmic contents leak out into the medium. Eventually cell and organelle membranes lyse and the contents are released *en masse*. Any cells which may undergo primary necrosis (accidental or traumatic cell death) lose membrane integrity and lyse to release cellular contents relatively quickly.

The appearance of the cytoplasmic enzyme lactate dehydrogenase (LDH) in the culture medium is indicative of the leaky membranes and lysis associated with cellular death (Wagner *et al.*, 1992). Extracellular LDH concentration has been used as a measure of cell death, lysis, and release of cellular contents (Chevalot *et al.*, 1994). In this experiment, it was found that extracellular LDH activity increased as population viability decreased (Figure 4.1.7a), more than doubling during the early decline phase during which time the viability fell from 75% to less than 40%. The extracellular LDH activity is proportional to the concentration of dead, but intact, cells until the end of the early decline phase, yielding 0.244 U/c (Figure 4.1.7b and c). Very little cellular debris was observed up to this time, suggesting that cell lysis was insignificant through to the end of the early decline phase.

As the population moves into the late decline phase, the concentration of dead cells begins to decrease, presumably due to the combination of declining viable cell concentration and increasing lysis of dead cells (input and output to the dead cell compartment). This is the point at which the extracellular LDH activity jumps from about 150 U/L to about 350 U/L (between 275 and 350 hours of culture time, Figure 4.1.7b). This pattern of sudden LDH release from cells into the culture medium can be explained as a consequence of the partial synchrony of this culture, in that a significant proportion of the population enters apoptosis at the same time. Since apoptosis (as a physiological process) is likely of a fixed length, this proportion of the population should commence secondary necrosis, culminating in cell lysis at approximately the same time. Thereafter, the release of LDH becomes inversely proportional to the dead cell concentration. This can be interpreted as release of LDH from the lysed cell compartment. Hence, the appearance of LDH in the culture medium should be considered to have two distinct sources: leakage through the membranes of intact dead cells, and release from lysed cells. The latter source is also indicative of the lysis of subcellular organelles,

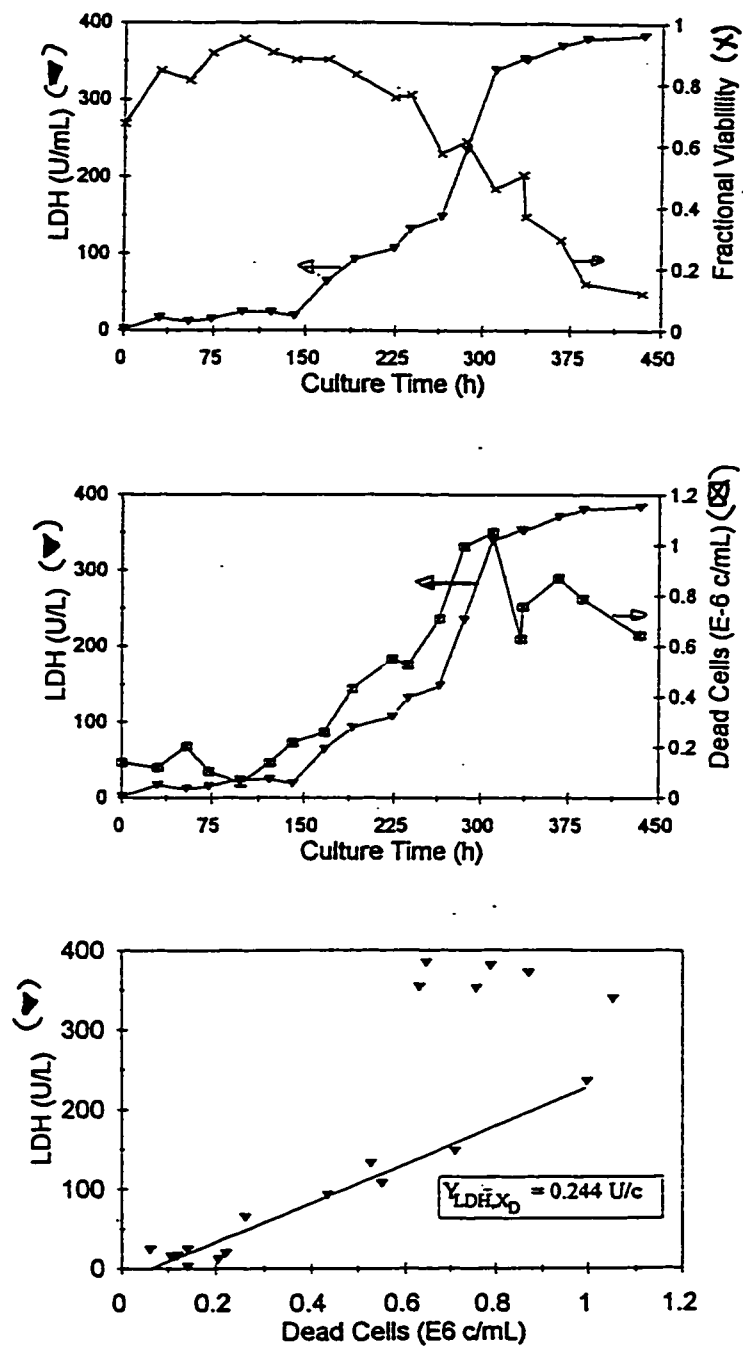


Figure 4.1.7: LDH as an indicator of 'leaky' membranes (and therefore, cell death).

- The extracellular LDH concentration increases as the viability of the population decreases.
- The accumulating extracellular LDH concentration is proportional to the accumulating dead cell concentration until the onset of significant cell lysis (300 hours), after which extracellular LDH continues to accumulate at a rate proportional to the rate of cell death, but is no longer proportional to the dead cell concentration because cells are leaving this subpopulation as a result of cell lysis.
- The extracellular LDH concentration can be expressed as a yield of LDH from dead cells until the point of significant cell lysis.

including lysosomes which would involve the concomitant release of proteases. Visual evidence of significant cell lysis (cellular debris) was not observed prior to the onset of the late decline phase.

The semi-synchronous growth pattern is more clearly depicted in Figure 4.1.8. In these plots, the accumulation of cells in the G1 phase during the lag phase of the population is seen during the first three days of the culture. The re-entry of the G1 arrested subpopulation into the cycling fraction appears to be consistent with the probabilistic model proposed by Smith and Martin (1973). This random re-entry into the cycling fraction is coupled with a portion of the population that was not arrested in G1, thereby preventing complete synchrony of the population. Peaks in the S phase at approximately 125 hours, 200 hours, and 290 hours, followed by peaks in the G2/M phase support the interpretation of semi-synchronous traverse of the viable population through the cell cycle.

In Figure 4.1.8a, the size of each of the four subpopulations is depicted as a fraction of the whole viable population. At 300 hours, well into the decline phase, cells are accumulating in the G1 phase. At approximately 340 hours there is a sharp decrease of cells in all of the cycling phases and a corresponding increase in the size of the A phase subpopulation. The fact that cells are accumulating in the G1 phase just prior to the increase in the A phase subpopulation suggests that cells enter apoptotic senescence from the G1 (or G0) phase. This is substantiated by considering the subpopulations of only the cycling fraction of the viable cells (Figure 4.1.8b). Here, it can be clearly seen that almost all of the cycling fraction resides in the G1 (or G0) phase by the end of the batch culture.

Further verification of the semi-synchrony of this population is found in the percentages residing in each of the cell cycle phases during the exponential growth phase. In asynchronous growth, 70 to 80% of the viable population resides in the S cell cycle phase during the early exponential growth phase (Lakhotia *et al.*, 1992). The proportion in S phase decreases through the remainder of the exponential growth phase, as the proportion in G1/G0 phase increases, presumably as cells arrest in G1/G0 in response to diminishing nutrient pools (Lakhotia *et al.*, 1992). The proportion of the population in G2/M remains relatively constant at 8 to 10 % until the late exponential growth phase, when it begins to increase. In contrast, in this culture the proportion of the viable population in S phase never rises above 60%, while the proportion in G1/G0 remains high during early exponential growth phase, only falling to approximately 20% in mid and late exponential growth phase (Figure 4.1.8a).

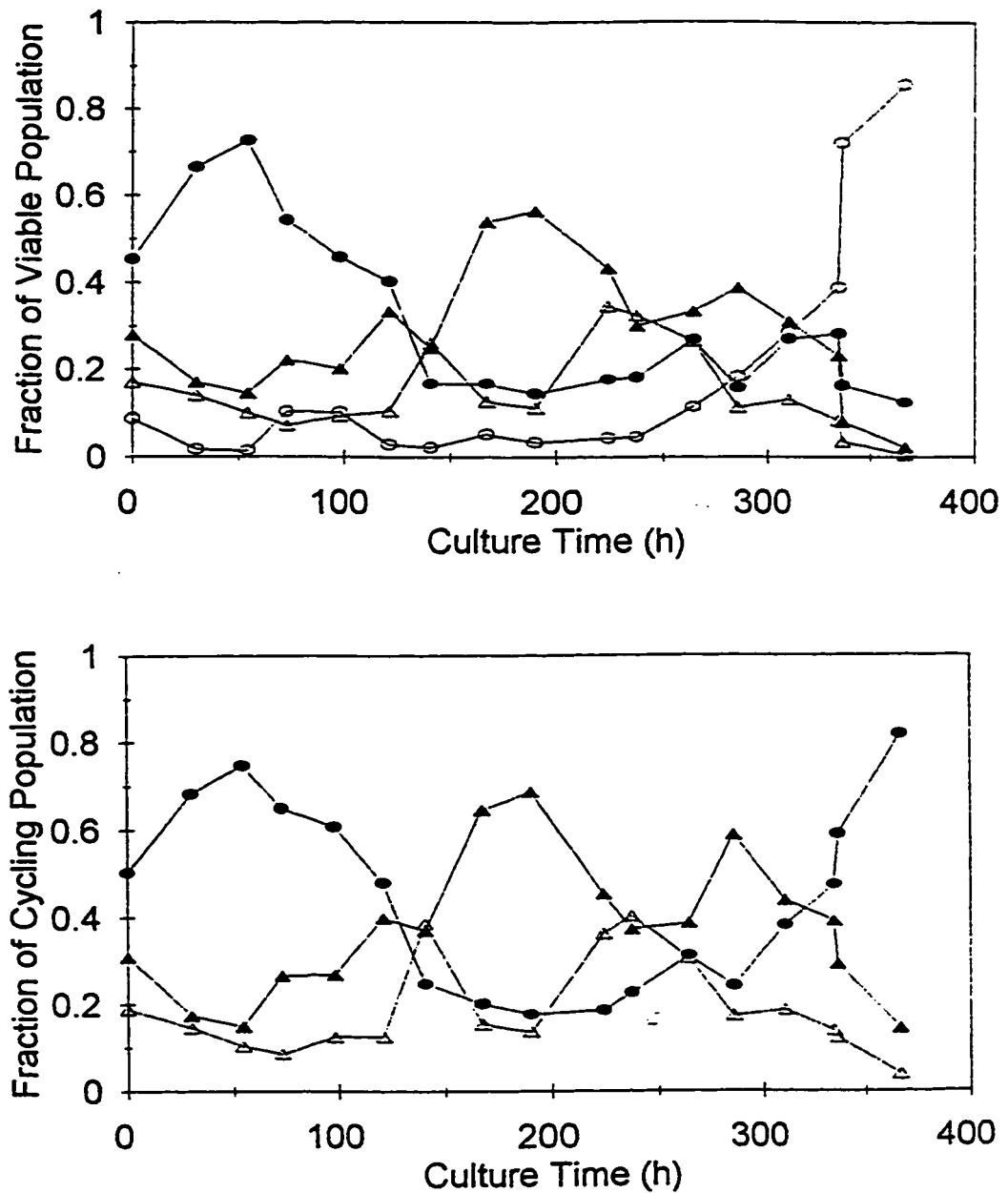


Figure 4.1.8: The semi-synchrony of CHO1-500 dispersed suspension batch culture is indicated by peaks in the subpopulations segregated by cell cycle phase. solid circles: G1/G0; open circles: A phase; solid triangles: S phase; open triangles: G2/M

a) entire viable population. The population accumulates in the apoptotic sub-compartment during the late decline phase.

b) the cycling fraction of the viable population (A phase excluded) The cycling fraction accumulates in G1/G0 during the lag phase and again during the late decline phase.

Population Segregation on the Basis of DNA Content

The above interpretation of the population growth dynamics is verified by considering the relative DNA profiles of the population over the course of the batch culture. In Figure 4.1.9, DNA population profiles are presented for four batch cultures cultivated under the conditions described previously. The batch cultures differed in terms of the initial concentrations of lactate, glucose, glutamine and serum. Nevertheless, the DNA population profiles all follow a remarkably similar trend. Again, it is seen that true asynchrony is only achieved for about 24 hours during the early exponential phase. The population accumulates in the G1/G0 phase during the first 3 days of culture, and the population resides primarily in the A phase by the end of the batch culture. The samples were gated based on a cell size between 8 and 20 μm in diameter, which is considered to be the range for intact dead CHO cells through to mitotic viable CHO cells in dispersed suspension, and which was verified microscopically (see Section 4.2). Greater than 99% of the particles in the samples fell within this gate through mid- exponential phase in all of these cultures. Thereafter the gated percentage of samples fell to approximately 95%, with the majority of the excluded particles having a diameter greater than 20 μm , and most likely representing 2 to 5 cell aggregates which were microscopically visualized from the mid exponential phase until the late decline phase. It was only in the late decline phase that the gated sample portions fell below 90%, and that the cellular debris indicative of lysis was microscopically visualized.

Necrotic cells, having ruptured or leaky cell membranes, would appear in DNA to RNA graphs as having a normal complement of DNA but a very low complement of RNA. In Figure 4.1.9, by virtue of this criterion, it can be seen that very few cells appear to leave the viable population through primary necrotic senescence. Swollen necrotic cells would also have a large size, corresponding to a large forward scatter (FS), but a low density, corresponding to a low side scatter (SS). Inspection of Figure 4.1.9a and Figure 4.1.9d substantiates the insignificant role of primary necrosis in these cultures. Cell death is discussed further in Section 4.2.

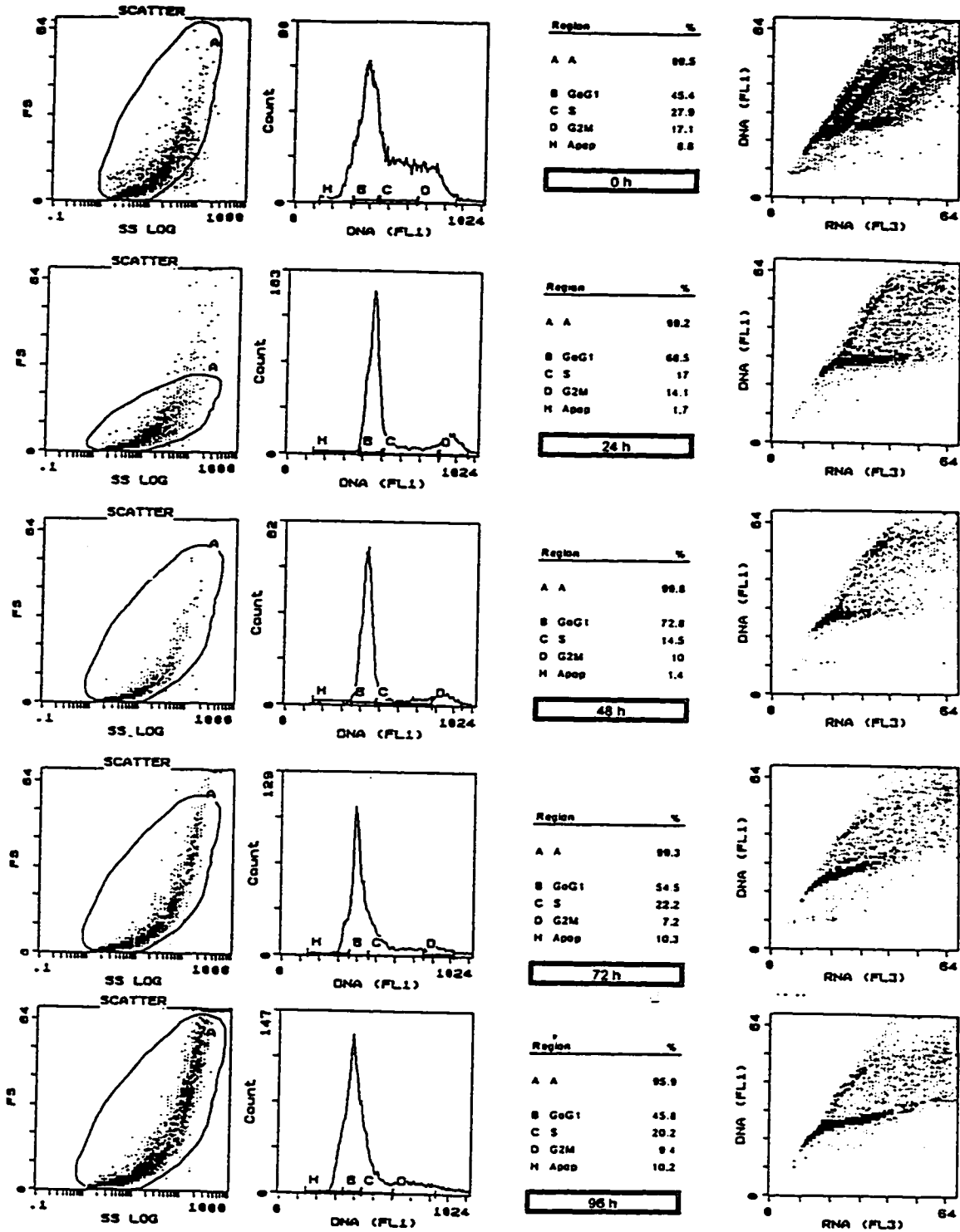


Figure 4.1.9: Flow cytometric profiles of CHO1-500 cells during dispersed suspension batch culture in serum-free medium. left-to-right: light scatter graphs; relative DNA profiles; proportion of population in the cell cycle phases; DNA vs. RNA

a) Initial substrate conditions: high GLC, low GLN, no LAC, no Serum

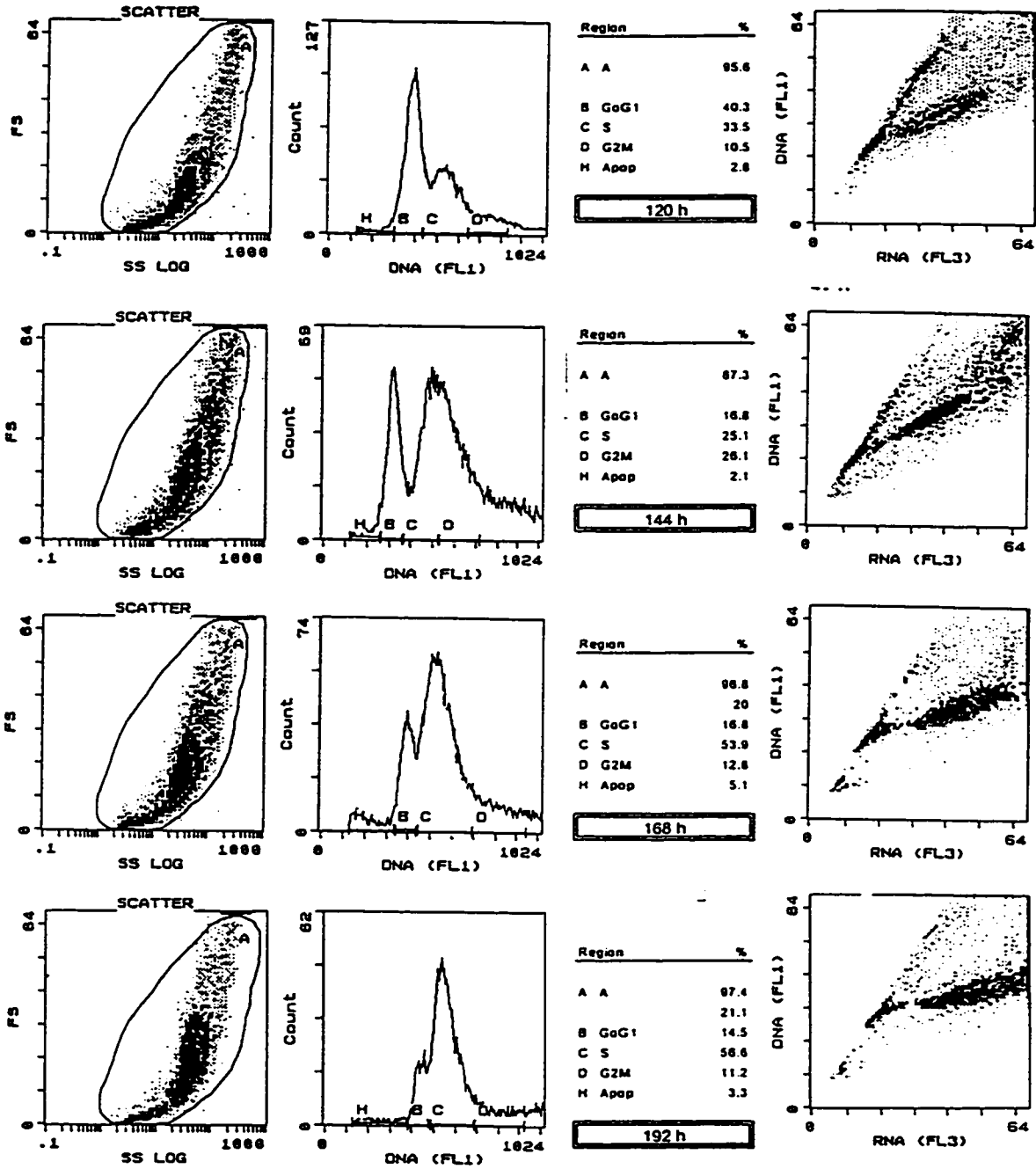


Figure 4.1.9a continued: 120 hours to 192 hours of batch culture time

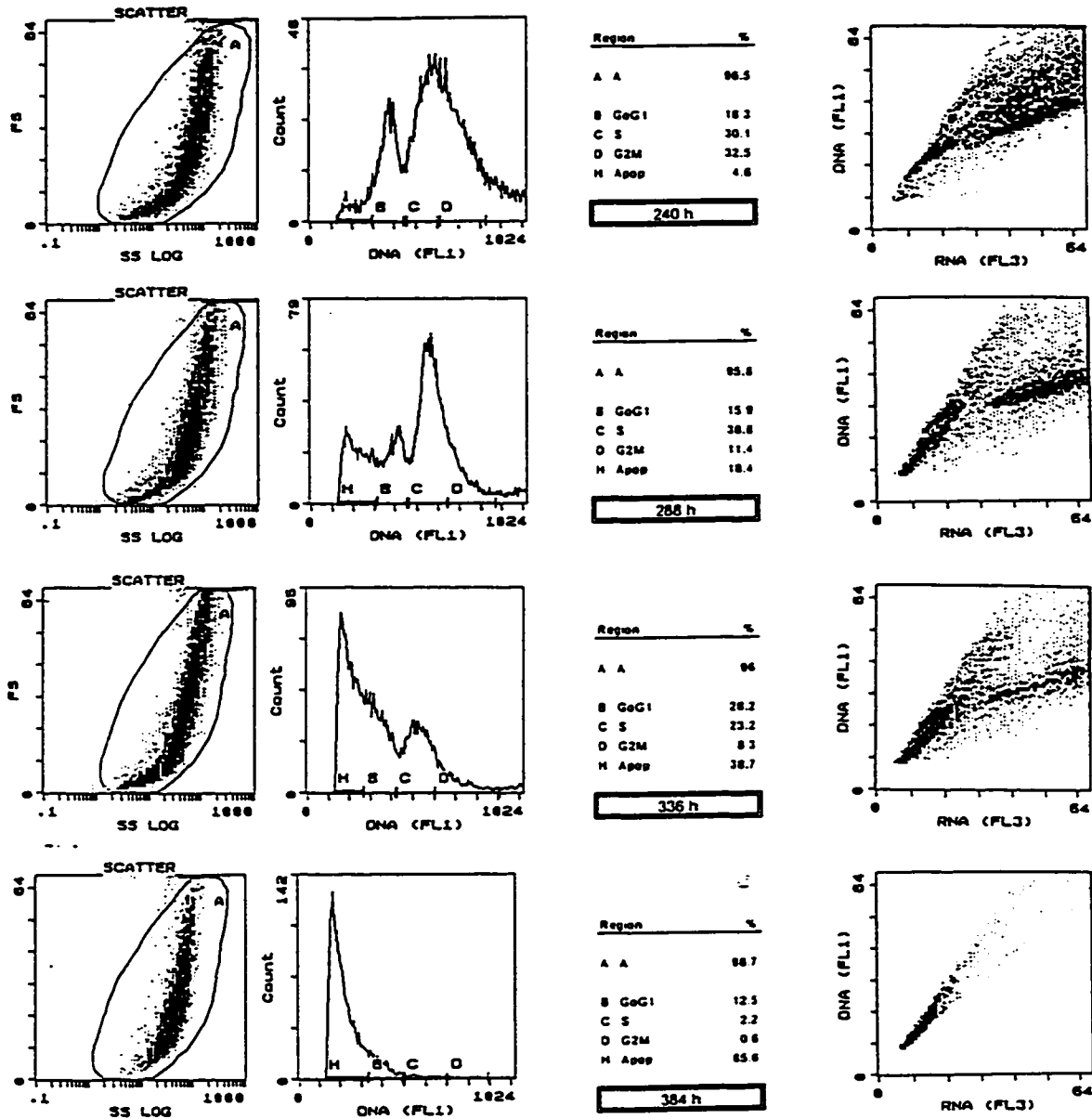


Figure 4.1.9a continued: 240 h to 384 h of batch culture time.

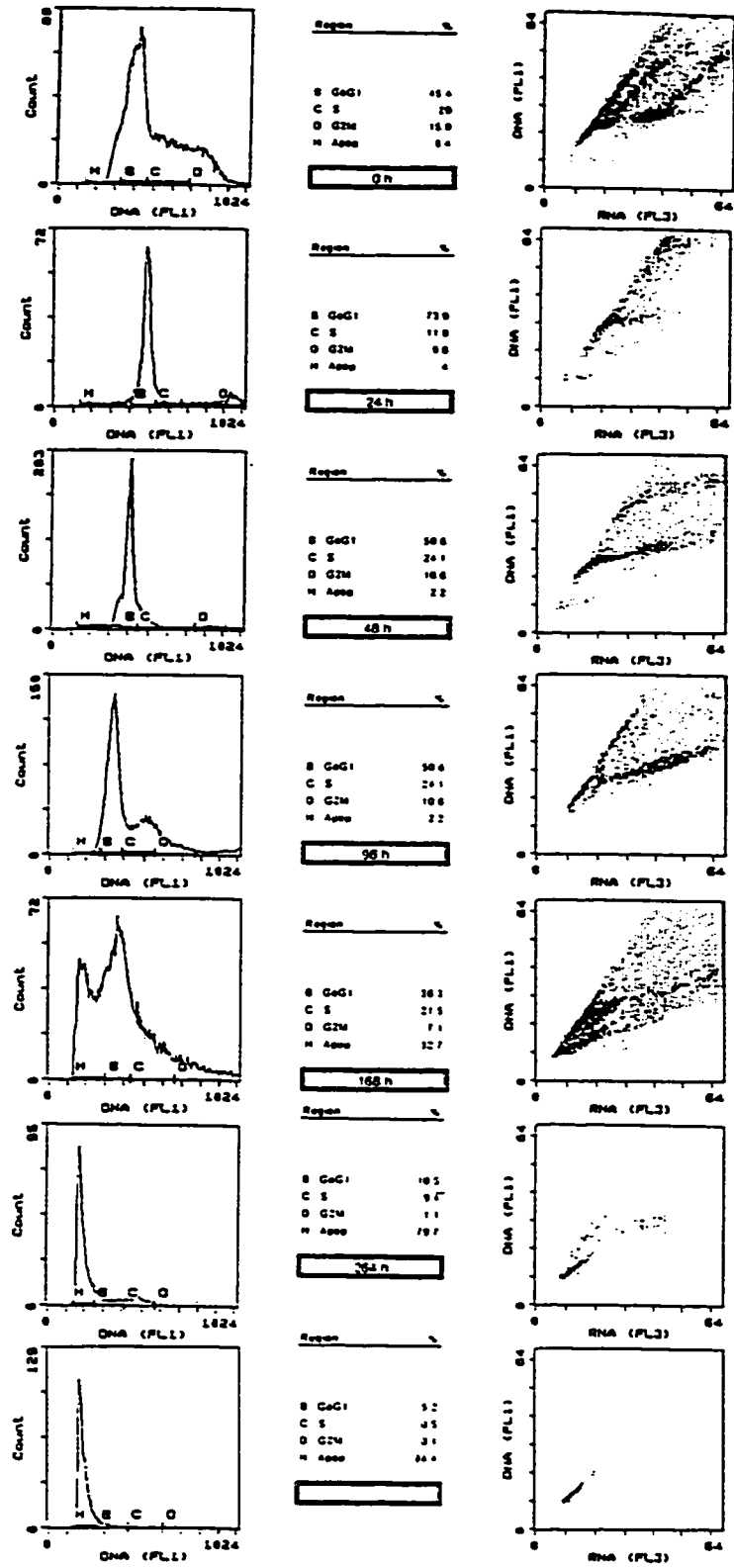


Figure 4.1.9b: Initial substrate conditions: low GLC, high GLN, high LAC, no Serum

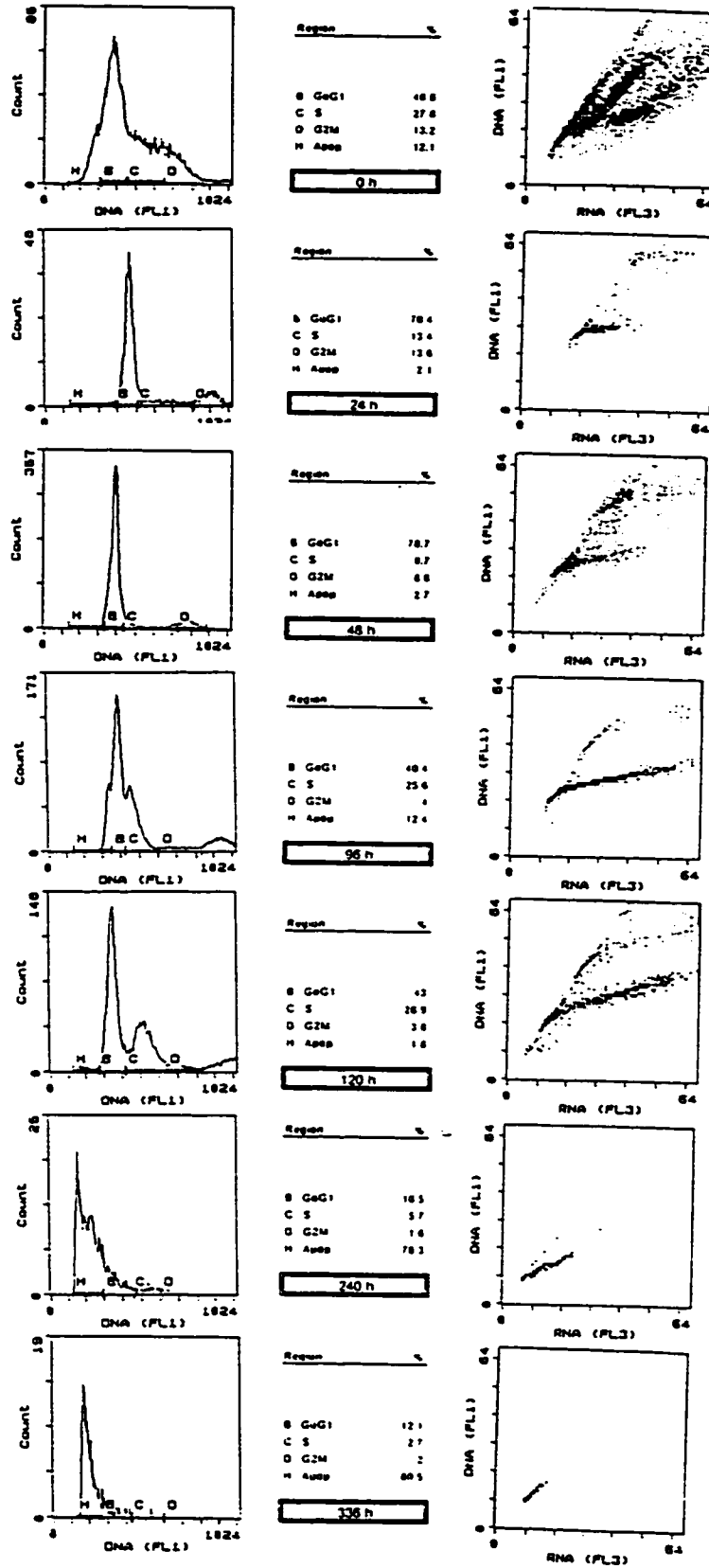


Figure 4.1.9c: Initial substrate conditions: high GLC, low GLN, high LAC, no Serum

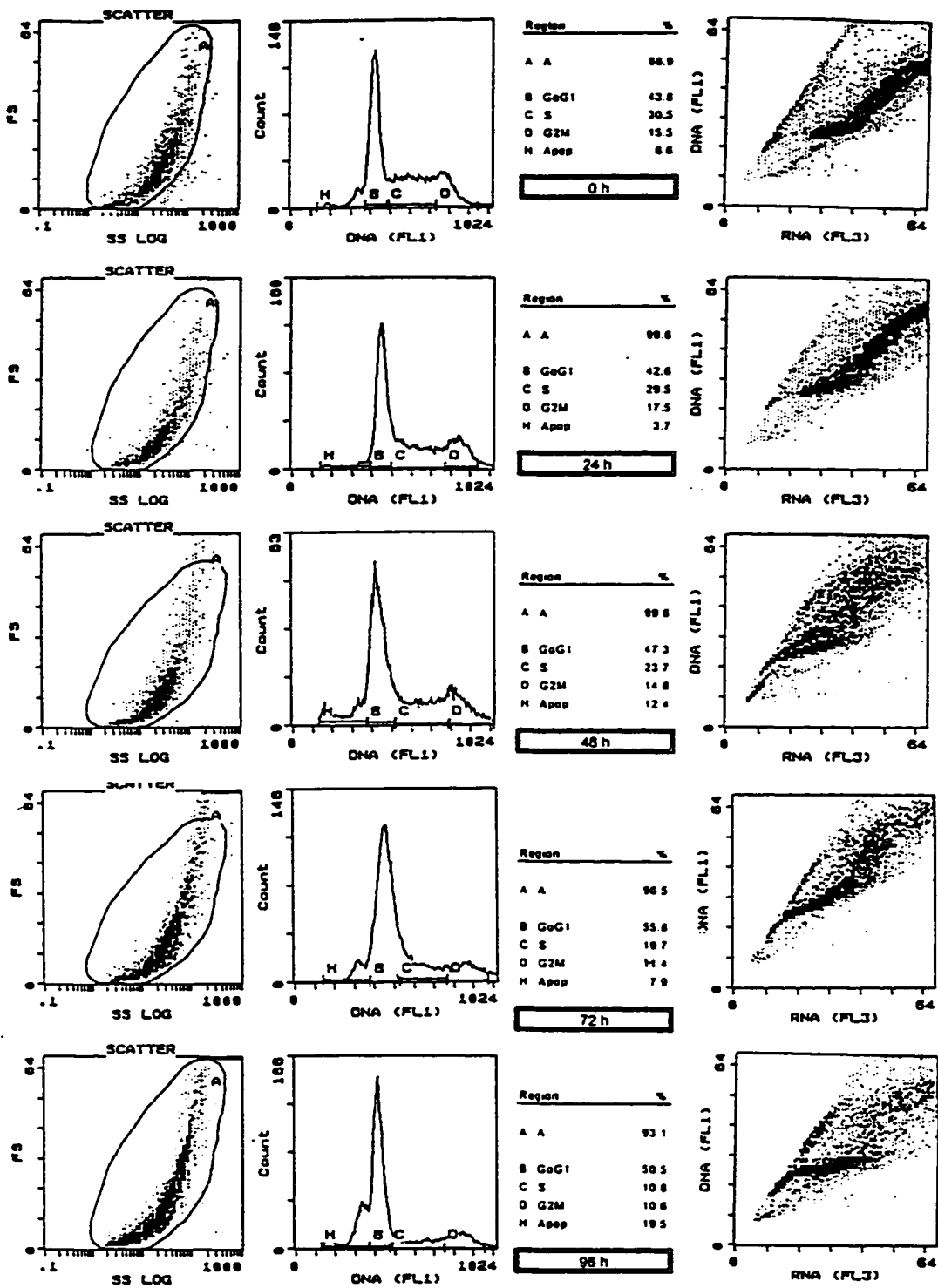


Figure 4.1.9d: Initial substrate conditions: high GLC, low GLN, low EAC, high Serum

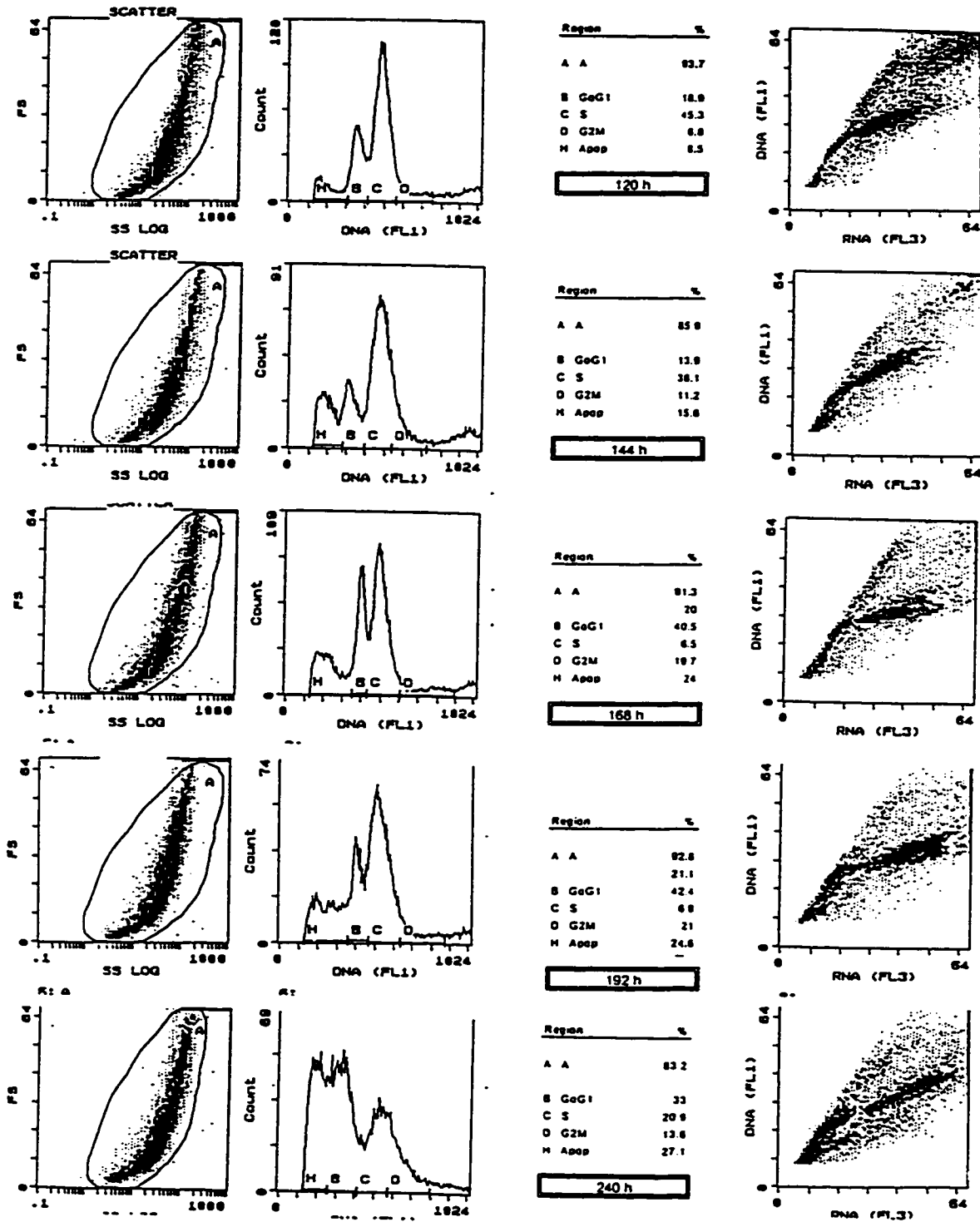


Figure 4.1.9d continued: 120 h to 240 h of batch culture time.

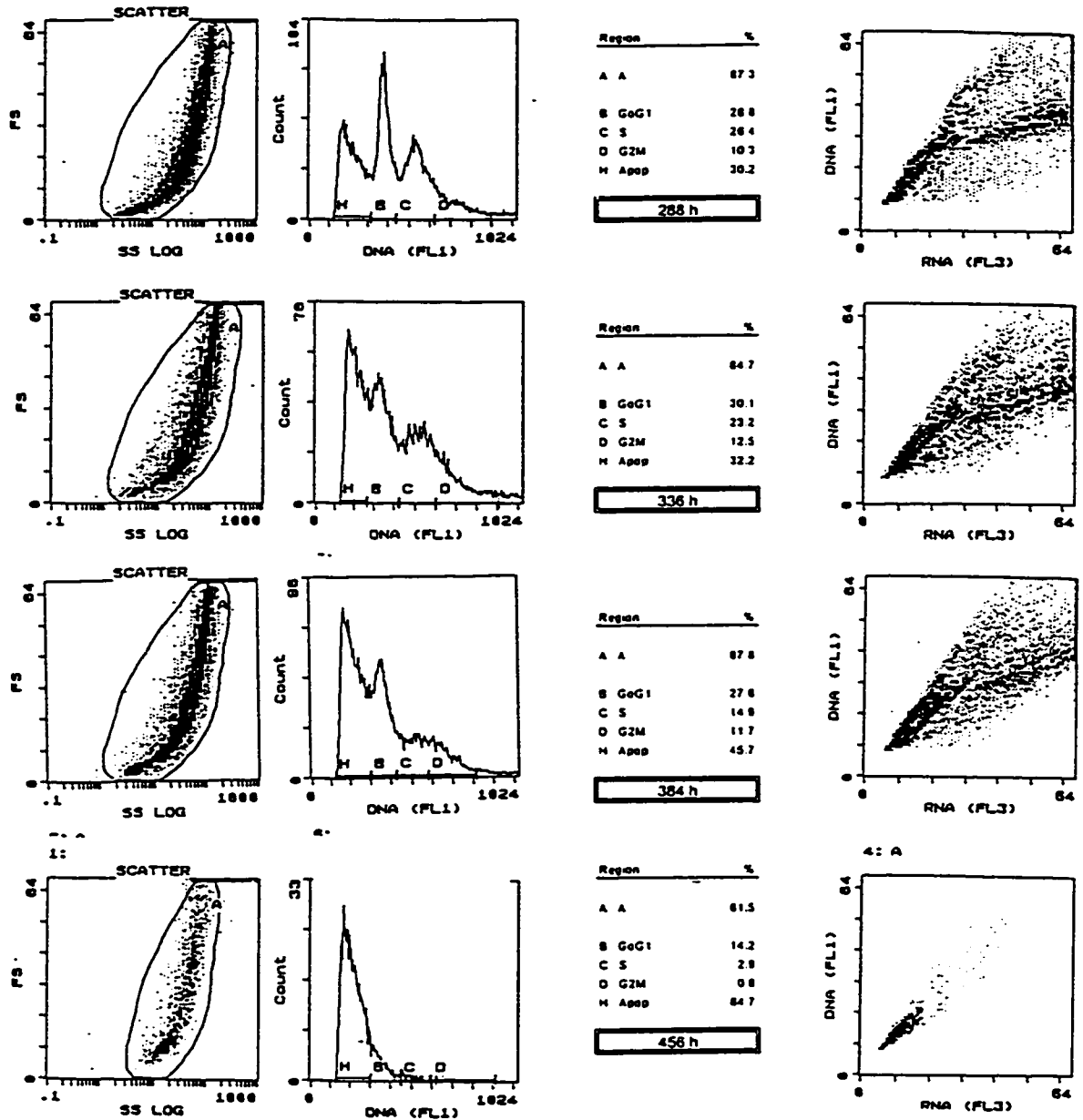


Figure 4.1.9d continued: 288 h to 456 h of batch culture time.

Estimating Concentrations in the Dead Cell and Lysed Cell Compartments

The inputs and outputs of the dead cell compartment and of the lysed cell compartment are presented in Figure 4.1.10. Contributions to the dead cell pool come from both the cycling fraction, through primary necrosis, and the apoptotic fraction, through secondary necrosis. Exit from the dead cell pool is through cell lysis, and *vice versa*, entry into the lysed cell pool is from the dead cell compartment. Considering the hypothesis shown in Figure 4.1.10, the change in the dead and lysed cell concentrations may be calculated from the following equations:

$$\frac{d[\text{dead cells}]}{dt} = k_n [\text{cycling cells}] + k_d [\text{apoptotic cells}] - k_l [\text{dead cells}] \quad (4.3)$$

$$\frac{d[\text{lysed cells}]}{dt} = k_l [\text{dead cells}] \quad (4.4)$$

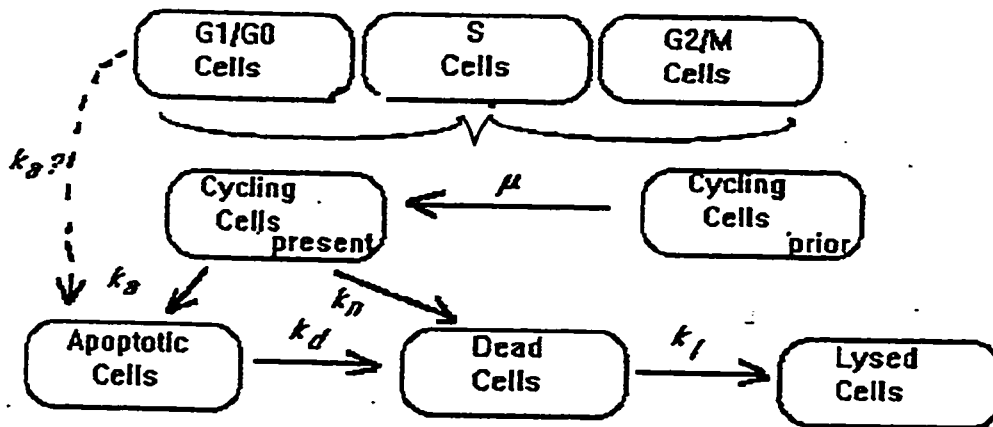


Figure 4.1.10: Subpopulation compartments based on cell cycle theory. The population can be segregated into a cycling fraction, an apoptotic fraction, a dead fraction, and a lysed fraction. The cycling fraction can be further subdivided into a G1/G0 fraction, an S fraction, and a G2/M fraction.

μ : cell cycle rate constant; k_a : rate constant of apoptosis entry; k_n : rate constant of primary necrosis;
 k_d : rate constant of secondary necrosis; k_l : rate constant of cell lysis

It may be concluded that primary necrosis plays an insignificant role in batch culture kinetics of this rCHO cell line under normal operating conditions such as those employed here. Thus, k_n is considered to be negligible, and contributions to the dead cell pool from the cycling fraction can be neglected. Significant amounts of cellular debris was not observed prior to 275 culture hours, so that exit from the dead cell pool through cell lysis can be considered to be negligible up to this point. Therefore, the rate of change in the dead cell pool can be calculated directly as the rate of increase in the measured dead cell concentration up to this point. From Figure 4.1.7b it can be seen that the concentration of dead cells actually decreases slightly up to mid exponential phase, at a rate of -310 c/mL/h. Since it is not likely that a significant number of cells are entering the dead cell pool during this time, this may be considered to be the rate of cell lysis during this time. From mid exponential phase through to the end of the exponential phase the dead cell pool is increasing at a constant rate of 3638 c/mL/h.

Recombinant Protein Productivity

As discussed in Section 4.1.1, productivity is associated with cell-hours rather than just the number of cells in the system. Thus, the first step in considering productivity kinetics is to convert cell numbers into cell-hours. When the unsegregated population is considered in terms of cumulative cell-hours (Figure 4.1.11), the existence of the lag phase is apparent. Under the conditions of this experiment there is apparently no metabolic switch, and the population proceeds smoothly through the exponential and decline phases. Balanced growth is characterized by time-invariant chemical, physical, and physiological state of the culture, while the population increases exponentially (Gu *et al.*, 1993). The exponential growth phase represents an approximately constant chemical state, in that nutrients are present in excess, and biowastes are at subtoxic levels. A constant average physiological state of the population occurs when growth is asynchronous and the relative size of each subpopulation is not changing. It can be seen that this condition is never fully attained during this batch culture. This is due to the partial synchrony of the cycling population.

The recombinant tPA productivity, as a function of the unsegregated population, is apparently growth-phase-associated. In Figure 4.1.12 it can be seen that the lag phase specific productivity is approaching four times that of the exponential and early decline phases. Although the productivity pattern observed here is not identical to the productivity pattern observed under different initial conditions (eg. see Section 4.1.1 and Appendix C), a high lag phase specific productivity is consistently observed. This is not consistent with S-phase specific protein production, the suggested pattern for this plasmid construct (Banik *et al.*, 1996; Gu *et al.*, 1993; Mariani *et al.*, 1981) (see Section 2.2), and which would correspond with maximum specific productivity during the exponential growth phase. However, here the protein is measured as the tPA titer in the culture medium, so that 'production' is the end point of

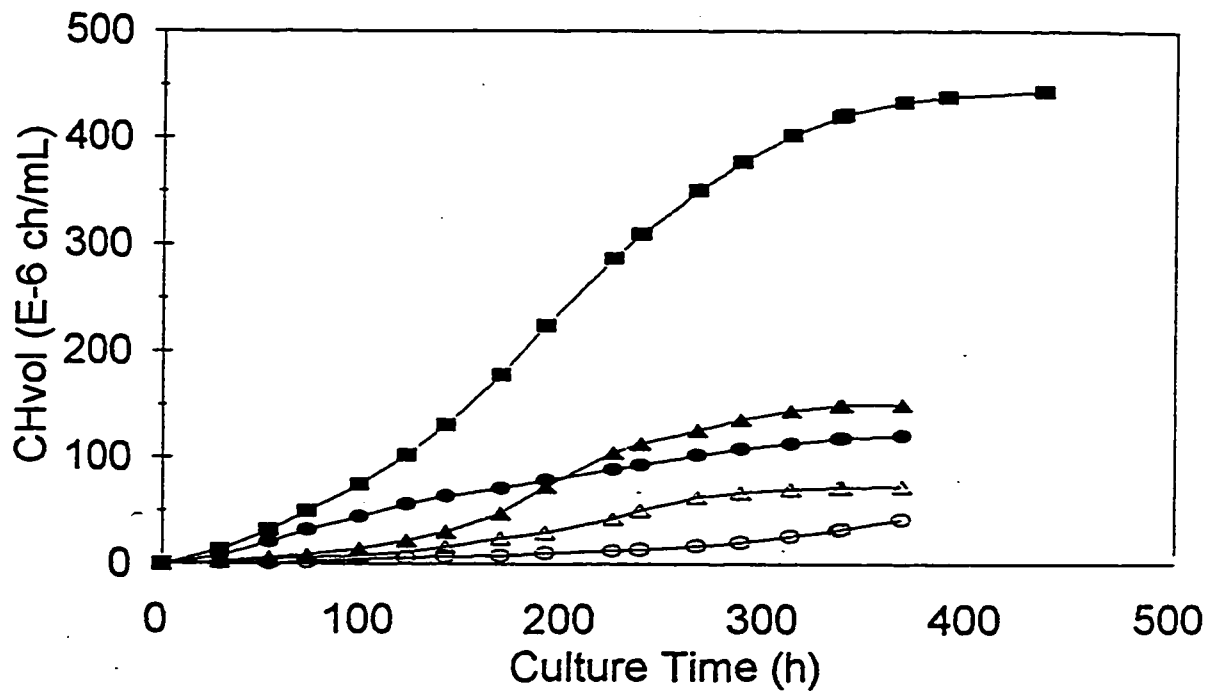


Figure 4.1.11: The viable population and subpopulations presented as cell-hours. Data recalculated from Figure 4.1.6.
 solid squares: viable population cell-hours; solid circles: G1/G0 cell-hours; open circles: A cell-hours; solid triangles: S cell-hours;
 open triangles: G2/M cell-hours.

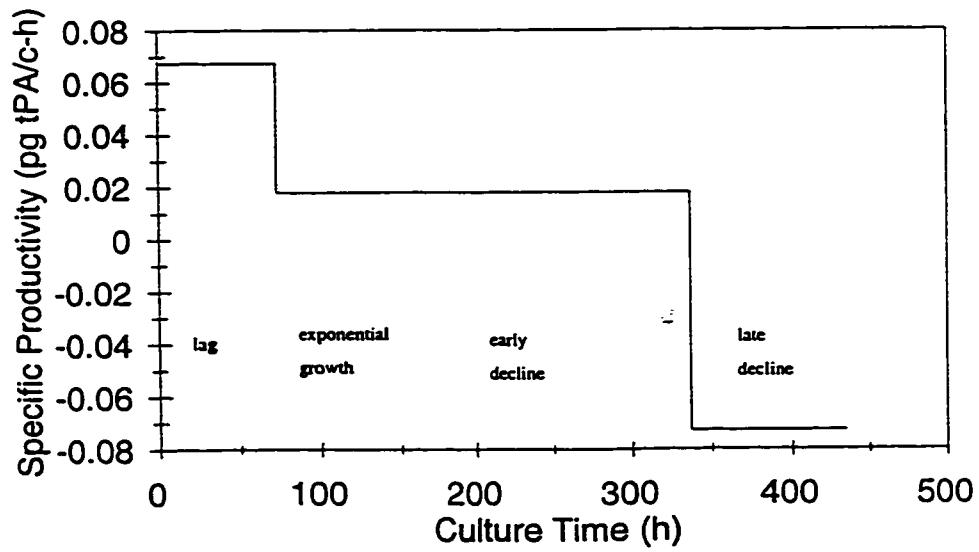
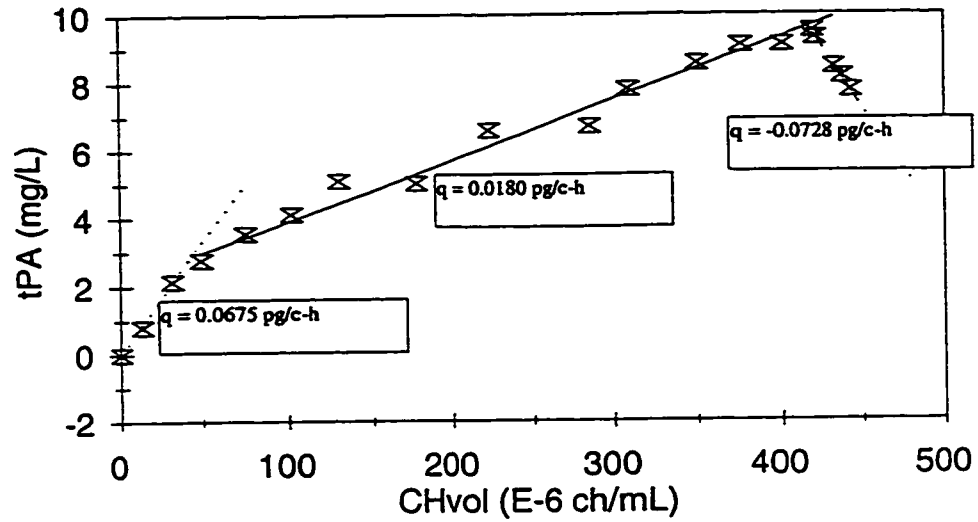


Figure 4.1.12: The specific productivity of h-tPA from the CHO1-5₅₀₀ cell line is growth-phase-associated.

synthesis and secretion. It is therefore possible that tPA synthesis occurs during the S phase, but that the observed increase in protein titer does not directly correlate with traverse through the S phase.

When the tPA concentration is plotted as a function of the individual subpopulations (Figure 4.1.13), it is seen that the tPA production is directly proportional to the hours that the viable population spends in the G1/G0 phase, strongly suggesting that secretion occurs during this cell cycle phase. This is in contrast with the findings of Kubbies *et al.* (1990) and Scott *et al.* (1987) who found a direct correlation of tPA production with the S phase, and Aggeler *et al.* (1982) who observed peak tPA production during the G2/M phases. All of these researchers measured extracellular tPA only, as is also the case here.

The Role of Dihydrofolate Reductase Expression

Dihydrofolate reductase, a key enzyme for thymidine nucleotide synthesis, is essential for the replication of DNA, as reviewed in Section 2.3. It should not be surprising, therefore, for the synthesis of both recombinant and endogenous DHFR to be cell cycle phase associated, irrespective of the nature of the transcription of the *dhfr* gene (constitutive or induced). The relative specific DHFR levels in the different cell cycle phases was investigated by comparing against relative DNA content profiles in the population (Figure 4.1.14). In Figure 4.1.14a about 73.5% of the cells of a density arrested population reside in the G1/G0 phase, with about 16% in the S phase. The corresponding DHFR associated fluorescence profile shows two distinct populations, a group comprising approximately 60% of the population with a relative DHFR content of 1, and a group comprising approximately 20% of the population with a relative DHFR content of 10. In Figure 4.1.14b, a population of cells in early exponential phase shows good correlations between the proportion of cells in G1/G0 phase and a relative DHFR content of 1, and between the proportion of cells in S phase and a relative DHFR content of 10. These correlations are further substantiated in the observed patterns in a mid-exponential phase population (Figure 4.1.14c). In the late decline phase population shown in Figure 4.1.14d, with essentially all of the viable population residing within the A phase (98.4%), there is no detectable DHFR associated fluorescence. Collectively, these graphs suggest that there is about 10X as much DHFR in S phase cells as in G1/G0 phase cells, and that DHFR is not expressed during apoptosis. These findings do not parallel the appearance of tPA in the culture medium for this culture system. The accumulation of extracellular tPA was found to be a linear function of the time spent in the G1/G0 phase (Figure 4.1.13).

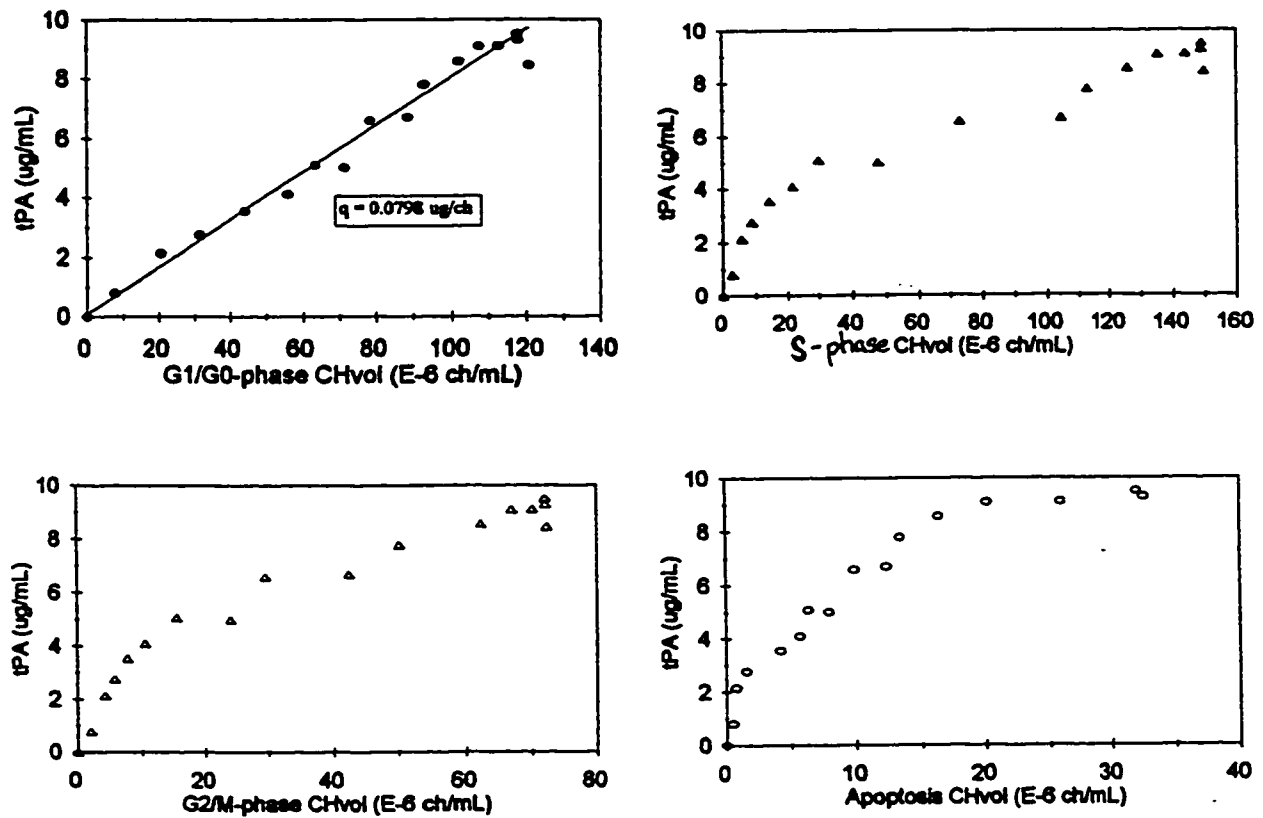
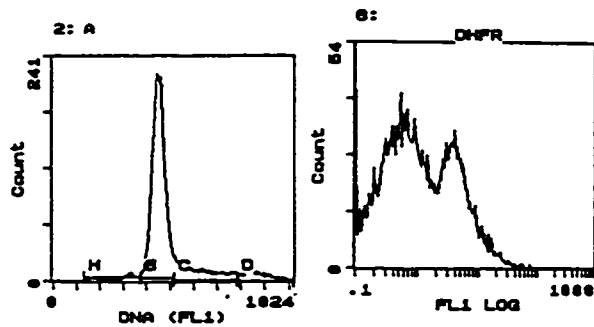
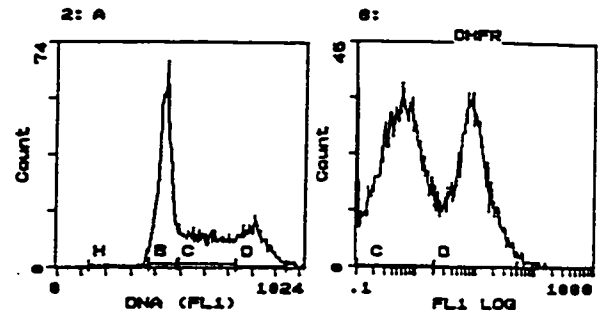


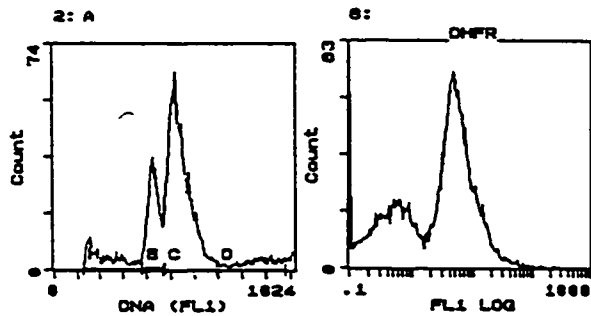
Figure 4.1.13: The appearance of tPA in the medium is a linear function of the time spent by the viable population in the G1/G0 cell cycle phase.



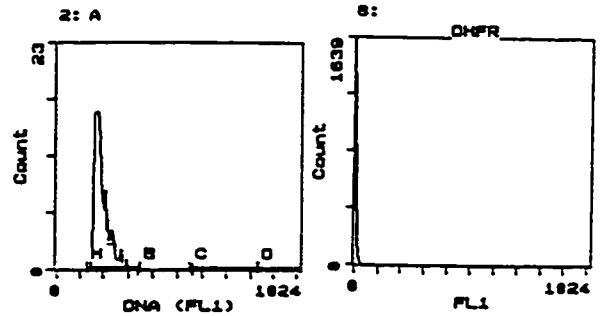
A) density arrested population
 G1/G0 73.5%; S 15.8%; G2/M 6.4%; A3.79%
 Relative DHFR: 1X - 60%; 10X - 20%



B) early exponential phase population
 G1/G0 44%; S 29%; G2/M 21%; A 1.5%
 Relative DHFR: 1X - 38%; 10X - 29%



A) mid exponential phase population
 G1/G0 18.6%; S 50.4%; G2/M 6.4%; A 9%
 Relative DHFR: 1X - 20%; 10X - 60%



B) late decline phase population
 G1/G0 1.1%; S 0.4%; G2/M 0%; A 98.4%
 Relative DHFR: 1X - 0%; 10X - 0%

Figure 4.1.14: Relative specific DHFR content and relative DNA content of CHO1-5₅₀₀ cells during the cell cycle phases. G1/G0 phase cells correlate to a relative DHFR content of 1X. S phase cells correlate to a relative DHFR content of 10X. DHFR associated fluorescence is absent in a population residing in the A phase.

When a foreign protein gene is co-transfected with *dhfr*, but the two genes are under the control of different promoters, the timing of the expression of the two genes may differ. The system used in the CHO1-5₅₀₀ cell line utilizes the constitutive SV40 early promoter for the expression of both proteins (tPA and DHFR), ensuring cotranscription. However, it is evident from Figures 4.1.13 and 4.1.14 and the results of other workers that the appearance of secreted tPA and the synthesis of DHFR may not occur in concert. Whether the genes are transcribed in concert or not, post-transcriptional modifications, translation, and post-translational modifications which collectively result in the appearance of the complete protein can be subject to different controlling influences. Furthermore, the appearance of a secreted protein in the culture medium is the endpoint of additional spatiotemporal processing.

Investigators working with the DHFR based expression systems in CHO cells tend to report solely on the levels of the complete proteins. Several report S phase associated synthesis of the protein product, and it has become generally assumed that this is coincident with S phase associated appearance of DHFR. Gu and co-workers (1993) found that intracellular levels (synthesis) of recombinant β -galactosidase in CHO cells increased exclusively during the S phase. In their system, *dhfr* was under control of the SV40 promoter, while *β -galactosidase* was under control of the constitutive hCMV promoter. These authors did not calibrate synthesis of DHFR to the phases of the cell cycle. Banik and co-workers (1996) found that the intracellular levels of recombinant β -galactosidase in CHO cells was directly proportional to the cell specific growth rate. This suggests that the synthesis of this recombinant protein, which is under the influence of the constitutive SV40 early promoter, is S phase associated. Similarly, the production of recombinant human interferon- γ by CHO cells was reported to be growth-associated (S phase dependent), but the promoter was not identified by the authors, and it was unclear as to whether intracellular or extracellular human interferon- γ levels were measured (Hayter *et al.*, 1993). This evidence of S phase associated protein synthesis is obviously not related to the control of transcription of the gene by constitutive promoters.

In agreement with the understanding of DHFR gene transcription and protein synthesis patterns (see Section 2.2), it was found in this study that DHFR levels are associated with the cycling fraction of the cell population, in a cell cycle phase dependent manner. DHFR protein appearance is apparently not restricted to the S phase, but is present in the G1/G0 phase as well, albeit at an order of magnitude lower level.

The Role of Native Plasminogen Activators

The activity of native tissue plasminogen activator in mammalian ovary cells is relatively high. Although not approaching the 720 Units per gram of fresh tissue found in human uterus samples, the human ovary is relatively rich in tissue plasminogen activator expression, yielding 210 Units per gram of fresh tissue compared with only 110 Units per gram of fresh skeletal muscle, 25 Units per gram of fresh testes, and 0 Units per gram of fresh liver (Rouf *et al.*, 1996). Native ovarian tPA perhaps plays a role in follicle maturation and traverses through the fallopian tubes. Native ovarian tPA expression and secretion may therefore be inducible, and tied to menstrual cycle. Turnover of differentiated ovarian cells is low, with the cells residing primarily in the G1/G0 state, so that expression and secretion of native ovarian tPA is likely associated with the G1/G0 cell cycle phase. Stimulation of the expression and secretion of native ovarian tPA may influence the expression and secretion of recombinant tPA.

Transformed cells contain and secrete excess levels of activators of plasminogen, when compared with normal cells (Scott *et al.*, 1987). The maximal plasminogen activator activity in the culture supernatant (maximal secretion of enzyme) of a rat prostate adenocarcinoma cell line was found to correspond with the S/G2 cell cycle interface (Scott *et al.*, 1987). In accordance with this finding, the levels of intracellular plasminogen activators have been shown to decrease during the active cell cycle and to accumulate in cells arrested in G1/G0 (Loskutoff and Paul, 1978).

The activity of both non-specific neutral proteinases and of plasminogen activators has been reported to be increased in mitotic cells (Aggeler *et al.*, 1982). These workers found that plasminogen activators were secreted from Chinese Hamster Ovary fibroblasts in culture during the G2 and M cell cycle phases, with the activity being about twice that associated with the early cell cycle phases. This cell cycle specific secretion of native plasminogen activator occurred both in serum-free medium and in medium containing 5% serum. As these adherent cell populations reached confluence, they became arrested in the G1 phase, and the secretion of plasminogen activators decreased by several fold. The synthesis of extracellular matrix proteins also altered as the population approached confluence. Cells secreted fibronectin and procollagen type III throughout the entire culture time, but procollagen type I was only secreted as the population approached confluence. Also, the ratio of fibronectin to procollagen increased at confluence. The authors suggest that a physiologic role for plasminogen activators on cultured mitotic fibroblasts may be to break cell-matrix attachments and alter surface proteins and proteoglycans, allowing cells to round up for division. This role of plasminogen activator would presumably be constitutive. Observations in the current study confirm these findings of these authors that only after cells were in contact with each other for extended times (24 to 48 hours, or longer) did they secrete and deposit significant amounts of fibronectin and procollagen type I, which is normally the major connective tissue protein produced by fibroblasts. It was also found in the current study that adherent confluent cells of the rCHO 9606 cell line arrest in G1 (Figure 4.1.5d) and became very firmly attached to

the substratum, requiring several hours of exposure to trypsin to achieve detachment. Aspects of cell-cell contact, and physiological and morphological consequences are discussed further in Section 4.2. From the above discussion, it is possible that native regulatory mechanisms involved in the processing of tPA after transcription influence the production of the recombinant tPA.

Concluding Remarks

When mid-exponential phase CHO1-5₅₀₀ cells are inoculated into HB-CHO serum-free medium (Immucor) and cultured as a dispersed suspension in a stirred flask at 150 rpm, a large proportion appear to be temporarily arrested in G1/G0 phase. The population then proceeds through the growth phases in a semi-synchronous pattern, with a low apparent specific growth rate of about 0.011 h⁻¹. Production of recombinant tPA which is measured as the accumulation of the secreted protein in the culture medium is a linear function of the time spent by the viable population in the G1/G0 phase. Although this is in contrast to the S phase associated maximum intracellular DHFR content, no conclusions can be drawn with respect to the probability of co-expression of DHFR and tPA, because intracellular tPA content was not measured. There is no reason to suppose, however, that post-transcriptional through post-translational processing of the complete DHFR and tPA proteins would be co-regulated. Native regulatory systems for the individual proteins may play a significant role in their processing. Native ovarian tPA secretion is likely associated with G1/G0 phase, as is the secretion of tPA from CHO1-5₅₀₀ cells.

4.2 Morphological Types

The Chinese Hamster Ovary cell line, CHO-K1, and many of the CHO cell lines derived from it, grow readily both as an adherent monolayer (or multilayer) and in stirred suspension culture (Winterbourne *et al.*, 1993; Nikolai and Hu, 1992; Varani *et al.*, 1996). Preliminary experiments with the recombinant CHO1-5₅₀₀ (ATCC # CRL 9606) cell line, which is derived from the CHO-K1 parental cell, revealed that it adapted easily to aggregate suspension in serum-free static culture. The impacts of morphological type (suspension versus adherent) on the growth and production kinetics were therefore investigated.

In preliminary studies, cells were cultivated in spinner flasks at 60, 100, and 150 rpm. In serum-free medium, aggregation of suspended cells was found to be an inverse function of agitation rate, with large, relatively loose aggregates forming at 60 rpm, and tighter, spherical aggregates forming at 100 rpm. At the highest agitation rate, aggregates did not form and the population grew as a dispersed suspension. It was also found that in medium containing 10% serum, microcarrier attached cells died or became detached at 150 rpm, while cultures initiated with agitation rates of 100 and 150 rpm failed to colonize microcarriers, and even at 60 rpm microcarrier colonization was reduced. In these cultures cells proliferated as aggregated or dispersed suspensions, even in the presence of 10% serum. Hence, three morphological types, which can be induced by agitation rate, are exhibited by the CHO1-5₅₀₀ cell line: substratum attached; aggregated suspension; and dispersed suspension.

It was assumed that a pretreatment such as silicone coating would be necessary to prevent adhesion of cells to the glass bioreactor walls. However, in preliminary studies pretreatment was not performed, but there was no evidence of cell adhesion to the bioreactor walls. This can be explained by a combination of two theories: 1. the consecutive mechanisms of stable cell-substratum attachment; and 2. the model of consecutive replacement of substratum adsorbed proteins by surface-active attachment proteins (see Section 2.1).

The experimental setup for the study of the impact of morphological type resulted in two major points of difference in the three systems (Table 4.2.1). In the microcarrier suspension system (MS), serum containing medium was utilized to ensure stable attachment of cells to the microcarriers. In the dispersed suspension system (DS), an agitation rate of 150 rpm was employed to prevent aggregation. These factors may impact on the observed growth and production

kinetics, and act to obscure interpretation of the results. Further experimentation is recommended to separate out the impact of these factors. For example, the use of fibronectin coating may permit the use of serum-free medium in the microcarrier suspension system.

Microcarrier Suspension Culture

To compare attached morphological type with dispersed suspension and aggregated suspension, a microcarrier suspension format in a 1 liter working volume (2 liter total volume) stirred tank bioreactor configuration was employed. Polystyrene (NUNC) microcarriers, with a diameter range of 90 to 180 μm were precoated with 100% FBS for approximately 5 hours prior to charging to the bioreactor at a final loading of 10 g/L. A serum concentration of 10% FBS in Ham's F12 medium was chosen to ensure a concentration of attachment factors during the batch culture that was adequate to prevent desorption of the attachment layer on the microcarriers. Cells were allowed to attach to microcarriers in the absence of hydrodynamic shear by operating with only occasional 30 rpm stirring during the first 12 hours. Thereafter, the batch culture was completed with an agitation rate of 60 rpm. Headspace aeration was employed, so that air-liquid interfacial phenomena and pneumatic shear were not complicating factors. The pH did not leave the reported optimal range for growth of 7.0 to 7.8 (Borys *et al.*, 1993). Apart from adverse physiological effects outside of this range (which may impact on the biological stabilization of adherence), pH can affect the charge on the surface of the cell and its substratum, due to the degree of ionization of the charge-bearing surface groups. This would affect the electrostatic forces which play a major role in the initial adherence of cells to surfaces, and may partially explain the effect of pH on the shear sensitivity of microcarrier based systems (Crouch *et al.*, 1985). The reproducibility of the four batch runs that were made at different times, from different inocula was acceptable (Appendix C).

Cells completed initial attachment within the first two hours of culture, with very few cells remaining in the medium. By 24 hours, close to 100% of the cells were attached to the microcarriers. Less than 5% of the total cell concentration was found in free suspension throughout the batch culture time, until late in the declining phase. The cells in free suspension had a high viability of at least 70%, until the late declining phase when detached and detaching cells were mostly dead.

Table 4.2.1: Points of difference in the conditions employed for batch culture of CHO1-5₅₀₀ cells in the three morphological types.

System	% Serum	rpm	tip speed (cm/s)
MS	10	60	47
AS	0	60	47
DS	0	150	118

Morphology of Microcarrier Attached Cells

The morphology of microcarrier attached cells was explored with the aid of scanning electron microscopy during the late-exponential phase (Figure 4.2.1a) and midway through the declining phase (Figures 4.2.1b, 4.2.1c). The late-exponential phase cells are stably attached with associated spreading. Many of the cells exhibit the hemiellipsoid shape which was routinely seen in static T-flask culture (using medium containing 10% FBS). This fibroblast like shape is in contrast to the epithelial origin of these cells, but has been observed by other investigators and may be an attribute of the transformed state of these cells (Chevalot *et al.*, 1994; Winterbourne *et al.*, 1993; Konstantopoulos and Clark, 1996). The fibroblast-like morphology is common in adherent transformed cells. Konstantopoulos and Clark (1996) have noted increased insulin receptor activity and dense formation of actin stress fibers running the length of CHO cells having this morphology. The pseudopodia-like extensions which are visible at the ends of some of these cells may be associated with migration of attached cells across the substratum surface (Borys and Papoutsakis, 1992). Cells may migrate either away from populated areas to new sites for colonization, or towards the conditioned microenvironment associated with populated areas.

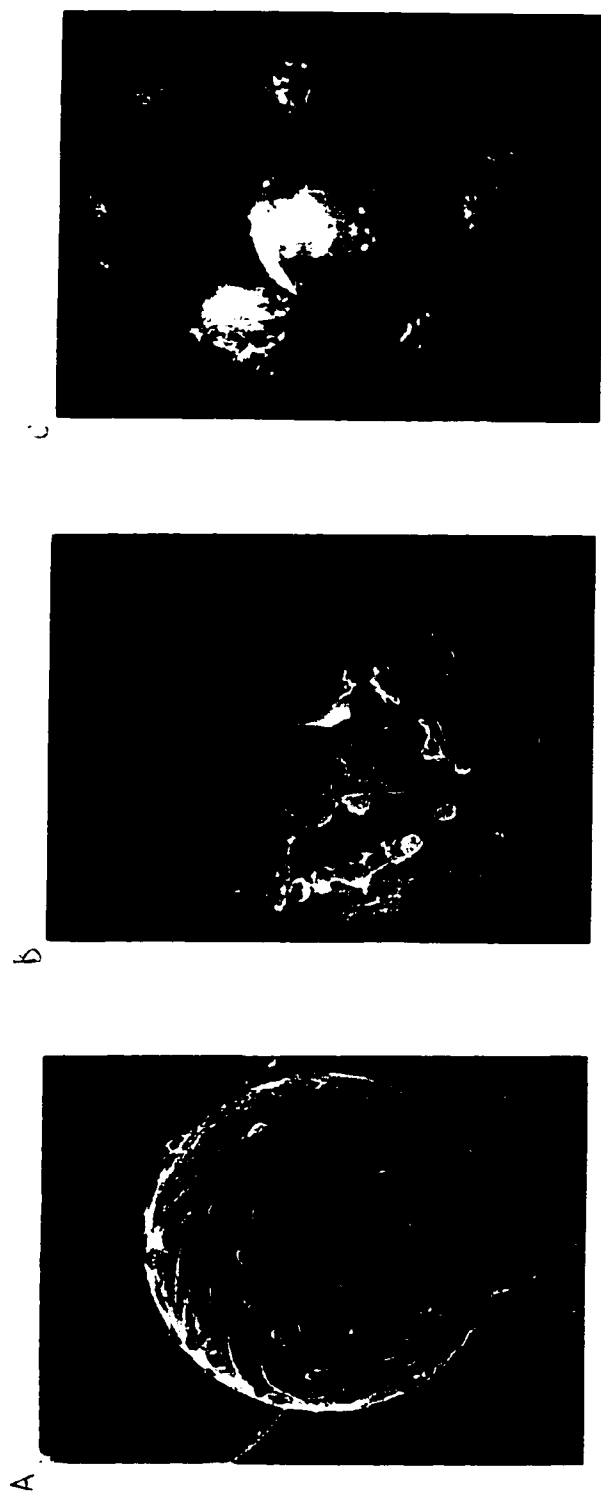


Figure 4.2.1: Polystyrene microcarrier attached cells. a. exponential phase b. declining phase c. declining phase

The rounded, but stably attached cells are likely mitotic or post-mitotic. The few detaching cells that are visible (right-hand side of view) are recognizable by their translucent appearance. These may be daughter cells which are being released from the non-attached side of their sister cells, or they may be apoptotic cells (magnification is not sufficient to see evidence of apoptosis). An aggregate formation can be seen at the lower left view of this microcarrier. Aggregate formation is seldom seen in static T-flask culture with serum-containing medium. Here, aggregate formation may be enhanced by hydrodynamic shear which may act to inhibit spreading. Many investigators have noted aggregation in microcarrier culture, even to the point of binding two or more small diameter ($< 60 \mu\text{m}$; $< 1 \mu\text{m}$) microcarriers together (Grinnel, 1980; Cheung and Juliano, 1984; Varani *et al.*, 1996; Nikolai and Hu, 1992). Evidence of intermicrocarrier aggregation can be seen in Figure 4.2.1c, but intermicrocarrier aggregation cannot be sustained with this size of microcarrier under hydrodynamic shear.

Although the cell coverage on the late-exponential phase microcarrier appears to be approximately 70%, there is a lack of the lateral alignment and close packing seen in confluent static T-flask cultures. This suggests that cell density per bead could be increased by a factor of 2 or 3 while still maintaining a monolayer. There is thus room for cell growth optimization in this culture system.

The declining phase cells (Figures 4.2.1b, 4.2.1c) are rounding up and detaching. This is consistent with the early stages of the process of apoptosis. In Figure 4.2.1b it can be seen that not all cells round up before detaching, and that cells are detaching in groups, or sheets. Long pseudopodia-like cytoplasmic bridges are also visible between cells. An explanation for this phenomenon is that cells in substratum attached colonies are physically connected by cytoplasmic bridging. When one or more of the cells in a colony enters apoptosis, rounds up, and detaches, it pulls neighboring cells with it. The neighboring cells may not be as advanced in the process of apoptosis, resulting in the detachment of non-rounded cells. In an asynchronous population, where cells do not enter apoptosis in concert, this has negative implications. Apoptotic cells may detach cycling cells which may then alter their metabolic and physiological states, which may in turn lead to premature failure of the production system. Bare patches can be seen on the microcarriers in Figure 4.2.1c where cells have detached as sheets.

The choice of microcarrier can impact on the phenomenon of *en masse* detachment. It has been shown in our laboratory (Dr. George Lu, personal communication) that CHO cells adhere strongly to dextran microcarriers (Cytodex), and do not detach even upon death. In such a system, cycling cells would not be prematurely ripped from the substratum by detaching apoptotic cells. However, intercellular signaling from apoptotic cells (Kim *et al.*, 1998; Fotedar *et al.*, 1996), and release of proteases from dead and lysed cells, may result in their exit from the cell cycle in any case.

Growth and Production Kinetics of Microcarrier Suspension Culture

A comparison of the kinetics of batch cultures using the adherent morphological type in static and stirred bioreactor configurations is presented in Table 4.2.2. Cells in microcarrier suspension batch culture grew relatively well, attaining a minimum doubling time of 26.5 hours which compares favorably with the 15 to 17 hour minimum doubling times seen in static T-flask culture for the recombinant CHO1-5₃₀₀ cell line, which is close to the reported minimum doubling time of wild type CHO-K1 (Winterbourne *et al.*, 1993). The maximum cell density of approximately 1.67×10^6 cells mL⁻¹ was only about half of the maximum densities achieved in static T-flask culture, reflecting the non-optimized state of this system. The average viable cell density of 0.73×10^6 cells mL⁻¹ (Table 4.2.3) could not be compared with T-flask culture where intermittent cell sampling is not possible.

Table 4.2.2: Batch population kinetics of the substratum-adherent morphological type in static and stirred bioreactor configurations.

Bioreactor Type	$X_{v_{max}}$ (E-6 c/mL)	μ_{max} (h ⁻¹)	[tPA] _{max} (mg/L)	P _{tPA} avg (mg/L/h)
Static (T-flask)	3.13 ± 0.54	0.043 ± 0.003	11.43 ± 0.6	0.076 ± 0.004
Stirred (MS)	1.67 ± 0.35	0.026 ± 0.006	10.11 ± 0.4	0.041 ± 0.003

Maximum product titer attained was similar, but production kinetics were reduced when compared with static T-flask culture. The product titer reached a maximum of 10.11 mg L^{-1} , but volumetric productivity was $0.041 \text{ mg L}^{-1} \text{ h}^{-1}$, which is about half of that found in static T-flask culture. The tPA concentration expressed as a percent of total supernatant protein was 0.42% (Table 4.2.4), which is similar to values obtained in static T-flask culture using serum-containing medium. Specific productivity was growth-phase-associated, with a pattern suggestive of G1 cell cycle phase association (see Section 4.1.2). The average specific productivity of $0.037 \text{ pg c-h}^{-1}$ (Table 4.2.4) could not be compared with the case of static T-flask culture where intermittent cell sampling is not possible.

Aggregate Suspension

Aggregate suspension culture was initiated by inoculating a dispersed suspension of cells into a 1 L working volume (2 L total volume) stirred tank bioreactor containing serum-free HB-CHO medium with a total protein concentration of 320 mg L^{-1} . The majority of the protein in the serum-free medium is BSA, and there are no known attachment factors present. The bioreactor was operated at an agitation rate of 60 rpm with headspace aeration. Acceptable reproducibility was seen in the three batch culture runs that were made (Appendix C).

Although the cell concentration did not increase significantly, small aggregates of 2 to 5 cells were visible under light microscopic examination after one day of culture. By mid-exponential phase the association of cells ranged from individual cells to large amorphous aggregates of several hundred cells. Although there were relatively few very large aggregates, they represented the majority of the total cell population. Similar observations have been made by other investigators (Peshwa *et al.*, 1993; Tolbert *et al.*, 1980). Under light microscopic observation, in agreement with these investigators, there was no visible sign of necrosis in even the largest aggregates until the declining phase. When the population entered the declining phase necrotic cores developed in the large aggregates, which subsequently deaggregated. This deaggregation is counter to the findings of Renner and co-workers (1993) who observed aggregates to form around dead cells. As the declining phase continued, aggregated and deaggregated cells underwent rapid lysis, in agreement with the observations of other investigators (Renner *et al.*, 1993; Chevalot *et al.*, 1994).

Morphology of Aggregates

In serum-free static T-flask culture, cells grew as large, loose aggregates of 200 to 500 μm in diameter. These very large aggregates, which were readily visible to the naked eye, contained hundreds to thousands of cells. Unlike spheroids, these loose aggregates contained large void volumes so that movement of nutrients and metabolites in and out of the aggregates was likely not mass transferred limited. Whole nuclei counts suggested void volumes of greater than 40% when compared to calculated maximum cell packing in the space occupied by the aggregates (calculated maximum cell density: $8.0 \times 10^6 \text{ cells mL}^{-1}$; whole nuclei count: ca. $4.76 \times 10^6 \text{ cells mL}^{-1}$).

In the absence of exogenous attachment factors such as can be found in serum, normally adherent but anchorage-independent cells will form cell-cell attachments. Initial cell-cell attachment may be cation mediated. Divalent cations such as Ca^{2+} may promote electrostatic interaction of the negatively charged surfaces of cells. In the absence of activated fibronectin ligands (fibronectin adsorbed to a substratum), fibronectin receptors on the membranes of cells interact with each other, leading to cell-cell attachment. CHO cell mutants which grow as dispersed suspension, even in serum-containing medium in static culture, have been reported to have low or no cell surface fibronectin receptor expression (Kurano *et al.*, 1990). Other transmembrane glycoproteins which promote aggregation through homophilic interaction, and which are not involved in cell-substratum attachment, have been identified (Lucka *et al.*, 1995). Cells of epithelial origin, such as CHO cells, form tight junctions which would further cement the cell-cell attachments (Peshwa *et al.*, 1993).

The above discussion does not explain the stability of very large, loose aggregates with in excess of 40% void space, even in static culture. Indeed, aggregates resisted mechanical and chemical disruption. Tolbert and co-workers (1980) similarly noted the tight binding of aggregated cells. An explanation of the stability of these cell-cell associations was sought through the examination of the gross morphology of the aggregates. In Figure 4.2.2 the non-homogenous nature of the static culture whole aggregate morphology is revealed. Rounded, elongated, and even flattened cells are visible. There are areas of bunched rounded cells. These grape-like bunches are joined to other grape-like bunches with long filament-like structures. It is likely that these filament-like structures confer the stability of the loosely packed whole aggregates.

Under conditions of even the relatively low hydrodynamic shear created by agitation rates of 60 rpm, aggregates are much tighter (Figure 4.2.3a). Even with this tighter overall structure, filament-like linkages are visible between bunches of cells. The surface morphology of individual rounded cells within the aggregate is visible in Figure 4.2.3b. It should be noted that there was considerable shrinkage associated with preparation of the samples for scanning electron microscopy, so that cells which appear here to be 6 to 10 μm in diameter were actually 10 to 16 or 17 μm in diameter *in vitro*. On average, rounded aggregate cells were smaller than dispersed suspension cells by about 10%.

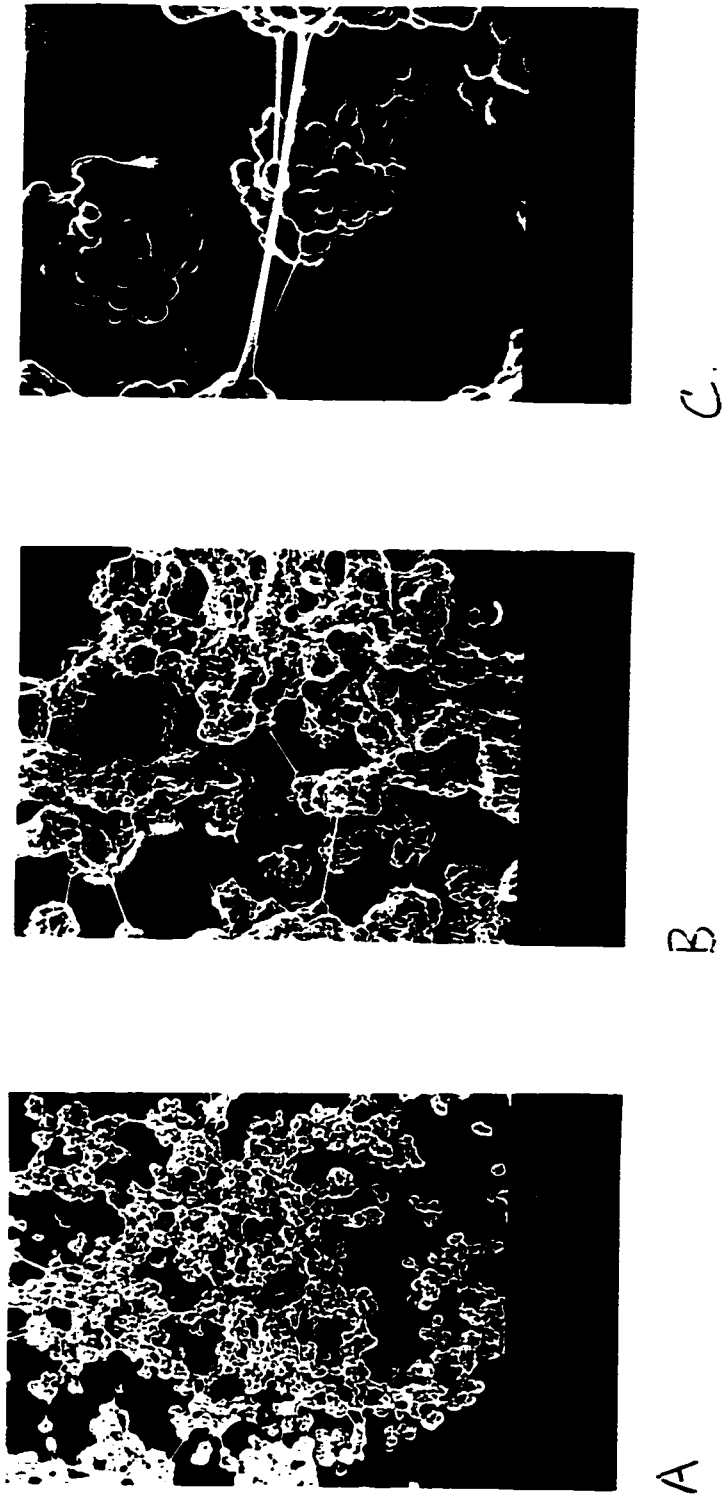


Figure 4.2.2: An aggregate formed in static T-flask culture



A.



B.

Figure 4.2.3: An aggregate formed in a 1 L working volume spinner flask at 60 rpm

There is considerable blebbing on these cells. Some investigators have noted that the phenomenon of aggregation is associated with suboptimal growth conditions (Renner *et al.*, 1993). The surface blebbing and small size of the aggregates may be indicative of apoptosis, which would be consistent with an assumption of suboptimal growth conditions. On the other hand, as this culture traversed the declining phase the cells deaggregated. Other investigators have reported different methods of inducing aggregation under good growth conditions (Peshwa *et al.*, 1993). The reduced size of the cells may be purely a result of aggregation and/or hydrodynamic shear. The blebbing may be formation of sites for cell-cell adhesion, but are likely merely microvilli indicative of the epithelial origin of these cells (Peshwa *et al.*, 1993). The majority of the blebbed rounded cells are also covered with fine filaments which may be polymerized actin (lamellipodia and focal adhesion sites) or other proteinaceous adhesion structures.

The long filament-like structures intraconnecting the aggregates are examined in Figure 4.2.4. In Figures 4.2.4a and 4.2.4b it can be seen that grape-like bunches of rounded cells serve as a substratum for the attachment, flattening, and spreading of other cells. In the absence of attachment factors in the medium, substratum adhesion molecules can only be supplied locally by autocrine secretion. In contrast to the rounded cells, the surface of the flattened and spread cells is smooth. Elongation of these cells can be seen, and it is clearly discernable in Figures 4.2.4a, 4.2.4b, and 4.2.4c that these cells are continuous with the connecting filaments. That is, the connecting filaments appear to be hyperextensions of flattening and spreading cells. This is consistent with the migratory pseudopodia visible in substratum attached cultures: the connecting filaments are membrane or cytoplasmic bridges. In Figures 4.2.4c and 4.2.4d it can be seen that the membrane bridges actually consist of more than one pseudopodia which are apparently flattened and spread along each other's lengths, providing an explanation of the mechanism of cytoplasmic bridging. The multiplicity of the pseudopodia within the cytoplasmic bridges supplies strength to these structures.

It has been observed here and by others (Peshwa *et al.*, 1993; Moreira *et al.*, 1995) that the size, concentration, and cell compactness of aggregates can be controlled by agitation rate. The physical strength of aggregates conferred by cytoplasmic bridging allows them to compact under hydrodynamic shear. This may explain the observed ability of natural aggregate cultures to withstand agitation rates which cause the death of cells attached to microcarriers (Moreira *et al.*, 1995). Thus natural aggregate culture has a distinct advantage for scale-up purposes when compared to microcarrier suspension culture. Aggregates fail to form at higher agitation rates in the CHO1-5₅₀₀ cell line. It would therefore be necessary to grow an inoculum of aggregates at lower agitation rates for culture at large scale.

This understanding of the morphology of aggregates may also explain how new aggregates are formed under agitation in stirred tank reactors, where dispersed suspensions fail to develop aggregates. Shearing may cause breakage of hyperextended cytoplasmic bridges so that an increase in the number of aggregates may come about from the fission of existing aggregates. Cell number within aggregates would continue to increase on the surface of bunched rounded cells within each aggregate.

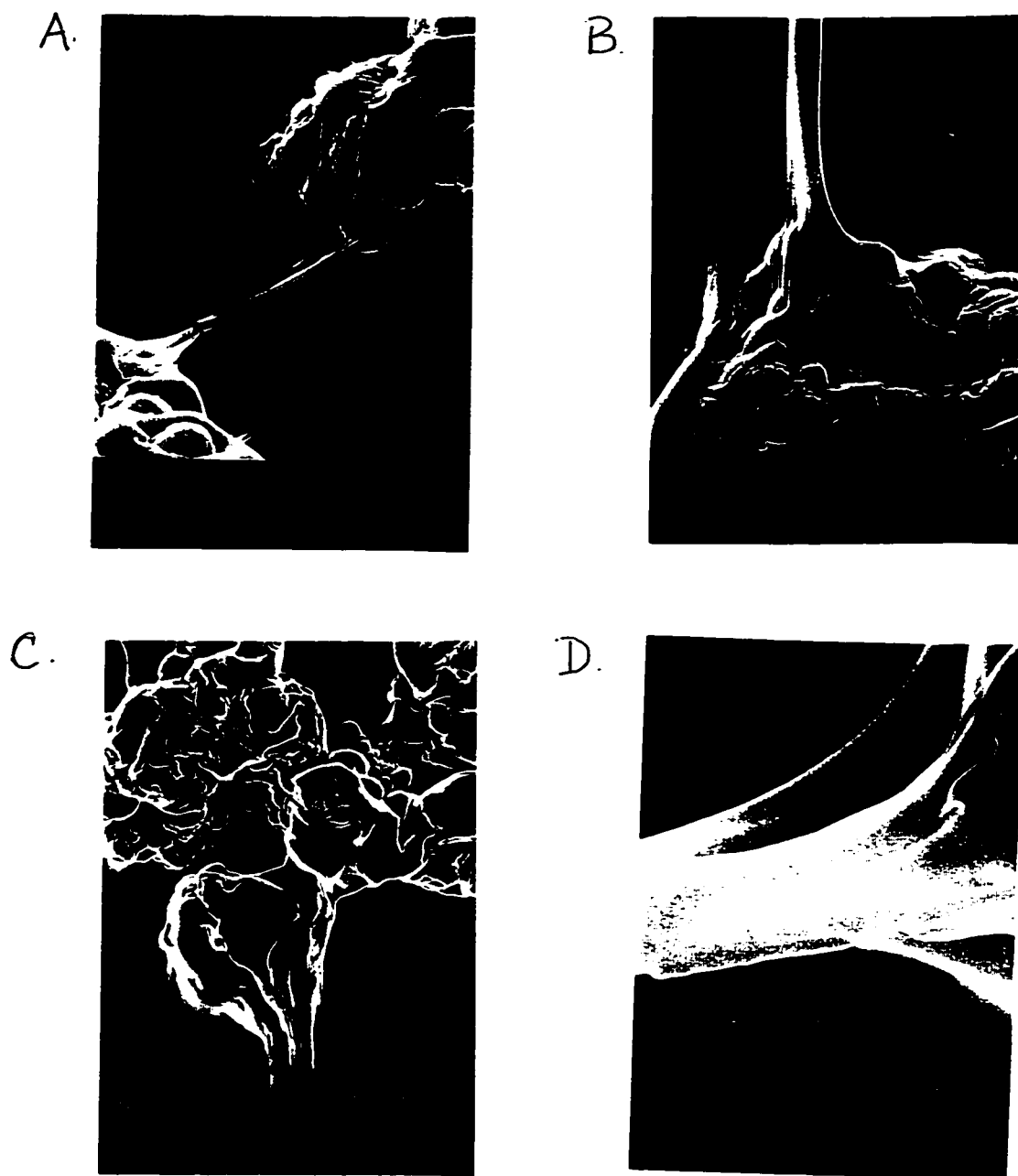


Figure 4.2.4: Morphological features of aggregated cells

Growth and Production Kinetics of Aggregate Suspension Culture

Growth parameters are presented in Table 4.2.3. In comparison with microcarrier suspension culture, the aggregate suspension culture expanded at a reduced rate with a maximum specific growth rate of 0.016 h^{-1} (a doubling time of approximately 43 hours). The culture reached a maximum concentration of $0.746 \times 10^6 \text{ cells/mL}$, which is a little less than one half of the density achieved in microcarrier suspension culture. The average cell density was also about one half of that maintained in the microcarrier suspension system. It has been suggested that the slower growth observed in aggregate suspension may be attributable to mass transfer limitations of nutrient delivery and metabolite clearance. The large void space of these aggregates is not consistent with a theory of mass transfer limitation.

The small size of many of the cells in the aggregates suggests that they have left the cycling fraction, and are either quiescent (G0 phase) or senescent (A phase). A critical cell size for the initiation of the cell cycle has been observed (Martens *et al.*, 1993). Here, in addition to the reduced size of rounded cells in the aggregates, the morphological examination revealed the presence of flattened and spread cells. It is generally accepted that anchorage-independent transformed cells have also lost the requirement to flatten and spread prior to entry into each cycle of division. While this may be true, it is possible that flattening and spreading is associated with enhanced proliferation rates of a population. Proliferation within aggregates may occur primarily by the division of cells which have been able to flatten and spread on the surface of bunched rounded cells.

Table 4.2.3: Growth of CHO1-5₅₀₀ cells in Microcarrier Suspension, Aggregate Suspension, and Dispersed Suspension systems.

System	CHvol (day 11) E-6 c-h/mL	Xv _{max} E-6 c/mL	Xv _{avg} E-6 c/mL	μ_{max} h ⁻¹
MS	221 ± 19	1.67 ± 0.35	0.73 ± 0.07	0.026 ± 0.006
AS	77 ± 23	0.75 ± 0.14	0.35 ± 0.05	0.016 ± 0.003
DS	191 ± 17	1.16 ± 0.21	0.59 ± 0.05	0.012 ± 0.002

Production parameters are presented in Table 4.2.4. In comparison with the microcarrier suspension system, the lower specific productivity combines with the lower average cell density to yield a reduced volumetric productivity and maximum product titer. Chevalot and co-workers (1994) also noted a reduced specific productivity in aggregate culture of rCHO cells encoding a non-secreted protein product when compared with microcarrier culture. In contrast, Kennard and Piret (1995) found no decrease in the specific protein production of another rCHO cell line encoding another non-secreted protein product in aggregate culture compared with microcarrier culture. As was found here, they noted a decrease in specific growth rate, but an increase in protein purity which they attribute to the absence of serum in the aggregate culture compared with the microcarrier culture. Avgerinos and co-workers (1990) also found no decrease in specific productivity of a secreted protein product from a rCHO cell line when cells grew as aggregates.

The impact of morphological type on specific productivity is likely a function of the protein product itself. It has been established that tPA production (where production is measured as the appearance of the product in the supernatant and is therefore the endpoint of transcription, translation, post-translational modification, intracellular transport, and secretion) is correlated with the G1 cell cycle phase, and is greatly reduced or absent in quiescent (G0 phase) and senescent (A phase) cells (see Section 4.1.2). The diminished specific productivity seen in this aggregate suspension system is consistent with depressed tPA productivity of cells in G0 and A physiological states. This is certainly a drawback to the use of aggregate suspension systems for the production of secreted recombinant proteins from *dhfr* transfected CHO cells. Prevention of entry into apoptosis may overcome this negative aspect of aggregate suspension

Table 4.2.4: Production of tPA from CHO1-5₅₀₀ cells in Microcarrier Suspension, Aggregate Suspension, and Dispersed Suspension systems.

System	[tPA] _{max} mg/L	P _{tPA_{avg}} mg L ⁻¹ h ⁻¹	Q _{tPA_{avg}} pg c-h ⁻¹	%tPA/Protein
MS	10.11 ± 0.4	0.041 ± 0.003	0.037 ± 0.004	0.42 ± 0.017
AS	5.03 ± 0.4	0.009 ± 0.002	0.021 ± 0.006	1.57 ± 0.125
DS	10.51 ± 0.5	0.034 ± 0.005	0.045 ± 0.005	3.29 ± 0.157

systems (Fotedar *et al.*, 1996). It must also be realized that these two systems varied not only in their growth behavior type (microcarrier suspension versus aggregate suspension), but also in the composition of the medium. In the microcarrier suspension system Ham's F12 basal medium was supplemented with 10% FBS. The composition of the HB-CHO serum-free medium is not known, but its differences from Ham's F12 with 10% FBS may be the causal factor in the reduced growth and productivity of the aggregate suspension system. Impact of initial concentrations of substrates is explored in Section 4.3.

In spite of the lower production kinetics, the tPA concentration in the aggregate suspension system is almost 4 fold greater than that of the microcarrier suspension system counterpart, when expressed as a percent of total supernatant protein, and inclusive of the differences in population density. This enhanced purity of tPA and associated enhanced recovery and ease of downstream processing may be sufficient to offset the lower absolute tPA production.

Dispersed Suspension

Dispersed suspension culture was initiated by inoculating a dispersed suspension of cells into a 1 L working volume (2 L total volume) stirred tank bioreactor containing serum-free HB-CHO medium with a total protein concentration of 320 mg L^{-1} . Agitation was started at inoculation at a rate of 150 rpm to prevent aggregate formation. Headspace aeration was employed so that complications arising from cell contact with the gas-liquid interface were avoided. Reproducibility of the four batch culture runs that were made was acceptable (Appendix C).

The dispersed suspension cells appeared healthy, exhibiting normal size, a smooth surface, and the spherical morphology seen in natural suspension cells such as lymphocytes and hybridomas. Very few cell-cell attachments formed over the course of the batch run, with a few 2 to 5 cell bunch-of-grapes-like aggregates appearing near the end of the exponential growth phase. These small aggregates persisted until midway through the declining phase, but did not increase in size or number and represented an insignificant proportion of the total population.

Growth parameters of the dispersed suspension system are presented in Table 4.2.3. The doubling time of this system (ca. 58 h) was the longest of the three, being about twice that of the microcarrier suspension system. The cells were of normal size, and the population did proliferate, so that it is apparent that flattening and spreading is not a

requirement prior to progression through the cell cycle. The relatively low specific growth rate does support the suggestion that flattening and spreading is associated with enhanced proliferative activity. A relatively reduced lag phase and enhanced maintenance of viability resulted in both the maximum cell concentration and the average cell concentration exceeding those seen in the aggregate suspension system. But these values did not approach the more successful growth of the microcarrier suspension system. After 11 days of culture, the volumetric cell-hours achieved in the dispersed suspension and microcarrier suspension systems were not dissimilar, demonstrating that a smaller proportion of the cells in the dispersed suspension system resided in the cycling fraction of the population.

The production parameters are presented in Table 4.2.4. In spite of the slower growth, the volumetric productivity is approximately 83% of that seen in the microcarrier suspension system, and the maximum titer is the same in both systems. The higher average specific productivity of the dispersed suspension system accounts for the similarity of the volumetric productivities of the two systems. The product concentration appears to be the maximum attainable due to the natural regulation of the extracellular concentration of this enzyme (see Section 4.1). On a percent of total supernatant protein basis, the dispersed suspension system is significantly superior, with twice the concentration seen in the aggregate suspension system and close to an 8 fold enrichment compared with the microcarrier suspension system. It should also be noted that conditions were not identical in any of the three systems. The dispersed suspension system was very similar to the aggregate suspension system, except for an agitation rate that was approximately twice as fast. This added shear may have impacted both on growth and production kinetics. In addition to the higher agitation rate, the dispersed suspension was cultured in serum-free HB-CHO medium, while the microcarrier suspension was cultured in Ham's F12 containing 10% FBS.

The titer is greatly in excess of endogenous levels, which can be attributed to the large copy number of the recombinant *tPA* gene. Further enhancement of titer may require techniques such as continuous removal of the product (by adsorption on silica, for example), destruction or inactivation of biosynthesized or serum-associated tPA inhibitors, extension of the exponential growth phase (enhanced maintenance of the majority of the population within the cycling fraction), further gene amplification (by MTX adaptation, for example), genetic engineering to prevent biosynthesis of tPA inhibitors, or genetic engineering to prevent or retard cell entry into apoptosis. It is doubtful that successful manipulations of the population growth characteristics would result in increased tPA titer. The natural regulatory mechanism of product titer is peculiar to tPA. Similar regulatory mechanisms would not necessarily be found in *dhfr* based genetic systems encoding for other recombinant protein products.

Concluding Remarks

In this set of experiments, it was found that growth kinetics of this rCHO cell line were superior in microcarrier suspension using Ham's F12 with 10% FBS, in agreement with the findings of others (Chevalot *et al.*, 1994). Production kinetics, however, were not significantly better in the microcarrier suspension system than in the dispersed suspension system. The maximum titer in both systems was approximately 10 mg L⁻¹. This apparent ceiling on the product supernatant titer may be a factor of the natural regulatory mechanisms peculiar to tPA. Further increases in tPA titer may require substantial processing and/or genetic engineering alterations to the system. The use of serum-free medium results in a marked enhancement of product purity. On a percent of total supernatant protein basis, the aggregate suspension system yielded a 4-fold improvement, and the dispersed suspension system yielded an 8-fold improvement, over the microcarrier suspension system.

Under the conditions of this set of experiments, dispersed suspension is the most attractive system. In addition to the best absolute and relative tPA concentrations, the dispersed suspension system is the simplest and cheapest to operate. The microcarrier suspension system requires pretreatment steps with attendant time costs and increased risks of contamination as well as the added direct costs of the microcarriers and the serum. The aggregate suspension system requires meticulous control of agitation rate (at least while aggregates are forming), and is difficult to monitor for growth.

The aggregate suspension system, however, may have advantages at the larger scale in stirred tank reactors where cells are subjected to greater shear forces. Large stirred tank reactors inoculated with already formed aggregates at a high density may result in improved production kinetics, but would require an increased number of seed culture steps. The possibility of such improvement is not indicated from this work and is purely speculative.

4.3 Metabolism of rCHO in Batch Culture

4.3.1 Population-Averaged Metabolism of rCHO Cells

Major Substrates and Metabolites

The metabolism of the rCHO batch culture run presented in Section 4.1.1 was evaluated in terms of the extracellular levels of substrates and metabolites. This batch culture run was one of several operated under similar conditions, with reproducible results (Appendix C). Several unique patterns of consumption and production were found to have occurred, notably the consumption of lactate. Rather than dismiss these findings as artifacts, a rational explanation was sought and is presented here.

Glucose, which is considered to be the major carbon and energy source for the cells, was supplied at an initial concentration of 8 mmol L^{-1} . It was rapidly depleted to less than 0.5 mmol L^{-1} in 4 days of culture, with a corresponding appearance of more than 9 mmol L^{-1} lactate in the medium accompanied by a rapid decrease of the extracellular pH (Figure 4.3.1). The specific consumption rate of glucose during this time was calculated to be $6.23 \times 10^{-11} \text{ mol c-h}^{-1}$, with a yield of lactate on glucose of $1.25 \text{ mol mol}^{-1}$ which are in agreement with the findings of other investigators for rCHO cells (Lin *et al.*, 1993, Tolbert *et al.*, 1980, Chevalot *et al.*, 1994). Assuming that all of the lactate is generated from glucose catabolism this indicates that only 62.5 % of the glucose is metabolized through anaerobic glycolysis. The rest of the glucose may have been metabolized through aerobic pathways, used to synthesize pentose moieties in nucleotides, and used in the formation of lipids and amino acids (proteins).

In normal mammalian cells, increased ATP (produced by oxidative phosphorylation) and citrate (the first intermediate of the TCA cycle) cause a concerted allosteric inhibition of phosphofructokinase, thereby decreasing the rate of glycolysis to pyruvate (Lehninger, 1989). Hence, pyruvate is produced only as fast as it is required to feed into the high energy yielding pathways of the TCA cycle and ETC. In cancer cells, this interlocking coordination is defective and glycolysis proceeds at a much higher rate than required by the citric acid cycle. As a result most of the pyruvate is reduced to lactate which is excreted (Lehninger, 1989). This is apparently the case with most transformed cell lines. As well, hybridomas have been shown to convert more than 90% of glucose to lactate (Phillips, 1991). In hybridoma systems the increasing lactate concentration exceeds the buffering capacity of the medium, toxic acidity conditions of less than 6.5 pH units develop, and the population enters a phase of rapid decline.

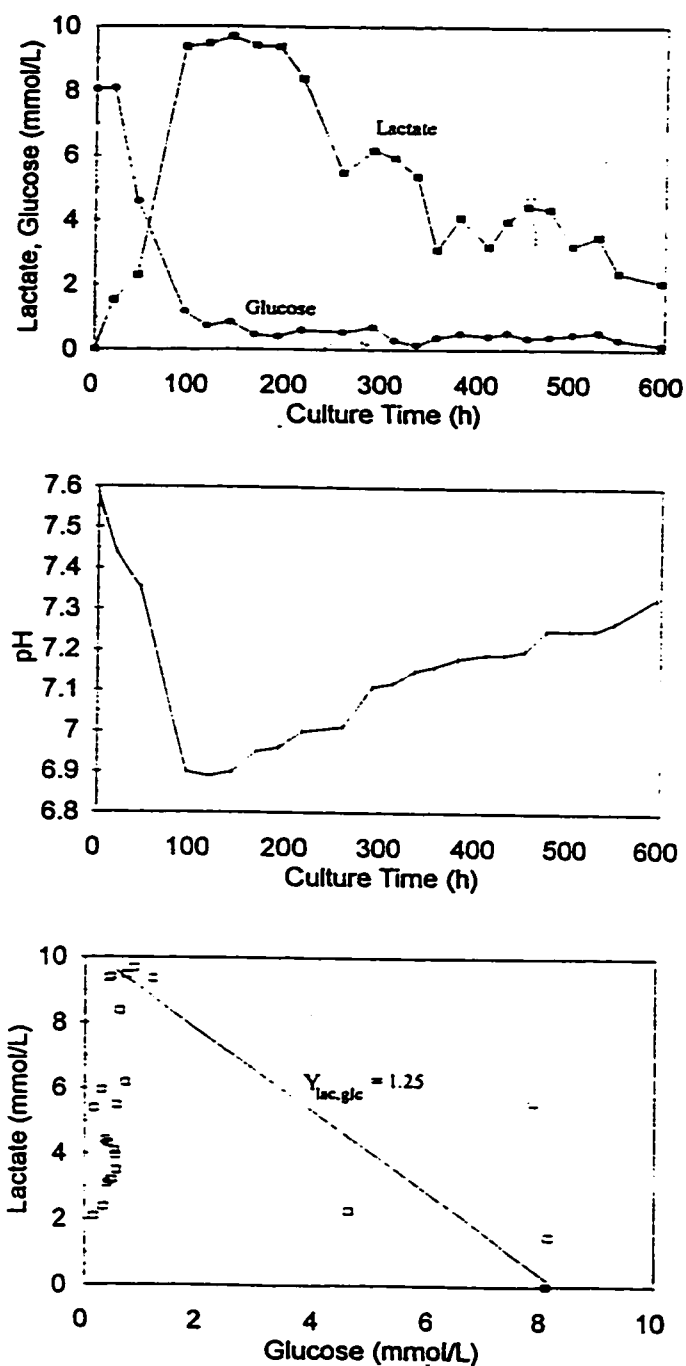
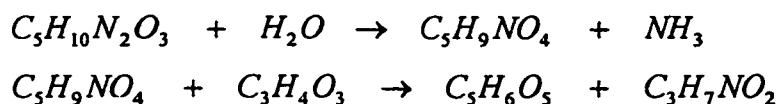


Figure 4.3.1: Dispersed suspension CHO1-S₅₀₀ in a stirred tank reactor operated in batch mode
a) top: Lactate and glucose trends b) middle: pH c) bottom: Lactate yield on glucose.

Here, with less of the glucose being metabolized to lactate, the pH fell to only 6.9 which is not considered a toxic acidity. Glucose was not exhausted, but remained at a constant low level for the last three weeks of the batch culture. No further evolution of lactate was observed once glucose reached a constant value. However, after remaining constant for approximately 5 days, the extracellular concentration of lactate declined exponentially over the next 7 days, while the pH rose. This surprising occurrence prompted further consideration of the growth kinetics of the culture. Referring to the viable cell concentration curve in Figure 4.3.2, it is apparent that the population drops significantly as the glucose concentration falls below 0.5 mmol L^{-1} , and then remains approximately constant for about one week before declining through the last one and half weeks of the batch culture period. The total cell concentration also drops significantly and abruptly as the glucose level reaches the low steady value of less than 0.5 mmol L^{-1} , indicating that a significant proportion of the population dies at this point, likely through necrosis with rapid cell lysis. The total cell concentration then remains constant for about 2 days, and then increases exponentially over the next two days, finally declining slowly for the last two weeks of the culture period. The exponential rise in the total population is not mirrored in the viable concentration, suggesting that while a portion of the population is replicating, another portion is dying, likely through the physiological process of apoptosis. During this time, the lactate concentration is declining exponentially.

As shown in Section 4.1.2, during the last two days of culture, almost the entire viable fraction of the population resides in the G1/G0 and A phases, with an insignificant number of cells in the S and G2/M phases. Therefore, the cycling fraction can be assumed to be approximately zero, which means that no new cells are being added to the total population. The rate of decrease in the total population during this time can therefore be assumed to be the rate of cell lysis, which is calculated here as 0.006 h^{-1} .

In addition to glucose, glutamine is the second major substrate for animal cells in culture. As discussed in Section 2.1, glutamine is utilized as a building block of proteins, a nitrogen source, a carbon source, and an energy source. This culture was supplied with a high initial concentration of glutamine of approximately 5.5 mmol L^{-1} (Figure 4.3.3). Glutamine was utilized immediately, with the extracellular concentration decreasing rapidly through the first 12 days of culture to a constant level of approximately 0.5 mmol L^{-1} . Glutamine consumption was accompanied during the first 8 days by the appearance of ammonia and alanine, with yields of 1.26 mol ammonia/mol glutamine and 0.45 mol alanine/mol glutamine, respectively. These yields suggest that about half of the glutamine is metabolized to ammonia and glutamate which is then transaminated with pyruvate to yield alanine.:



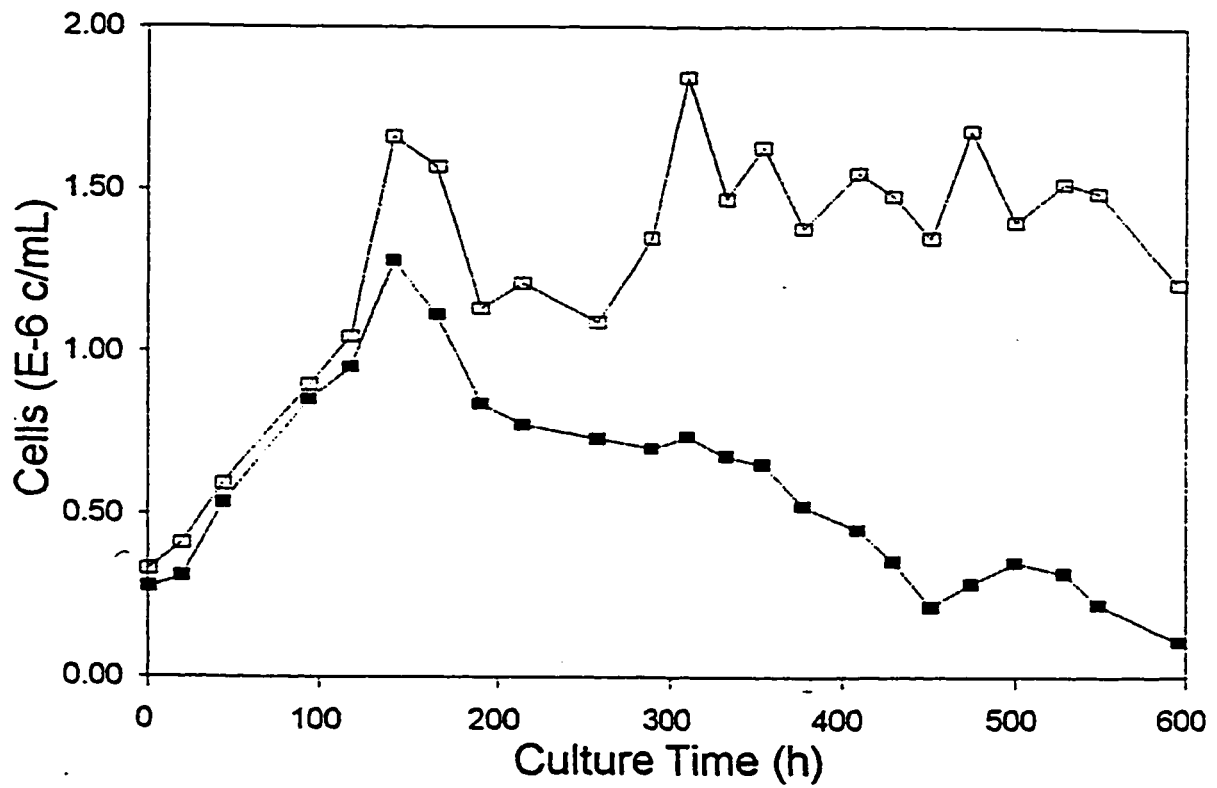


Figure 4.3.2: Comparison of total cell population (open squares) with viable cell population (filled squares). Cell lysis occurs primarily in the late decline phase.

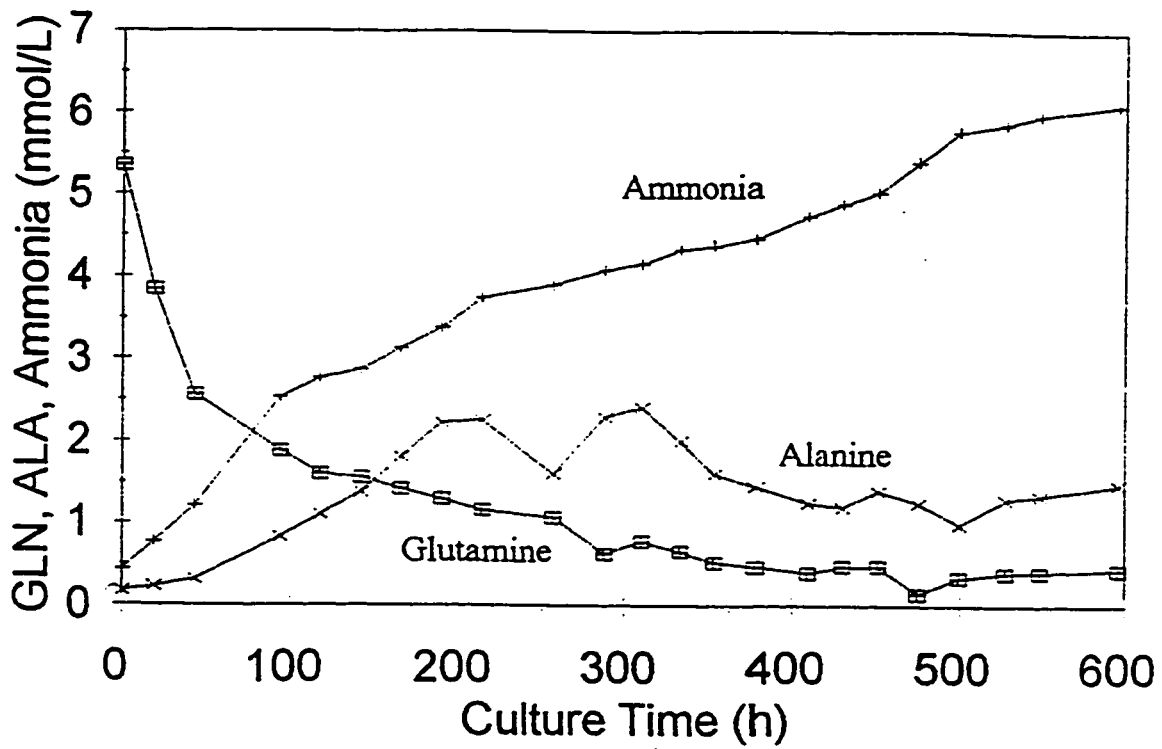
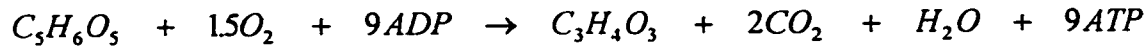


Figure 4.3.3: Alanine decreases during the decline phase (as glutamine falls below 1 mmol L^{-1}), while ammonia accumulates at the same rate from mid-exponential phase (100 culture hours) through the remainder of the batch culture run.

The other product in the transamination step, α -ketoglutarate, enters the TCA cycle to generate 9 moles of ATP equivalents:



If alanine is conserved, this pathway would liberate 0.5 moles of ammonia for every mole of glutamine consumed via all pathways. Some of the remaining half of the glutamine is chemically degraded. It has been shown that glutamine in culture medium has a first order half life of 6.7 days at 37 °C (Seaver, 1987). Two moles of ammonia is released per mole of glutamine which is chemically degraded, here accounting for 0.25 moles of ammonia for every mole of glutamine consumed via all pathways. To close the balance with respect to ammonia, it is then assumed that one fourth of the glutamine is oxidized, either completely to carbon dioxide or incompletely to lactate, liberating 0.5 moles of ammonia per mole of glutamine consumed via all pathways. The energy yield, in terms of ATP equivalents, differs significantly in these last two pathways. Complete oxidation of glutamine generates 27 ATP equivalents per mole of glutamine, while incomplete oxidation generates only 9 moles of ATP per mole of glutamine. This assumption is obviously an oversimplification as some of the glutamine is used to produce proteins, nucleic acids, and other nitrogenous compounds, and as some of the ammonia comes from the metabolism of other amino acids.

Following 12 days in culture, the glutamine is maintained at a low concentration, but unexpectedly the alanine concentration declined, and the ammonia concentration continued to increase at the same rate.

Serendipitously, the analytical method utilized to follow alanine and glutamine concentrations also generated data for 8 other amino acids (Figure 4.3.4), which with the rest of the data suggests some possible mechanisms. Specific consumption and accumulation rates and yields, together with tPA production and growth parameters are presented in Table 4.3.1. The amino acids examined include four of the thirteen essential amino acids: glutamine, threonine, tyrosine, and arginine. Threonine and tyrosine decrease rapidly during the exponential growth phase to steady concentrations which are then maintained throughout the rest of the batch culture. The glutamine, initially at a high concentration, declines exponentially to a low constant concentration as discussed above and as expected. The large standard deviation and scatter of the arginine data proved inconclusive. Aspartic acid, glutamic acid, and serine all decrease rapidly to low constant concentrations, while asparagine is completely consumed. As discussed above, alanine, which is expected to increase as glutamine is transaminated through glutamate, initially increases, but then decreases during the last 16 days of the batch culture period. Glycine unexpectedly increases throughout the batch culture period.

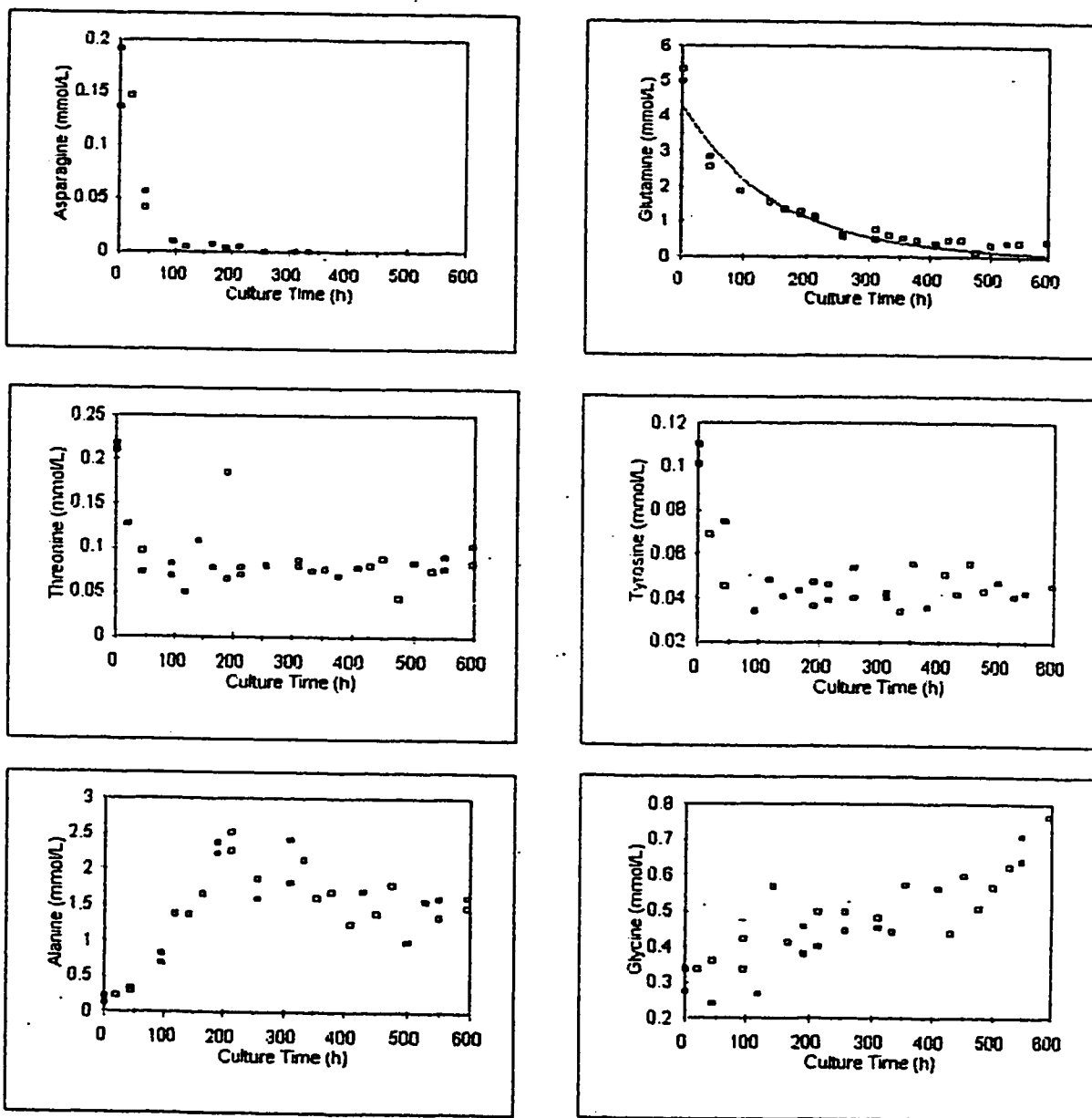


Figure 4.3.4: Amino acid profiles over batch culture duration of dispersed suspension morphological type. Alanine increases as glutamine decreases until the end of the exponential phase (200 culture hours). Thereafter, alanine unexpectedly decreases. Glycine increases at a constant rate throughout the batch culture run.

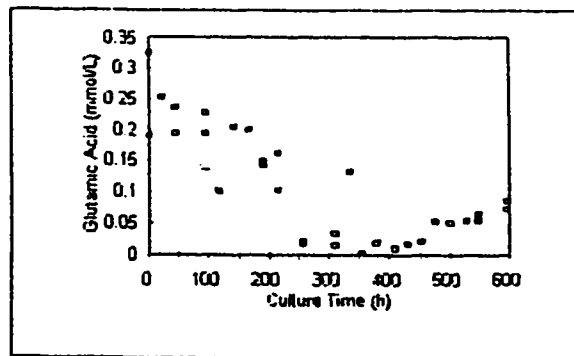
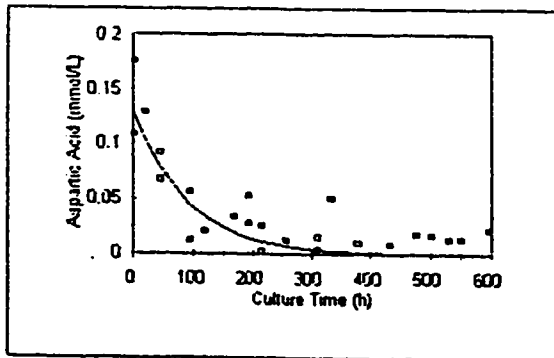
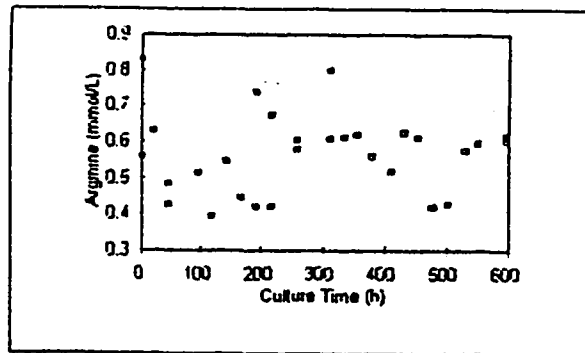
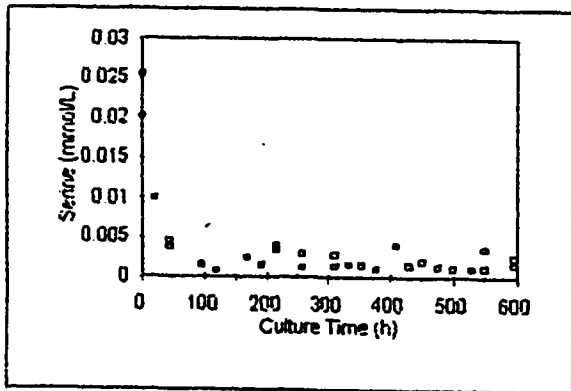
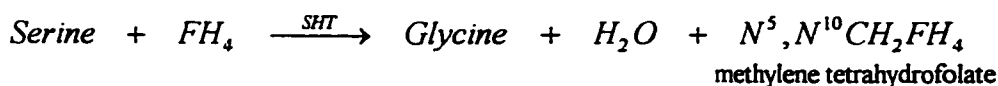


Figure 4.3.4 (continued): amino acid profiles

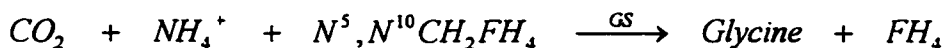
DHFR and the Production of Glycine

An understanding of the ammonia and glycine linkage in this cell line can be explained by considering the B complex vitamin, folic acid. Folic acid is enzymatically reduced to its active coenzyme form, tetrahydrofolic acid (FH₄). Tetrahydrofolate functions as an intermediate carrier of 1-carbon groups in a number of complex enzymatic reactions in which methyl, methylene, methenyl, formyl, or formimino groups are transferred from one molecule to another.

The reduction of folic acid occurs in two steps in which successive pairs of hydrogen atoms are added to the molecule. In the first step, folic acid is reduced enzymatically to dihydrofolate (FH₂). In the second step, the reduction of FH₂ to FH₄ is catalyzed by DHFR. Tetrahydrofolate acts as the coenzyme in a number of bioreactions, including the biosynthesis of glycine from serine (Lehninger, 1993):



In this reaction, which is catalyzed by the enzyme serine hydroxymethyltransferase (SHT), the tetrahydrofolate serves as an acceptor of the β carbon atom of serine during its cleavage to yield glycine. The 1-carbon unit derived from serine and carried by tetrahydrofolate can be transferred to various acceptor molecules. In vertebrates, when glycine is biosynthesized enzymatically from carbon dioxide and ammonium ion, it acts as the acceptor molecule (Lehninger, 1993):



In this reaction, which is catalyzed by glycine synthase (GS), the two additional hydrogen atoms which are required to form the glycine molecule are supplied by the oxidation of the reduced form of nicotinamide adenine dinucleotide (NADH). This reaction can be coupled to the glycine production from serine reaction through the cycling of the various forms of the folate coenzyme (Figure 4.3.5). While this reaction would serve to restore tetrahydrofolate from its methylene derivative, and would account for an increasing concentration of glycine, it would also consume ammonia. In addition, this reaction for the biosynthesis of glycine has been shown to occur primarily in the liver of vertebrates (Lehninger, 1993). As a net ammonia consumption is not occurring in this ovarian cell line it is unlikely that this reaction is taking place.

Table 4.3.1.: Growth, Protein production, and metabolism kinetics of CHO1-5₅₀₀ in dispersed suspension batch culture.

Rate Constant	0 - 50 Cell-Hours	50 - 200 Cell-Hours	> 200 Cell-Hours
Metabolism:			
qConsumption (pmol/c-h)			
qGLC	0.143	0.001	0.0001
qGLN	0.060	0.008	0.002
qLAC	-0.185	0.00035	0.030
qAMM	-0.041	-0.011	-0.011
qALA	-0.014	-0.014	0.005
qSER	0.001	0	0
qGLY	-0.001	0.001	0.001
Protein Production:			
qProduction (pg/c-h)			
qtPA	0.076	0.018	0.042
ktPA	0	0	-0.069
Growth:			
μ (h⁻¹)			
μ	0.012		
k(d)	0.0001	0.0035	0.0046

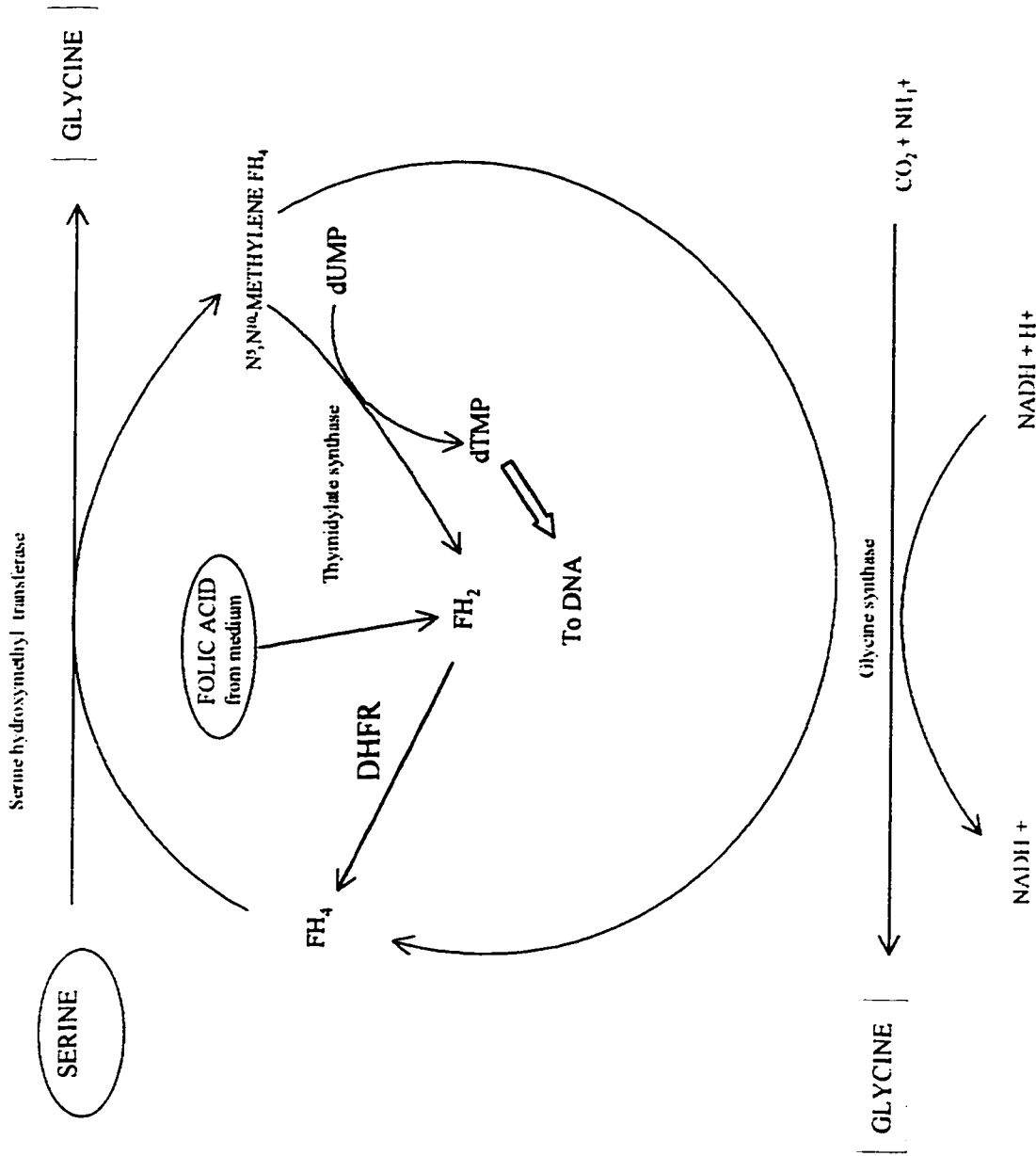


Figure 4.3.5: Glycine synthesis and the role of folates.

FH₄: tetrahydrofolate, FH₂: dihydrofolate, dUMP: deoxyuridylylate monophosphate, dTMP: deoxythymidylate monophosphate

Other routes by which tetrahydrofolate can be restored from N^5,N^{10} -Methylenetetrahydrofolate involves the biosynthesis of DNA building blocks such as the formation of deoxythymidylate (dT) from deoxyuridylate (dU), or the formation of deoxythymidylate monophosphate (dTMP) from deoxyuridylate monophosphate (dUMP). In these reactions the entire methylene group is donated from the methylene derivative of tetrahydrofolate, leaving the vitamin in the dihydrofolate form. Dihydrofolate is then reduced to tetrahydrofolate enzymatically via DHFR as mentioned above. One of these reaction systems coupled with the reaction of glycine formation from serine would result in a net production of glycine without consumption of ammonia (Figure 4.3.5). The high recombinant *dhfr* copy number in this cell line supports the plausibility of this mechanism. The steady accumulation of glycine suggests that DHFR expression is constitutive.

Attention is now turned to the fate of serine. The initial concentration of approximately 0.25 mmol L^{-1} serine is rapidly depleted to less than $0.001 \text{ mmol L}^{-1}$, with a corresponding increase in glycine during the first 5 days of the batch culture period. Glutamine and glucose decrease while alanine, ammonia, and lactate increase during this time period, reflective of the glycolysis and glutamine metabolism commonly seen in hybridoma culture. This metabolic pattern is held until the end of the exponential growth phase. The last three weeks of the batch culture period correspond to steady state concentrations of amino acids indicative of their roles as intermediates as noted above. The unusual behavior of lactate and alanine is also observed during the last three weeks of the batch culture period. The steady state concentration of serine during this time period is approximately $0.002 \text{ mmol L}^{-1}$. Possible metabolic pathways which would account for the observed metabolite and substrate profiles are presented below.

Glucogenic Compound Metabolism in Animal Cells

All life forms require a carbon source for use as building blocks of biomaterials, and/or as energy for life processes. Many life forms are capable of utilising simple organic compounds as sources of carbon and energy. For example, lactate catabolism occurs in many yeast and mold species of Fungi, and in both Gram negative and Gram positive bacterial species, as well as in many plant species.

In the higher heterotrophs (animals), carbohydrates (in particular, glucose), fatty acids, and amino acids are degraded via converging catabolic pathways to enter the citric acid cycle and to yield their energy-rich bond electrons to the respiratory train, providing energy to make ATP. Conversely, anabolic pathways use chemical energy in the form of ATP and NADPH to synthesize important cell components from simple precursor molecules. Catabolism and anabolism proceed simultaneously in a dynamic steady state, such that the energy-yielding degradation of cell components is counterbalanced by biosynthetic processes (Lehninger, 1982).

The first principle of this metabolic/energy dynamics, is that the pathway taken in the biosynthesis of a biomolecule is not usually identical to the pathway taken in its degradation. Secondly, biosynthetic pathways are controlled by different regulatory enzymes from those controlling the corresponding catabolic pathways. And thirdly, energy-requiring biosynthetic processes are obligatorily coupled to the energy-yielding breakdown of ATP, in such a way that the overall process is essentially irreversible, just as the overall process of catabolism is irreversible. Thus, the total amount of ATP (and NADPH) energy used in a given biosynthetic pathway always exceeds the minimum amount of free energy required to convert the precursor into the biosynthetic product (Lehninger, 1982).

The biosynthesis of D-glucose is an absolute necessity in all higher animals, since the brain and nervous system, as well as the kidney medulla, the testes, erythrocytes, and embryonic tissues, require D-glucose from blood as their sole or major fuel source. Animals constantly make D-glucose from simpler precursors in a set of carefully regulated biosynthetic reactions, and then pass the glucose into the blood. Unlike plants, animals cannot bring about the net conversion of CO₂ into new glucose. In animals, the formation of D-glucose from noncarbohydrate precursors is called **gluconeogenesis** ("formation of new sugar"). Fox (1993) defines gluconeogenesis as the formation of glucose from noncarbohydrate molecules such as amino acids and lactic acid. The important precursors of D-glucose in animals are lactate, pyruvate, glycerol, most of the amino acids, and the intermediates of the citric acid cycle (Figure 4.3.6). In animals gluconeogenesis occurs largely in the liver, and to a lesser extent in the kidney cortex.

The glycolytic conversion of glucose into pyruvate is a central pathway of catabolism of carbohydrates, while the conversion of pyruvate into glucose is a central pathway in gluconeogenesis. Although not identical, seven enzymatic reactions of glycolysis also take part in gluconeogenesis: all seven are freely reversible (Figure 4.3.7) (Lehninger, 1982). There are, however, three steps in glycolysis that are essentially irreversible, and cannot therefore be utilized in gluconeogenesis. These reactions are bypassed by an alternate set of enzymes, catalyzing different reactions with different stoichiometries; they function in gluconeogenesis but not in glycolysis. These bypass reactions are nearly irreversible in the direction of glucose synthesis (Figure 4.3.7) (Lehninger, 1982). Thus, both glycolysis and gluconeogenesis are essentially irreversible processes in cells.

Gluconeogenesis consists of two phases: generation of hexose derivatives from lactate, amino acids, glycerol, and other substances (phase I); and conversion of such hexose derivatives to glucose (phase II) (Hanson and Mehlman, 1976). The biosynthetic (anabolic) pathway to glucose, allows the net synthesis of glucose not only from pyruvate, but also from various precursors of pyruvate or phosphoenol pyruvate. All of the citric acid cycle (Krebs cycle) intermediates (citrate, isocitrate, α -ketoglutarate, succinate, fumarate, and malate) may undergo oxidation to yield oxaloacetate, which is converted into phosphoenol pyruvate by phosphoenol pyruvate carboxykinase. Mammals can be classed according to their intracellular location of phosphoenol pyruvate carboxykinase: firstly, animals with the

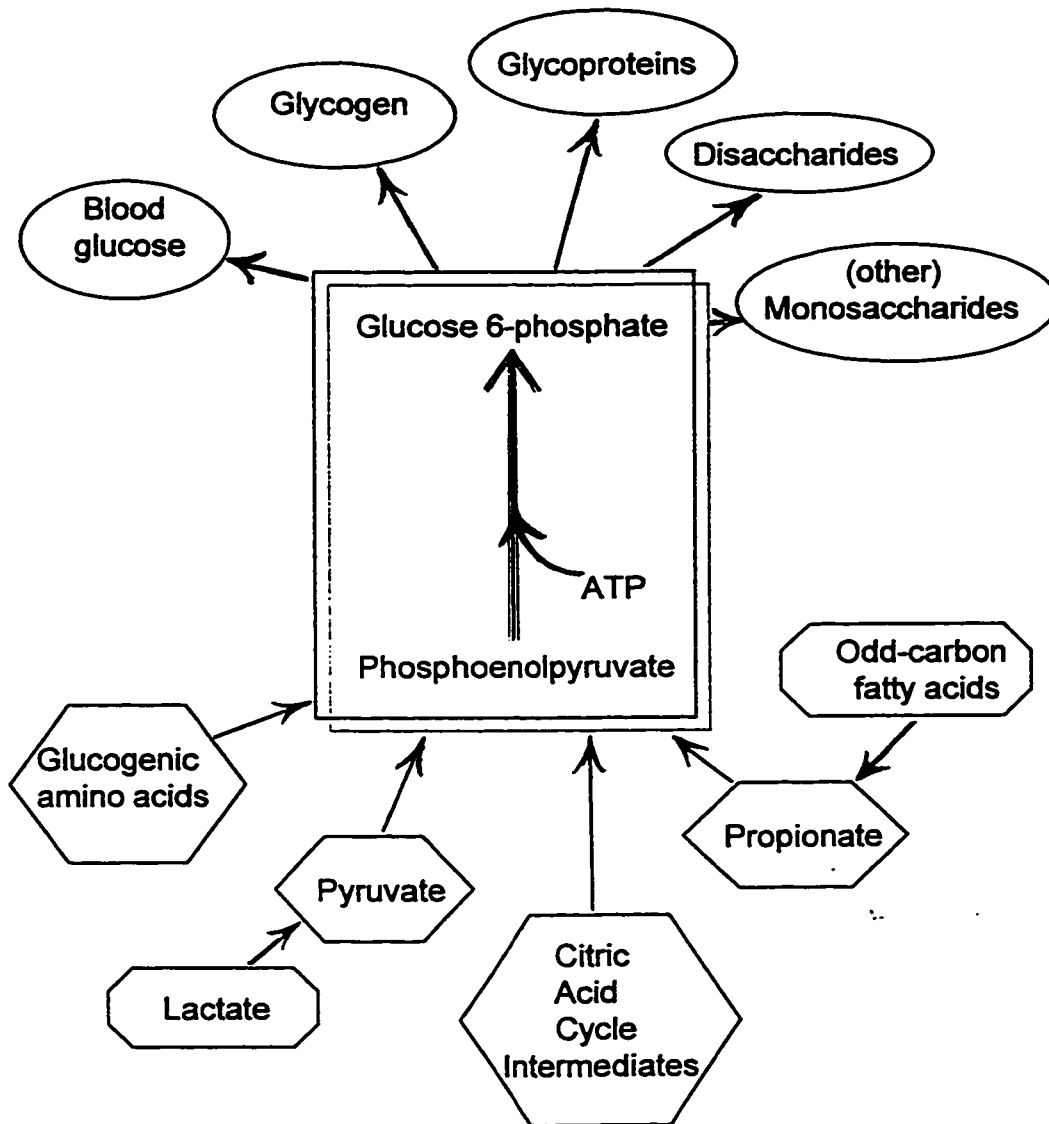


Figure 4.3.6: Many different precursors feed into the common gluconeogenesis pathway to produce glucose-6-phosphate from phosphoenolpyruvate.

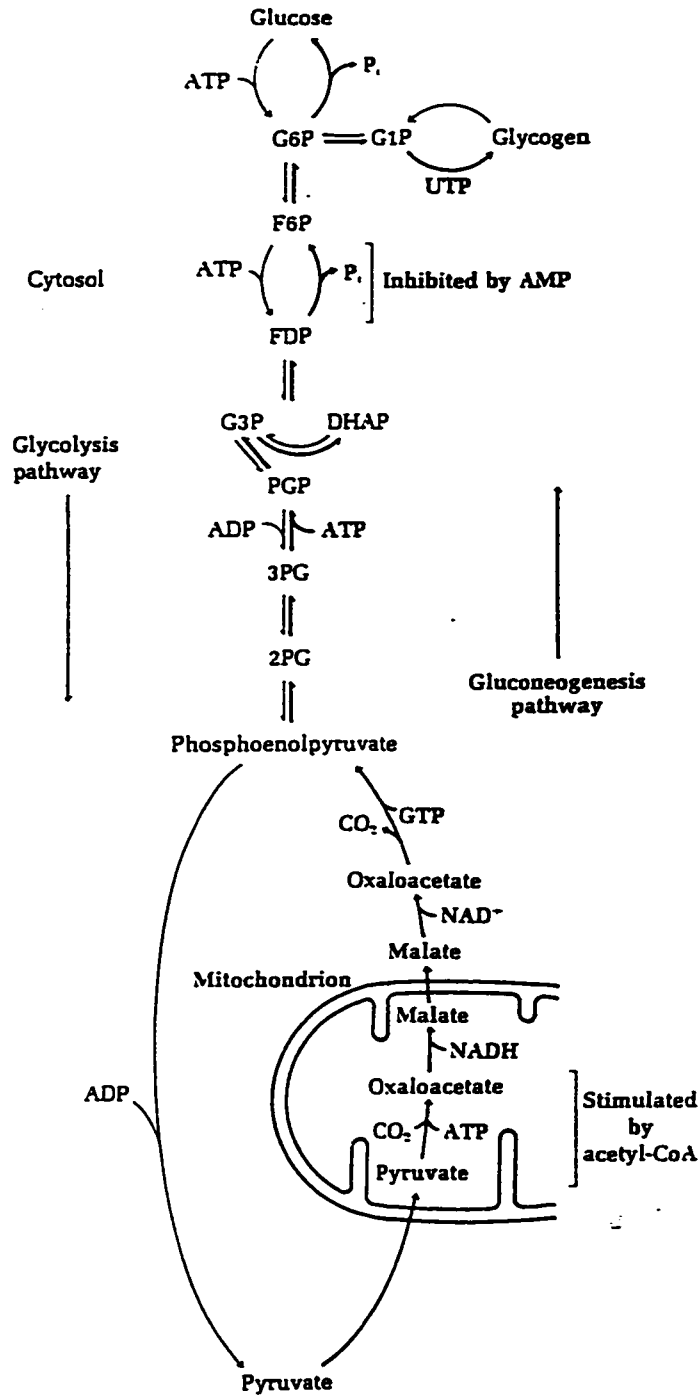


Figure 4.3.7: The opposing pathways of glycolysis and gluconeogenesis. There are three essentially irreversible steps in each pathway.

enzyme predominantly cytosolic (rat, mouse, and hamster); secondly, animals with the enzyme predominantly mitochondrial (chicken, pigeon, and rabbit); and thirdly, animals with the enzyme almost equally distributed between cytosol and mitochondria (most animals, including guinea pig, sheep, ox, dog, cat, primates (including man)). In contrast, pyruvate carboxylase, which catalyses pyruvate conversion to oxaloacetate, is totally mitochondrial (Hanson and Mehlman, 1976). Gluconeogenesis is thus complicated in animals having cytosolic phosphoenol pyruvate carboxykinase, by the transport oxaloacetate from the mitochondria to the cytosol. Hamsters fall into this category.

Some or all of the carbon atoms of many of the amino acids derived from proteins are ultimately converted by animals into either pyruvate or certain intermediates of the citric acid cycle. Such amino acids can therefore undergo net conversion into glucose and glycogen and are called glucogenic amino acids (Table 4.3.2). Obvious examples are alanine, glutamate, and aspartate, which on deamination yield pyruvate, α -ketoglutarate, and oxaloacetate, respectively, all of which are direct precursors of phosphoenol pyruvate. The large ATP yield that would result prohibits the complete oxidation of amino acids to CO_2 , whereas the partial oxidation of amino acids as they are converted to glucose provides exactly the energy needed to support gluconeogenesis (Jungas, *et.al.*, 1992). Even this partial oxidation of the normal daily dietary supply of amino acids accounts for about one-half of the daily O_2 consumption of the liver in mammals, making amino acids the major fuel utilized by liver for ATP production. Gluconeogenesis from amino acids must, therefore, be regarded as a normal prandial (digestive) process, not one limited to periods of fasting, and/or intense (muscular) exertion (Jungas, *et.al.*, 1992).

Amino acid oxidation generates relatively strong non-volatile acids. This metabolic fixed-acid load is normally largely neutralised by the metabolic generation of bicarbonate associated with the hepatic oxidation of dietary organic acids, or the renal oxidation of glutamine (Jungas, *et.al.*, 1992). In addition to bicarbonate buffering, ammonia acts to counterbalance the production of acidic compounds in cell culture systems.

In mammals some of the potential gluconeogenic precursor, propionyl-CoA, is directly oxidized to CO_2 in the muscle, rather than being secreted as alanine to be later converted to glucose by liver. Of the propionyl-CoA converted to glutamine, secreted by muscle, and taken up by the gut, one-third is oxidized to CO_2 . The remainder of the glutamine secreted by muscle is metabolised in the kidneys, where 20% is oxidized to CO_2 . Overall, approximately 30% of the propionyl-CoA generated will go to CO_2 , while the remaining 70% will go to glucose via alanine (muscle), lactate (gut), or serine (kidneys) (Jungas, *et.al.*, 1992).

During prolonged starvation in whole mammalian organisms, when the hepatic glycogen reserve has been depleted, gluconeogenesis, especially from amino acids, must provide the carbohydrate energy source for metabolism. This switch from glucose to ketone body utilization is an essential adaptive mechanism for sparing body protein during starvation (Hanson and Mehlman, 1976).

Table 4.3.2: Glucogenic amino acids

Pyruvate family:

alanine
serine
cysteine
glycine

Oxaloacetate family:

asparagine
aspartate

Succinyl-CoA family:

valine
threonine
methionine

α -ketoglutarate family:

glutamate
glutamine
proline
arginine
histidine

Carbon atom donors:

phenylalanine
tyrosine
isoleucine
tryptophan
lysine

Six high-energy phosphate groups of ATP are ultimately expended to rebuild one glucose molecule from two molecules of lactate, whereas only two molecules of ATP were originally obtained from the anaerobic breakdown (glycolysis) of a molecule of glucose (Figure 4.3.7). The complete oxidative metabolism (glycolysis plus aerobic respiration) of one glucose molecule to CO₂ and water, is accompanied by a gross yield of 38 ATP. Thus, metabolism of one lactate molecules, would yield 16 ATP equivalents (or 32 ATP equivalents from two lactate molecules). This energy yield calculation is made assuming that the complete metabolism of lactate to CO₂ and water, occurs as the sum of two steps: the anabolic process of gluconeogenesis to produce glucose, followed by the aerobic catabolism of the glucose. In the metabolism of lactate, it is possible to bypass the second phase of gluconeogenesis, and to proceed directly into the citric acid cycle from pyruvate. In this case, the metabolism of one lactate molecule would yield 18 ATP equivalents, or 36 ATP equivalents from two lactate molecules. This is the same yield per carbon atom as that obtained through the post-glycolysis complete oxidation of glucose.

Gluconeogenesis and Glucogenic Compound Catabolism in Animal Cell *in vitro* Systems

Gluconeogenesis occurs in the liver, and, under certain physiological conditions, the kidney cortex of whole mammalian organisms, and has been studied extensively in rodent species. Almost all mammalian cells can transaminate or deaminate key amino acids into tricarboxylic acid cycle intermediates and, by conversion into phosphoenol pyruvate, reverse glycolysis to produce glucose. The occurrence of gluconeogenesis in hepatic and renal *in vitro* systems has been well documented (Table 4.3.3). Liver and kidney organ cultures, tissue cultures, and primary cell cultures actively undergo gluconeogenesis. Established cell lines of hepatocytes and various renal cells have been shown to be capable of deriving energy from amino acids, pyruvate, and/or lactate. Gluconeogenesis has been observed *in vitro* in striated muscle cells, neural cells, and spermatozoa. Gluconeogenesis has also been observed in non-mammalian *in vitro* animal cell systems: In particular, gluconeogenesis has been frequently observed in fish hepatocyte culture.

Many studies have been conducted with respect to the regulation of gluconeogenesis and of the catabolism of glucogenic compounds (Table 4.3.4). Phorbol esters, angiotensin II, p-kinase C, and various hormones such as vasopressin and somatostatin, are all regulators of the metabolism of glucogenic compounds (Garcia, *et.al.*, 1986; Dileepan *et.al.*, 1985). Nitrite (Wiechetek, *et.al.*, 1993) and somatotropic (growth) hormone (Rogers, *et.al.*, 1989) have both been shown to stimulate gluconeogenesis. Chemical species which appear to enhance the metabolism of glucogenic compounds include epidermal growth factor (Moule, *et.al.*, 1988), plasma prolactin and various amino acids (Abu *et.al.*, 1987) including glutamine (Hanson and Mehman, 1976), manganese (Tolbert, *et.al.*, 1981), and methotrexate and various cytostatics (Hudakova, 1992). Inhibitors include metals such as cadmium, zinc, and copper

Table 4.3.3: Occurrence of gluconeogenesis and/or glucogenic compound catabolism in animal cells in culture

Cell Culture Type	Reference
Rat hepatocytes	Valera <i>et al.</i> 1993
skipjack tuna hepatocytes	Buck <i>et al.</i> 1992
Rat liver organ culture	Rosa <i>et al.</i> 1992
Human hepatocytes	Takahashi <i>et al.</i> 1994
Rat hepatocytes	Wiechetek <i>et al.</i> 1993
Perfused mammalian livers	Donato <i>et al.</i> 1993
Parenchymal cells	Tolbert <i>et al.</i> 1980
Renal proximal tubules	Yanagawa <i>et al.</i> 1983
Rabbit renal proximal tubule	Jans <i>et al.</i> 1989
Amphibian retina	Goldman 1989
Neural cells	Baines <i>et al.</i> 1988
Rabbit kidney cortex tubules	Michalik <i>et al.</i> 1987
Rabbit kidney cell line LLC-RK	Williams <i>et al.</i> 1990
Various cultured mammalian cells	Kier <i>et al.</i> 1995
Spermatozoa	Hanson and Mehlman 1976
Striated muscle cells	Hanson and Mehlman 1976
V 79B cell line	Hudakova 1992
Hepatoma cells	Lauris <i>et al.</i> 1986

Table 4.3.4: Chemical factors affecting gluconeogenesis and/or glucogenic compound metabolism

<i>Chemical Factor</i>	<i>Effect</i>	<i>Reference</i>
Monocarboxylate transporter	Inhibit/Enhance	Garcia <i>et al.</i> 1994
Various hormones	Inhibit/Enhance	Pilo <i>et al.</i> 1993
Various neurotransmitters	Inhibit/Enhance	Pilo <i>et al.</i> 1993
Various regulatory enzymes	Inhibit/Enhance	Rosa <i>et al.</i> 1992
Lithium	Inhibits	Bosch <i>et al.</i> 1992
Cytostatics	Enhance	Hudakova 1992
Phenobarbital	Inhibits	Argaud <i>et al.</i> 1991
Cd, Zn, Cu	Inhibit	Tolbert <i>et al.</i> 1981
Manganese	Enhance	Tolbert <i>et al.</i> 1981
Insulin	Inhibits	Lauris <i>et al.</i> 1986
Epidermal growth factor	Enhance	Moule <i>et al.</i> 1988
Various neurotransmitters	Inhibit/Enhance	Baines <i>et al.</i> 1988
Gentamicin	Inhibits	Michalik <i>et al.</i> 1987
Plasma prolactin	Enhance	Abu <i>et al.</i> 1987
Various amino acids	Enhance	Abu <i>et al.</i> 1987
Glucose	Inhibits	Lauris <i>et al.</i> 1986
Phorbol esters, vasopressin, angiotensin II, p-kinase C	Regulate	Garcia <i>et al.</i> 1986
Somatostatin	Regulate	Dileepan <i>et al.</i> 1985
Growth hormone	Stimulates	Rogers <i>et al.</i> 1989
Glutamine	Enhance	Hanson and Mehlman 1976
Nitrite	Stimulates	Wiechetek <i>et al.</i> 1993
Methotrexate	Enhance	Hudakova 1992

(Tolbert, *et.al.*, 1981), and lithium (Bosch, *et.al.*, 1992), phenobarbital (Argaud, *et.al.*, 1991), gentamicin (Michalik, *et.al.*, 1987), and (of course) glucose (Lauris, *et.al.*, 1986). Some chemical species can play the role of inhibitor or enhancer, depending upon their concentration. This class of dual role regulators includes monocarboxylate transporter (Garcia, *et.al.*, 1994), various hormones (Pilo, *et.al.*, 1993), various neurotransmitters (Pilo, *et.al.*, 1993; Baines, *et.al.*, 1988), and various regulator proteins (Rosa, *et.al.*, 1992).

All mammalian cells are capable of metabolism of various glucogenic compounds. The following survey of the CHO cell literature suggests that these cells may be capable of the metabolism of glucogenic compounds.

When glucose was replaced with galactose as the carbon source for a CHO cell culture, the specific growth rate was depressed, the lactate concentrations initially increased, but then unexpectedly decreased (Barngrover *et al.*, 1985). When CHO cells were arrested in the G1/G0 cell cycle phase, the lactate production significantly declined (Jenkins and Hovey, 1993). These observations are consistent with the enhancement of gluconeogenesis by cytostatic agents (Hudakova, 1992).

When Ogata *et al.* (1993) utilized serum-free medium for CHO cell culture, they observed that the specific production rate of recombinant protein increased, while lactate production significantly decreased. Specifically, they measured the yield of lactate on glucose as $0.049 \text{ mol mol}^{-1}$. (Commonly, yields of lactate on glucose in CHO culture are approximately 1.2 mol mol^{-1} .) Both of these observations are consistent with the cytostatic effect of the absence of serum in the medium. The very low apparent yield of lactate on glucose reported by Ogata *et al.* (1993) may be an artifact, created by the biodegradation of lactate in the absence of serum. *i.e.* The low apparent yield of lactate on glucose may be indicative of lactate metabolism (gluconeogenesis).

In 1994, the Ogata group reported results from further work with CHO cells in serum-free medium. In this paper the authors cite a "remarkable" increase in specific recombinant protein production, and a decrease in lactate production. They suggest the "CHO K1 cells exhibit different physiological characteristics in response to serum removal from the medium". In their work, the cell density was not determined directly, but was estimated from the glucose consumption rate. The approach assumed that specific glucose consumption rate is approximately constant, which is not necessarily consistent with their assertion of altered physiological characteristics. Moreover, the specific recombinant protein production rate is estimated from the lactate production to glucose consumption ratio. Using this approach, it is not only assumed that the specific glucose consumption rate is approximately constant, but that the yield of lactate on glucose is also approximately constant, and that the specific recombinant protein production rate is correlated with this yield. Obviously, any change in glucose consumption and/or lactate yield, would impact on calculated cell density and specific recombinant protein production rate; while lactate biodegradation would have a

significant effect on these calculations. Changes in the rates of glucose consumption and lactate production, and/or the occurrence of lactate biodegradation, which may well accompany "different physiological characteristics" associated with cells cultured in serum-free medium, may explain the authors' finding of a (calculated) "remarkable" increase in recombinant protein production.

Hayter's group (1993) studied the physiology of a recombinant CHO cell line in glucose-limited chemostat culture. As the rCHO 320 cell line contains the DHFR-based plasmid, the group used methotrexate to amplify the recombinant protein gene expression. Their reported data contains some interesting anomalies: 1. The glucose consumption data suggests that there is no maintenance energy requirement for these CHO cells. 2. The specific lactate production rate decreases with the specific growth rate (compare this finding to the assumption of constant specific lactate production rate utilized by Ogata *et al.*, 1993). Regression of their data indicates that no lactate would be produced when the specific growth rate falls below 0.011 h^{-1} . As the specific growth rate is directly correlated to the glucose concentration, this observation may be indicative of lactate biodegradation under conditions of low glucose concentration (recall that glucose inhibits gluconeogenesis (Lauris, *et al.*, 1986)). 3. The apparent ammonia yield from glutamine is very high at low specific growth rates. Normally, the moles of glutamine consumed is approximately equal to the moles of ammonia produced. This suggests that glutamine consumption is not following the usual catabolic pathway. 4. The specific alanine production rate decreased with specific growth rate. Regression of their data indicates that no alanine would be produced when the specific growth rate falls below 0.011 h^{-1} . This again suggests that glutamine consumption is not following the usual catabolic pathway, and/or that alanine, a glucogenic compound, is being consumed. 5. Serine levels decreased sharply with growth rate, and once again, extrapolation of data indicates that no serine would be produced when specific growth rate falls below 0.011 h^{-1} . This also suggests that serine, a glucogenic compound, is being consumed. 6. Both asparagine and glycine uptake rates were abnormally high, while the glutamate production rate remained constant through all growth rates. Here, again, both asparagine and glycine are glucogenic compounds, while glutamate is a byproduct of the biodegradation of many amino acids.

The authors suggest that glucose is not the sole energy source in the medium. They attempt to account for their data via the utilization of glutamine, through the citric acid cycle, as an energy source. However, this would also yield alanine and serine, which their data indicate are both decreased under conditions of low glucose concentrations. The authors especially noted that the specific products of glucose catabolism approach zero as the specific growth rate decreases. Finally, the authors noted that similar phenomena are observed in HeLa cells and in rat hepatoma cells. Although not mentioned by Hayter *et al.* (1993), both of these cell lines have been shown elsewhere to undergo gluconeogenesis.

Metabolism of dhfr-System Recombinant Chinese Hamster Ovary Cells

The above discussion and observed data support the plausibility that gluconeogenesis functions in the metabolism of the recombinant CHO1-5₅₀₀ cell line. Above some critical threshold concentrations, it appears that glucose and glutamine are the primary substrates for metabolism, and that gluconeogenesis does not occur, or plays an insignificant role. The utilization patterns for these two substrates have been discussed above. The critical concentrations of glucose and glutamine observed in this cell line may be 0.5 mmol L⁻¹ and 0.5 mmol L⁻¹, respectively.

Following glucose depletion (here, defined as decrease to a constant concentration of 0.5 mmol L⁻¹), lactate is no longer produced, but is not consumed until glutamine is also depleted to its critical level. It therefore appears that glucose and glutamine are preferentially utilized and that gluconeogenesis only occurs in their absence. Another interpretation is that gluconeogenesis is inhibited by glucose above 0.5 mmol L⁻¹, and that the lag between glucose depletion and the start of lactate consumption reflects the time necessary for the biosynthesis of the enzymes and intermediates of gluconeogenesis. The decrease in the viable population which occurs when glucose is depleted suggests that some cells were not able to switch to lactate metabolism. The phase I gluconeogenesis pathway utilises the two pyruvate family glucogenic compounds which are available in excess: lactate and alanine. These substrates can be utilized as carbon, nitrogen, and energy sources.

The high concentrations of DHFR in this rCHO cell line also play a role in its metabolism. DHFR may drive the production of glycine from serine, which in turn is derived from 3-phosphoglycerate, which is an intermediate of glycolysis. The 3-phosphoglycerate may come from phase I gluconeogenesis of lactate and alanine. Production of serine from 3-phosphoglycerate requires glutamate as a co-substrate and yields α -ketoglutarate as a co-product. The consumption of glutamate and production of α -ketoglutarate serve, in turn, to facilitate the entry of alanine into the gluconeogenesis pathway via alanine transamination. This interlocking pathway mechanism is illustrated in Figure 4.3.8.

A side benefit of the three phase metabolic batch culture pattern in this rCHO cell line is that the pH of the system is restored to physiologically compatible values as the lactate is consumed. When pH falls below 6.5 animal cell cultures enter into rapid necrotic cell death (Phillips, 1991). The major contributing factor to falling pH is the increasing concentration of lactate from the glycolysis of glucose. In this culture, only 62.5% of the glucose is metabolised to lactate, so that the pH fall is not as rapid as that observed in hybridoma cultures. Secondly, the consumption of lactate coupled with the continued production of ammonia in the latter half of the culture period restores the pH to physiologically compatible levels. The avoidance of toxic acid conditions may be the controlling factor in the extended maintenance of viability which results in the long (4 week) batch culture period. Lactate and alanine are not depleted by the end of the culture period. The accumulation of ammonia may be the controlling factor in the entry of the

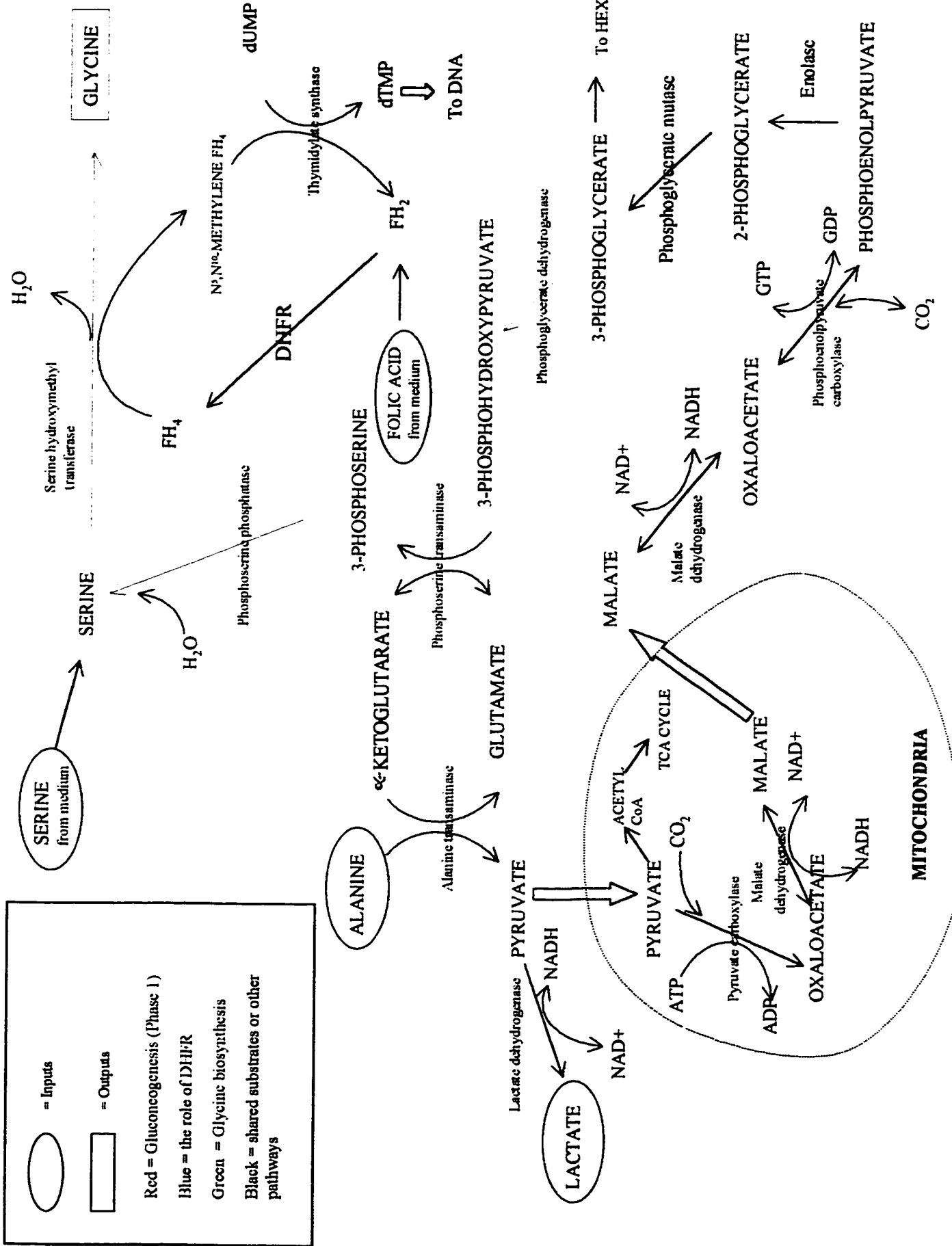


Figure 4.3.8: Lactate and alanine consumption through the gluconeogenesis Phase I pathway, serine synthesis, and glycine production mediated by DHFR. FH₄: tetrahydrofolate; FH₂: dihydrofolate; dUMP: deoxyuridylylate monophosphate; dTMP: deoxythymidylylate monophosphate

population into apoptosis. In this culture the viable cell concentration begins to decrease from a steady state value of approximately 0.8 mmol L^{-1} when ammonia reaches a concentration of 4.5 mmol L^{-1} . This occurs at approximately 325 hours, several days after lactate consumption began, and at a physiologically compatible pH of approximately 7.15. A summary of the overall metabolic equations which are the major contributors that can account for the metabolite patterns observed during the three metabolic phases of this rCHO cell line in batch culture is presented in Figure 4.3.9.

Concluding Remarks

The metabolism of rCHO cells in batch culture is more complex than that of hybridomas in batch culture. On the basis of substrate consumption and metabolic byproduct accumulation, the metabolic pattern of this batch culture of rCHO can be partitioned into three phases. The first phase is characterized by relatively high specific consumption rates of glucose and glutamine, with significant amounts of lactate, ammonia, and alanine accumulating. This metabolic phase is similar to the metabolic patterns observed in batch hybridoma culture, except for significantly smaller yields of lactate on glucose, ammonia on glutamine, and alanine on glutamine. At the end of the first metabolic phase the viability decreases abruptly. In the second metabolic phase, glucose consumption ceases and a steady concentration of approximately 0.5 mmol L^{-1} is maintained, while lactate accumulation ceases. The glutamine specific consumption rate is reduced, but the yield of ammonia on glutamine is increased to about 2 mol mol^{-1} . The total cell concentration drops at the beginning of the second metabolic phase, but then increases exponentially through the remainder of the second metabolic phase. This exponential increase is not reflected in the viable cell population, which following the initial drop is maintained at an approximately constant concentration through the remainder of the second metabolic phase. This suggests that while a portion of the viable population resides in the cycling fraction, another portion is entering senescence, perhaps because these cells were unable to make the metabolic switch. In the third metabolic phase both glucose and glutamine concentrations are approximately constant at 0.5 mol mol^{-1} . The notable phenomenon associated with the third metabolic phase is the consumption of lactate and alanine. Viability is maintained, suggesting that lactate and alanine are being utilized as carbon, nitrogen, and energy sources. The pH does not fall to toxic levels, probably as a result of the consumption of lactate. The maintenance of a physiologically compatible pH level also contributes to the maintenance of viability. Viability drops significantly as ammonia levels rise above 4.5 mmol L^{-1} . Lactate and alanine are not depleted by the end of the batch culture, suggesting that toxic levels of ammonia are the controlling factor in loss of viability.

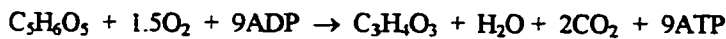
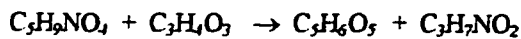
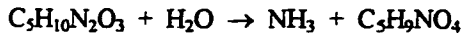
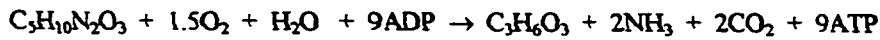
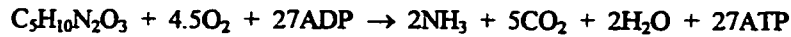
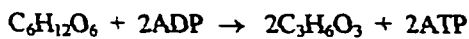
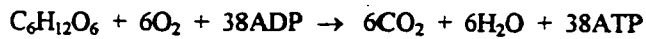
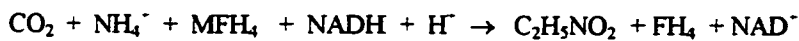
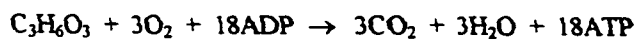
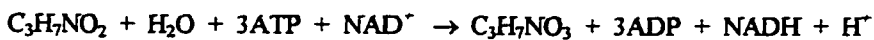
Glutamine:**Glucose:****Serine:****Ammonia:****Lactate:****Alanine:**

Figure 4.3.9: Summary of overall pathways for the consumption of major substrates by rCHO

The specific production rate of tPA is greatest during the lag population phase and the early exponential population phase, which also corresponds to the first metabolic phase. This is in contrast to the expectation that tPA production would be maximal during the exponential phase when the proportion of the population in S phase is maximal and the DHFR concentration is therefore also maximal (see Section 4.1.2). The drop in tPA productivity at the end of the first metabolic phase may be the result of the natural regulatory mechanisms of the concentration of the protein, or may be the result of the altered metabolism of the population. Production of tPA continues at a decreased but steady rate until the viability drops when ammonia reaches 4.5 mmol L^{-1} part way through the third metabolic phase. The tPA concentration declines as the total cell concentration declines, suggesting a correlation with cell lysis. Acid proteases released into the medium from dead and lysing cells may degrade the tPA.

Gluconeogenesis, which would account for the consumption of lactate and of alanine, may be a part of the metabolism of this rCHO cell line. Besides the present observations, phenomena supporting the possibility of gluconeogenesis has been widely reported. The elevated levels of DHFR in this rCHO cell line may drive a metabolic scheme consisting of phase I of gluconeogenesis coupled to serine biosynthesis and its transamination into glycine. Although the elevated levels of DHFR may not be sufficient to extend population growth, they may be sufficient to extend the viability of a batch culture by driving lactate and alanine consumption.

There may be significant offshoots of these interpretations. For example, unique, unexpected patterns in biochemical consumption and accumulation (eg. alanine, glycine, lactate, etc.) observed in the batch culture of the CHO1-5₅₀₀ cell line has been explained by considering that cells that are both transformed and genetically engineered are not normal. Depending upon plasmids, vector constructs, and host cell, complicated interactions between recombinant protein production and metabolic pathways should not be unexpected. With such cells, these patterns should not be dismissed as artefacts, but actively studied. Furthermore, by understanding these unique expression patterns, it may be possible for biochemical engineers to monitor productivity indirectly and inexpensively. Tissue plasminogen activator, as a case in point, is both costly and notoriously difficult to measure. Therefore, batch production could be easily monitored via the patterns of one of the above-mentioned metabolites. By understanding that tPA production is directly correlated with metabolic phase one of a batch culture, optimised batch length may be determined from monitored levels of glucose, glutamine, and lactate. These correlations may be applied to the design of fed-batch protocols which could enhance the productive portion of a batch culture by extending the length of the first metabolic phase.

4.3.2 Preliminary Modeling of Growth and rProtein Production

A working model for the growth and production kinetics of a cell culture system can be useful in process monitoring, control, and optimization strategies. A good model can be used to predict outcomes of optimization strategies without recourse to actual experimentation. However, good working models for animal cell culture systems are difficult to develop, primarily because of the lack of knowledge of these highly complex systems (see Section 2).

An attempt was made to adapt an existing kinetic model, developed for hybridoma cells, to the CHO1-5₅₀₀ cell line. The complexity of the observed CHO1-5₅₀₀ metabolite patterns in batch culture rendered this task more challenging than was originally anticipated. Three metabolic phases were identified for this rCHO cell line (see Section 4.3.1), based on the consumption of three major substrates. In addition to the significant utilization of glucose and glutamine, as seen in hybridoma cells and many other animal cells, this rCHO cell line also utilized lactate to a considerable extent. Net lactate consumption was not observed when glucose and glutamine levels were greater than 0.5 mmol L⁻¹, and the growth and metabolite kinetics could be adequately described by the Phillips's model by instigating appropriate parameter values reflective of the metabolism of the CHO1-5₅₀₀ cell line. However, these equations required adjustments in order to describe the third metabolic phase. The equations describing the kinetics of glutamine, glucose, the viable population concentration, the dead population concentration, alanine, and lactate were developed as follows:

Glutamine:

It was noted that glutamine consumption was about twice as great during the lag phase as at any other time. This was interpreted as indicating the G1/G0 phase cells use about twice as much glutamine as cells in other physiological states. (An interesting implication with respect to protein synthesis ...):

$$demand = 2f_{G1} + (1 - f_{G1})$$

where f_{G1} is the G1 fraction of the viable population

Therefore, the equation describing glutamine consumption is:

$$\frac{dGLN}{dt} = -demand \left[\frac{G_s GLN X_v (A\mu + B)}{G_s GLN (9 + 18f_1) + GLC (2 + 36f_2)} \right] \quad \text{M-1}$$

where
 GLN is the glutamine concentration (mmol L⁻¹)
 GLC is the glucose concentration (mmol L⁻¹)
 G_s is the substrate preference index
 X_v is the viable cell concentration (million cells/mL)
 A is the specific biosynthetic energy rate (moles ATP/cell)
 B is the specific maintenance energy rate (moles ATP/cell/time)
 f₁ is the fraction of glutamine completely oxidized
 f₂ is the fraction of glucose completely oxidized
 and *demand* is a function of the G1 fraction of the population

Glucose:

$$\frac{dGLC}{dt} = -\frac{1}{G_s} \frac{GLC}{GLN} \left[\frac{G_s GLN X_v (A\mu + B)}{G_s GLN (9 + 18f_1) + GLC (2 + 36f_2)} \right] \quad \text{M-2}$$

Viable Cells:

$$\frac{dX_v}{dt} = (\mu - k_d) X_v \quad \text{M-3}$$

where μ is the specific growth rate (h⁻¹)
 and k_d is the specific death rate (h⁻¹)

Dead Cells:

$$\frac{dX_d}{dt} = k_d X_v - k_l X_d \quad \text{M-4}$$

where k_l is the specific rate of cell lysis (h⁻¹)
 and X_d is the dead cell population (million cells/mL)

Lysed Cells:

$$\frac{dX_l}{dt} = -k_l \frac{dX_d}{dt} \quad \text{M-5}$$

Alanine:

$$\frac{dALA}{dt} = -q_{ALA} X_V \quad \text{M-6}$$

where ALA is the alanine concentration (mmol L⁻¹)
 and q_{ALA} is the specific consumption rate of alanine
 (can be greater than or less than zero)

Lactate:

$$\frac{dLAC}{dt} = -Y_{LAC,GLC} \frac{dGLC}{dt} - q_{LAC} X_V \quad \text{M-7}$$

where LAC is the lactate concentration (mmol L⁻¹)
 and $Y_{LAC,GLC}$ is the yield of lactate on glucose
 q_{LAC} is the specific consumption rate of lactate

In addition to the equations explicitly describing the kinetics of the viable cell population, the dead cell compartment, glucose, glutamine, alanine, and lactate, equations were developed to follow the kinetics of ammonia, serine, glycine, and the G1 and G0 phase population. These equations are based on observed stoichiometric relationships, assuming the primary use of the interconnecting metabolic pathways shown in Figure 4.3.8 and the relationship between the physiological states of the cells (Section 2.1).

Serine:

$$\frac{dSER}{dt} = q_{SER} X_V \quad \text{M-8}$$

where: SER is the serine concentration (mmol L⁻¹)
 q_{SER} is the specific consumption rate of serine
 X_V is the viable cell concentration

Ammonia:

$$\frac{dNH_3}{dt} = -Y_{ALA,GLN} \frac{dGLN}{dt} - (1 - Y_{ALA,GLN}) Y_{NH_3,GLN} \frac{dGLN}{dt} - Y_{GLY,NH_3} \frac{dSER}{dt} \quad \text{M-9}$$

where NH_3 is the ammonia concentration
 $Y_{ALA,GLN}$ is the yield of alanine on glutamine
 $Y_{NH_3,GLN}$ is the yield of ammonia on glutamine
 Y_{GLY,NH_3} is the yield of glycine on ammonia
 GLN is the glutamine concentration
 and SER is the serine concentration

Glycine:

$$\frac{dGLY}{dt} = -\frac{dSER}{dt} - f_3 \frac{dLAC}{dt} - f_4 \frac{dALA}{dt} ; \quad \text{M-10}$$

where, $f_3 = 0$ when $dLAC/dt > 0$; and, $f_4 = 0$ when $dALA/dt > 0$

where: GLY is the glycine concentration (mmol L^{-1})
 SER is the serine concentration (mmol L^{-1})
 LAC is the lactate concentration (mmol L^{-1})
 ALA is the alanine concentration (mmol L^{-1})
 f_3 is the fraction of lactate consumed for serine biosynthesis
 and f_4 is the fraction of alanine consumed for serine biosynthesis

G1 phase Cells:

$$\frac{dG1}{dt} = f_5 \frac{X_V}{dt} \quad \text{M-11}$$

where $G1$ is the concentration of G1 phase cells (cells/mL)
 and f_5 is the fraction of the viable population in the G1 phase

G0 phase Cells:

$$\frac{dG0}{dt} = -f_6 \frac{dG1}{dt} \quad \text{M-12}$$

where: $G0$ is the G0 phase cell concentration (cells/mL)
 and f_6 is the fraction of the cells leaving G1 which enter G0

The equation describing the protein production kinetics in the Phillips's model was not used. Instead, the relationship of extracellular tPA accumulation to the G1 cell cycle phase was reflected by expressing the tPA concentration as a direct linear function of the G1 phase cell-hours. The proportionality constant is the specific productivity with respect to the G1 phase cell-hours. Similarly, product degradation kinetics were incorporated as a direct function of the lysed cell concentration. To this extent, the model was segregated.

tPA:

$$\frac{dtPA}{dt} = q_{tPA} \frac{dG1CH}{dt} - k_{tPA} \frac{dX_l}{dt} \quad \text{M-13}$$

where tPA is the product titre (mg/L)
 q_{tPA} is the G1 specific productivity rate
 $G1CH$ is the volumetric G1 phase cell-hours
 and k_{tPA} is the product degradation rate constant

Finally, equations were incorporated for the cumulative volumetric cell-hours for the viable population and for the G1 phase fraction of the population:

Cell-Hours:

$$CH = \int X_v dt \quad \text{M-14}$$

G1 Phase Cell Hours:

$$G1CH = \int G1 dt \quad \text{M-15}$$

The rCHO cell line was observed to pass through three metabolic phases over the course of a batch culture (Section 4.3.1). Several of the parameters altered value with switches in metabolism. The two metabolic switches appeared to coincide with depletion of glucose to a steady state concentration and depletion of glutamine to a steady state concentration, respectively. The depletion points were assumed to be the triggers for the metabolic switches resulting in step changes in the values of some of the parameters (Table 4.3.5).

The model was tested by simulating the batch culture dynamics observed in the experiment analyzed in Sections 4.1.1 and 4.3.1. Once the parameter values were determined and the initial values of the variables were set, the simulation was achieved through a process of orthogonal collocation. The model contains a total of 15 equations and 24 parameters, 19 of which were determined from experimental data. Four of the five estimated parameters were used as adjustable parameters to fit the observed batch culture dynamics. The four adjustable parameters were the specific biosynthetic energy rate (A), the specific maintenance energy rate (B), the fraction of consumed lactate utilized for serine synthesis (and ultimately glycine synthesis) (f_3), and the fraction of consumed alanine utilized for serine synthesis (and ultimately glycine synthesis) (f_4). From the simulation results are presented graphically in Figure 4.3.10, it is apparent that the model fits the data well, with the exception of ammonia during the last half of the culture period (Figure 4.3.10g).

The third step in modeling comprises model refinement through simulations of different sets of experimental data (see Section 2.3). To this end, the dynamics of a second dispersed suspension batch culture were simulated. The simulation results are presented in graphical form in Appendix B. The model was successful in simulating the first metabolic phase and the first metabolic switch, but failed to accurately simulate the remainder of the batch culture dynamics. It was concluded that the assumptions that steady state glucose and glutamine concentrations are the sole controlling elements determining metabolic phases were incorrect, at least in as much as the specific values assigned.

The impact of the initial substrate concentrations on the batch culture dynamics were then investigated in an exploratory factorial experiment. Four factors were considered: lactate concentration, glucose concentration, glutamine concentration, and the presence of serum. Due to equipment and time constraints, only two levels of each variable were tested, in an experimental matrix with only a single replicate of eight separate treatment combinations

Table 4.3.5: Model parameters and initial conditions for a dispersed suspension batch culture of CHO1-S₅₀₀ cells.

Initial Conditions	Parameter Values
Glucose: 8 mmol/L	A: 50
Glutamine: 5.5 mmol/L	B: 0.2
Lactate: 0 mmol/L	q _{tPA,G1} : 0.0975 pg/c-h
Alanine: 0.2 mmol/L	ktPA: 35 pg/c-h
Serine: 0.0225 mmol/L	Y _{amm,gln} : 0.016 mol/mol
Glycine: 0.30 mmol/L	Y _{lac,glc} : 1.25 mol/mol
Ammonia: 0 mmol/L	q _{ALA} : 0.006 nmol/c-h
tPA: 0 mg/L	q _{LAC} : 0.036 nmol/c-h
X _v : 0.25 E6 c/mL	q _{SER} : 0.0012 nmol/c-h
X _d : 0.0075 E6 c/mL	f _{amm→gly} : 0
X _l : 0 c/mL	f _{gln→amm} : 1.2
XG ₁ : 0.175 E6 c/mL	G _s : 0.365
XG ₀ : 0 c/mL	f ₁ : 0.725
Pop-CHvol: 0 c-h/mL	f ₂ : 0.367
G1-CHvol: 0 c-h/mL	f ₃ : 0.035
	f ₄ : 0.010
	f ₅ : 0.85
	ck _{gln} : 0.002
	μ _{max} : 0.0155 h ⁻¹
	kd-1: 0.0001 h ⁻¹
	kd-2: 0.0035 h ⁻¹
	kd-3: 0.0046 h ⁻¹

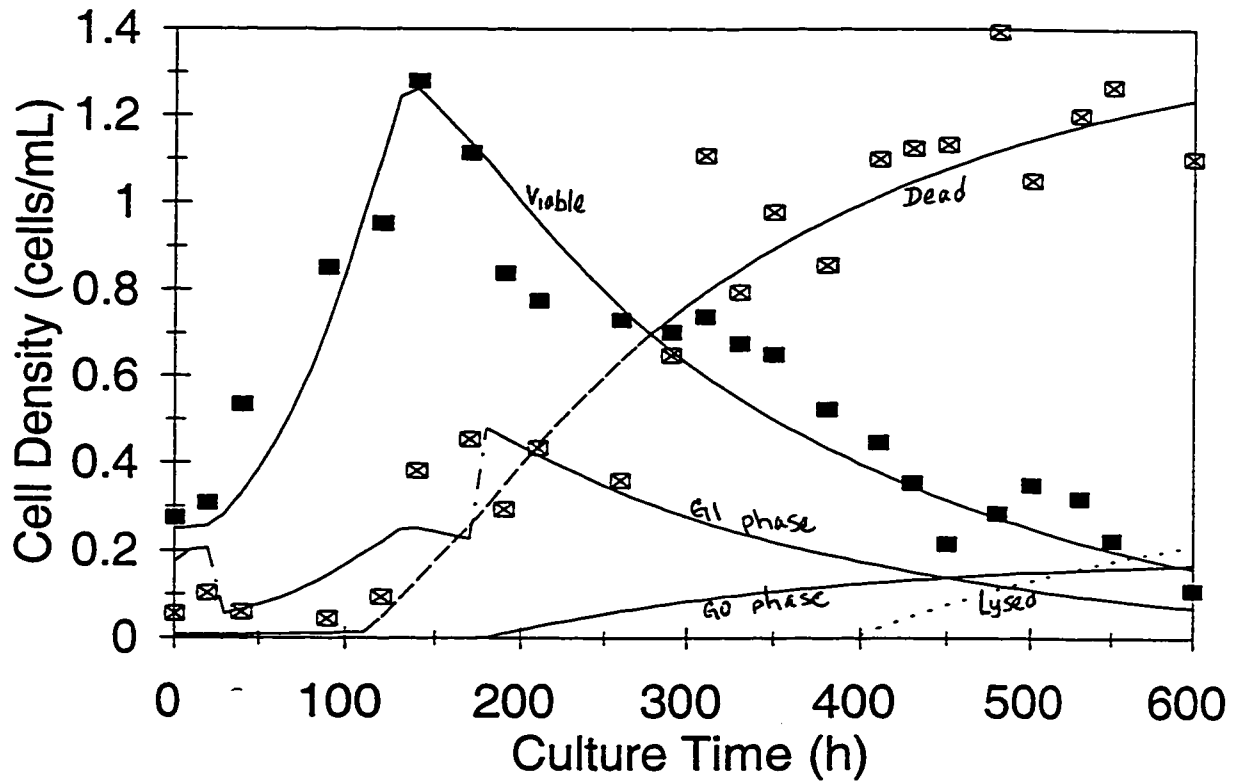


Figure 4.3.10a: Model simulations of the batch culture dynamics of dispersed suspension CHO1-5₅₀₀ cells in a stirred tank bioreactor with serum-free medium. symbols = data : solid squares- viable cells ; x-in-squares- dead cells

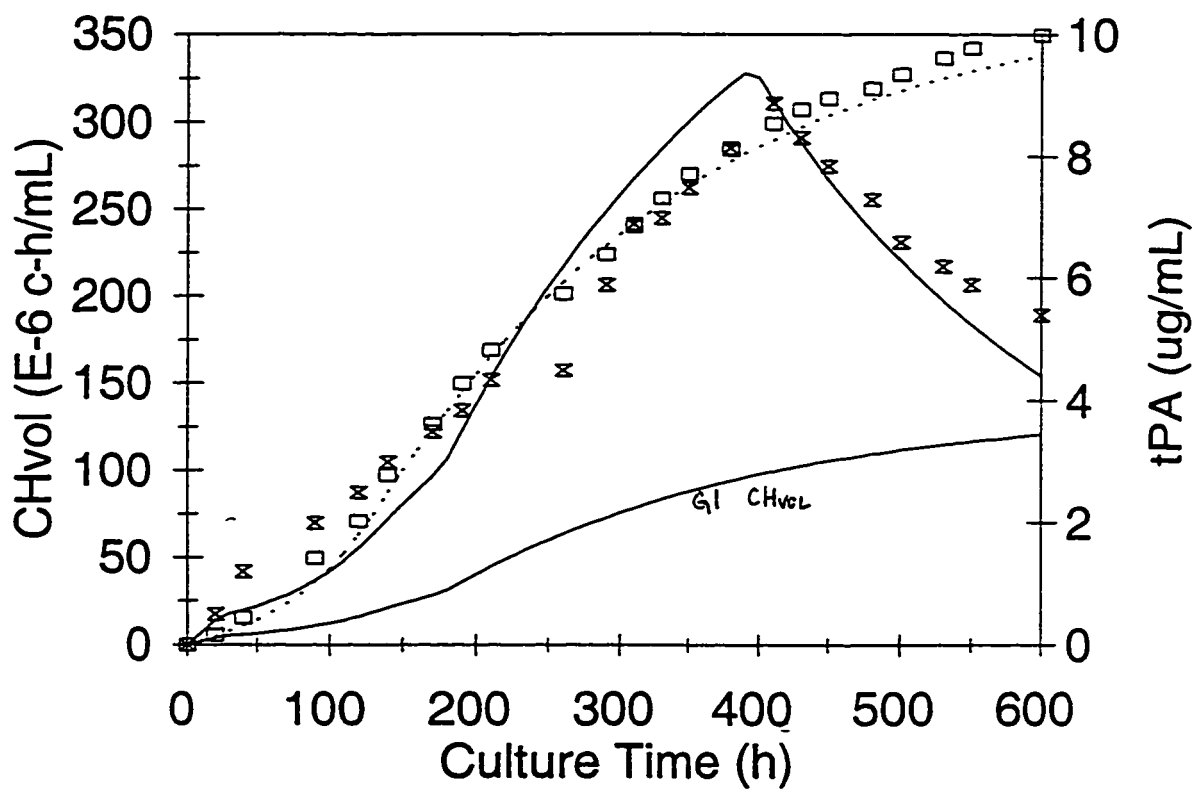


Figure 4.3.10b: X - tPA ; □ CHvol

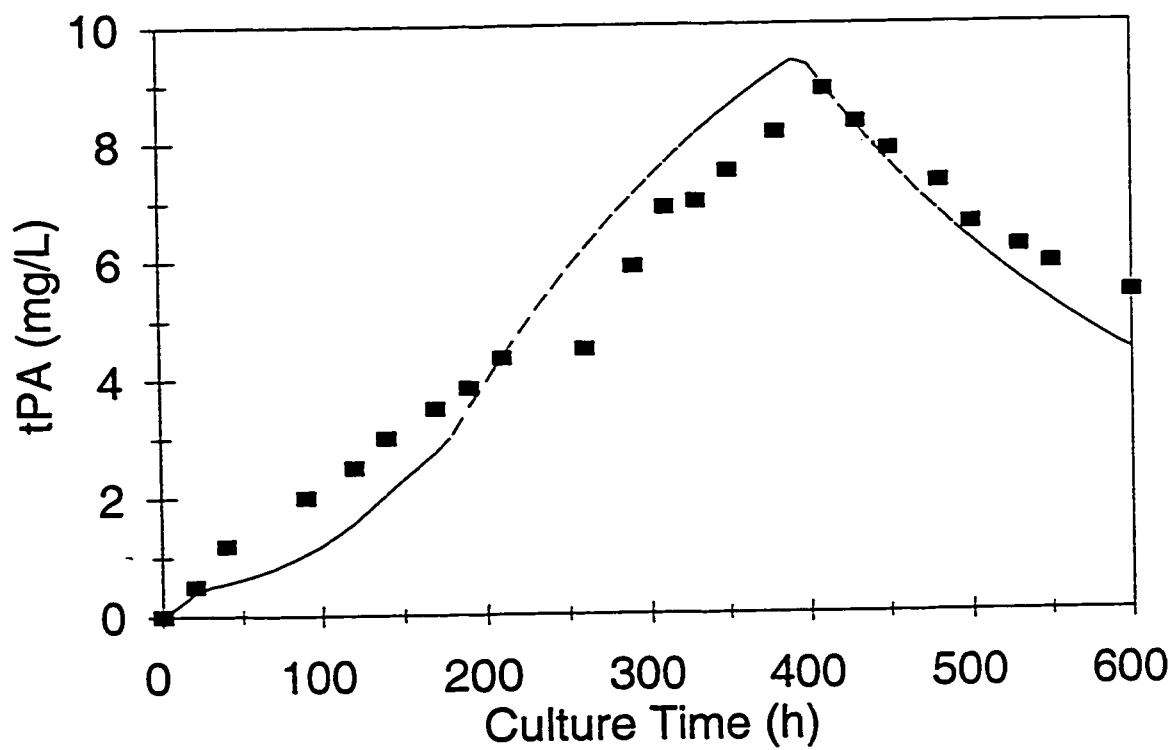


Figure 4.3.10c

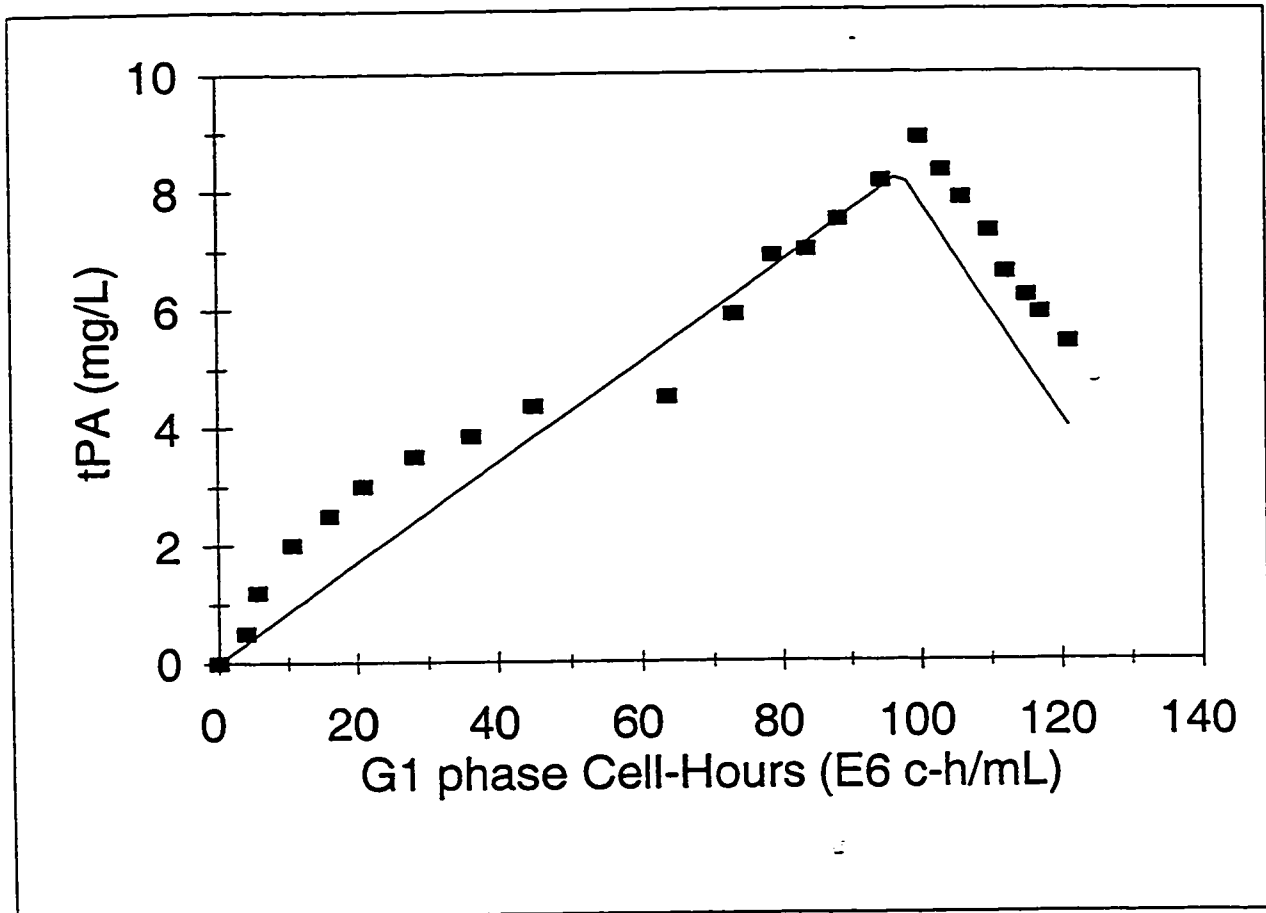


Figure 4.3.10d

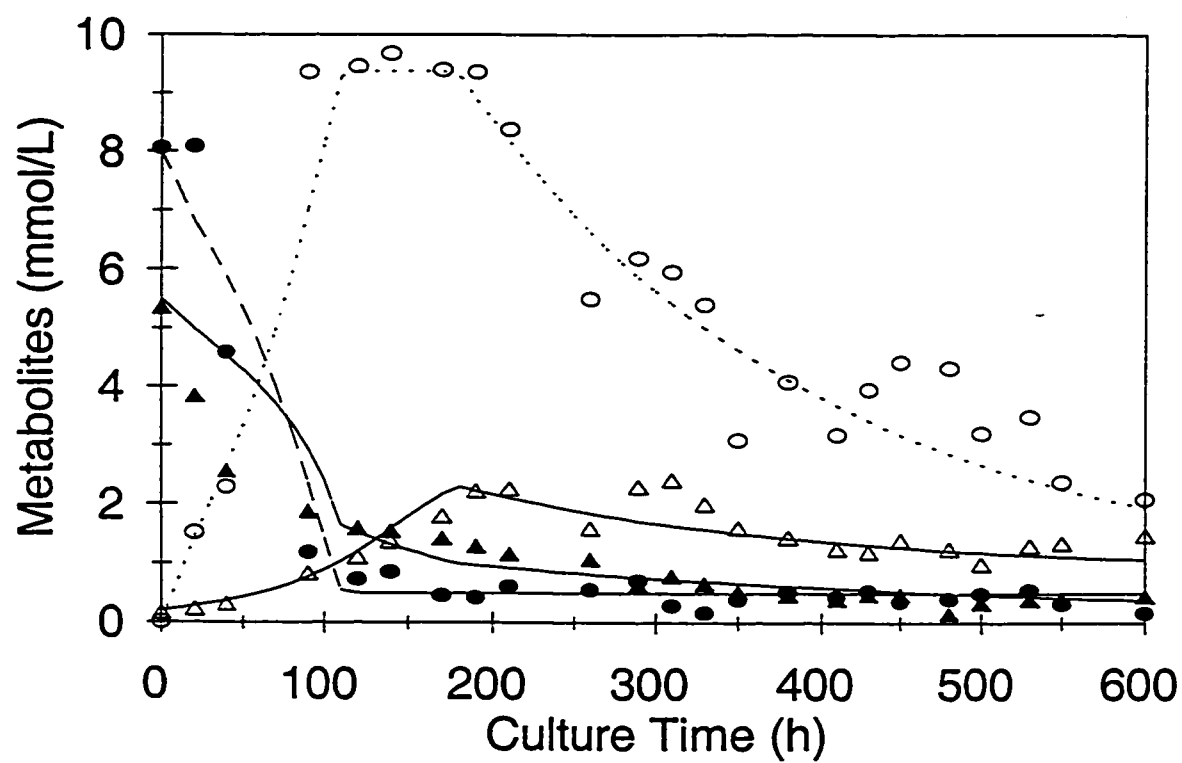


Figure 4.3.10e: solid circles - glucose; open circles - lactate; solid triangles - glutamine; open triangles - alanine

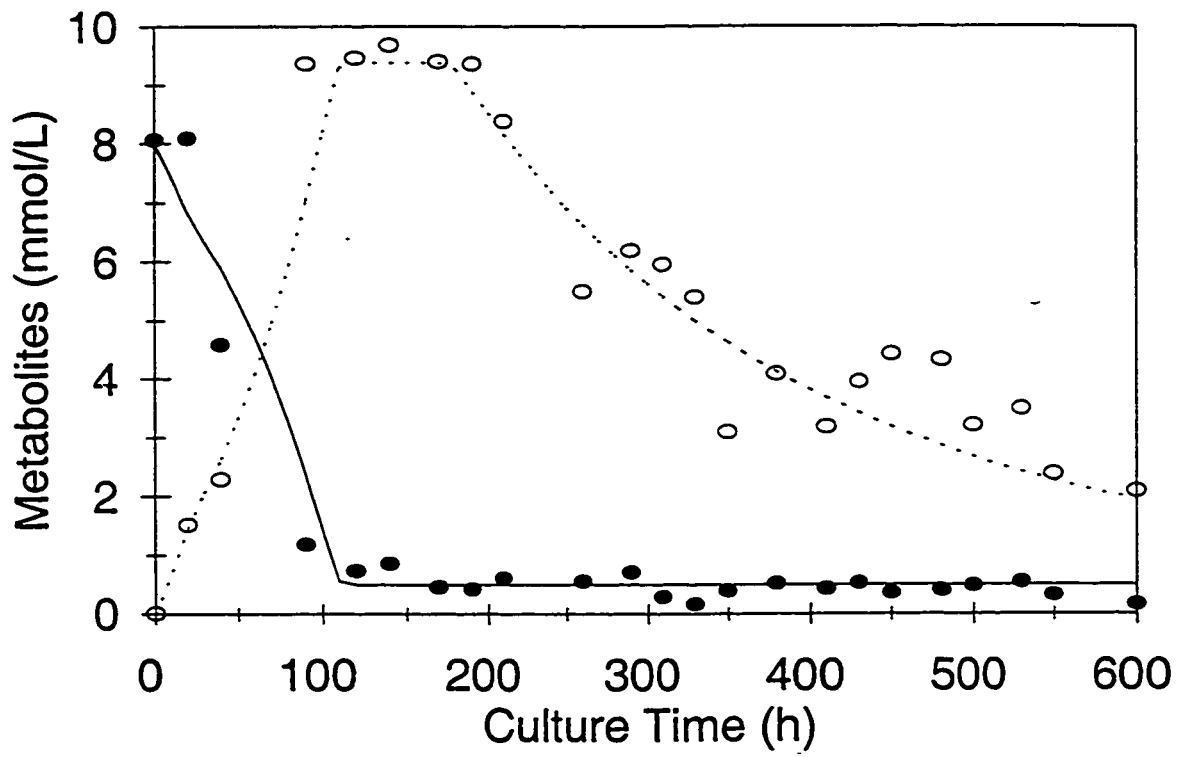


Figure 4.3.10f: solid circles - glucose; open circles - lactate

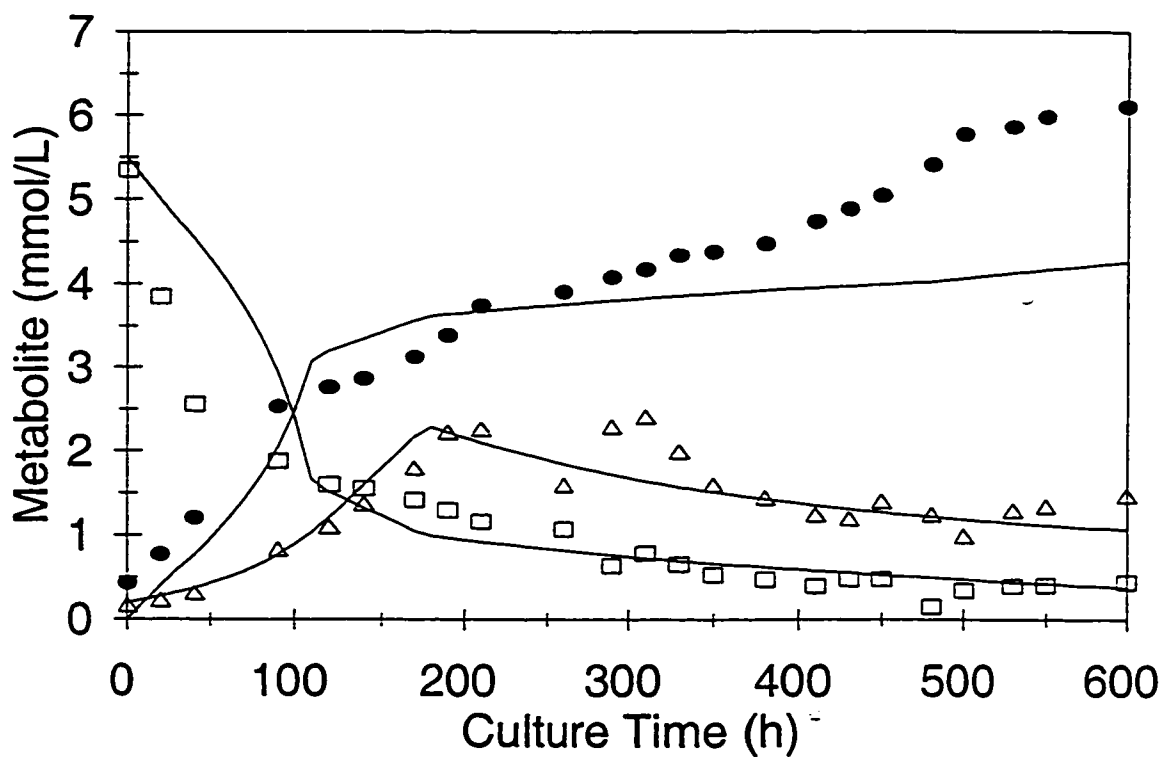


Figure 4.3.10g: solid circles - ammonia; open squares - glutamine; open triangle - alanine

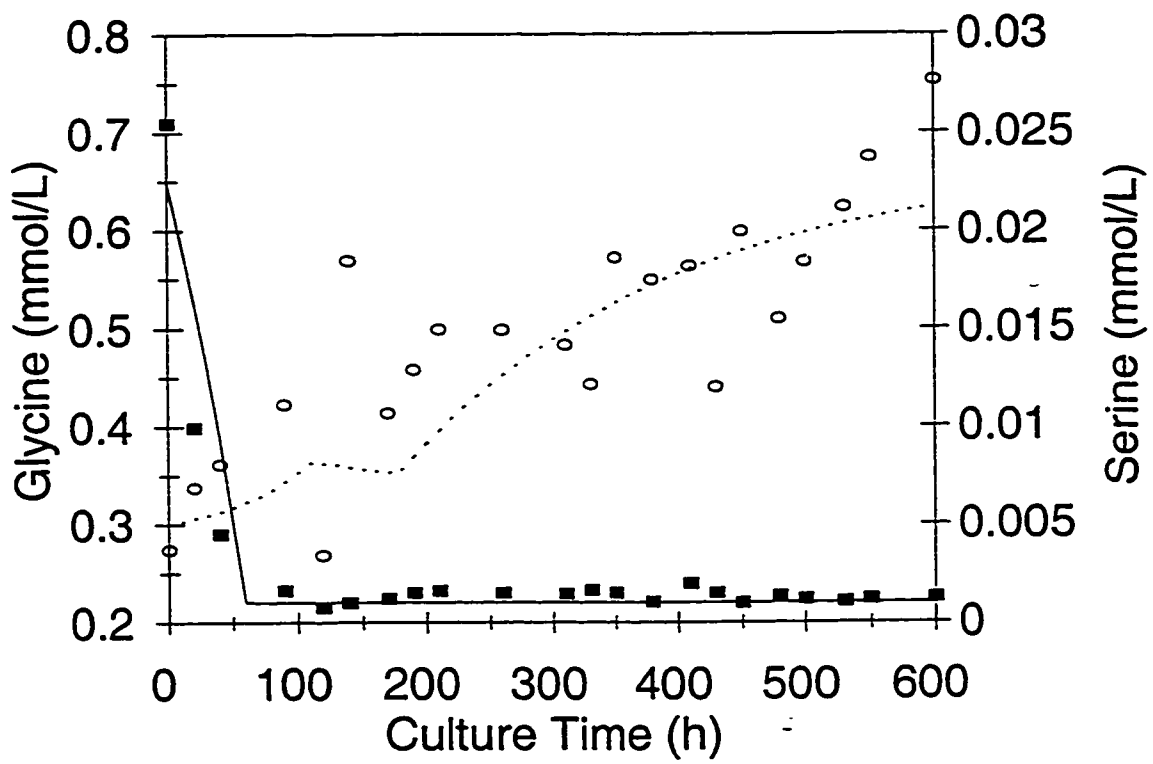


Figure 4.3.10h: solid squares - serine; open circles - glycine

(Table 4.3.6). The available degrees of freedom for the design did not allow for examination of treatment interactions on a statistical basis (Systat 6.0 for Windows, SPSS Inc., Chicago, Ill.), although strong interactions were to be expected. Some important trends are, however, quite apparent and are presented in Tables 4.3.7 through 4.3.11.

In Table 4.3.7 it can be seen that growth is viability is depressed in the presence of high lactate levels ($X_{v_{avg}}$), while the biological capacity for production is enhanced when serum containing medium is used (CHvol). In Table 4.3.8 it can be seen that product titre is depressed by low glutamine levels and/or by the presence of serum. The volumetric productivity and the specific productivity appear to be enhanced by a combination of high glutamine levels and high lactate levels. Metabolic trends were difficult to discern from this preliminary experiment, but it was observed that the glucose consumption rate is significantly increased at high glucose levels in the absence of serum (not surprising). Initial substrate concentration experiments are likely to provide valuable insight into the metabolism of the cell line, and it is recommended that such investigations be undertaken, using multiple replicates of each treatment.

The general model framework appears to be adequate to describe the batch culture dynamics of the CHO1-5₅₀₀ cell line. It is recommended that model refinement be pursued, as this may in turn lead to refinements in the understanding of the metabolism and ultimately the productivity of this rCHO cell line.

Table 4.3.6: Initial substrate concentrations for 100 mL spinner flask batch cultures of rCHO in dispersed suspension.

CULTURE	[GLUCOSE] mmol L ⁻¹	[GLUTAMINE] mmol L ⁻¹	[LACTATE] mmol L ⁻¹	[SERUM] v/v%
1	10.5	1.56	15.9	0
2	41.3	1.46	16.5	0
3	10.3	8.38	18.9	0
4	28.5	8.27	18.2	0
5	31.5	1.31	0.27	0
6	37.0	8.16	0.18	0
7	35.8	1.07	2.02	10
8	30.2	7.92	1.82	10

Table 4.3.7: Population growth parameters of the spinner flask initial substrate concentration experiment.

CULTURE	$X_{V_{max}}$ E-6 c/mL	$X_{V_{avg}}$ E-6 c/mL	CHVol E-6 c-h/mL	μ_{max} h ⁻¹	k_{davg} h ⁻¹	k_{lavg} h ⁻¹
1	0.73	0.53	288	0.0153	0.0025	0.0011
2	0.71	0.48	253	0.0100	0.0030	0.0014
3	0.59	0.30	130	0.0162	0.0060	0.0029
4	0.97	0.70	374	0.0258	0.0023	0.0011
5	2.12	1.01	443	0.0100	0.0137	0.0055
6	1.71	0.79	345	0.0270	0.0083	0.0045
7	2.92	2.20	1008	0.0300	0.0035	0.0022
8	2.26	1.33	605	0.0310	0.0047	0.0007

Table 4.3.8: Production parameters of the spinner flask initial substrate concentration experiment

CULTURE	$[\text{tPA}]_{\text{max}}$ mg L ⁻¹	%tPA _{pro} mg mg ⁻¹	P_{tPAavg} mg L ⁻¹ h ⁻¹	Q_{tPAavg} pg c-h ⁻¹	$Q_{\text{tPA-M1}}$ pg c-h ⁻¹	$Q_{\text{tPA-M2}}$ pg c-h ⁻¹	$Q_{\text{tPA-M3}}$ pg c-h ⁻¹
1	5.70	1.78	0.026	0.008	0.187	0.008	-0.025
2	5.96	1.86	0.026	0.017	0.131	0.011	-0.022
3	9.15	2.86	0.075	0.053	0.098	0.013	NA
4	10.62	3.32	0.088	0.027	0.173	-0.002	NA
5	9.50	2.97	0.028	0.021	0.058	0.030	0.015
6	10.4	3.25	0.034	0.023	0.083	0.014	-0.016
7	6.99	0.29	0.021	0.007	0.020	0.013	0.004
8	7.00	0.29	0.030	0.008	0.045	0.000	-0.006

Table 4.3.9: Substrate and ammonia concentrations at the switches between metabolic phases in the spinner flask initial substrate concentration experiment

CULTURE	CHvol E6 c-h mL ⁻¹	[GLUCOSE] mmol L ⁻¹	[GLUTAMINE] mmol L ⁻¹	[LACTATE] mmol L ⁻¹	[AMMONIA] mmol L ⁻¹
FIRST METABOLIC SWITCH					
1	NA	NA	NA	NA	NA
2	40.16	34.71	0.63	21.83	1.53
3	77.34	2.64	4.09	22.44	4.51
4	60.44	15.89	5.97	23.72	4.24
5	49.15	26.62	0.14	10.89	1.85
6	74.49	32.34	5.43	14.94	4.28
7	65.10	21.87	0.26	17.50	1.68
8	141.00	16.67	3.50	16.67	4.83
SECOND METABOLIC SWITCH					
1	63.20	3.97	0.25	25.06	1.81
2	125.65	29.58	0.14	20.17	2.32
3	NA	NA	NA	NA	NA
4	NA	NA	NA	NA	NA
5	74.75	23.34	0.14	11.94	2.09
6	280.58	11.56	1.03	20.00	8.06
7	281.00	15.77	0.04	15.77	1.89
8	334.00	12.56	1.53	22.56	6.88

Table 4.3.10: Specific substrate consumption rates during the metabolic phases for the spinner flask initial substrate concentration experiment (units are $\mu\text{mol c}\cdot\text{h}^{-1}$)

CULTURE	FIRST METABOLIC PHASE			SECOND METABOLIC PHASE			THIRD METABOLIC PHASE			
	q _{GLC}	q _{GLN}	q _{ALA}	q _{GLC}	q _{GLN}	q _{ALA}	q _{GLC}	q _{GLN}	q _{ALA}	
1	0.090	0.020	NA	0.000	NA	NA	0.000	0.000	0.036	0.001
2	0.176	0.023	NA	0.060	0.006	0.004	0.094	0.001	0.004	0.004
3	0.088	0.054	NA	0.022	0.043	-0.044	NA	NA	NA	NA
4	0.214	0.030	NA	0.044	0.014	-0.060	NA	NA	NA	NA
5	0.095	0.023	NA	0.128	0.000	-0.041	0.034	0.000	-0.014	0.002
6	0.062	0.034	NA	0.087	0.011	-0.009	0.060	0.004	-0.095	0.001
7	0.096	0.120	NA	0.025	0.001	NA	0.008	0.000	0.012	0.012
8	0.092	0.027	NA	0.021	0.010	-0.027	0.030	0.003	0.015	-0.011

Table 4.3.11: Yields of byproducts on substrates during the three metabolic phases for the spinner flask initial substrate concentration experiment

CULTURE	$Y_{LAC,GLC}(M1)$ mol mol ⁻¹	$Y_{AMM,GLN}(M1)$ mol mol ⁻¹	$Y_{AMM,GLN}(M2)$ mol mol ⁻¹	$Y_{AMM,GLN}(M3)$ mol mol ⁻¹	$Y_{ALA,GLN}(M1)$ mol mol ⁻¹	$Y_{ALA,GLN}(M2)$ mol mol ⁻¹	$Y_{ALA,GLN}(M3)$ mol mol ⁻¹
1	1.36	1.33	1.33	0.76	0.56	-1.32	-1.32
2	0.69	1.40	1.08	0.21	0.86	-0.04	-4.43
3	0.48	0.96	0.67	NA	0.56	-0.41	NA
4	0.22	1.03	0.56	NA	0.54	0.10	NA
5	1.86	1.49	ND	-0.05	0.72	ND	-2.11
6	2.94	1.43	1.60	0.78	0.84	0.71	-2.60
7	1.07	1.83	0.92	-0.57	0.90	0.96	-3.46
8	1.11	1.07	0.96	0.89	0.69	0.55	1.86

5. Conclusions and Recommendations

5.1 Conclusions

In contrast to microbial cells, in mammalian cells the production of proteins and proliferation of cells lie within time domains of different orders. The epigenetic time domain is in the order of hours while the genetic time domain is in the order of days. Protein production is not usually restricted to a single cell cycle phase within cycling fraction (eg. S phase) of the genetic time domain, and, in any case, the proportion of the population in any given physiological state does not remain constant through a batch run. Hence, correlations of protein production to growth rate are impractical. These two important aspects of animal cell culture (growth and production) can be placed on the same basis by considering growth in terms of cell-hours, which represent the biological capacity for production.

Frequently, protein productivity changes with the average physiological state of the population. This is observed as growth-phase-association or partial-growth-phase-association. The rCHO cell line investigated in this study exhibited growth-phase-association, with specific productivity maxima in the lag and early decline phases. Compartmentalization of the population into the cell cycle phases, quiescent phase, and apoptotic phase revealed that protein production was directly proportional to the G1 phase cell-hours. This is in agreement with the observed partial-growth-phase-association pattern, as the proportion of the population in the G1 cell cycle phase is maximal in the lag and early decline growth phases.

The *dhfr*-based system of producing foreign proteins in mammalian cells likely results in incidental transcription of the protein-gene with transcription of *dhfr*. However, it must not be assumed that synthesis of the protein occurs simultaneously with synthesis of DHFR. Although the plasmid is designed for co-transcription of *tPA* and *dhfr*, there is no reason to assume that post-transcriptional modifications of the *tPA* transcript are under the control of the regulatory mechanisms for the post-transcriptional modifications of the *dhfr* transcript. Also, the definition of protein

production of secretory glycoproteins usually is inclusive of transcription, post-transcriptional modifications, translation, post-translational modifications, and secretion, while DHFR is an intracellular protein. Secretion is usually the rate limiting step in the appearance of secretory proteins in the supernatant. Therefore, there is a time and space separation between the rate of appearance of DHFR within the cell and the rate of appearance of the recombinant protein outside of the cell. If this time lag is not accounted for, correlations of extracellular protein appearance to intracellular DHFR appearance are phenomenological at best, and should not be used as a basis of concluding the degree of co-regulation of the translation of the two molecules. In this study, while the production of the recombinant tPA strongly correlated with the G1 cell cycle phase, DHFR content increased sharply in the S cell cycle phase.

The transformed and genetically engineered mammalian cell investigated in this study exhibited unusual patterns in the appearance and disappearance of metabolites in the culture medium. On the basis of these patterns three population-averaged metabolic phases were identified during a batch culture run. The first metabolic phase is similar to that observed in hybridoma culture, with glutamine and glucose being co-utilized, and ammonia, alanine, and lactate accumulating. When glucose is depleted to a constant level, lactate accumulation also ceases. During this second metabolic phase, lactate and glucose levels are constant, glutamine is being utilized and alanine and ammonia are accumulating. When glutamine is depleted to a constant level, the culture switches to a third metabolic phase in which alanine and lactate are consumed, glucose is constant, glutamine is disappearing at a rate consistent with its chemical degradation, and ammonia is accumulating. These observations may be due to the utilization of the phase I gluconeogenesis metabolic pathway.

Throughout the batch culture run, glycine accumulates. Glycine may be formed from serine, which in turn may be formed from a molecule synthesized in the phase I gluconeogenesis pathway. Tetrahydrofolate functions as the carbon acceptor in the cleavage of serine to form glycine. The carbon is removed from the folic acid derivative by the formation of thymidine compounds from uridine compounds, leaving this B complex vitamin in the dihydrofolate form. The restoration of dihydrofolate to tetrahydrofolate is catalyzed by DHFR. Hence DHFR may drive glycine production, which in turn drives the formation of serine from the consumption of alanine and lactate. Thus the high levels of DHFR in this CHO1-5₅₀₀ cell line may serve to enhance the utilization of the phase I gluconeogenesis pathway.

Tissue plasminogen activator is apparently not produced during the third metabolic phase, while the percentage of the population in apoptosis increases sharply when the culture enters the second metabolic phase. Maximal population expansion and tPA production should correlate to maximal extension of the first metabolic phase. Initial substrate concentrations may impact on the duration of the first metabolic phase. Relative levels of the various metabolites might trigger the different metabolic phases and might therefore form the basis of fed-batch protocols designed to extend the first metabolic phase.

The extracellular concentration of tPA from the CHO1-5₅₀₀ cell line reaches an apparent ceiling of approximately 10 mg L⁻¹. This maximum of the extracellular level of tissue plasminogen activator is likely a consequence of natural regulatory mechanisms. Further processing and/or genetic manipulations are known to improve the tPA titers. Degradation of accumulated tPA occurs during the late decline phase, which is correlated to the dead cell and lysed cell concentrations. Batch cultures should not be permitted to proceed into the late decline phase, and harvest should take place before the second metabolic switch into the third metabolic phase takes place.

The CHO1-5₅₀₀ cell line was found to be capable of growth in three morphological types (substratum adherent, aggregated, and dispersed suspension) which are easily induced by agitation rate and serum content. The most favourable growth kinetics ($\mu_{\max} = 0.026 \text{ h}^{-1}$) and volumetric productivity (0.041 mg L⁻¹ h⁻¹) are associated with the substratum-attached growth behavior type. Dispersed suspension culture exhibits a similar volumetric productivity to that observed in microcarrier suspension culture. Dispersed suspension culture is therefore the most attractive format as it is both simpler and cheaper than microcarrier suspension culture. Aggregate suspension culture exhibited the least favourable growth and production kinetics. However, aggregate suspension culture may have an advantage at a larger scale, in terms of better resistance to shear damage.

Extensive cytoplasmic bridging was observed between aggregated and substratum-attached cells. The cytoplasmic bridges apparently function to strengthen aggregates with large void volumes. The large void volumes ($\cong 50\%$) within aggregates are assumed to preclude mass transfer limitations. The cytoplasmic bridges may be instrumental in the cell-sheet detachment pattern observed in substratum-attached culture, and this may result in the premature failure of these systems.

Modeling of growth, production, and metabolism dynamics can improve the understanding of the system. Successful models can be used for optimization and prediction of culture behavior. A partially structured and partially segregated metabolic cell-cycle model which was developed in this study could successfully simulate the first metabolic phase of batch culture of the CHO1-5₅₀₀ cell line, substantiating the assumed major metabolic pathways utilization. Initial substrate conditions impact significantly on the metabolic patterns of the CHO1-5₅₀₀ cell line during batch culture. Further model development could shed light on the metabolic patterns and controls of this and other transformed and transfected cell lines.

A better understanding of metabolism and growth behavior, and their impacts on growth and production kinetics, may enable further optimization of batch mammalian cell culture. In this study some of the unique aspects of the metabolism, growth behavior, and growth and production kinetics of the CHO1-5₅₀₀ cell line have been identified.

5.2 Recommendations

The complex metabolism of this transformed and transfected cell line should be investigated in greater detail through the use of bioassay methodologies. The concentrations of metabolic enzymes such as pyruvate carboxylase, thymidylate synthase, serine hydroxymethyl transferase, and phosphoserine transaminase should be measured. The dynamics of the rest of the amino acids should be investigated. The impact of initial concentrations of major substrates should be studied in depth. This would enable the identification of the major inputs and outputs to population metabolism, with their associated overall kinetics. This information can then be used to refine modeling and thence to facilitate optimization of the system.

The relationship of tPA synthesis and tPA secretion to the cell cycle phases should be investigated. Intracellular levels of tPA protein and of tPA mRNA should be measured. Synchronized cell populations should be employed in these investigations, but the synchronization method must be carefully chosen so that metabolic and production dynamics are not significantly influenced by the process of synchronization. This information could be used to refine modeling and to optimize the system.

The impact of scale-up (and hence increasing shear) on the growth and production dynamics of the three morphological types should be investigated. Relative dynamics observed at the 1 liter scale may not hold at the larger scales employed industrially.

Model development should be continued. Fine tuning of the model may serve to improve simulations as well as to augment the understanding of the metabolism and related growth and production kinetics of this cell line. An accurate model can be used to simulate the impacts of process variations without the need to actually perform costly and lengthy experiments.

APPENDIX A:
Experimental Data

Microcarrier Suspension: Spinner #1 Ham's F12 with 10% FBS
 NUNC polystyrene microcarrier beads (90 - 180 μ m) 1 L spinner @ 60 rpm 10g/L of beads

Time h	cells/bead	viable E6 c/mL	CHVol E6 ch/mL	tPA mg/L	tPA-0 mg/L	GLC mM	LAC mM
0	0	0.25	0	1.979	0	7.38	3.95
24	79	0.243683	5.9238775	4.154	2.175	7.25	4.2
96	523	1.613246	58.093995	8.432	6.453	6	
120	571	1.761307	98.562625	10.46	8.476	7.1	6.48
144	724	2.23325	146.27344	10.03	8.048	5.98	
168	834	2.572556	203.84717	9.865	7.886	5.42	
192	461	1.422001	250.4256	10.42	8.436	5.34	
264	354	1.091948	340.40536	10.45	8.47	4.19	
288	213	0.65702	360.95298	10.51	8.526	3.77	10.51
312	255	0.786573	378.22949	11.22	9.239	3.12	
336	109	0.336221	390.94656	10.91	8.926	2.08	
360	145	0.447267	400.28512	9.08		2.18	

Microcarrier Suspension: Spinner #2 HAM's F12 with 10% FBS
 NUNC polystyrene microcarrier beads (90 - 180 um) 1 L spinner @ 60 rpm 10g

Time h	cells/bead	viable E6 c/mL	CHvol E6 ch/mL	tPA mg/L	tPA-0 mg/L	GLC mM	LAC mM
0	0	0.23	0	2.92	0	8	
24	74	0.22826	5.4990984	3.31	0.39	7.82	3.65
48	162	0.499705	13.813604	4.83	1.91	6.33	
120	184	0.567566	52.183548	6.04	3.12	5.28	
144	343	1.058018	71.08357	7.86	4.94	4.86	6.79
168	229	0.706373	91.9729	8.934	6.014	4.01	
192	137	0.42259	105.23016	10.35	7.43	2.84	
216	49	0.151145	111.5664	10.07	7.147	1.91	
288	23	0.070946	119.20116	8.153	5.233	1.17	10.23

Microcarrier Suspension: Spinner #3 Ham's F12 with 10% FBS
 NUNC polystyrene beads (90 - 180 μ m) 1 L spinner @ 60 rpm 10g/L of beads

Time h	cells/bead	viable E6 c/mL	CHVol E6 ch/mL	tPA mg/L	tPA-0 mg/L	GLC mM	LAC mM
0	0	0.28	0	0.574	0	9.88	2.06
24	149	0.459605	8.697972	1.2	0.626	7.35	2.28
48	277	0.854434	23.979913	2.368	1.794	6.64	4.42
72	448	1.381901	50.310689	4.552	3.978	5.63	6.91
96	374	1.15364	80.65481	6.555	5.981	4.84	8.24
168	383	1.181402	164.71237	7.055	6.481	3.77	9.96
192	134	0.413336	182.26489	7.4	6.826	4.25	11.02
216	64	0.197414	189.27765	7.53	6.956	3.58	10.86
240	24	0.07403	192.29674	9.055	8.481	3.53	11.04
264	20	0.061692	193.92091	8.81	8.236	2.81	11.4

Microcarrier Suspension: Spinner #4 Ham's F12 with 10% FBS
 NUNC polystyrene beads (90 - 180 um) 1 L spinner @ 60 rpm 10g/L of beads

Time h	cells/bead	viable E6 c/mL	CHvol E6 ch/mL	tPA mg/L	tPA-0 mg/L	GLC mM	LAC mM
0	0	0.128	0	1.1	0	11.5	
24	34	0.104876	2.7853082	1.814	0.714	9.26	1.997
48	226	0.69712	10.289283	2.478	1.378	8	5.5
72	415	1.280109	33.311734	4.706	3.606	88	
96	497	1.533046	66.978431	6.984	5.8835	7.1	7.98
168	538	1.659515	181.85048	7.966	6.866	6.41	
192	177	0.545974	205.89003	8.95	7.85	4.56	
216	193	0.595328	219.57711	9.75	8.65	5.27	10.15
240	84	0.259106	229.27728	11.56	10.456	4.88	
264	65	0.200499	234.76252	12.26	11.16	4.72	11.33

Aggregate Suspension: Spin Serum Free HB-CHO Spinner #1
 1 L ; 60 rpm ; 0-200s amorphous aggregates in suspension

Sample	Time h	pH	[Total] E6 c/mL	V-fac	[Viable] E6 c/mL	CHvol E6 c-h/mL	GLC mM	LAC mM
0	0	7.5	0.112	0.82	0.09184	0.00	14.6	0
1	22	7.4	0.148	0.97	0.14356	2.55	13.2	0.44
2	46	7.5	0.187	0.94	0.17578	6.37	13	0.49
3	70	7.4	0.246	0.9	0.2214	11.11	12.9	
4	98	7.5	0.255	0.965	0.24608	17.65	12.6	1.24
5	120	7.6	0.275	0.72	0.198	22.52	12.7	1.61
6	144	7.6	0.293	0.64	0.18752	27.14	13	2.56
7	166	7.5	0.289	0.69	0.19941	31.40	11.7	2.84
8	190	7.4	0.288	0.68	0.19584	36.14	10.1	3.8
9	215	7.4	0.311	0.81	0.25191	41.71	9.92	3.8
10	239	7.4	0.338	0.79	0.26702	47.93	8.38	5.45
11	261	7.4	0.358	0.8	0.2864	54.02	7.09	6.11
12	311	7.2	0.703	0.83	0.58349	74.89	5.94	9.51
13	334	7.1	0.754	0.79	0.59566	88.45	6.94	12
14	358	7	1.029	0.77	0.79233	104.99	5.06	13.3
15	383	6.9	1.302	0.6	0.7812	124.66	3.28	14.4
16	407	6.9	1.51	0.55	0.8305	144.00	2.82	14.6
17	430	6.9	1.49	0.49	0.7301	161.92	1.72	13.3
18	473	6.8	1.45	0.5	0.725	193.20	1.38	15.2
19	505	6.8	1.375	0.4	0.55	213.47	0.81	16.9
20	527	6.9	1.199	0.35	0.41965	224.08		15.9
21	550	6.9	1.49	0.45	0.6705	236.39	0.56	14
22	571	7	0.979	0.4	0.3916	247.28		11.2
23	595	7	0.981	0.2	0.1962	254.07		
24	626	6.9	0.985	0.18	0.1773	259.85		13.2
25	647	7	1.02	0.16	0.1632	263.42		12
26	667	7	0.85	0.13	0.1105	266.13		12.3
27	691	7	0.845	0.22	0.1859	269.60		
28	715	6.9	0.985	0.23	0.22655	274.54		

Aggregate Suspension: Spinner #2 Serum Free HB-CHO
 1 L ; 60 rpm ; 0-200s amorphous aggregates in suspension

Sample	Time h	pH	[Total] E6 c/mL	V-frac	[Viable] E6 c/mL	CHvol E6 c-h/mL	GLC mM	LAC mM	tPA-0 mg/L
0	0	7.2	0.099	0.85	0.08415	0.00	16.5	0	0
1	22	7.2	0.15	0.98	0.147	2.48	15.7	0	
2	46	7.2	0.216	0.97	0.20952	6.71	14.3	0.42	0.1
3	70	7.3	0.176	0.96	0.16896	11.24	13.1	0.44	
4	98	7.3	0.162	0.96	0.15552	15.78	12.9	0.96	0.3
5	120	7.4	0.164	0.87	0.14268	19.06	12.5	1.02	
6	144	7.3	0.315	0.9	0.2835	23.98	10	1.21	0.3
7	166	7.2	0.404	0.97	0.39188	31.34	9.75	2.38	
8	190	7.1	0.646	0.94	0.60724	43.14	8.76	3.23	0.73
9	215	7.1	0.701	0.9	0.6309	58.62	8.31	3.92	
10	239	7	0.98	0.75	0.735	74.98	5.7	4.97	2
11	261	6.8	0.96	0.74	0.7104	90.88	4.91	6.98	
12	311	6.8	0.96	0.63	0.6048	123.68	3.91	9.65	2.2
13	334	6.9	1.48	0.55	0.814	139.88	3.83	9.16	
14	358	6.8	1.57	0.42	0.6594	157.50	3.68	9.32	2.4
15	383	6.8	1.63	0.37	0.6031	173.27	3.71	9.43	
16	407	6.8	1.36	0.34	0.4624	185.98	3.5	9.34	3.44
17	430	6.8	1.66	0.27	0.4482	196.45	3.06	9.46	
18	473	6.7	1.85	0.3	0.555	217.94	2.96	9.68	3.61
19	505	6.8	1.67	0.29	0.4843	234.54	2.6	9.03	
20	527	6.8	1.585	0.21	0.33285	243.43	2.39	8.55	3.8
21	550	6.8	1.37	0.29	0.3973	251.80	1.71	7.6	
22	571	6.8	1.03	0.29	0.2987	259.06	1.76	8.34	4.4
23	595	6.8	1.051	0.27	0.28377	266.05	1.15	7.74	
24	626	6.8	1.12	0.23	0.2576	274.43	1.28	8.4	4.5
25	647	6.8	0.958	0.19	0.18202	279.00	1.22	8.51	
26	667	6.8	0.951	0.2	0.1902	282.72		8.44	5.3
27	691	6.8	0.995	0.24	0.2388	287.85		7.53	
28	715	6.8	0.925	0.18	0.1665	292.66			

Aggregate Suspension: Spinner #3 Serum Free HB-CHO
 1 L ; 60 rpm ; 0-200s amorphous aggregates in suspension

Sample	Time h	pH	[Total] E6 c/mL	V-fraction	[Viable] E6 c/mL	CHvol E6 c-h/mL	GLC mM	LAC mM	tPA-0 mg/L
0	0	7.5	0.092	0.91	0.08372	0.00	7.19	0	0
1	22	7.5	0.137	0.96	0.13152	2.33	6.29	0.38	
2	46	7.4	0.192	0.96	0.18432	6.08	6.3	0.89	1.1
3	70	7.5	0.286	0.95	0.2717	11.49	5.97	0.62	
4	98	7.5	0.276	0.95	0.2622	18.96	5.68	0.76	
5	120	7.6	0.276	0.92	0.25392	24.64	3.36	0.58	
6	144	7.4	0.351	0.88	0.30888	31.37	3.17	2.18	1.9
7	166	7.4	0.397	0.91	0.36127	38.73	2.48	3.67	
8	190	7.3	0.549	0.85	0.46665	48.61	1.97	5	3.9
9	215	7.3	0.757	0.79	0.59803	61.85	0.74	5.56	
10	239	7.3	0.992	0.5	0.496	74.94	0.31	6.57	3.7
11	261	7.4	0.995	0.423	0.42089	85.00	0.14	6.35	
12	311	7.4	1.71	0.24	0.4104	105.78	0.17	4.89	0.6
13	334	7.5	1.64	0.13	0.2132	112.71	0.29	4.32	
14	358	7.5	1.57	0.15	0.2355	118.09	0.51	3.93	0.4
15	383	7.5	1.62	0.093	0.15066	122.84	0.69	4.04	

Dispersed Suspension: Spinner #1 Serum Free HB-CHO
1 L; 150 rpm

Sample	Time h	pH	[Total] E6 c/mL	V-fraction	[Viable] E6 c/mL	CHvol E6 c-h/mL	GLC mM	LAC mM	GLN mM	ALA mM	AMM mM	tPA-0 mg/L
	0				0.2763	0.00						
0	0.5	7.6	0.333	0.83	0.27639	0.14	8.056	0.009	5.354	0.174	0.433	0
1	19.5	7.4	0.413	0.75	0.30975	5.70	8.089	1.514	3.85	0.232	0.775	0.5
2	44	7.4	0.595	0.9	0.5355	15.80	4.578	2.291	2.562	0.32	1.215	1.2
3	94	6.9	0.897	0.95	0.85215	49.88	1.178	9.367	1.88	0.834	2.532	2
4	117.7	6.9	1.046	0.91	0.95186	71.21	0.728	9.464	1.6	1.108	2.763	2.5
5	141.7	6.9	1.662	0.77	1.27974	97.80	0.85	9.678	1.558	1.382	2.869	3
6	166	7	1.568	0.71	1.11328	126.86	0.456	9.402	1.425	1.805	3.13	3.5
7	190.2	7	1.132	0.74	0.83768	150.28	0.417	9.364	1.299	2.228	3.386	3.85
8	213.5	7	1.21	0.64	0.7744	169.08	0.606	8.381	1.163	2.266	3.743	4.35
9	256.5	7	1.09	0.67	0.7303	201.42	0.55	5.491	1.074	1.603	3.91	4.5
10	288	7.1	1.35	0.52	0.702	223.97	0.7	6.189	0.635	2.3	4.082	5.9
11	310.3	7.1	1.845	0.4	0.738	240.05	0.289	5.953	0.788	2.418	4.171	6.9
12	333.3	7.2	1.471	0.46	0.67666	256.31	0.161	5.4	0.66	2	4.34	7
13	354.5	7.2	1.63	0.4	0.652	270.37	0.389	3.086	0.533	1.608	4.385	7.5
14	378	7.2	1.38	0.38	0.5244	284.14	0.511	4.089	0.475	1.45	4.474	8.15
15	409	7.2	1.55	0.29	0.4495	299.20	0.428	3.178	0.401	1.25	4.741	8.88
16	429.5	7.2	1.48	0.24	0.3552	307.41	0.528	3.956	0.483	1.2	4.89	8.32
17	451	7.2	1.35	0.16	0.216	313.43	0.361	4.422	0.483	1.4	5.044	7.85
18	474.7	7.3	1.68	0.17	0.2856	319.33	0.4	4.322	0.154	1.25	5.41	7.3
19	499.5	7.3	1.4	0.25	0.35	327.19	0.478	3.2	0.346	0.992	5.775	6.6
20	528	7.3	1.52	0.21	0.3192	336.72	0.544	3.489	0.403	1.3	5.864	6.2
21	549	7.3	1.49	0.15	0.2235	342.36	0.322	2.378	0.413	1.35	5.985	5.9
22	596	7.3	1.21	0.09	0.1089	349.85	0.156	2.089	0.447	1.48	6.112	5.4

Dispersed Suspension: Spinner #2 Serum Free HB-CHO

1 L ; 150 rpm

Sample	Time h	pH	[Total] E6 c/mL	V-frac	[Viable] E6 c/mL	CHvol E6 c-h/mL	GLC mM	LAC mM	GLN mM	ALA mM	AMM mM	tPA-0 mg/L	Protein mg/L	
	0				0.3693	0.00								
	0	0.5	8.8	0.445	0.83	0.36935	0.18	7.96	0	4.72	0.17	0.119	0	141.89
	1	21.3	7	0.626	0.92	0.57592	9.87	7.14	0.71		0.28	0.462	2.6	121.3
	2	45.3	7	0.531	0.86	0.45666	22.21	6.87	1.61	3.87	0.48	1.118	1.8	148.75
	3	70	7	0.751	0.91	0.68341	36.08	6.46	1.96		0.73	2.018	3.2	112.91
	4	94.2	6.8	0.859	0.87	0.74733	53.36	4.77	2.53	3.01	1.4		3.6	154.85
	5	118	6.8	1.015	0.85	0.86275	72.11	3.13	5.57	2.22	1.4		6.6	179.26
	6	161	6.7	0.825	0.48	0.396	97.88		6.04	1.29	1.27	4.046	7.6	204.43
6p		192	6.7	0.935	0.5	0.4675	111.45	2.76	6.49			4.42	8.9	167.06
	7	214	6.8	1.635	0.42	0.6867	124.18	2.45	6.59	1.05	1.76	4.598	10	205.19
	8	238	6.8	1.532	0.48	0.73536	141.24	1.04	6.16				10.95	203.67
	9	260	6.8	1.68	0.54	0.9072	158.56	0.62	6.13	0.57	2.57	5.186	11.65	225.79
	10	283	6.8	1.36	0.52	0.7072	177.44	0.28	4.64	0.4			9.5	162.48
	11	314	6.9	1.48	0.4	0.592	197.52	0.24	4.72	0.26	2.79	5.311	7.8	187.65
	12	335	6.9	1.52	0.38	0.5776	209.51	0.46	4.09	0.17			5.4	205.96
	13	356	7	1.96	0.21	0.4116	220.04	0.52	3	0.18	2.04		4.9	177.74
	14	380	7	2.09	0.28	0.5852	231.80		2.4					222.73
	15	405	7.1	2.14	0.25	0.535	245.60	0.57	2.56	0.17	1.97			275.36
	16	432	7.1	2.26	0.18	0.4068	258.47	0.41	2.11	0.24		5.579	6.6	237.23
	17	454	7.1	2.35	0.16	0.376	267.08	0.72	1.99	0.17	2.1			219.68
	18	501	7.2	1.05	0.05	0.0525	274.80	0.71		0.22	2.15		6	141.89

Dispersed Suspension: Spinner #3
1 L ; 150 rpm

Serum Free HB-CHO

Sample	Time h	pH	[Total] E6 c/mL	V-frac	[Viable] E6 c/mL	CHvol E6 c-h/mL	GLC mM	LAC mM	GLN mM	ALA mM	AMM mM	tPA-0 mg/L	Protein mg/L
	0				0.1618	0.00							
0	1	7.9	0.195	0.83	0.16185	0.16	8.74	0.03	3.87	0.2	0.018	0	343.37
1	21.5	7.8	0.26	0.9	0.234	4.17	7.97	0.54			0.249	1.259	287.71
2	43	7.7	0.398	0.92	0.36616	10.52	7.7	1.48	3.11	0.35	1.14	1.949	296.85
3	69.3	7.5	0.624	0.94	0.58656	22.84	6.99	2.61			1.799		198
4	92.5	7.4	1.027	0.92	0.94484	40.25	6.86	3.59	2.18	0.76	3.26		281.07
5	117	7.2	1.217	0.93	1.13181	65.27		6.09			3.207		308.48
6	139	7	0.942	0.91	0.85722	86.85		9.92	1.04	1.01	3.653	8.686	359.16
7	162	7.1	1.254	0.78	0.97812	108.38		9.89			4.276	12.01	346.69
8	186	7.1	1.515	0.61	0.92415	131.20	1.39	9.51	0.81	1.12	4.686	13.02	295.19
9	214	7.1	1.635	0.44	0.7194	153.68		7.87					300.17
10	236	7.2	1.48	0.41	0.6068	168.68	0.47	8.59	0.64	1.19	4.401	11.91	199.66
11	271	7.2	1.38	0.42	0.5796	189.44	0.22	7.81	0.49	1.27	4.757		283.56
12	306	7.2	1.19	0.45	0.5355	208.85	0.12	7.33	0.38	1.09	5.238	11.66	310.97
13	331	7.1	2.075	0.28	0.581	222.89	0.11	6.78					395.71
14	354	7.2	2.223	0.21	0.46683	234.63	0.1	6.14	0.32	1.04	5.541	12.3	465.49
15	378	7.3	2.091	0.17	0.35547	244.51	0.03	5.53			5.882		459.67
16	403	7.4	2.17	0.19	0.4123	253.96	0.01	5.83	0.39	1.27	5.648		423.12
17	430	7.5	2.05	0.29	0.5945	267.57	0.01	5.39			5.844	13.02	442.23
18	458	7.5	2.21	0.22	0.4862	282.55	0.03	5.12	0.36	1.4	5.951	13.02	392.38

Dispersed Suspension: Spinner #4
1 L; 150 rpm

Serum Free HB-CHO

Sample	Time h	pH	[Total] E6 c/mL	V-frac	[Viable] E6 c/mL	CHvol E6 c-h/mL	GLC mM	LAC mM	GLN mM	ALA mM	AMM mM	tPA-0 mg/L
	0				0.15	0.00						
0	1	7.6	0.181	0.83	0.15023	0.15	8.34	0	3.3	0.16	0.196	0
1	21.5	7.6	0.208	0.91	0.18928	3.61		0.5			0.553	0.195
2	43	7.5	0.32	0.92	0.2944	8.73	7.46	1.21	4.11	0.43	1.052	0.2
3	69.3	7.4	0.556	0.91	0.50596	19.02		2.22			1.925	1.3
4	92.5	7.4	0.82	0.91	0.7462	33.34	6.89	2.89	2.67	0.77	2.691	4.1
5	117	7.2	0.81	0.95	0.7695	51.66		2.74			3.135	
6	139	7.2	0.911	0.87	0.79257	68.71	2.69	4.41	1.58	1.05	3.601	5.2
7	162	7.1	1.021	0.89	0.90869	88.67	0.93	7.04			4.012	5.1
8	186	6.9	1.42	0.9	1.278	114.66	0.51	7.43	0.89	1.18	3.994	7.83
9	214	7	1.581	0.83	1.31223	150.27	0.27	8.23			4.67	8.5
10	236	7	1.95	0.64	1.248	179.28		7.94	0.6	1.22	4.812	7.8
11	271	7.1	1.575	0.56	0.882	216.19		7.29	0.46	1.18	4.777	6
12	306	7.1	1.79	0.41	0.7339	244.25	0.07	6.29	0.55	1.28	4.973	5.9
13	331	7.1	1.62	0.47	0.7614	263.06	0.02	6.18			5.062	5.5
14	354	7.2	1.855	0.21	0.38955	275.55		5.33	0.35	1.23	5.006	5.3
15	378	7.3	2.105	0.13	0.27365	283.48		5.41			4.884	5
16	403	7.4	2.153	0.11	0.23683	289.76		5.38	0.44	1.23	5.383	3.1
17	430	7.4	2.06	0.13	0.2678	296.65		5.73			5.543	2.7
18	458	7.5	1.87	0.15	0.2805	304.28		5.7	0.48	1.22	5.489	2.4

Factorial: Initial Substrate Concentrations Spinner #2
 100 mL; 150 rpm; dispersed suspension

Hour	Sample	pH	(Total) V _{fraction}	NH ₃	LAC	GLC	IPA-0	GIN	ALA	
h			E5 g/ml	mm	mm	mm	mg/L	mm	mm	
	medium	7.65		0.12	16	44.23		1.517	0.17	
0	0	7.7	4.45	0.7162162	0.123	16.5	41.28	0	1.462	0.197
30.25	1	7.84	4.8	0.8333333	1.005	19.83	40.7	1.7321	1.285	0.408
54.5	2	7.75	5	0.8125	1.287	20.67	37.52	4.2573	0.757	0.563
72.92	3	7.8	5.4	0.7946429	1.506	22	36.56	4.4461	0.7	0.876
98.1	4	7.76	6	0.86	1.533	21.83	34.71	5.0428	0.631	1.092
121.3	5	7.78	7.2	0.8958333	1.773	20.17	33.79	5.1259	0.457	1.141
140.8	6	7.78	9.4	0.8297872	1.693	19.39	29.99	5.4129	0.307	1.281
167.5	7	7.84	9.25	0.76	1.818	20.17	29.98	5.5035	0.213	1.272
190.5	8	7.82	8.95	0.7924528	1.943	19.11	29.83	5.6319	0.15	1.089
223.8	9	7.87	9.25	0.6787879	2.317	20.17	29.58	5.8812	0.136	0.982
237.3	10	7.87	8.9	0.6814159	2.317	19.33	28.03	5.9491	0.116	0.933
264.5	11	7.89	7.2	0.6181818	2.21	21.44	27.73	5.9567	0.079	0.818
285.8	12	7.93	7.05	0.7375887	2.174	19.78	27.07	5.9265	0.081	0.8
310.5	13	7.96	7	0.7071429	2.424	20	26.17	5.7075	0.07	0.79
334.8	14	8.04	7.05	0.6764706	2.103	20	25.33	5.5262	0.074	0.778
336.8	15	8.07	6.95	0.622807	2.273	20.28	23.84	5.4658	0.065	0.7
366.4	16	8.12	6.8	0.6041667	2.29	20.63	23.11	5.3751	0.059	0.673
387.5	17	8.11	5.7	0.5505618	2.273	20.64	23.03	5.2241	0.055	0.672
434.5	18	8.13	5.65	0.5755396	2.29	19.94	21.53	4.4386	0.05	0.6
481.3	19	8.14	5.5	0.556701	2.397	19.78	19	4.4084	0.047	0.576
553.5	20	8.15	4.85	0.4758621	2.301	18.33	17.36	3.721	0.04	

Factorial: Initial Substrate Concentrations Spinner #3
 100 mL; 150 rpm; dispersed suspension

Hour	Sample #	pH	(Total) Viscosity cP/mL	NHS mM	IAC mM	GIC mM	IPA-O mM	GIN mM
	medium	7.65		0.328	17.72	11.81		8.555
0	0	7.61	5.18	0.6911197	0.189	18.94	10.31	0
30.25	1	7.8	6.8	0.8602941	1.822	21.89	6.861	3.8797
54.5	2	7.76	7.75	0.8129032	3.087	21.89	5.883	6.0297
72.92	3	7.77	7.6	0.7746479	3.992	23.39	4.711	7.4396
98.1	4	7.75	7.4	0.7905405	4.189	22.89	3.983	8.3233
121.3	5	7.83	6.95	0.7563025	4.67	22.39	3.344	9.1465
140.8	6	7.83	6.55	0.7309942	4.509	22.44	2.639	7.3716
167.5	7	7.95	6.55	0.7175573	4.848	22.56	2.489	7.5
190.5	8	7.96	6.4	0.5952381	5.418	20.56	2.328	7.636
223.8	9	8.03	6.05	0.3801653	5.828	21	2.317	6.7296
237.3	10	8	4.55	0.3186813	6.096	20.67	2.139	7.9305
264.5	11	8.02	4.05	0.4074074	6.269	23.06	2.044	6.5257
285.8	12	8.03	4.45	0.2857143	5.614	22.67	1.978	7.281
310.5	13	8.04	4.25	0.2	6.666	22.5	1.911	7.5151
334.8	14	8.07	3.7	0.1818182	6.274	21.5	1.789	7.4698
336.8	15	8.07	3.2	0.2021277	6.817	22.67	1.761	7.2734
366.4	16	8.09	3.25	0.2	6.568	23.83	1.761	6.9411
387.5	17	8.09	4.7	0.1276596	6.176	26.22	1.467	6.5332
434.5	18	8.1	2.95	0.220339	6.978	24.67	1.433	6.3746

Factorial: Spinner #4 (continued)

(Vols)	CHV	(G/G)	(S)	(G2/M)	(A)
ES c/ml	ES c/ml	ES c/ml	ES c/ml	ES c/ml	ES c/ml
2.62	0	1.21044	0.75456	0.40348	0.25414
5.722605	12.013289	4.332012	0.606596	0.618041	0.137343
6.85	27.216626	5.5074	0.6987	0.5343	0.1096
7.437097	40.367632	4.930795	1.346115	0.379292	0.788332
8.529389	60.438039	4.349989	2.524699	0.469116	1.177056
9.424453	81.202383	5.814887	2.450358	0.914172	0.245036
9.65	99.799107	3.86	3.667	1.93	0.2316
9.6	125.54592	5.3952	2.688	0.9984	0.5184
8.7	146.57395	3.2103	2.958	0.6438	1.8966
7.9	174.15007				
6.65	183.94711	2.86615	1.064	0.3458	2.4073
6.138889	201.36269				
7.8	216.10238	1.1232	0.3822	0.078	6.2556
6.65	233.94644				
7.6	251.19894	1.2312	0.1824	0.1216	6.0952
7.196703	252.67824				
6.16326	272.45815	0.739591	0.117102	0.055469	5.27575
6	285.27746				
5.922086	313.29396				
5.45	339.86093	0.4905	0.09265	0.02725	4.8396

Factorial: Initial Substrate Concentrations Spinner #5
 100 mL; 150 rpm; dispersed suspension

Hour	Sample	pH	[Total] V-fraction E5 c/mL	NH3 mM	LAC mM	GLC mM	LDH U/L	IPA-01 mg/L	GLN mM	ALA mM	
0	medium	7.7		0.121	0.167	30.05			1.364	0.115	
30.25	0	7.8	4.26	0.6713615	0.127	0.267	31.46	2.09	0	1.307	0.036
54.5	1	7.9	7.7	0.8441558	0.868	5.644	27.88	16.72	0.8056	0.832	0.38
72.92	2	7.7	11	0.8136364	1.476	9	26.17	12.12	2.1501	0.427	0.629
98.1	3	7.7	10.75	0.9023256	1.854	10.89	26.62	15.45	2.7694	0.141	0.899
121.3	4	7.6	11.25	0.9463415	2.085	11.94	23.34	24.24	3.5473	0.146	1.262
140.8	5	7.5	14.5	0.9034483	1.889	11.61	24.03	24.15	4.1138	0.165	1.145
167.5	6	7.5	18.3	0.8797814	1.854	13.17	20.03	19.23	5.1	0.168	0.796
190.5	7	7.5	21.4	0.8785047	1.818	13.5	19.67	64.37	5.0126	0.049	1.01
223.8	8	7.4	25.5	0.829582	1.818	13.83	18.24	92.8	6.5911	0.009	1.02
237.3	9	7.4	22.5	0.7556561	1.978	14.28	18.51	107	6.7044	0.087	0.798
264.5	10	7.4	22.3	0.7639752	1.836	15	16.49	131.8	7.792	0.058	0.425
285.8	11	7.3	23.4	0.5746269	1.961	15	15.17	148	8.5624	0.02	0.666
310.5	12	7.3	18.4	0.6141304	1.961	15.28	14.62	235.4	9.0836	0.009	0.567
334.8	13	7.3	19.4	0.4587629	1.916	16.22	13.89	339	9.1062	0.006	0.411
336.8	14	7.3	12.7	0.503937	1.729	16.72	12.89	353.6	9.499	0.128	0.655
366.4	15	7.3	12	0.36875	1.782	16.67	11.58	352	9.2875	0.076	0.824
387.5	16	7.3	12.3	0.2926829	1.961	16.94	10.36	370.8	8.4416	0.05	0.7
434.5	17	7.3	9.3	0.1530055	1.907	17.56	9.195	380	8.1546	0.021	0.64
	18	7.3	7.35	0.122449	2.085	18.06	8.889	384.2	7.7392	0.097	0.616

Factorial: Initial Substrate Concentrations
100 mL; 150 rpm; dispersed suspension

Spinner #6

Hours	Sample	pH	Total Verraction E5 c/mL	NH3 mM	LAC mM	GEC mM	tPA-0 mg/L	GEN mM	
	medium	7.65		0.303	0.167	38.01		7.292	
0	0	7.72	4.62	0.6320346	0.228	0.178	37.01	0	8.162
30.25	1	7.82	7.7	0.8571429	1.777	6.133	35.46	1.7925	6.447
54.5	2	7.65	8.55	0.8245614	2.934	9.833	34.24	2.7304	6.285
72.92	3	7.59	12.2	0.8606557	4.001	10.56	33.17	4.1352	5.358
98.1	4	7.42	12.95	0.9305019	4.278	14.94	32.34	6.3746	5.425
121.3	5	7.31	15.3	0.9019608	5.276	15.72	30.4	6.756	3.16
140.8	6	7.23	20.5	0.8341463	5.311	18.83	23.65	7.3026	2.596
167.5	7	7.2	19.2	0.7762712	6.416	17.61	22.69	8.0816	2.223
190.5	8	7.17	16.6	0.6596386	6.666	18.33	14.86	8.4517	1.938
223.8	9	7.16	21	0.6142857	7.201	19.67	15.42	8.5876	1.337
237.3	10	7.15	17.8	0.4494382	7.771	18.33	12.75	8.8973	1.366
264.5	11	7.08	19.5	0.3641026	8.056	20	11.56	9.7508	1.026
285.8	12	7.07	24.1	0.3029046	8.199	19.44	11	10.317	0.99
310.5	13	7.06	23.1	0.3246753	8.341	20.39	10.97	10.4	0.984
334.8	14	7.02	25.1	0.1434263	7.236	21.67	11.08	9.7054	1.06
336.8	15	7.03	17.3	0.1676301	8.422	22.61	10.56	9.5242	0.933
366.4	16	7.04	17.2	0.1337209	7.976	23.11	8.806	9.2372	0.89
387.5	17	7.03	20.4	0.0735294	7.949	24.56	7.639	9.0559	0.847
434.5	18	7.04	16.05	0.0939227	8.208	26.64	7.306	9.1616	0.586

Factorial: Spinner #6 (continued)

(Viable) E5 c/mL	CHvol E6 ch/mL	(G1/G0) E5 c/mL	(S) E5 c/mL	(G2/M) E5 c/mL	(A) E5 c/mL	CH-G1/G0 E6 ch/mL	CH-S E6 ch/mL
2.92	0	1.45416	0.81468	0.58108	0.0438	0	0
6.6	13.650755	3.5904	1.584	0.792	0.6336	7.1496728	3.4999953
7.05	30.195382	2.7918	2.41815	0.5499	0.7614	14.847533	8.2815015
10.5	46.148533	5.8275	1.9425	0.7875	0.84	22.446048	12.281681
12.05	74.494215	6.3383	2.2172	1.3496	0.49405	37.753786	17.511122
13.8	104.36982	4.9266	4.416	1.5042	0.4002	50.724361	24.899078
17.1	134.38243	5.3523	6.6006	1.197	1.5732	60.740556	35.497963
14.90441	177.12109	4.456418	5.663675	1.311588	2.310183	73.823153	51.869469
10.95	206.62035	6.7452	1.43445	0.79935	1.8177	86.523704	58.95261
12.9	246.18246					86.523704	58.95261
8	260.02758	2.272	2.4	0.888	2.16	105.74147	67.722881
7.1	280.57694					ERR	ERR
7.3	295.87596	1.5184	1.3651	0.2701	3.8033	114.81078	76.618485
7.5	314.18984					ERR	ERR
3.6	327.07526	0.9108	0.234	0.09	2.3616	120.63606	79.761032
2.9	327.72274					ERR	ERR
2.3	335.40258	0.1656	0.0345	0.0138	2.0953	122.02046	80.091072
1.5	339.3479						
1.507459	346.41541						

Factorial: Spinner #6 (continued)

CH-G2/M	CH-A	CHvol(10)
E6 ch/mL	E6 ch/mL	E7 ch/mL

0	0	0
2.0603446	0.6677729	1.3650755
3.669589	2.3544677	3.01953823
4.8882645	3.828172	4.61485332
7.5156404	5.4693914	7.4494215
10.81568	6.5006744	10.4369824
13.437956	8.1716113	13.4382434
16.790857	13.30267	17.7121091
19.170016	18.027126	20.6620345
19.170016	18.027126	24.6182459
23.110565	27.302003	26.0027577
ERR	ERR	28.0576941
25.628517	41.389235	29.5875957
ERR	ERR	31.4189842
26.431523	56.213766	32.7075261
ERR	ERR	32.772274
26.56022	63.26286	33.5402583
		33.9347895
		34.6415408

Factorial: Initial Substrate Concentrations
100 mL; 150 rpm; dispersed suspension

Spinner #7
10% FBS

Hour	Sample	pH	(Total) V-fraction E5 c/ml	NH3 mM	LAC mM	GIC mM	LDH U/L	IPA-0 mM	GLN mM	ALA mM	
	medium	7.65		0.123	1.611	39.89	54.57	0.2452	1.285	0.178	
0	0	7.77	5.52	0.7355072	0.128	2.022	35.82	65.02	0	1.074	0.114
30.25	1	7.77	14.2	0.9577465	0.982	7.6	32.31	63.4	0.0252	0.495	0.238
54.5	2	7.22	21.5	0.972093	1.679	17.5	21.87	65.49	1.2513	0.263	0.978
72.92	3	7.07	25.15	0.9561753	1.729	20.78	19.01	66.18	2.4295	0.2	1.16
98.1	4	7.01	25.9	0.9737991	1.814	21.33	17.26	83.37	3.4038	0.135	1.504
121.3	5	7.05	27.6	0.9673913	1.875	19.83	17.28	109.4	3.721	0.102	1.162
140.8	6	7.14	29.5	0.9207547	1.889	18.56	15.77	4.1289	0.013	1.24	
167.5	7	7.21	33.9	0.8967552	2.103	17.17	15.24	147.5	4.9068	0.042	1.332
190.5	8	7.25	34	0.8588235	2.05	16.06	15.12	172.1	4.9673	0.04	1.085
223.8	9	7.32	34	0.847619	2.157	16.56	14.4	201.6	5.5111	0.01	1.352
237.3	10	7.37	34.7	0.8027211	1.943	14.28	13.7	5.783	0.006	0.746	
264.5	11	7.39	34.6	0.7641509	2.085	14.28	13.1	244.8	6.6667	0.04	0.631
285.8	12	7.41	33.2	0.8793103	2.174	13.06	12.58	6.8026	0.049	0.801	
310.5	13	7.44	33	0.8532423	2.055	12.94	12.36	263.1	6.5685	0.005	0.411
334.8	14	7.48	29.1	0.7591623	1.925	12.11	11.89	281.1	6.9839	0.01	0.607
336.8	15	7.46	26.1	0.796875	1.952	11.67	11.75	6.8102	0.093	0.842	
366.4	16	7.53	24.05	0.7544484	2.103	10.83	11.25	6.6062	0.01	0.7	
387.5	17	7.55	24.15	0.7907801	1.943	10.11	10.1	6.9914	0.009	0.5	
434.5	18	7.62	19.8	0.7777778	1.952	10.17	9.5	6.2286	0.01	0.443	
481.3	19	7.66	16.65	0.7440273	2.014	8.889	8.222	5.0881	0.008	0.494	
553.5	20	7.68	15.9	0.7721893		7.611	6.5	1.8479	0.006	0.306	

Factorial: Initial Substrate Concer Spinner #8: GLC=high, GLN=high, LAC=0, Seru
100 mL; 150 rpm; dispersed suspension 10% FBS

Hour h	Sample	pH	(Total) E5 C/ml	V-fraction	NH3 mM	LAC mM	GLC mM	IPA=0 mg/L	GLN mM
	medium	7.65			0.356	1.567	30.22		7.209
0	0	7.74	4.52	0.7477876	0.274	1.822	28.55	0	7.921
30.25	1	7.82	11.5	0.9391304	1.732	5.689	27.58	2.9859	5.724
54.5	2	7.35	19.1	0.973822	2.994	8.889	23.65	3.2402	5.287
72.92	3	7.14	20.5	0.9756098	3.85	13.89	18.43	6.0272	4.607
98.1	4	7.05	21.6	0.962963	4.831	16.67	16.67	6.7145	3.5
121.3	5	7.04	26.2	0.8778626	5.704	18.56	15.39	6.2613	2.658
140.8	6	7.07	29.1	0.7766323	5.864	19.44	13.93	6.2236	1.823
167.5	7	7.11	27.6	0.6521739	6.809	19.78	13.38	6.3897	1.814
190.5	8	7.13	30.9	0.6479218	6.88	22.56	12.56	6.5785	1.534
223.8	9	7.17	30.8	0.4837662	7.058	23.28	12.18	6.3444	1.308
237.3	10	7.21	29.3	0.492228	6.916	22.06	11.76	7.0091	1.262
264.5	11	7.16	26.1	0.5186335	6.948	22	10.98	6.3595	0.665
285.8	12	7.14	23.2	0.4439655	7.103	21.28	9.472	5.9819	1
310.5	13	7.13	25.95	0.4420063	7.156	21.67	7.945	5.4758	0.943
334.8	14	7.14	24	0.4392857	7.254	20.11	7.689	5.2568	1.045
336.8	15	7.11	21.6	0.3965517	7.468	20.06	7.222	5.7553	1.006
366.4	16	7.13	15.8	0.2848101	7.664	19.89	6.728	5.6495	0.9
387.5	17	7.14	20.7	0.352657	7.735	19.61	6.378	5.0529	0.66
434.5	18	7.14	21.35	0.5682819	8.065	19.39	5.783	5.8384	0.47
481.3	19	7.12	19.2	0.5260417	8.145	19.06	5.889	6.5483	0.299
553.5	20	7.05	19.1	0.1675393		19.06	5.783	6.1556	0.067

APPENDIX B:

Model Computer Code and Simulation Graphs

MODEL COMPUTER CODE:

```

                'DIFFERENTIAL EQUATIONS

                'first equation (GLUTAMINE)
600
    IF Y(1) < 0 THEN Y(1) = 0

    IF Y(2) < .5 AND nFLAG = 1 THEN 'delay between glucose exhaustion and growth cessation
    teatime = X
    nFLAG = 0
    END IF

    IF Y(1) > 1 AND Y(2) > .5 THEN
    spgr = con(11)
    frac = 1
    ELSE
    IF Y(2) < .5 THEN frac = .5
    IF Y(1) < 1 THEN frac = .03
    spgr = 0
    IF X - teatime < (.5 * LOG(2) / con(11)) THEN spgr = con(11)
    END IF

    FG1 = Y(10) / Y(3)          'G1 fraction
    demand = 2 * FG1 + (1 - FG1) 'demand for substrate

    Gs = con(19)
    f1 = .725
    f2 = .367
    ckGLN = .002          '.00275

    IF Y(2) > .5 THEN
    DY = -demand * Y(1) * Y(3) * (con(1) * spgr + frac * con(2))
    DY = DY / (Gs * Y(1) * (9 + 18 * f1) + Y(2) * (2 + 36 * f2))
    DY = DY - ckGLN * Y(1)
    ELSE
    DY = -demand * Y(3) * frac * con(2) / (9 + 18 * f1)
    DY = DY - ckGLN * Y(1)
    END IF

    IF Y(2) <= .5 AND Y(1) <= .5 THEN
    'DY = -ckGLN * Y(1)
    END IF

    dYdt(1) = DY

    RETURN

```


'second equation (GLUCOSE)

605

IF Y(2) < .495 THEN Y(2) = .495

IF Y(2) > .5 THEN

DY = (1 / Gs) * (Y(2) / Y(1)) * (dYdt(1) + ckGLN * Y(1))

ELSE

DY = 0

END IF

dYdt(2) = DY

RETURN

'third equation (VIABLE CELLS)

610

IF Y(3) < 0 THEN Y(3) = 0

IF X <= 24 THEN

DY = .1 * spgr * Y(3)

ELSE

IF Y(1) > 1 AND Y(2) > .5 THEN

DY = spgr * Y(3) - con(12) * Y(3)

END IF

IF Y(1) > 1 AND Y(2) <= .5 THEN

DY = spgr * Y(3) - con(13) * Y(3)

END IF

IF Y(1) <= 1 AND Y(2) <= .5 THEN

DY = spgr * Y(3) - con(14) * Y(3)

END IF

END IF

dYdt(3) = DY

RETURN

'fourth equation (ALANINE)

615

IF Y(4) < 0 THEN Y(4) = 0

IF Y(1) > 1 THEN

DY = con(4) * Y(3)

ELSE

DY = -con(5) * Y(3)

END IF

dYdt(4) = DY

RETURN

'fifth equation (LACTATE)

620

IF Y(5) < 0 THEN Y(5) = 0

IF Y(2) > .5 THEN

DY = -1.25 * dYdt(2)

END IF

IF Y(2) <= .5 AND Y(1) > 1 THEN

DY = 0

END IF

IF Y(2) <= .5 AND Y(1) <= 1 THEN

DY = -con(6) * Y(3) 'preferred form

END IF

dYdt(5) = DY

RETURN

'sixth equation (TPA)

625

IF Y(6) <= 0 THEN Y(6) = 0
DY = con(3) * dYdt(15) - con(17) * dYdt(13)

dYdt(6) = DY

RETURN

'seventh equation (SERINE)

630

IF Y(7) < .001 THEN Y(7) = .001

IF Y(2) > .5 THEN
DY = -con(7) * Y(3)

ELSE
DY = 0
END IF

dYdt(7) = DY

RETURN

'eighth equation (AMMONIA)

635

DY = -con(4) * dYdt(1) - (1 - con(4)) * con(20) * dYdt(1) - con(8) * dYdt(7)

IF Y(1) < .5 THEN
DY = -2 * dYdt(1) - con(8) * dYdt(7)
END IF

dYdt(8) = DY

RETURN

```
                'ninth equation (GLYCINE)
640
    f3 = con(9)
    f4 = con(10)
    IF Y(9) < 0 THEN Y(9) = 0

    IF Y(1) > 1 AND Y(2) > .5 THEN
    DY = -dYdt(7)
    ELSE
    DY = -f3 * dYdt(5) - f4 * dYdt(4)
    END IF

    dYdt(9) = DY

    RETURN

                'tenth equation (G1 PHASE)
645
    IF Y(10) < 0 THEN Y(10) = 0

    IF X < 24 THEN
    YO(10) = .8 * Y(3)
    Y(10) = YO(10)
    END IF

    IF X = 24 THEN                ' re-define G1 fraction
    YO(10) = .2 * Y(3)
    Y(10) = YO(10)
    END IF

    IF Y(1) <= 1 AND G1FLAG = 0 THEN
    YO(10) = .44 * Y(3)          ' re-define G1 fraction
    Y(10) = YO(10)
    G1FLAG = 1
    END IF

    DY = dYdt(3) * Y(10) / Y(3)

    dYdt(10) = DY

    RETURN
```

'eleventh equation (G0 PHASE CELLS)

650

IF Y(11) < 0 THEN Y(11) = 0

IF Y(1) <= 1 AND Y(2) <= .5 THEN

DY = -.4 * dYdt(10)

ELSE

DY = 0

END IF

dYdt(11) = DY

RETURN

'twelveth equation (DEAD CELLS)

655

IF Y(1) > 1 AND Y(2) > .5 THEN

DY = con(12) * Y(3)

END IF

IF Y(1) > 1 AND Y(2) <= .5 THEN

DY = con(13) * Y(3)

END IF

IF Y(1) <= 1 AND Y(2) <= .5 THEN

DY = con(14) * Y(3)

END IF

dYdt(12) = DY

RETURN

'thirteenth equation (LYSED CELLS)

660

DY = 0

IF Y(1) <= .6 THEN

DY = con(18) * dYdt(12)

END IF

dYdt(13) = DY

RETURN

'fourteenth equation (CELL HOURS)

665

DY = Y(3)

dYdt(14) = DY

RETURN

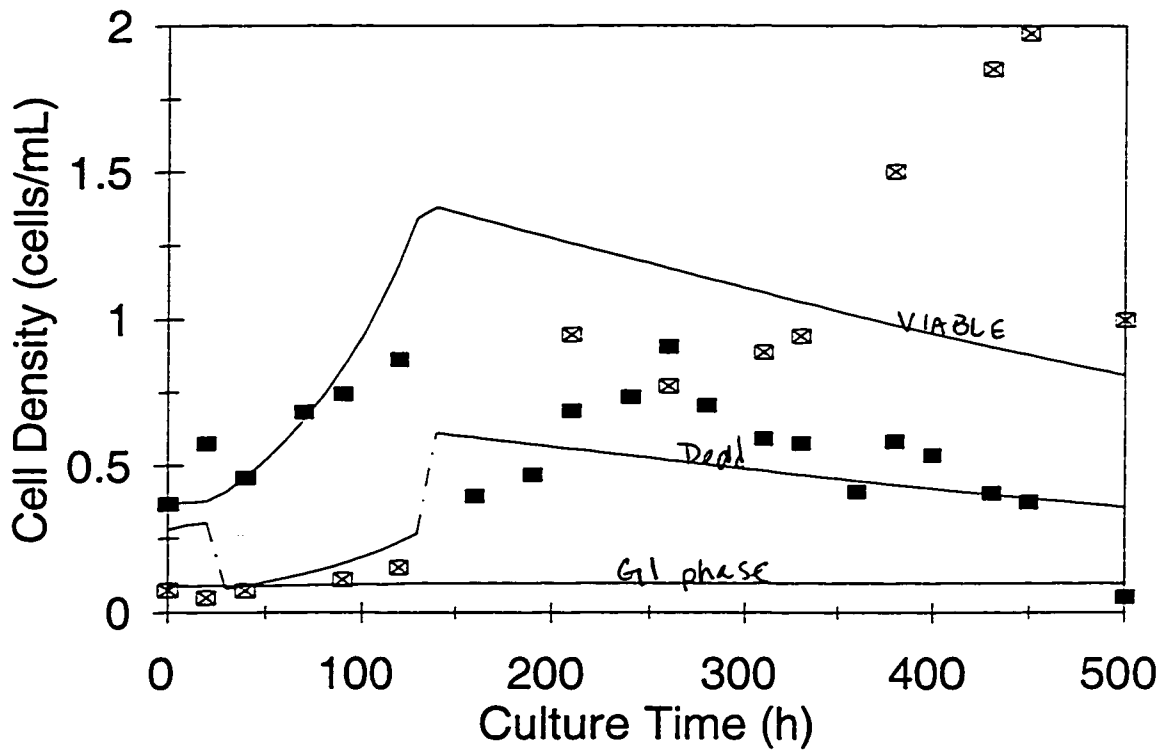
'fifteenth equation (G1 PHASE CELL HOURS)

670

DY = Y(10)

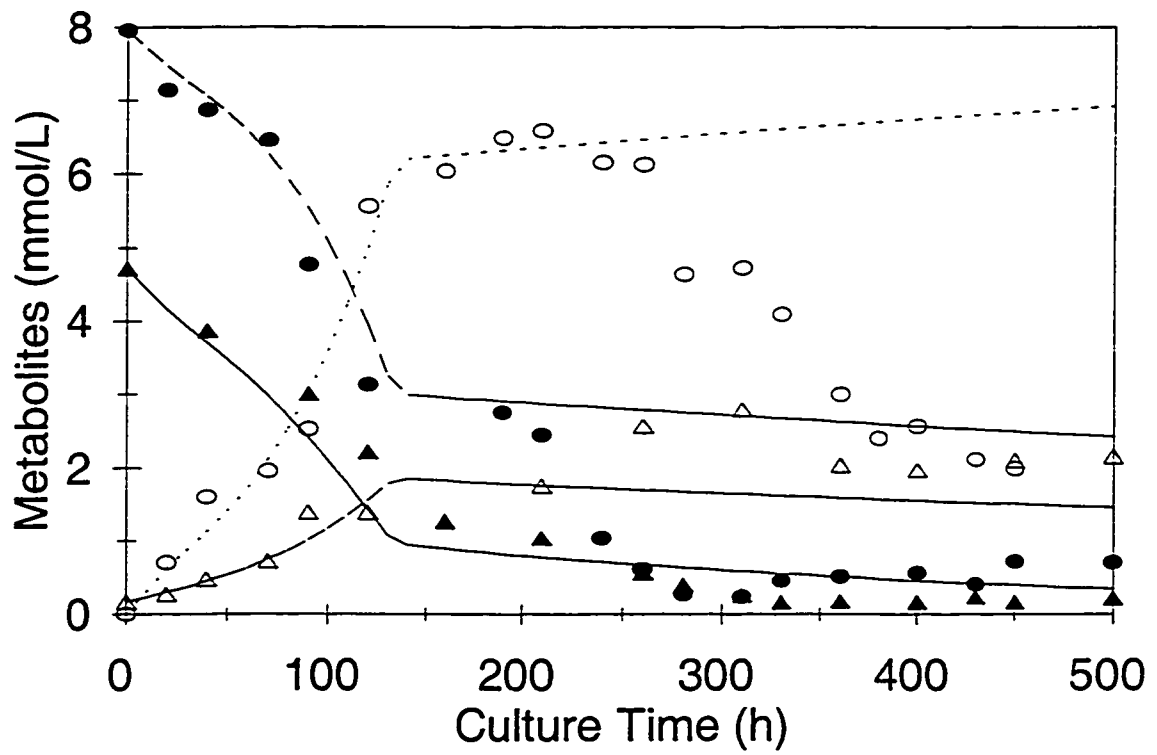
dYdt(15) = DY

RETURN

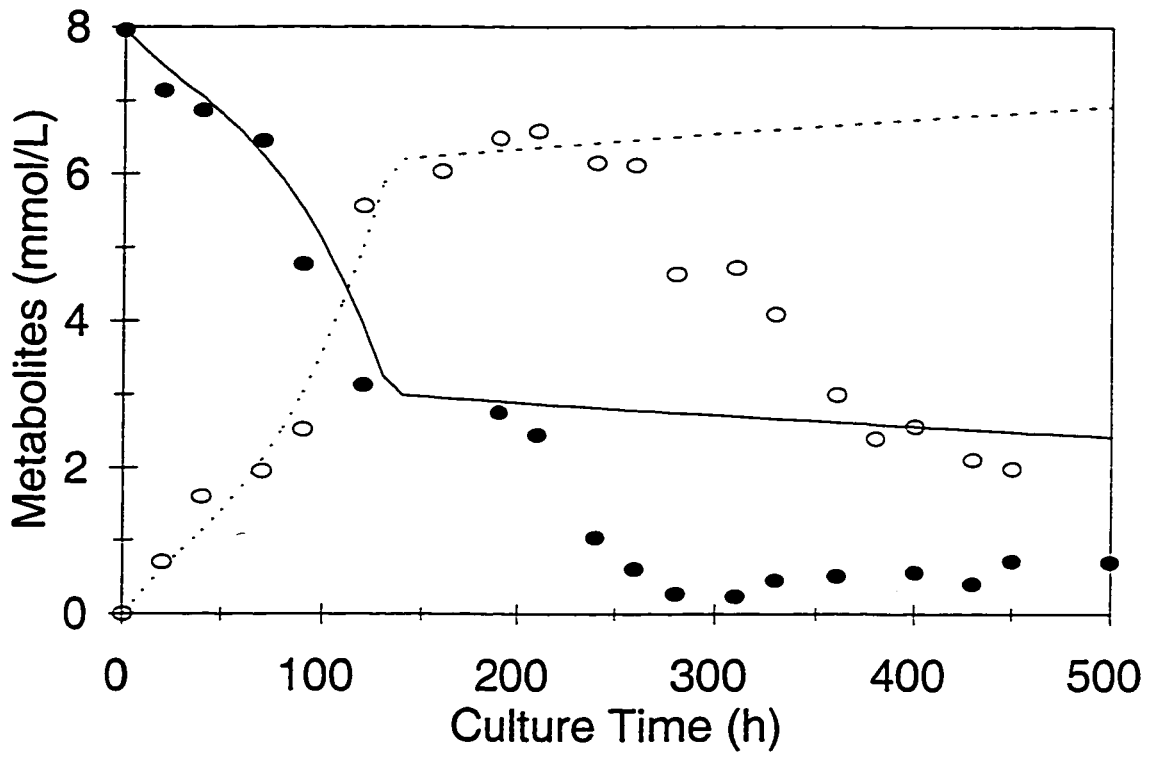


Simulation only successful during the first metabolic phase.

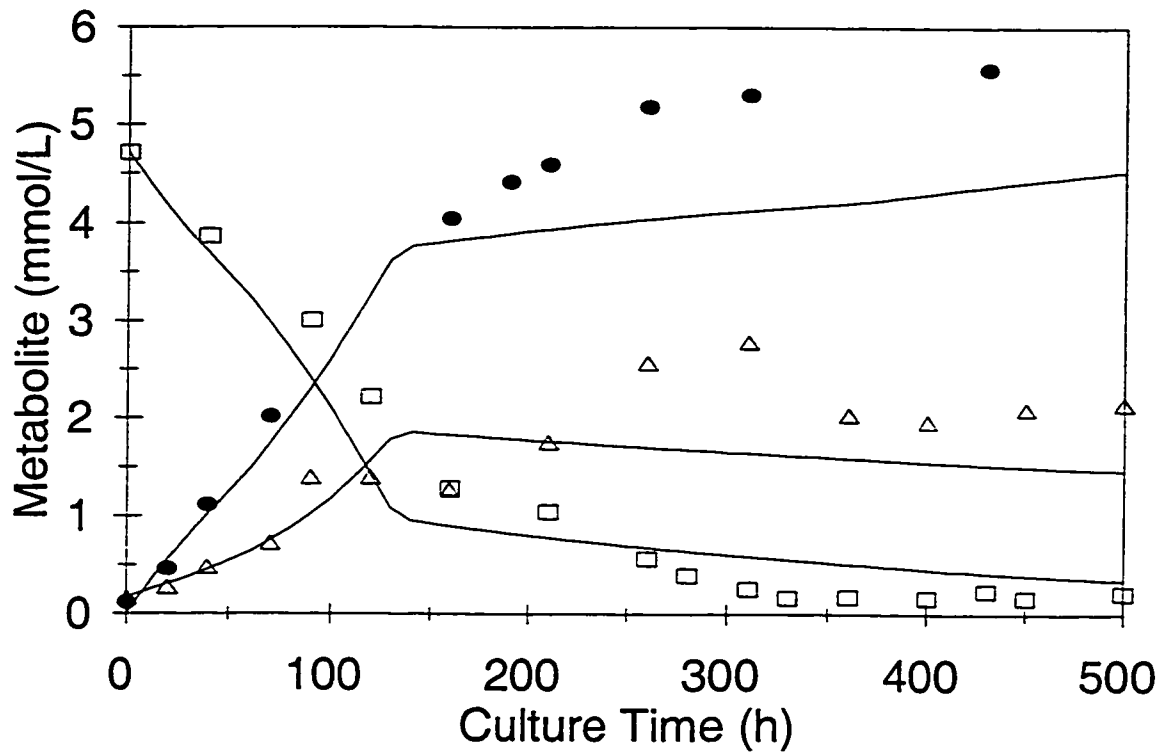
- viable cells/ml
- ⊠ dead cells/ml



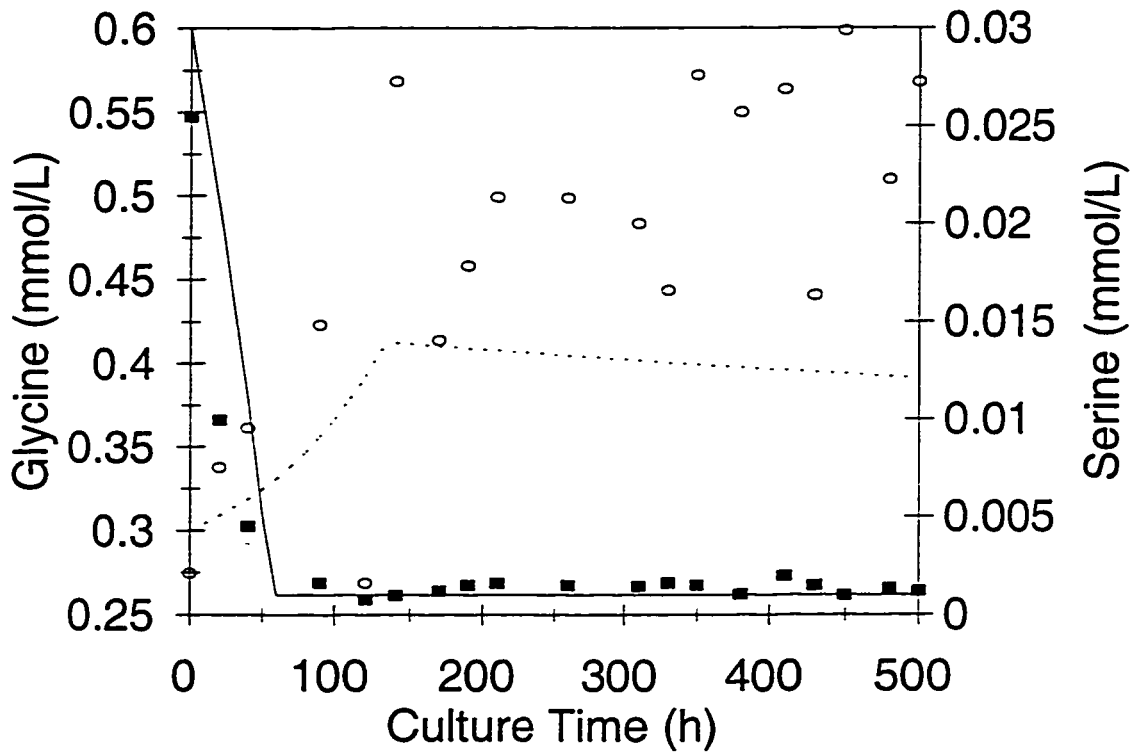
- Lactate.
- GLUCOSE
- ▲ GLUTAMINE
- △ ALANINE



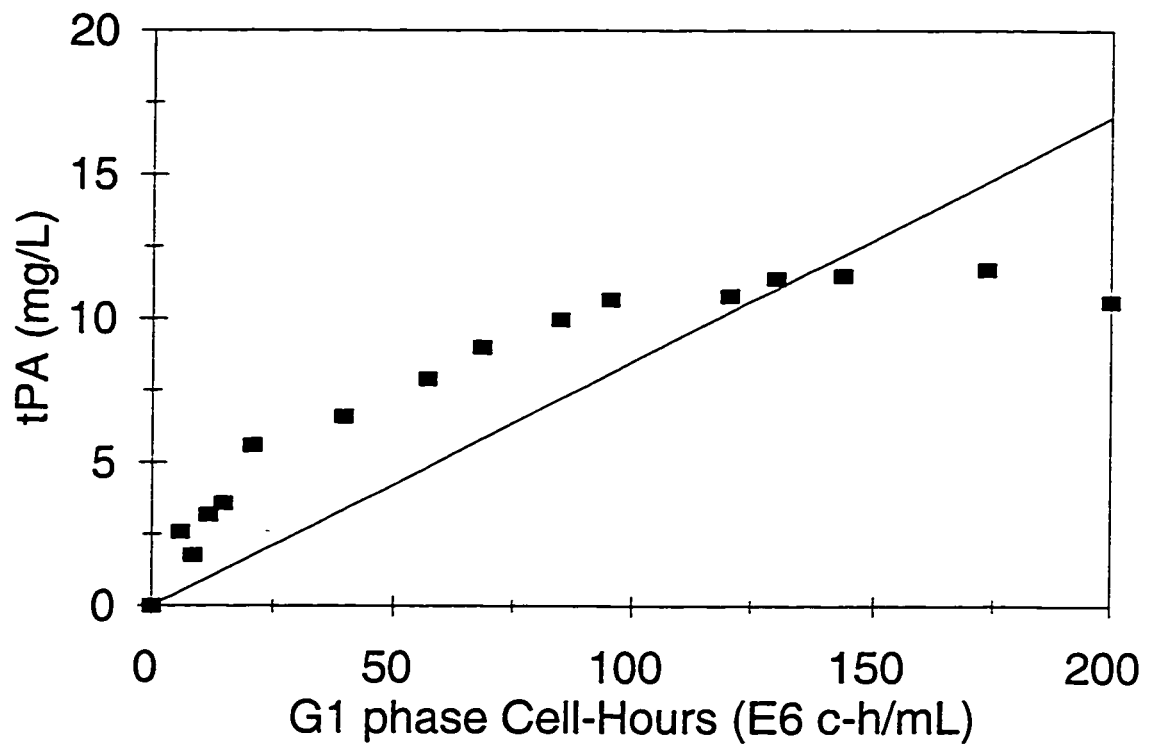
● GLUCOSE
○ LACTATE

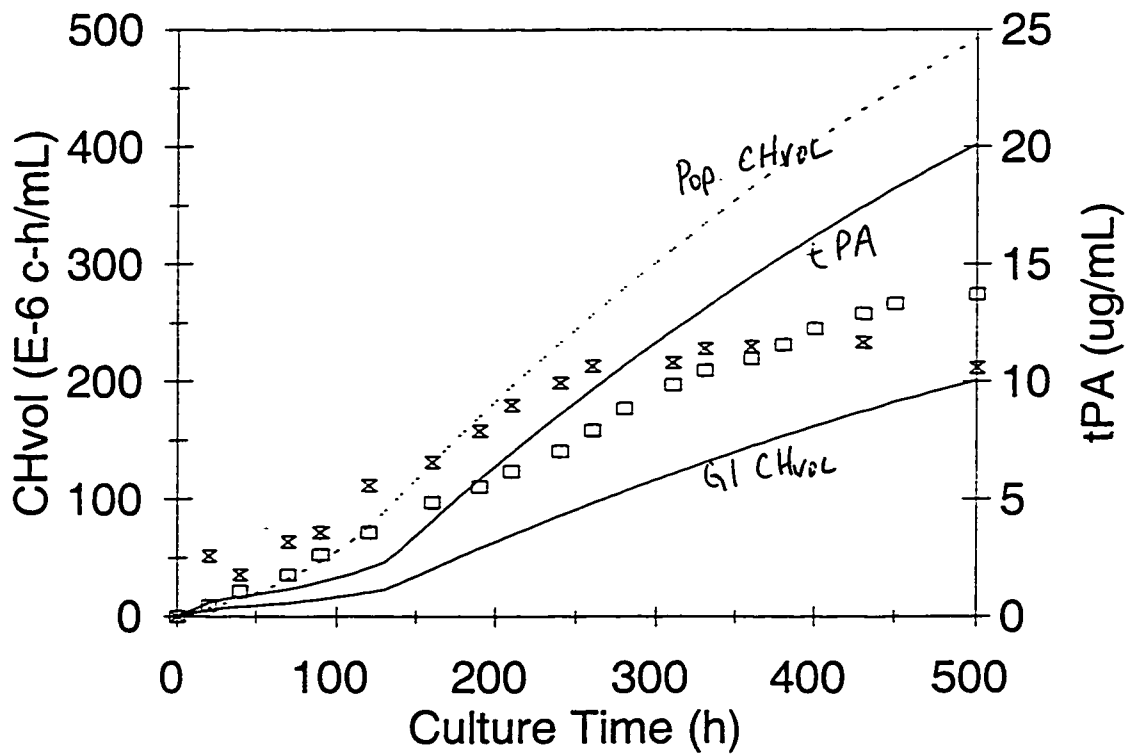


- GLUTAMINE
- △ ALANINE
- AMMONIA

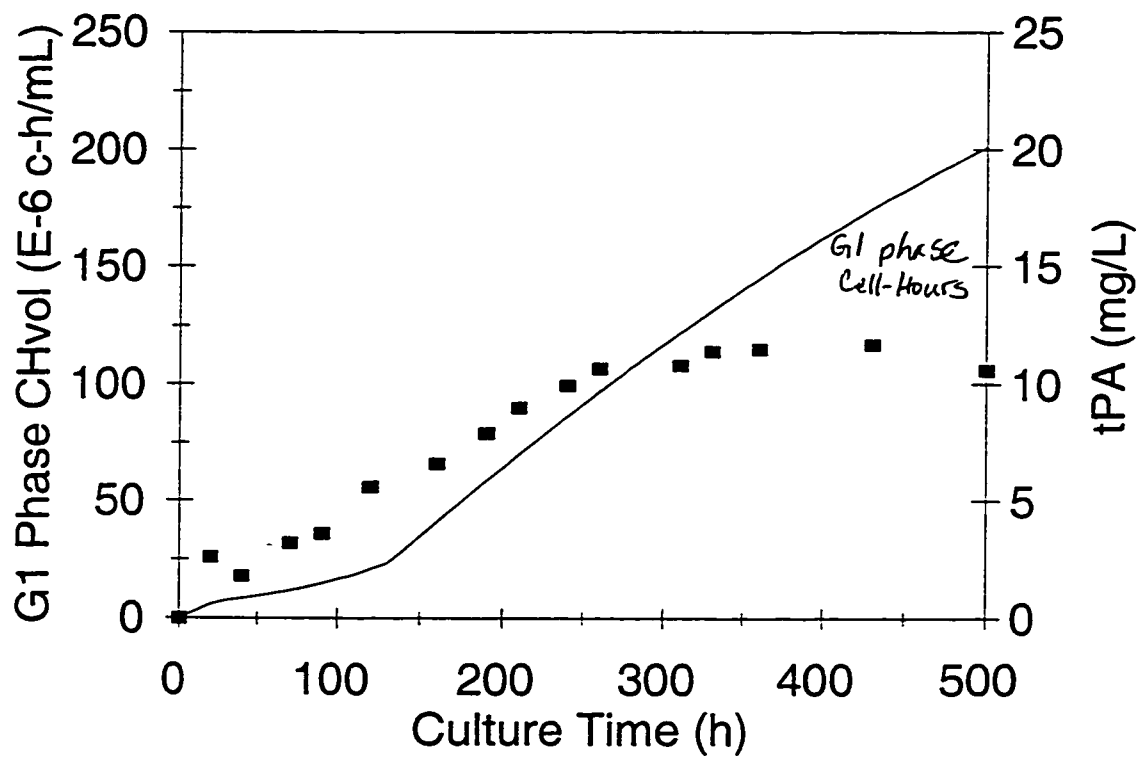


■ SERINE
○ GLYCINE





x tPA
 □ viable population cell-hours.



■ tPA

APPENDIX C:

Preliminary Experiments and Reproducibility

Preliminary Experiments and Reproducibility	page 224
Reproducibility of the Morphological Types Experimental Set	page 233
Graphical Evaluation of the Impact of Initial Substrate Concentrations Preliminary Factorial Experiment	page 234

Preliminary Experiments

A set of preliminary experiments were undertaken. The goals of this preliminary investigation included:

- identify a cell line, representative of a commercial host/plasmid system, for use as the research model.
- identify and/or develop a reliable assay for the rDNA protein product.
- assess reproducibility/suitability of the chosen research model.
- establish population parameters of the chosen research model.
- establish culture requirements of the chosen research model.

The cell line chosen for preliminary investigation was a rCHO cell line expressing h-t-PA, as mentioned above. This cell line is derived from a DHFR⁻ CHO mutant, which has been transfected with an expression vector coding for DHFR and for h-t-PA. The expression vector contains an SV40 promoter for each of the two proteins.

HB-CHO, a commercially available serum-free medium specifically designed to support CHO cell populations, was employed in the preliminary investigation. Initially, the cells were placed in HB-CHO containing 10% (v/v) FBS. The cells were maintained as a surface adherent monolayer in T-flasks, in a 5% CO₂, 37 °C incubator. Following 5 days of maintenance as a confluent monolayer, the populations were adapted to serum-free HB-CHO by step reductions in the concentration of serum over a two week

period. At 2% (v/v) FBS, the cells began to detach from the surface, and once 0% serum conditions were achieved, no cells remained attached to the surface.

Two days after serum-free conditions were achieved, the suspended cells began to form aggregates. Aggregates were loose with respect to cell-to-cell proximity. Aggregates were amorphous in shape, attaining a maximum longitudinal axis of approximately 2 mm. Aggregates were maintained in serum-free HB-CHO medium in T-flasks, in a 5% CO₂, 37 °C incubator for three weeks. Viability and growth remained high.

In a second preliminary experiment, ease of cell line adaptability to serum-free conditions was evaluated. The cells were initially grown to confluence (about 5 days) in HB-CHO containing 10% (v/v) serum. The confluent population was then subjected to a step change to 0% serum. The cells detached from the surface over approximately 12 hours, and then continued to grow, and to form aggregates. These suspended aggregates were once again maintained in serum-free conditions for three weeks. No impairment of growth or viability was observed. Indeed, the maximum cell concentration was at least 2-fold greater than concentrations attained as monolayers of cells in medium containing 10% (v/v) serum (data not shown).

The h-t-PA concentration was determined using the Chromozym t-PA method (Boehringer Mannheim). Single chain t-PA cleaves the Chromozym t-PA (N-Mehtylsulfonyl-D-Pher-Gly-Arg-4-nitranilide acetate) to 4-nitraniline. The 4-nitraniline is a chromophore which absorbs at 405 nm. The absorbance is linearly proportional to the concentration of 4-nitraniline, and therefore to the concentration of single chain t-PA, up to a concentration of 1.5 µg/mL of single chain t-PA. The absorbance was calibrated against pure h-t-PA (Sigma). Concentrations of h-t-PA in the three week rCHO cultures were determined to be greater than 1.5 µg/mL of medium. The Chromozym t-PA assay, which requires a total volume of 1.6 mL, was adapted to

microassay be performed as a microassay in 96 well microplates (Section 5.4.9). h-t-PA concentrations from sample replicates, using the microassay technique, were found to be accurate to within 11%.

Reproducibility and population parameters were assessed from twelve 200 mL, stationary batch runs in T-flasks cultured under 5% CO₂ at 37 °C. Cell concentration could not be determined directly from cells growing as aggregates. Initially, cells were dispersed into single cell suspension by the addition of DNase I. However, disaggregation via this method required at least six hours to achieve. Therefore, this method was not used during this experiment. Instead, aggregates were disrupted into a nuclear suspension by the addition of citric acid and Triton-X 100. Whole nuclei were then counted, corresponding to total cell concentration. Viability could not be quantitatively determined. By qualitative visual inspection, it was apparent that viability was high, even in the largest aggregates, until the decline phase of the batch runs. Total cell concentrations of the twelve runs had an average standard deviation of the between population means of less than 12% (Figure 1), indicating high reproducibility between batch stationary runs. The maximum cell concentration was similar to the maximum cell concentrations obtained as microcarrier adherent monolayers suspended in stirred tanks (Phillips, not published). The maximum apparent growth rate of the total cell population, μ_{app} , was 0.024 h⁻¹; which corresponds to a maximum doubling time of 30 hours. This growth rate is similar to that found in microcarrier adherent monolayers suspended in stirred tanks (Phillips, not published).

The batch stationary suspended aggregate rCHO cell cultures attained a maximum h-t-PA titre of 4.0 µg/mL after 15 days (Figure 2). The average standard deviation of the population means of the h-t-PA concentration measurements was approximately 14%. The specific productivity was found to be partially growth associated (Figure 3).

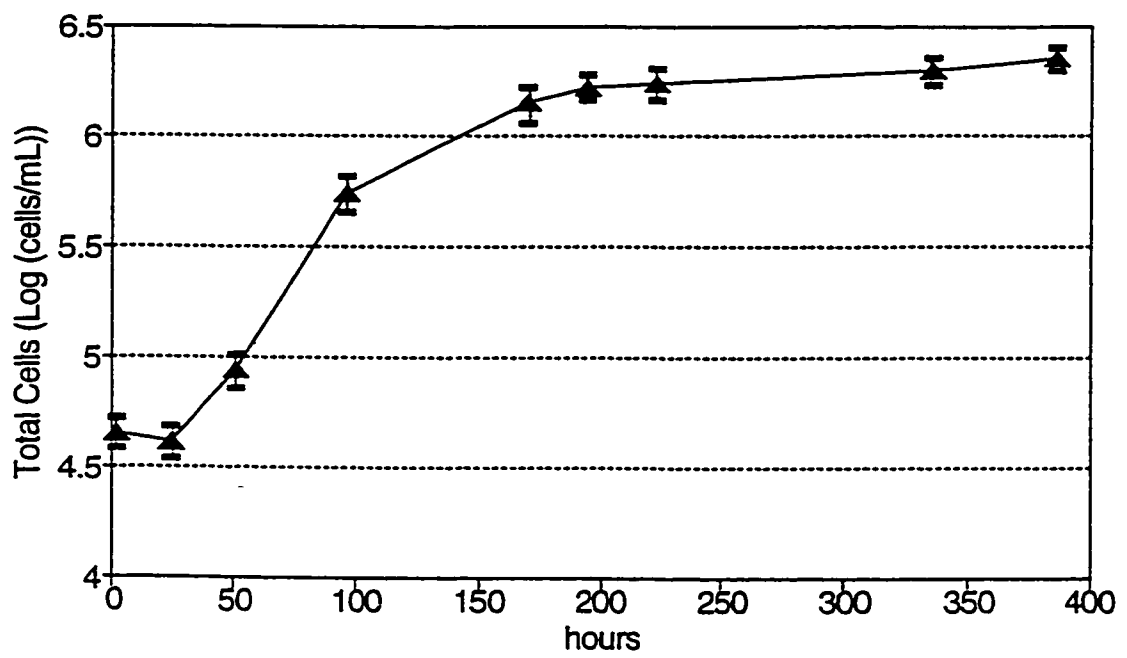


Figure 1: CHO aggregates in suspension in serum-free, 200 mL stationary batch culture. Data points are the between population means of 12 separate runs.

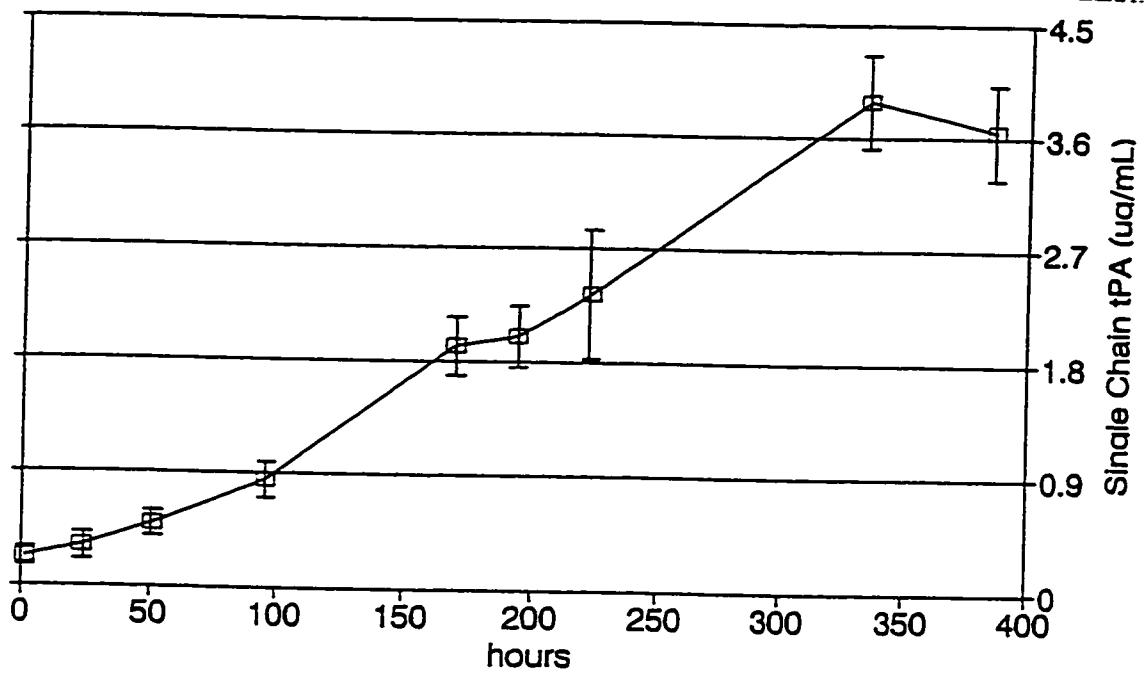


Figure 2: Volumetric productivity of single chain h-t-PA by CHO cell aggregates in suspension in serum-free, 200 mL stationary batch culture. Data points are the between population means of 12 separate runs.

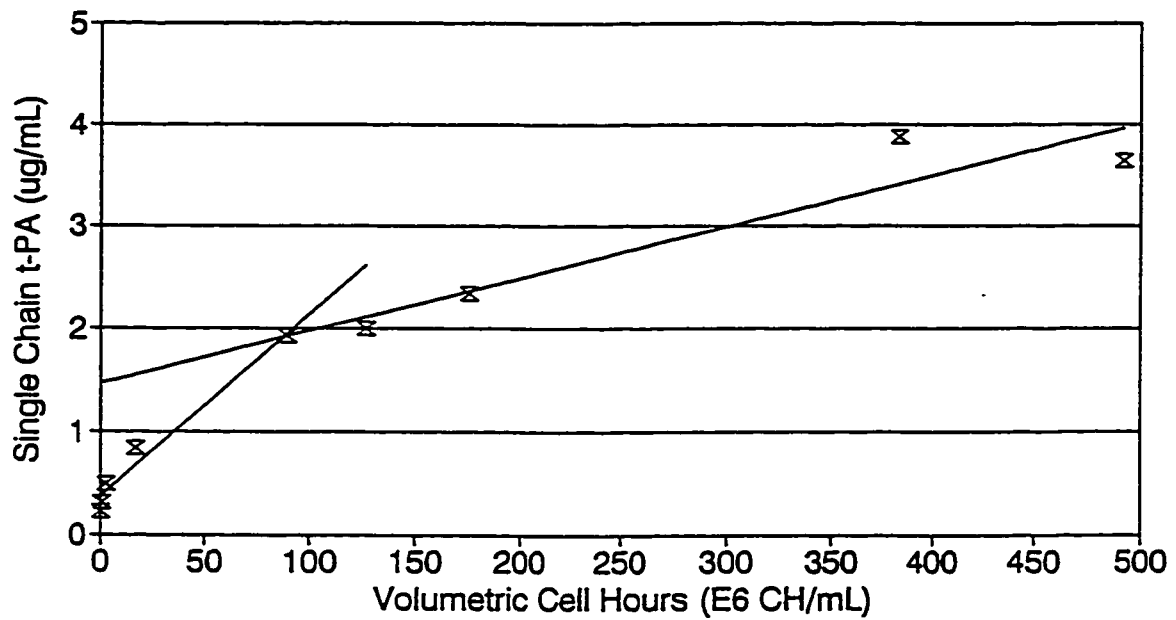


Figure 3: Specific productivity of single chain h-t-PA by CHO cell aggregates in suspension in serum-free, 200 mL stationary batch culture. Data points are the between population means of 12 separate runs.

It was calculated to be 0.018 $\mu\text{g}/\text{million cell-hours}$ during the population lag and early exponential phases, and 0.005 $\mu\text{g}/\text{million cell-hours}$ thereafter. The productivity of suspended aggregate cultures is approximately 20 to 25% greater than that seen in suspended microcarrier-adherent cultures.

Aggregate suspension culture, as a bioprocessing type, has inherent potential benefits when compared with microcarrier-adherent suspension culture. For example, 1) aggregates do not require serum proteins, or specific proteins, to act as ligands in their formation; 2) aggregates do not require a surface for cell growth; 3) aggregates require no bioprocessing preparatory steps; etc.

Population RNA/DNA ratios were also measured during the first eight days of the batch runs. An interesting pattern of RNA/DNA population ratios during the batch cultivations was observed (Figure 4). It may be possible to correlate RNA/DNA population ratios to population growth phase, and perhaps to percent viability. This may be of particular value in cases where cell concentrations and/or viabilities are difficult or impossible to measure directly.

The preliminary findings, which are summarized in Table 1, formed the basis for the formulation of the specific research objectives. This preliminary investigation demonstrated that: 1) the cell line is appropriate for use as a representative of the rCHO cell line type; 2) the productivity of the rDNA protein can be monitored reliably; and 3) the host/plasmid system can be cultured reproducibly.

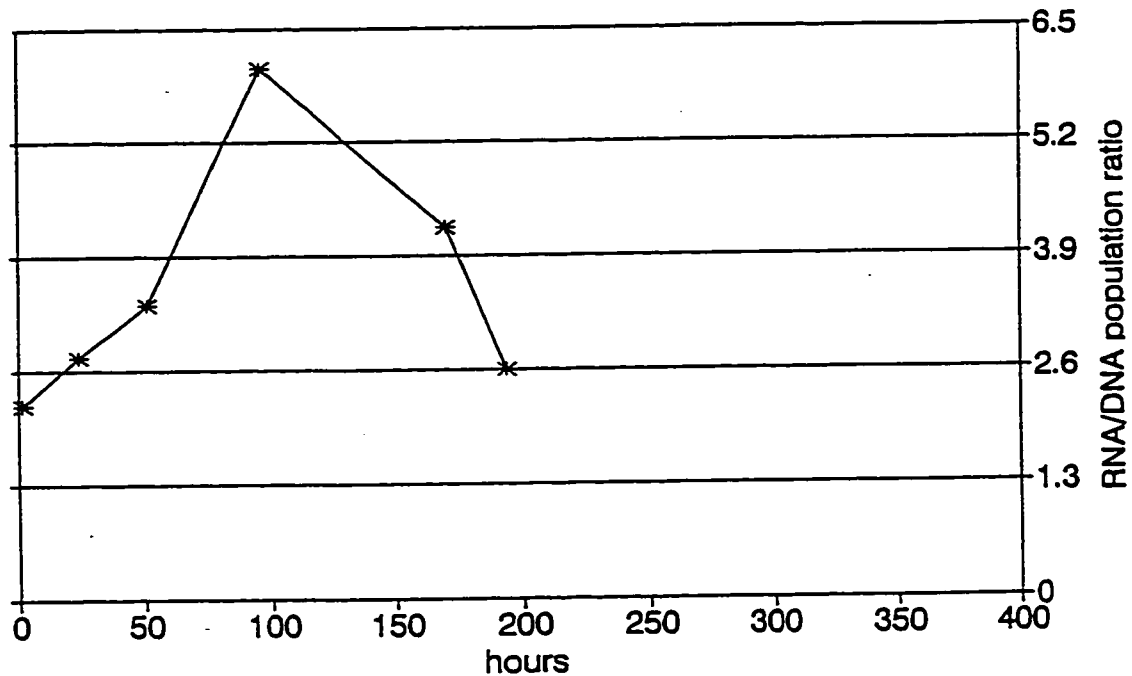
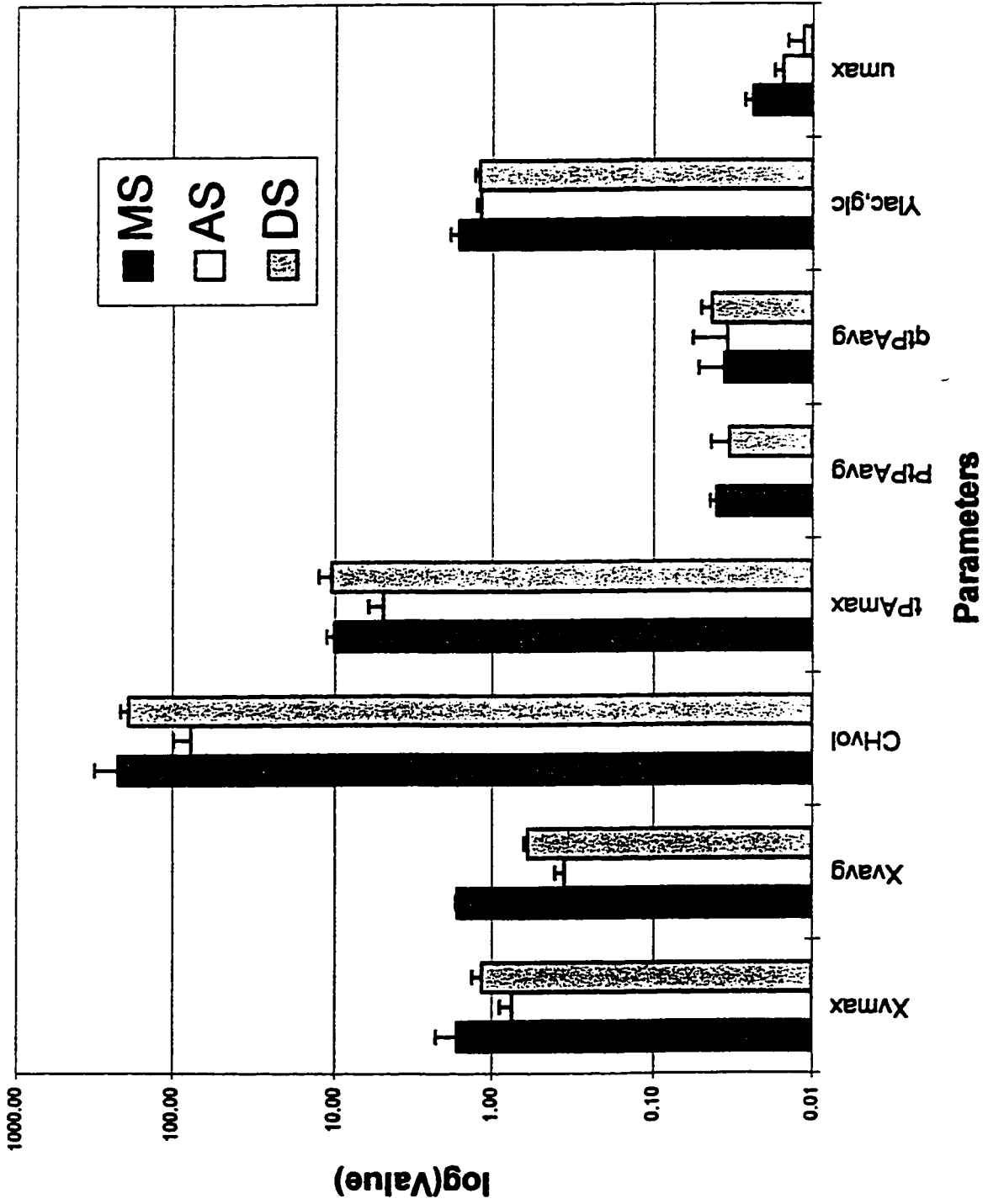


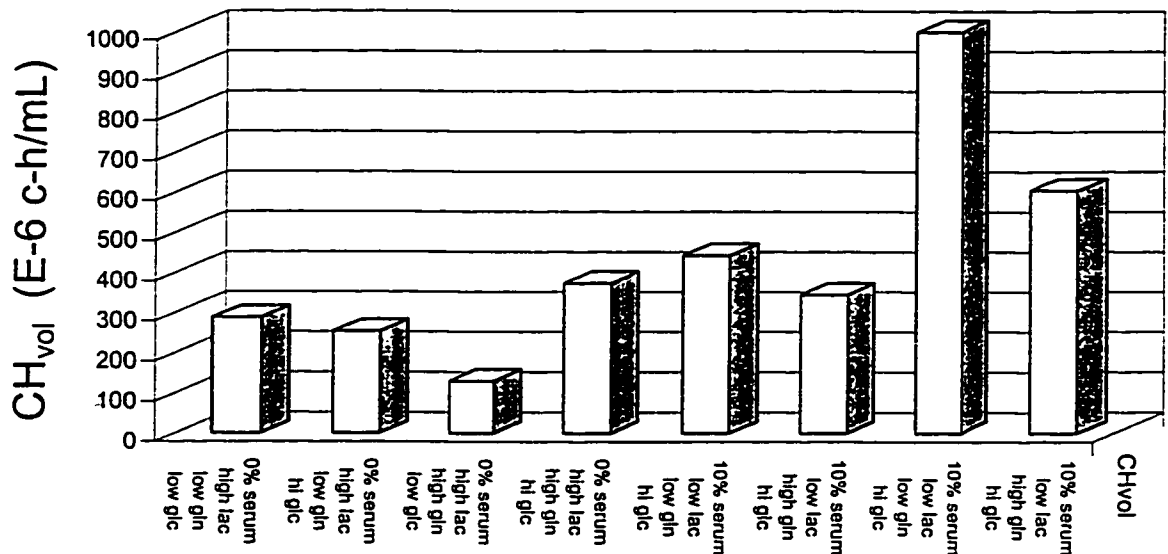
Figure 4: RNA/DNA population ratios of CHO cell aggregates in suspension in serum-free, 200 mL stationary batch culture. Data points are the between population means of 12 separate runs.

Table 1: Summary of findings from preliminary investigation of rCHO cells producing h-t-PA

PRELIMINARY FINDINGS
rCHO grows and produces h-t-PA reproducibly in serum free stationary batch culture
$\mu_{\max} \approx 0.024 \text{ h}^{-1}$ ($t_d \approx 30 \text{ h}$)
$P_{\max} \approx 4 \mu\text{g/mL}$
productivity is partially growth associated
rDNA protein assay accurate [t-PA] $\pm 11\%$
cells grow as non-surface adherent aggregates
cell-cell adhesion very strong: can break with DNase I in 6 -12 hours
viability difficult to assess in aggregates: total cell counts can be made from whole nuclei counts of detergent disrupted aggregates
RNA/DNA population ratios vary with population growth phase
aggregates yield potential benefits w.r.t. bioprocessing

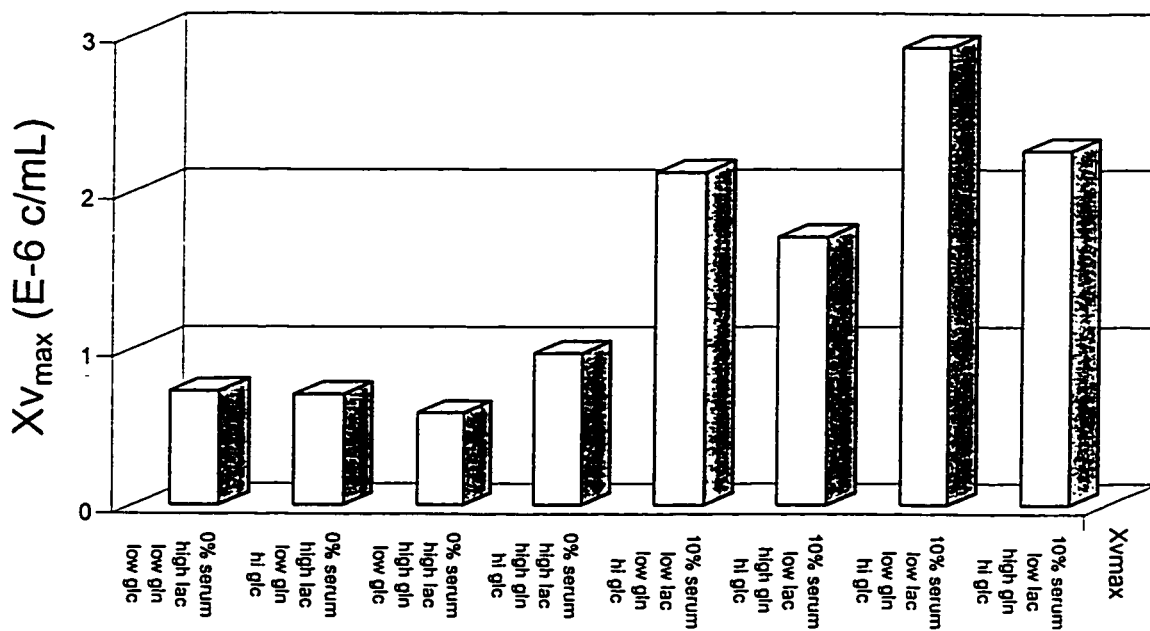


Growth Parameters as a Function of Initial Substrate Combinations (1) - Cell Hours



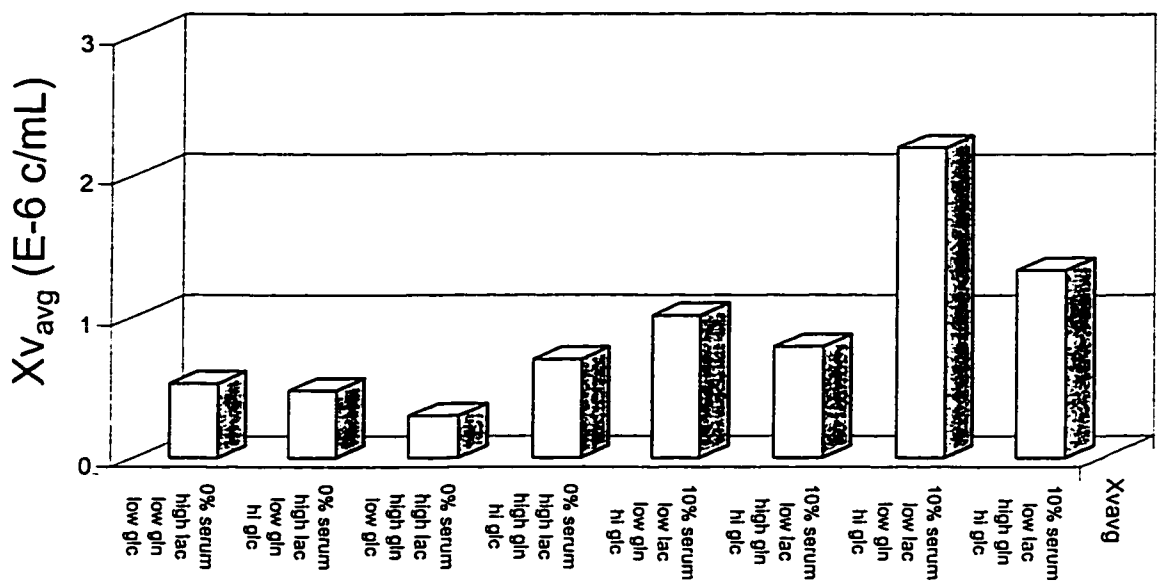
Growth Parameters as a Function of Initial Substrate Concentrations

(2) - $X_{v_{max}}$

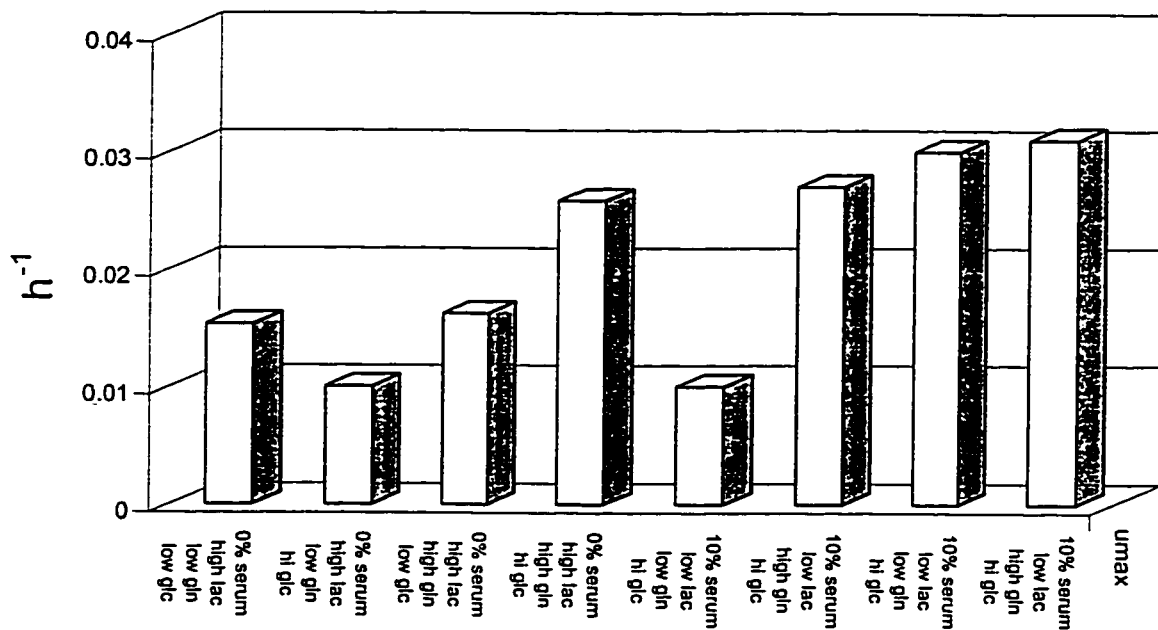


Growth Parameters as a Function of Initial Substrate Concentrations

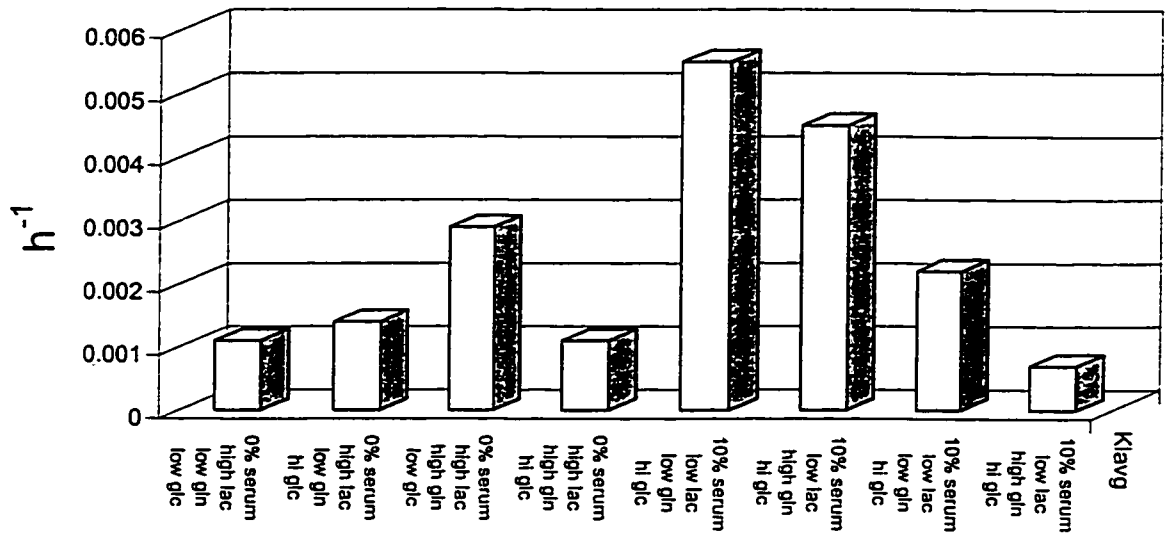
(3) - $X_{V_{avg}}$



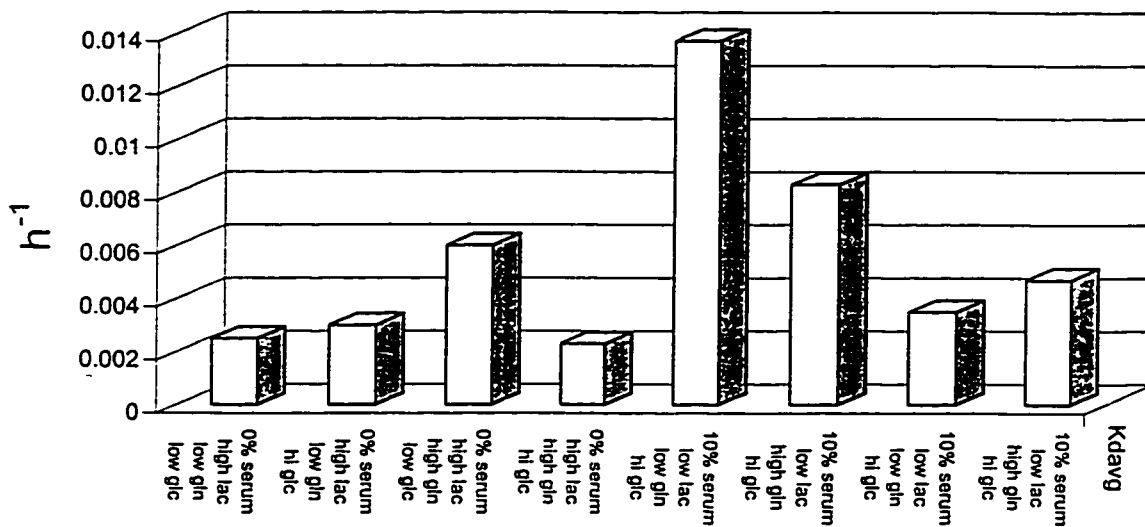
Growth Parameters as a Function of Initial Substrate Concentrations (4) - u_{max}



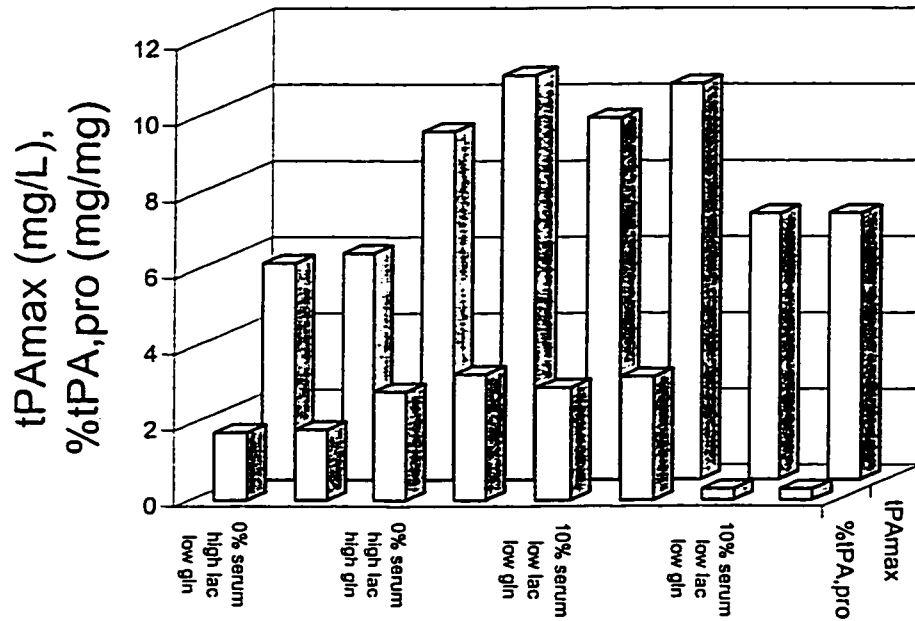
Growth Parameters as a Function of Initial Substrate Concentrations (5) - $K_{I_{avg}}$



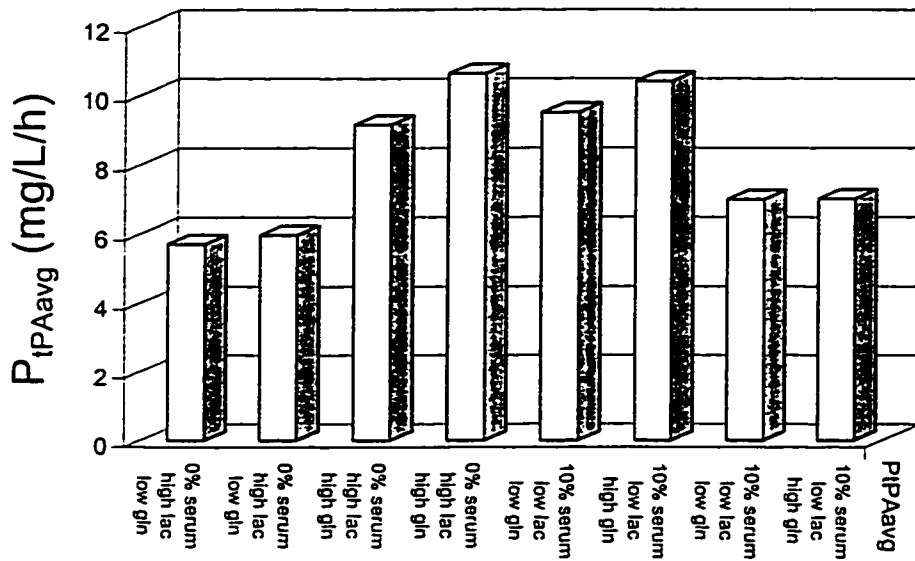
Growth Parameters as a Function of Initial Substrate Combinations (6) - $K_{d_{avg}}$



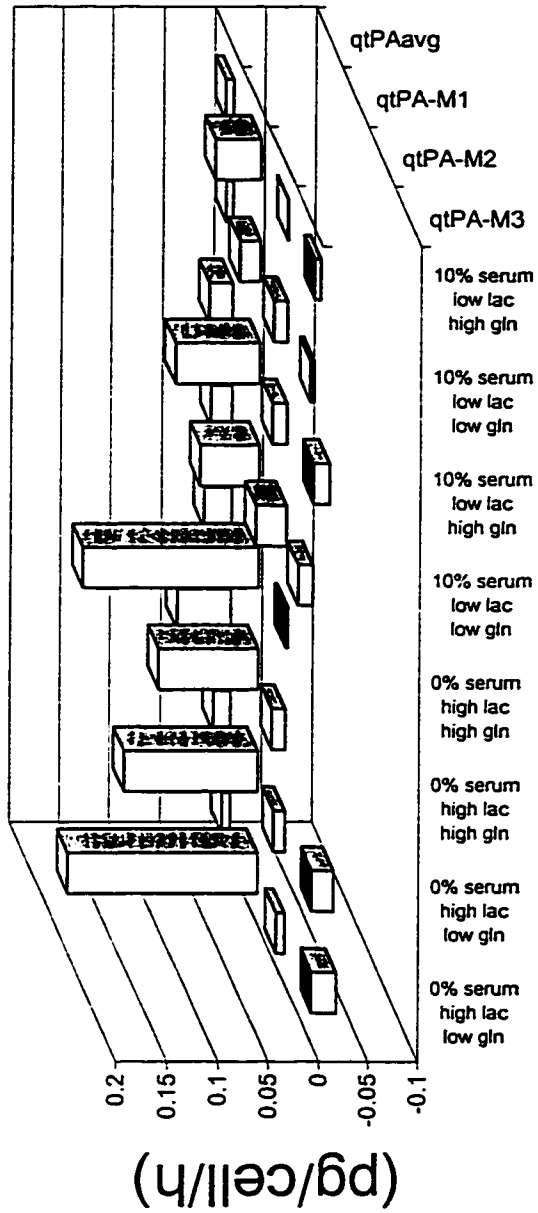
tPA Production Parameters as a Function of Initial Substrate Combinations -(1)

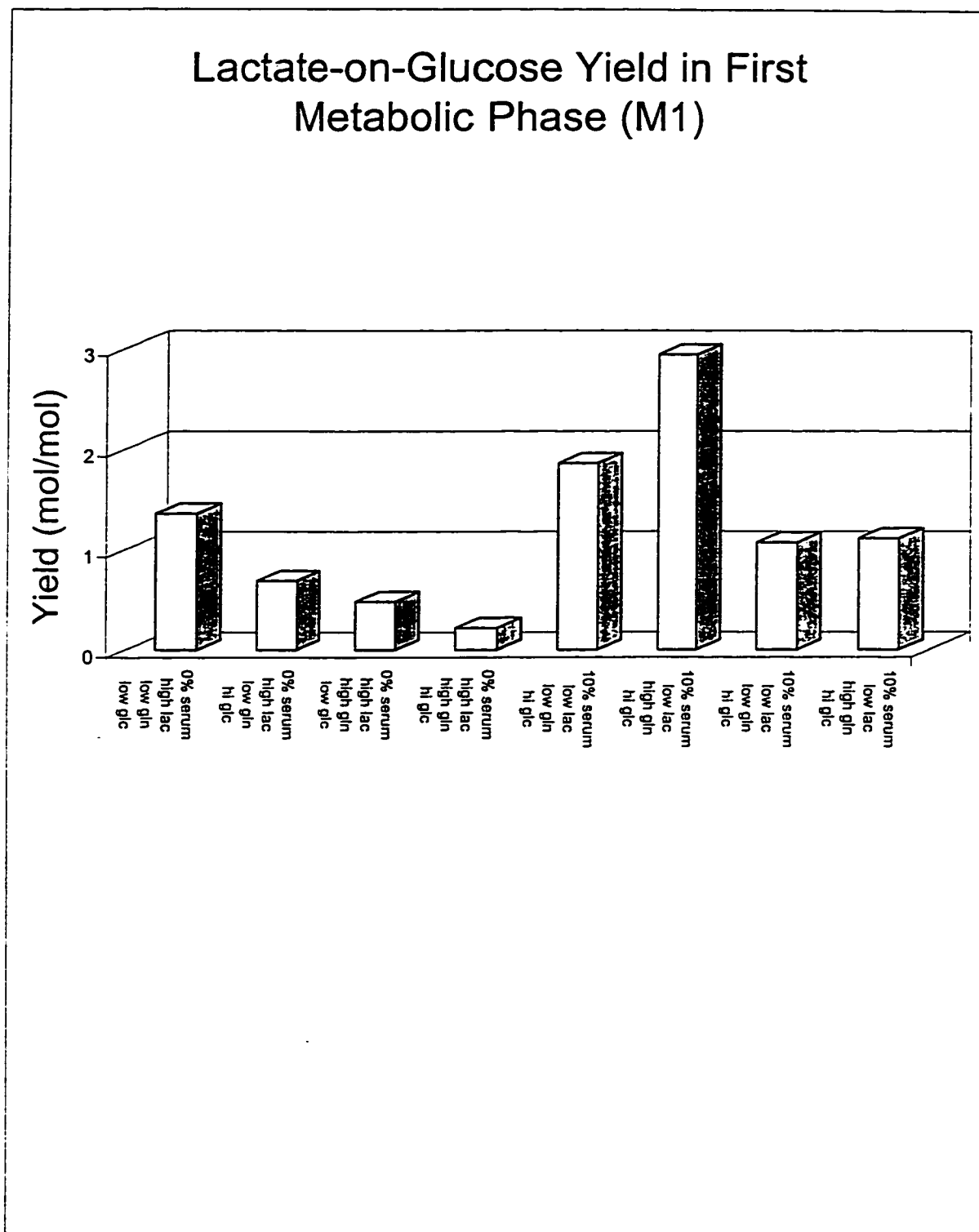


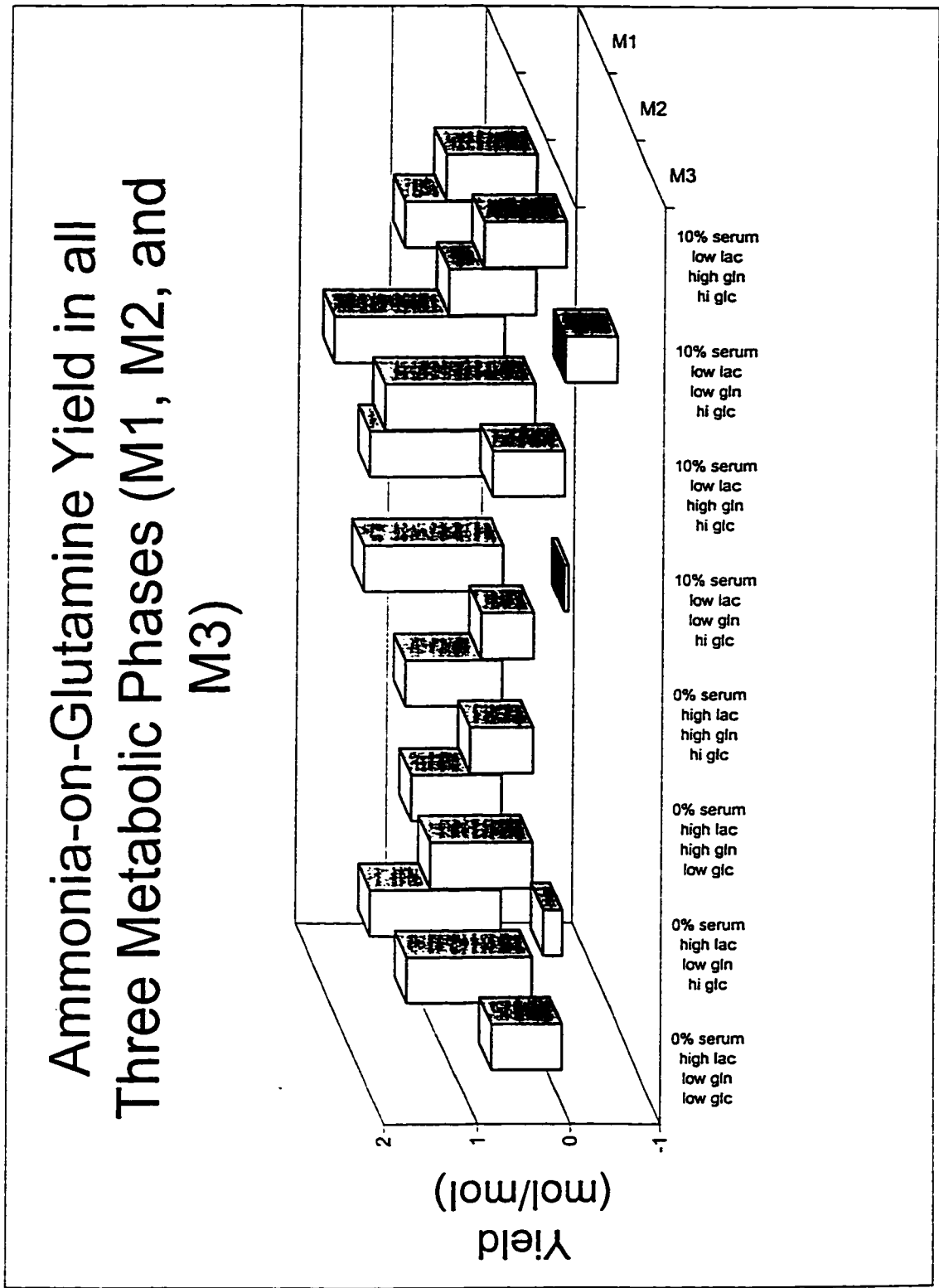
tPA Production Parameters as a Function of Initial Substrate Combinations -(2)

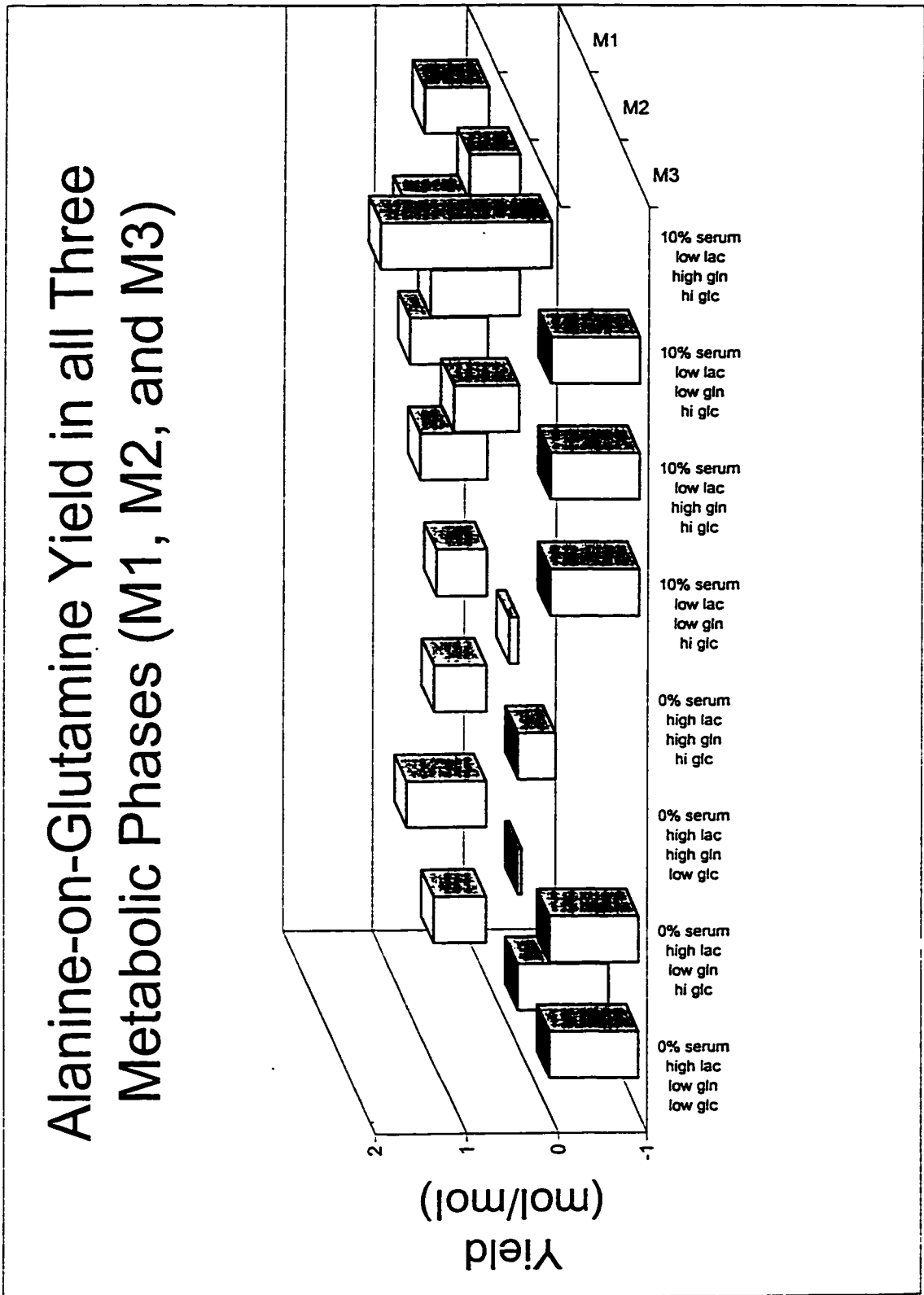


tPA Production Parameters as a Function of Initial Substrate Combinations -(3)





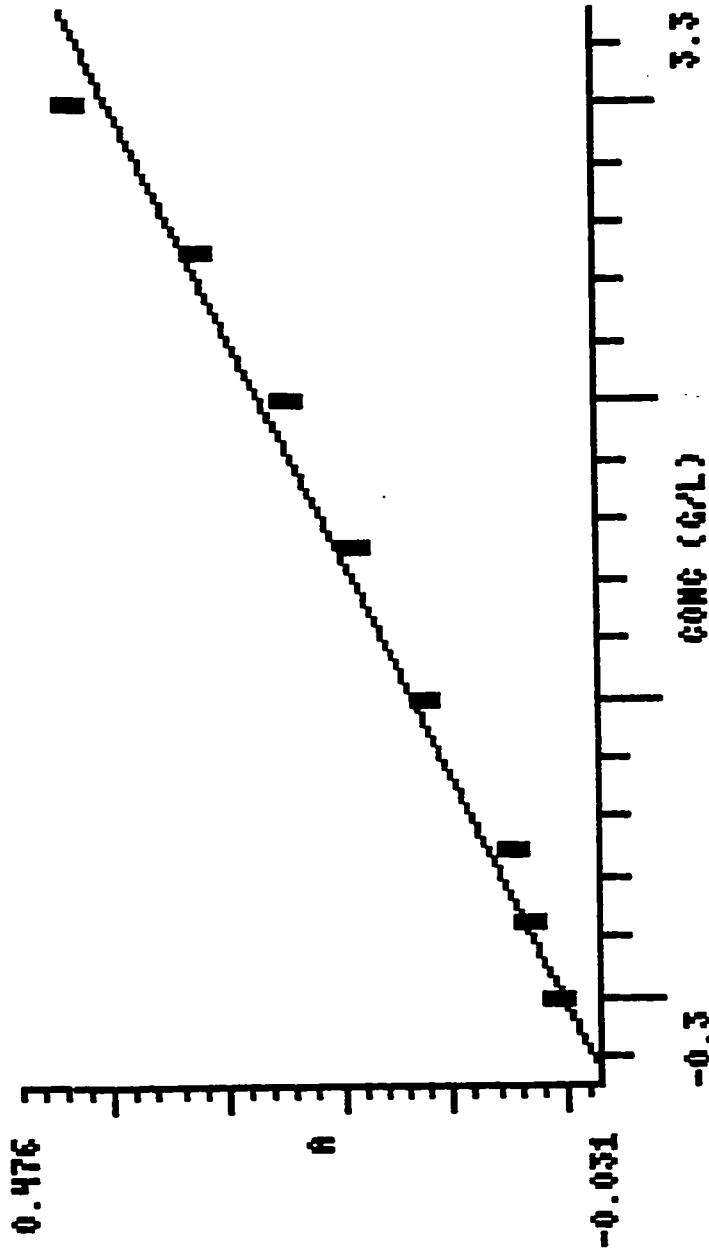




APPENDIX D:
Standard Curves

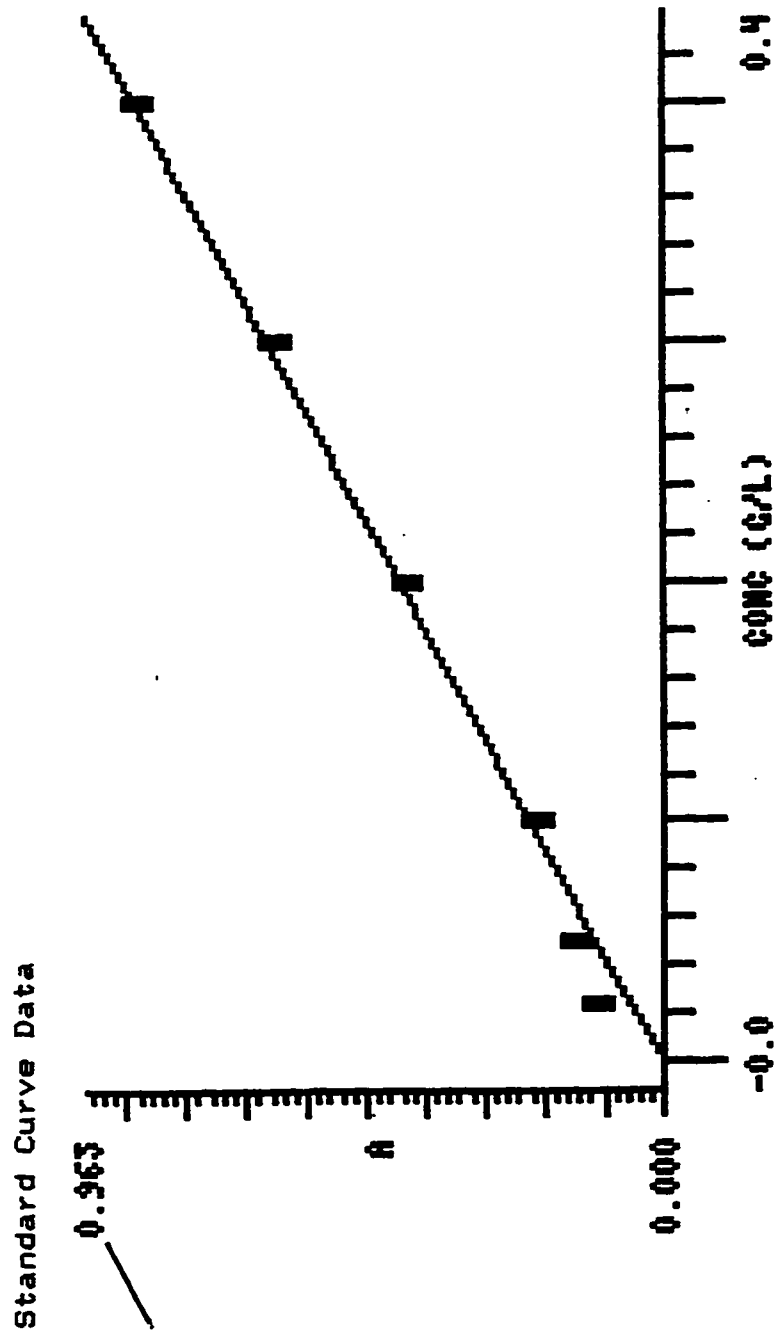
Typical Glucose Standard Curve	page 245
Typical Lactate Standard Curve	page 246
Typical Set of Amino Acid Standards HPLC Peaks	page 247
Typical Set of Amino Acids Standard Curves	page 253
Typical tPA Standard Curve	page 263
Typical ELISA Standard Curve	page 264

Glucose Assay Standard Curve



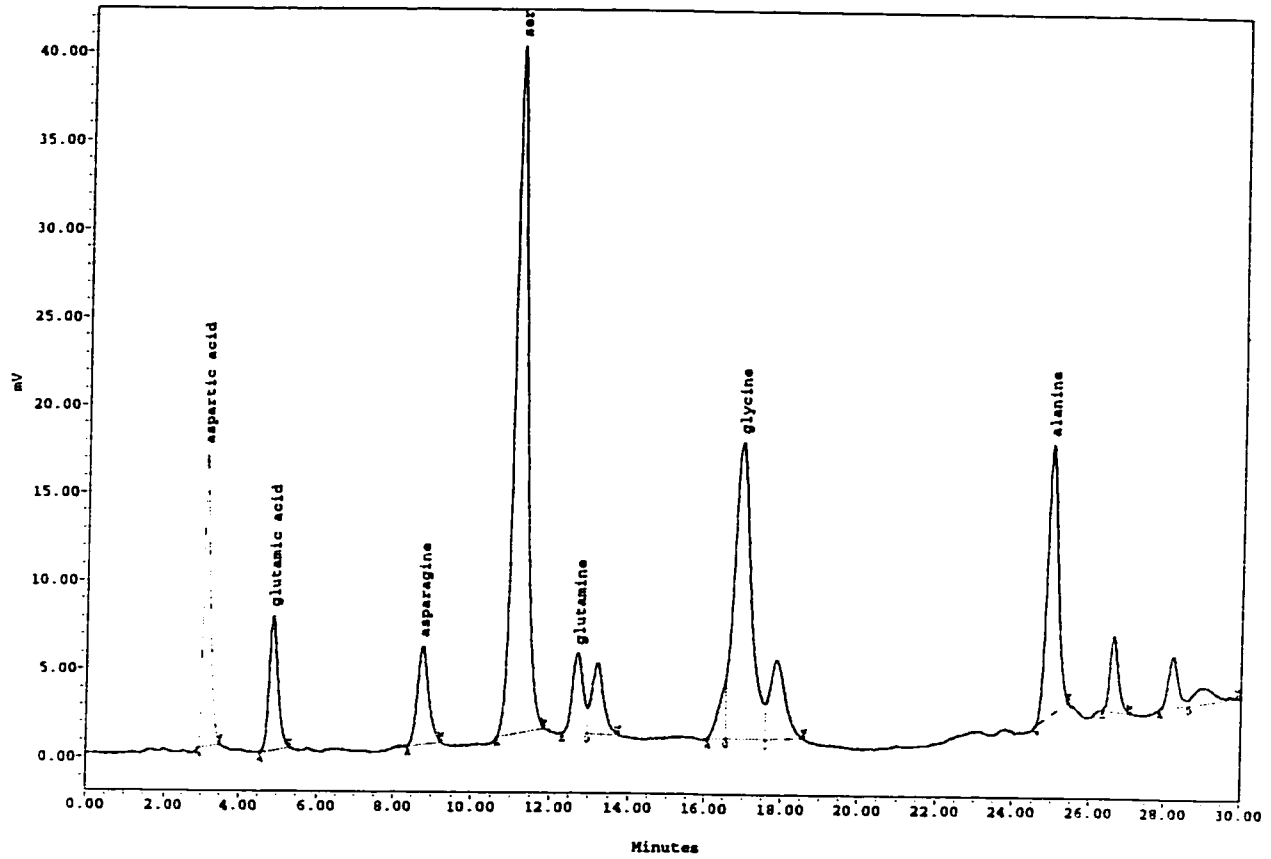
Slope 0.133
Intercept 0.000
Corr. Coeff. 0.993
Std. Deviation 0.0180

Lactate Assay Standard Curve



Slope 2.209
Intercept 0.000
Corr. Coeff. 0.998
Std. Deviation 0.0345

week of Dec 01 STD. SET



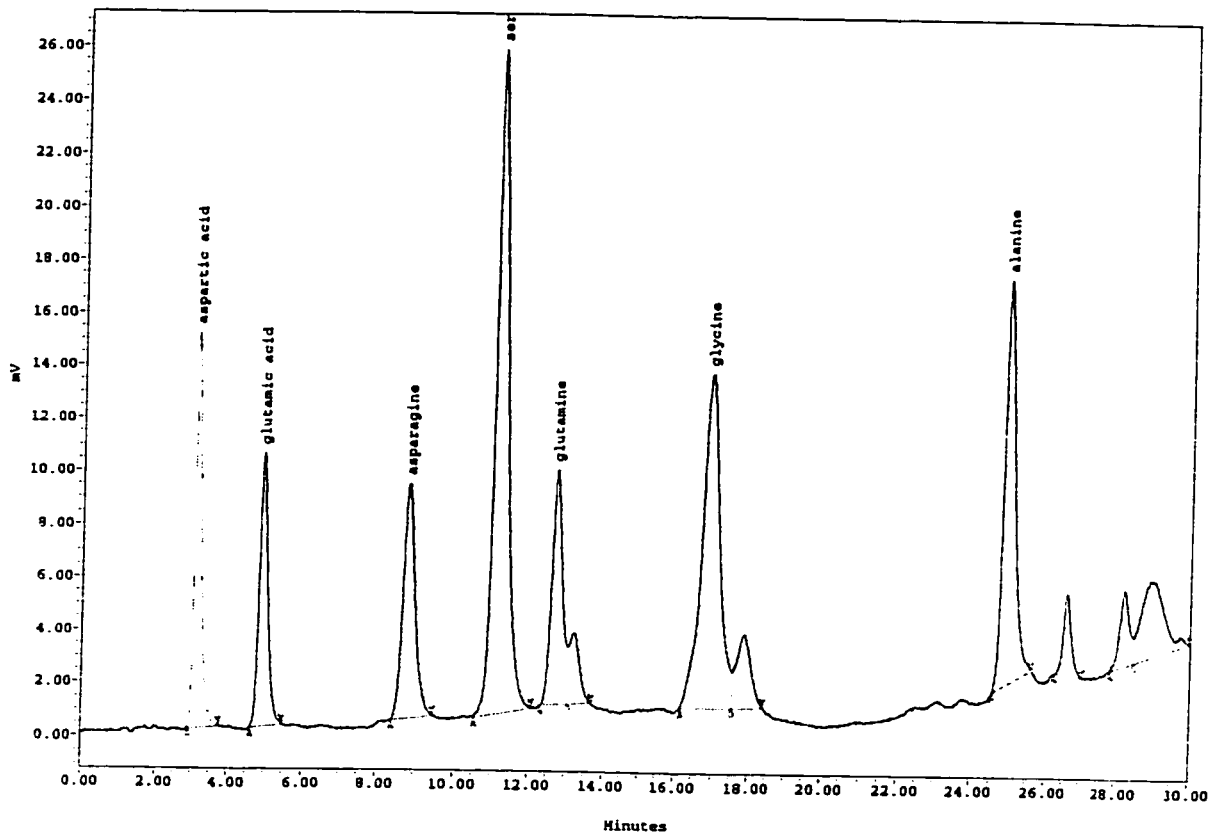
Result Table

#	Name	Retention Time (min)	Type	Amount	Units	Area (uV*sec)	Height (uV)	Response	Int Type	Start Time (min)	End Time (min)
1	aspartic acid	1.100	Found	0.022	uM	207134	16650	207133.985	HM	2.933	3.517
2	glutamic acid	4.883	Found	0.087	uM	118187	7601	118187.000	BB	4.567	5.333
3	asparagine	8.767	Found	0.094	uM	111514	5560	111514.000	BB	8.400	9.267
4	serine	11.133	Found	0.022	uM	837436	38924	837436.219	HM	10.683	11.867
5	glutamine	12.717	Found	0.094	uM	86396	4584	86395.515	BV	12.333	12.967
6		13.200	Unknown			86080	4056		VB	12.967	13.750
7		16.567	Unknown			40992	3499		BV	16.083	16.567
8	glycine	16.933	Found	0.087	uM	503664	16856	503664.434	VV	16.567	17.567
9		17.867	Unknown			133499	4509		VB	17.567	18.600
10	alanine	24.983	Found	0.175	uM	300150	15384	300149.784	HM	24.600	25.433
11		26.617	Unknown			66144	4396		BB	26.317	27.050
12		28.217	Unknown			49640	2896		BV	27.883	28.633
13		28.950	Unknown			16581	931		VB	28.633	29.950

Result Table

#	Baseline Start (min)	Baseline End (min)	Slope	Offset	% Area	% Height	% Amount
1	2.933	3.517	0.272570	-0.246539	8.04	13.25	3.77
2	4.567	5.333	0.319130	-1.225696	4.59	6.04	15.09
3	8.400	9.267	0.200769	-0.956462	4.33	4.42	16.12
4	10.683	11.867	0.405402	-3.045046	32.49	30.95	3.77
5	12.333	13.750	-0.046588	2.046588	3.35	3.65	16.12
6	12.333	13.750	-0.046588	2.046588	3.34	3.23	
7	16.083	18.600	0.013113	1.053106	1.59	2.78	
8	16.083	18.600	0.013113	1.053106	19.54	13.40	15.09
9	16.083	18.600	0.013113	1.053106	5.18	3.59	
10	24.600	25.433	1.422409	-37.713372	11.65	12.23	30.02
11	26.317	27.050	-0.308182	11.278318	2.57	3.42	
12	27.883	29.950	0.287903	-4.755702	1.93	2.30	
13	27.883	29.950	0.287903	-4.755702	1.42	0.74	

5.



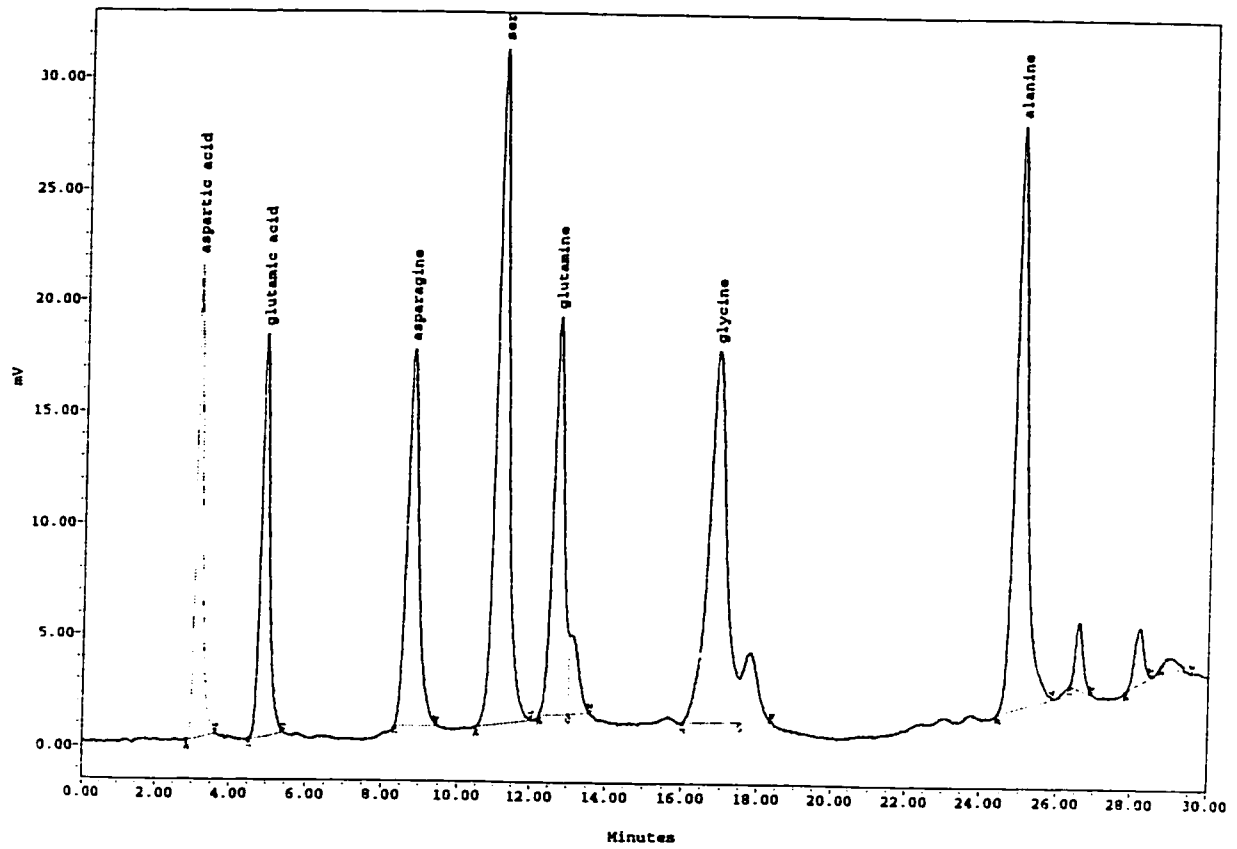
Result Table

#	Name	Retention Time (min)	Type	Amount	Units	Area (uV*sec)	Height (uV)	Response	Int Type	Start Time (min)	End Time (min)
1	aspartic acid	3.133	Found	0.044	uM	189019	14925	189019.340	SM	2.933	3.767
2	glutamic acid	4.933	Found	0.175	uM	165806	10315	165806.226	SM	4.617	5.500
3	asparagine	8.817	Found	0.188	uM	188311	8863	188311.000	SM	8.417	9.467
4	serine	11.183	Found	0.044	uM	567529	25062	567529.466	SM	10.567	12.100
5	glutamine	12.733	Found	0.188	uM	179412	8850	179412.000	SM	12.317	13.083
6		13.217	Unknown			51248	2685		VB	13.083	13.700
7	glycine	16.950	Found	0.175	uM	410692	12679	410692.498	SM	16.183	17.583
8		17.900	Unknown			79073	2790		VB	17.583	18.433
9	alanine	24.967	Found	0.250	uM	319280	15293	319279.920	SM	24.583	25.633
10		26.617	Unknown			49016	3102		VB	26.283	27.050
11		28.217	Unknown			52562	2915		VB	27.850	28.500
12		28.933	Unknown			126725	2930		VB	28.500	30.000

Result Table

#	Baseline Start (min)	Baseline End (min)	slope	OffSet	% Area	% Height	% Amount
1	2.933	3.767	0.107717	-0.021734	7.94	13.52	4.14
2	4.617	5.500	0.110509	-0.167802	6.97	9.34	16.45
3	8.417	9.467	0.183810	-0.910064	7.91	8.03	17.67
4	10.567	12.100	0.231522	-1.683415	23.85	22.70	4.14
5	12.317	13.700	0.071566	0.365542	7.54	8.02	17.67
6	12.317	13.700	0.071566	0.365542	2.15	2.43	
7	16.183	18.433	0.013333	0.999222	17.26	11.48	16.45
8	16.183	18.433	0.013333	0.999222	3.32	2.53	
9	24.583	25.633	0.803807	-17.777264	13.42	13.65	23.50
10	26.283	27.050	-0.270000	9.842501	2.09	2.81	
11	27.850	30.000	0.473488	-10.331639	2.21	2.64	
12	27.850	30.000	0.473488	-10.331639	5.33	2.65	

4/2

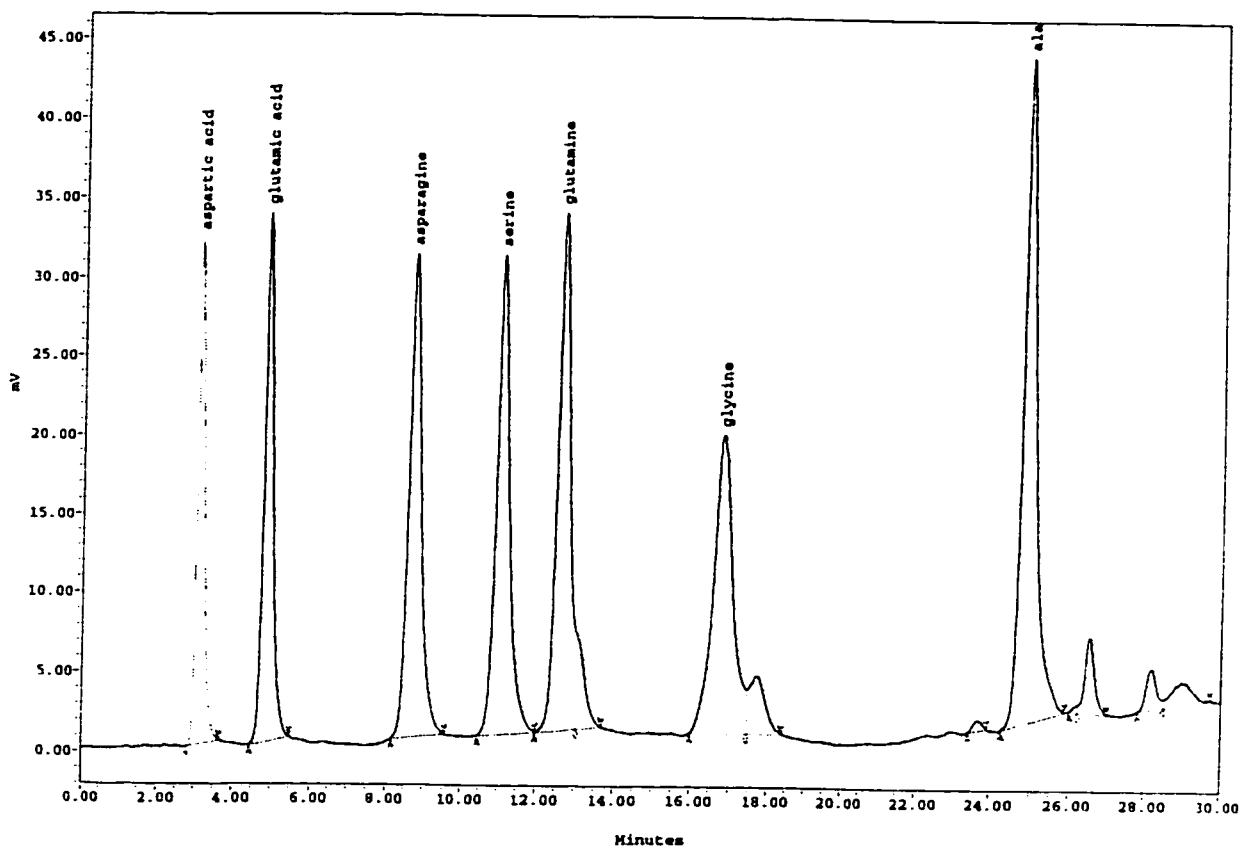


Result Table

#	Name	Retention Time (min)	Type	Amount	Units	Area (uV*sec)	Height (uV)	Response	Int Type	Start Time (min)	End Time (min)
1	aspartic acid	3.117	Found	0.087	uM	264105	21382	264105.000	BB	2.883	3.633
2	glutamic acid	4.883	Found	0.250	uM	292794	18858	292794.000	BB	4.533	5.467
3	asparagine	8.733	Found	0.175	uM	370108	16901	370307.899	HW	8.350	9.450
4	serine	11.100	Found	0.087	uM	698682	30322	698681.593	HW	10.517	12.033
5	glutamine	12.667	Found	0.375	uM	370692	17930	370691.923	HW	12.250	13.017
6		13.017	Unknown			65277	3669		VB	13.017	13.600
7	glycine	16.850	Found	0.250	uM	552627	16734	552627.207	HW	16.017	17.533
8		17.800	Unknown			90158	3187		VB	17.533	18.400
9	alanine	24.917	Found	0.500	uM	596500	26211	596499.906	HW	24.433	25.883
10		26.567	Unknown			45883	3105		BB	26.317	26.933
11		28.183	Unknown			38945	2523		BB	27.867	28.500
12		29.033	Unknown			11672	674		HW	28.783	29.583

Result Table

#	Baseline Start (min)	Baseline End (min)	Slope	Offset	% Area	% Height	% Amount
1	2.883	3.633	0.401333	-0.866178	7.77	13.32	4.57
2	4.533	5.467	0.328929	-1.159143	8.62	11.25	12.98
3	8.350	9.450	-0.016366	1.110655	10.90	10.53	19.47
4	10.517	12.033	0.191778	-1.040727	20.56	18.89	4.57
5	12.250	13.600	0.091110	0.368900	10.91	11.17	19.47
6	12.250	13.600	0.091110	0.368900	1.92	2.29	
7	16.017	18.400	0.034606	0.667933	16.27	10.43	12.98
8	16.017	18.400	0.034606	0.667933	2.65	1.99	
9	24.433	25.883	0.494287	-10.240791	17.56	16.33	25.96
10	26.317	26.933	-0.575676	18.258865	1.35	1.93	
11	27.867	28.500	1.051579	-26.351002	1.15	1.57	
12	28.783	29.583	-0.493922	18.361855	0.34	0.30	

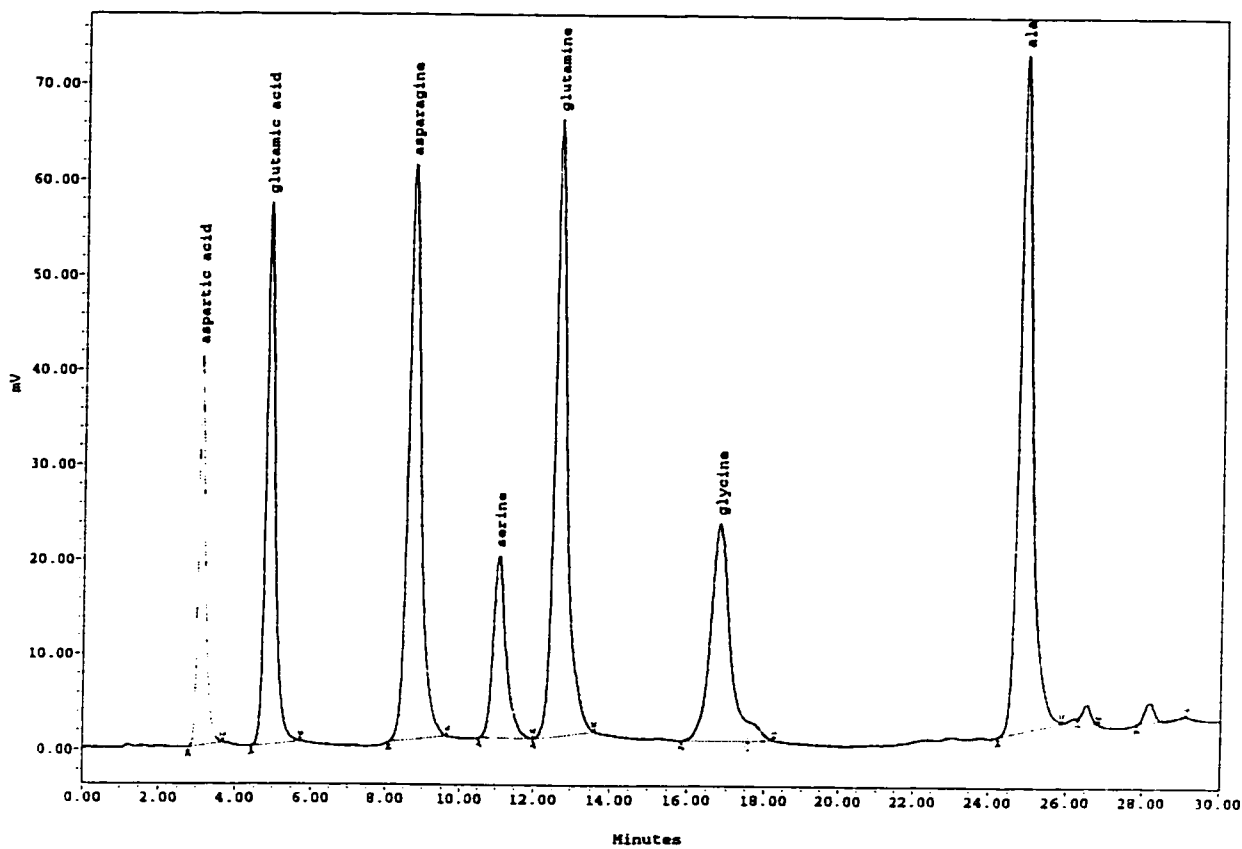


Result Table

#	Name	Retention Time (min)	Type	Amount	Units	Area (uV*sec)	Height (uV)	Response	Int Type	Start Time (min)	End Time (min)
1	aspartic acid	3.100	Found	0.175	uM	401064	32017	401064.000	BB	2.817	3.667
2	glutamic acid	4.850	Found	0.500	uM	549120	33421	549120.000	BB	4.467	5.500
3	asparagine	8.700	Found	0.750	uM	704410	30518	704410.000	BB	8.150	9.567
4	serine	11.067	Found	0.175	uM	718190	30322	718190.046	BB	10.467	12.000
5	glutamine	12.633	Found	0.750	uM	730691	32690	730690.716	BV	12.000	13.050
6		13.067	Unknown			87804	6059		VB	13.050	13.700
7	glycine	16.817	Found	0.500	uM	659868	18957	659868.005	BV	16.000	17.483
8		17.733	Unknown			111831	3714		VM	17.483	18.400
9		23.700	Unknown			11746	694		BB	23.417	23.933
10	alanine	24.883	Found	1.000	uM	998559	42105	998559.000	BB	24.283	25.900
11		26.217	Unknown			2832	408		BV	26.050	26.233
12		26.533	Unknown			83669	4852		VB	26.233	26.983
13		28.167	Unknown			46799	2601		BV	27.833	28.467
14		28.967	Unknown			57108	1477		VM	28.467	29.733

Result Table

#	Baseline Start (min)	Baseline End (min)	Slope	Offset	% Area	% Height	% Amount
1	3.817	3.667	0.502353	-1.153961	7.77	13.35	4.55
2	4.467	5.500	0.468387	-1.709129	10.43	13.93	12.99
3	8.150	9.567	0.196941	-0.778071	13.64	12.72	19.48
4	10.467	12.000	0.142175	-0.413095	13.91	12.64	4.55
5	12.000	13.700	0.215294	-1.290529	14.15	13.43	19.40
6	12.000	13.700	0.215294	-1.290529	1.70	2.53	
7	16.000	18.400	-0.007916	1.426651	12.78	7.90	12.99
8	16.000	18.400	-0.007916	1.426651	2.17	1.95	
9	23.417	23.933	0.431613	-0.552936	0.23	0.29	
10	24.283	25.900	0.683505	-14.844784	19.34	17.56	25.97
11	26.050	26.983	-0.202500	8.221126	0.05	0.17	
12	26.050	26.983	-0.202500	8.221126	1.62	2.02	
13	27.833	29.733	0.382364	-7.639971	0.91	1.00	
14	27.833	29.733	0.382364	-7.639971	1.11	0.62	

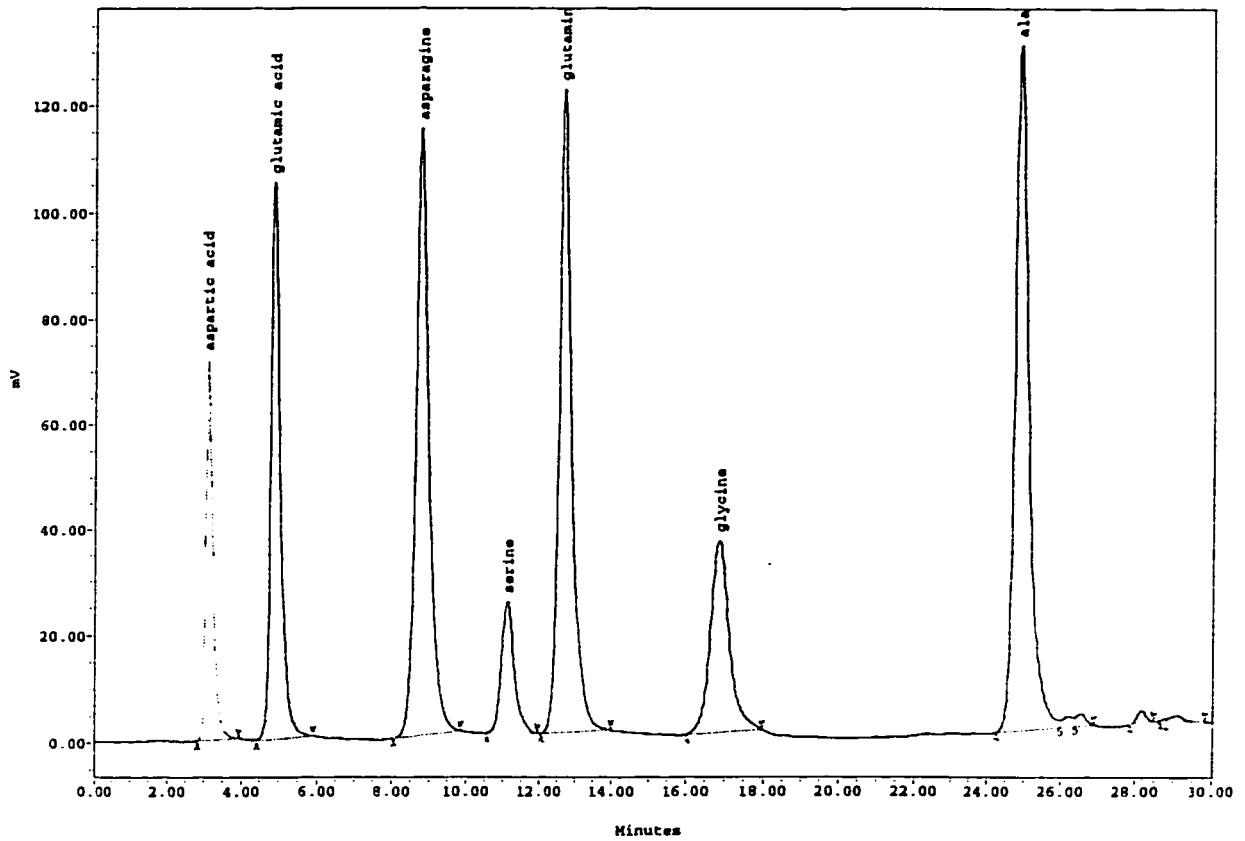


Result Table

#	Name	Retention Time (min)	Type	Amount	Units	Area (uV*sec)	Height (uV)	Response	Int Type	Start Time (min)	End Time (min)
1	aspartic acid	3.100	Found	0.250	uM	525010	41356	525010.000	BB	2.800	3.700
2	glutamic acid	4.850	Found	1.000	uM	965332	57063	965332.385	BB	4.417	5.750
3	asparagine	8.700	Found	1.500	uM	1441166	60612	1441166.000	BB	8.100	9.667
4	serine	11.067	Found	0.250	uM	459613	19238	459613.000	BB	10.550	12.000
5	glutamine	12.650	Found	1.500	uM	1535968	64854	1535968.000	BB	12.000	13.600
6	glycine	16.817	Found	1.000	uM	761157	22859	761156.946	NV	15.867	17.567
7		17.583	Unknown			42588	1979		NV	17.567	18.267
8	alanine	24.883	Found	2.000	uM	1712917	71263	1712917.000	BB	24.250	25.900
9		26.550	Unknown			26802	1853		BB	26.300	26.850
10		28.167	Unknown			38801	2184		BB	27.867	29.150

Result Table

#	Baseline Start (min)	Baseline End (min)	Slope	Offset	% Area	% Height	% Amount
1	2.800	3.700	0.541111	-1.263111	6.99	12.05	3.33
2	4.417	5.750	0.368582	-1.244349	12.86	16.62	13.33
3	8.100	9.667	0.425106	-2.600362	19.19	17.66	20.00
4	10.550	12.000	-0.033103	1.714242	6.12	5.60	3.33
5	12.000	13.600	0.440625	-3.970500	20.45	18.89	20.00
6	15.867	18.267	0.030000	0.682998	10.14	6.66	13.33
7	17.567	18.267	0.030000	0.682998	0.57	0.58	
8	24.250	25.900	0.913333	-20.414335	22.81	20.76	26.67
9	26.300	26.850	-1.290909	37.664909	0.36	0.54	
10	27.867	29.150	0.671254	-15.569051	0.52	0.64	

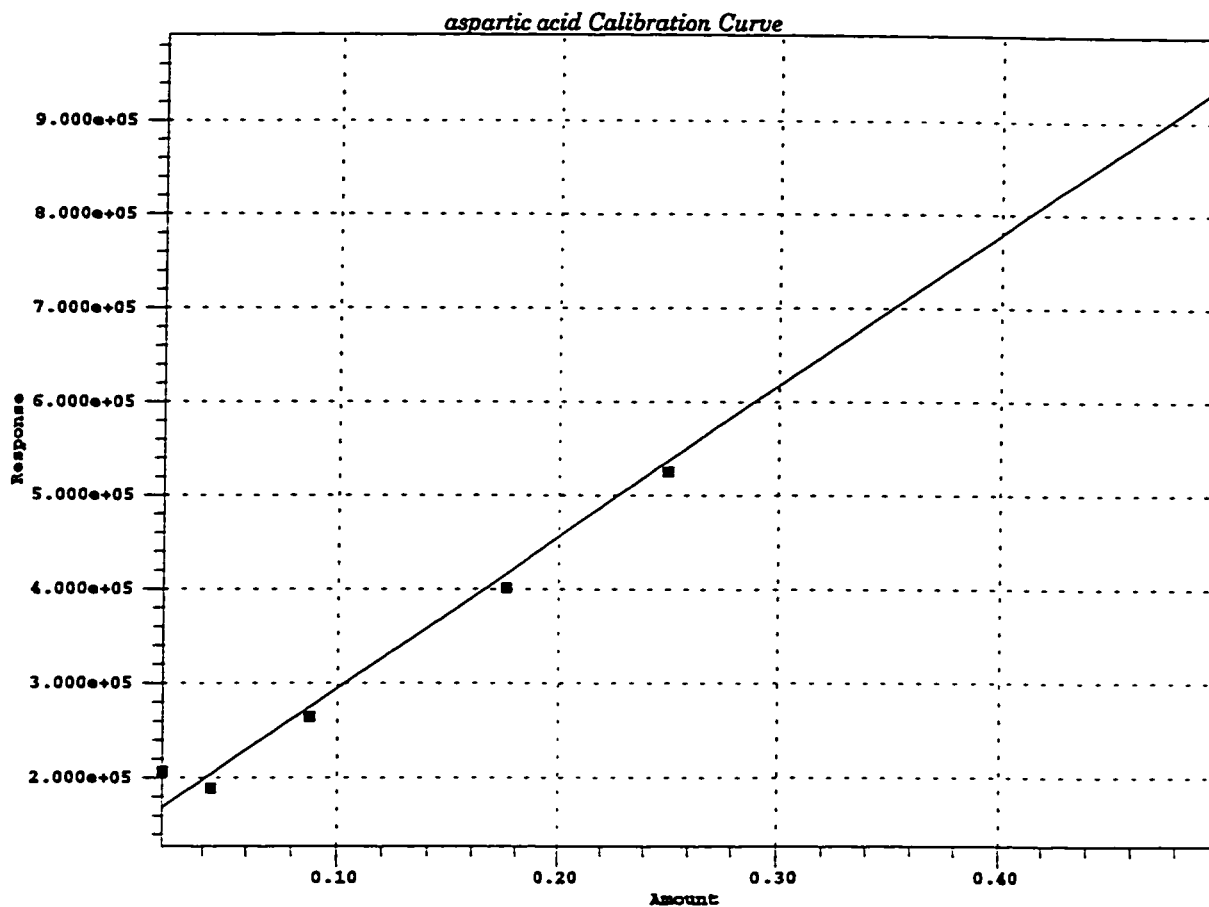


Result Table

#	Name	Retention Time (min)	Type	Amount	Units	Area (uV*sec)	Height (uV)	Response	Int Type	Start Time (min)	End Time (min)
1	aspartic acid	3.117	Found	0.500	uM	952391	72027	952390.995	BM	2.850	3.933
2	glutamic acid	4.900	Found	2.000	uM	1814901	105046	1814901.163	BM	4.417	5.917
3	asparagine	8.783	Found	3.000	uM	2795904	114476	2795903.682	BM	8.083	9.867
4	serine	11.133	Found	0.500	uM	595198	24548	595198.000	BB	10.567	11.983
5	glutamine	12.700	Found	3.000	uM	2939488	121228	2939488.392	BM	12.067	14.000
6	glycine	16.867	Found	2.000	uM	1195896	36181	1195895.877	BM	16.033	17.950
7	alanine	24.900	Found	4.000	uM	3262613	129359	3262613.000	BV	24.267	26.000
8		26.233	Unknown			42063	1956		VV	26.000	26.400
9		26.550	Unknown			40025	2268		VB	26.400	26.900
10		28.183	Unknown			36723	2298		BB	27.867	28.500
11		28.833	Unknown			2144	438		BV	28.667	28.833
12		29.100	Unknown			22845	1043		VW	28.833	29.833

Result Table

#	Baseline Start (min)	Baseline End (min)	Slope	Offset	% Area	% Height	% Amount
1	2.850	3.933	0.509539	-1.137185	6.94	11.79	3.33
2	4.417	5.917	0.459943	-1.527326	13.37	17.20	13.33
3	8.083	9.867	0.738669	-5.149204	20.38	18.74	20.00
4	10.567	11.983	-0.123529	3.153294	4.34	4.02	3.33
5	12.067	14.000	0.338830	-2.398624	21.42	19.85	20.00
6	16.033	17.950	0.484589	-6.222376	8.72	5.92	13.33
7	24.267	26.900	0.554430	-11.535178	23.78	21.18	26.67
8	24.267	26.900	0.554430	-11.535178	0.31	0.32	
9	24.267	26.900	0.554430	-11.535178	0.29	0.37	
10	27.867	28.500	0.702632	-16.058001	0.27	0.38	
11	28.667	29.833	-0.219595	10.498261	0.02	0.07	
12	28.667	29.833	-0.219595	10.498261	0.17	C.../	



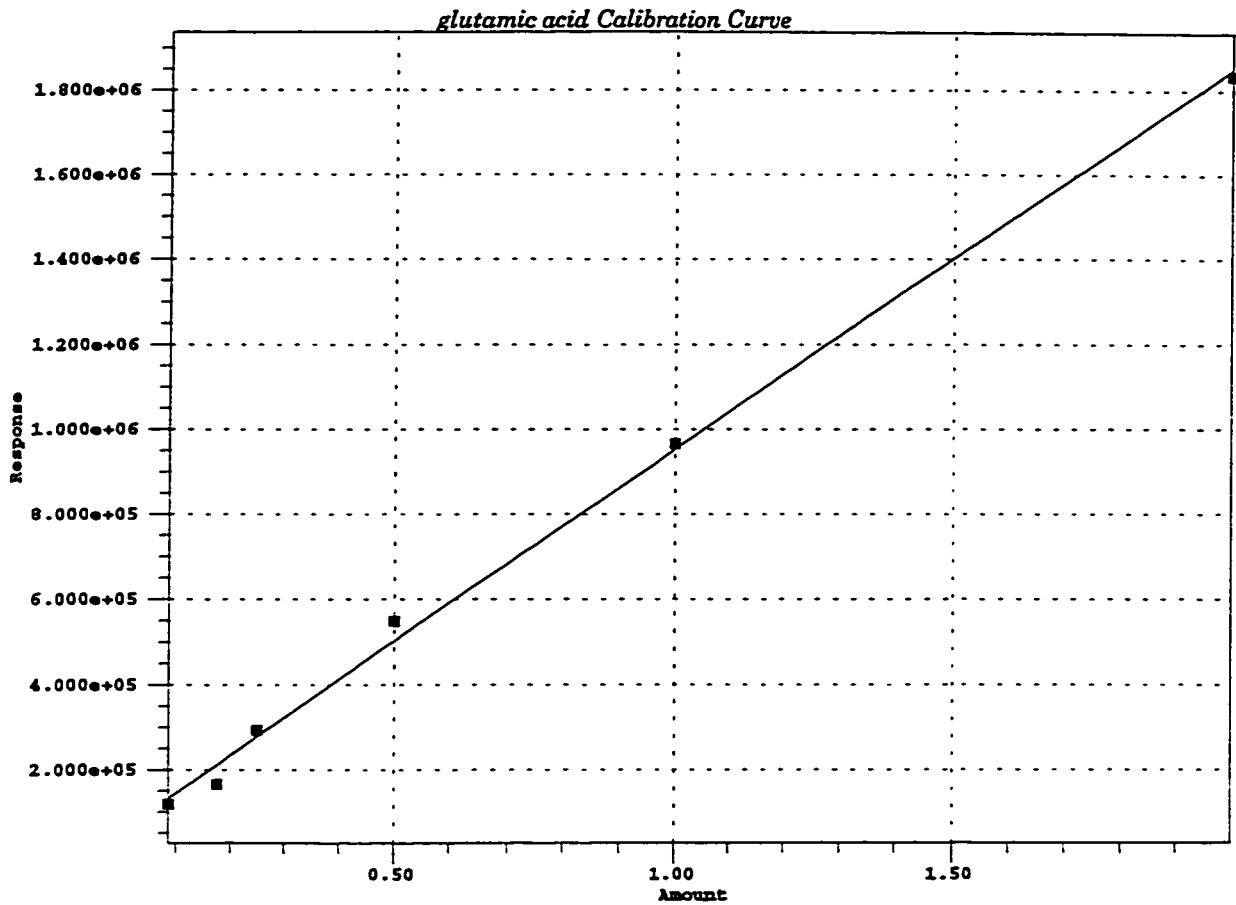
aspartic acid Calibration Information

Processing Method	roshni_29nov96	System	FLUORESCENCE_OPA
Channel	SATIN	Date	02-DEC-96
Type	LC	Name	aspartic acid
Retention Time	3.119 min	Order	1
A	133084.950560	B	1614111.180237
C	0.000000	D	0.000000
E	0.000000	F	0.000000
R	0.997225	R ²	0.994457
Standard Error	24059.372197		

aspartic acid Point Table

#	Amount	Response	Calc. Amount	% Deviation	Manual	Ignore?
1	0.021875	207133.985197	0.045876	109.719	No	No
2	0.043750	189019.339700	0.034653	-20.792	No	No
3	0.087500	264105.000000	0.081172	-7.232	No	No
4	0.175000	401064.000000	0.166023	-5.130	No	No
5	0.250000	525010.000000	0.242812	-2.875	No	No
6	0.500000	952390.994656	0.507590	1.518	No	No

Table 'aspartic acid Average Table' contains no data.



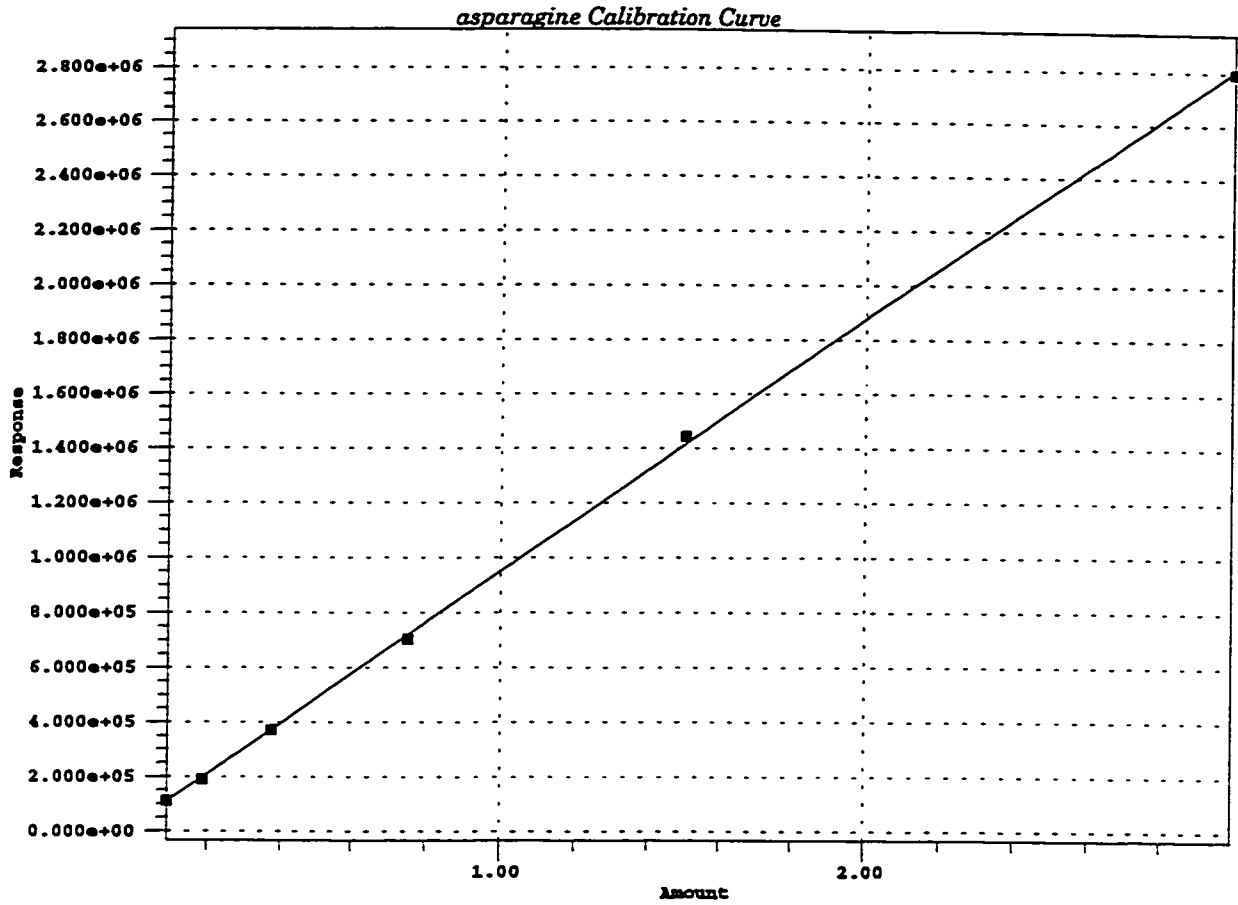
glutamic acid Calibration Information

Processing Method	roshni_29nov96	System	FLUORESCENCE_OPA
Channel	SATIN	Date	02-DEC-96
Type	LC	Name	glutamic acid
Retention Time	4.875 min	Order	1
A	53492.989480	B	898487.410999
C	0.000000	D	0.000000
E	0.000000	F	0.000000
R	0.998841	R ²	0.997684
Standard Error	35353.645397		

glutamic acid Point Table

#	Amount	Response	Calc. Amount	% Deviation	Manual	Ignore?
1	0.087500	118187.000000	0.072003	-17.711	No	No
2	0.175000	165804.225655	0.125000	-28.571	No	No
3	0.250000	292794.000000	0.266338	6.535	No	No
4	0.500000	549120.000000	0.551624	10.325	No	No
5	1.000000	965332.285287	1.014860	1.486	No	No
6	2.000000	1834901.162573	1.982675	-0.866	No	No

Table 'glutamic acid Average Table' contains no data.



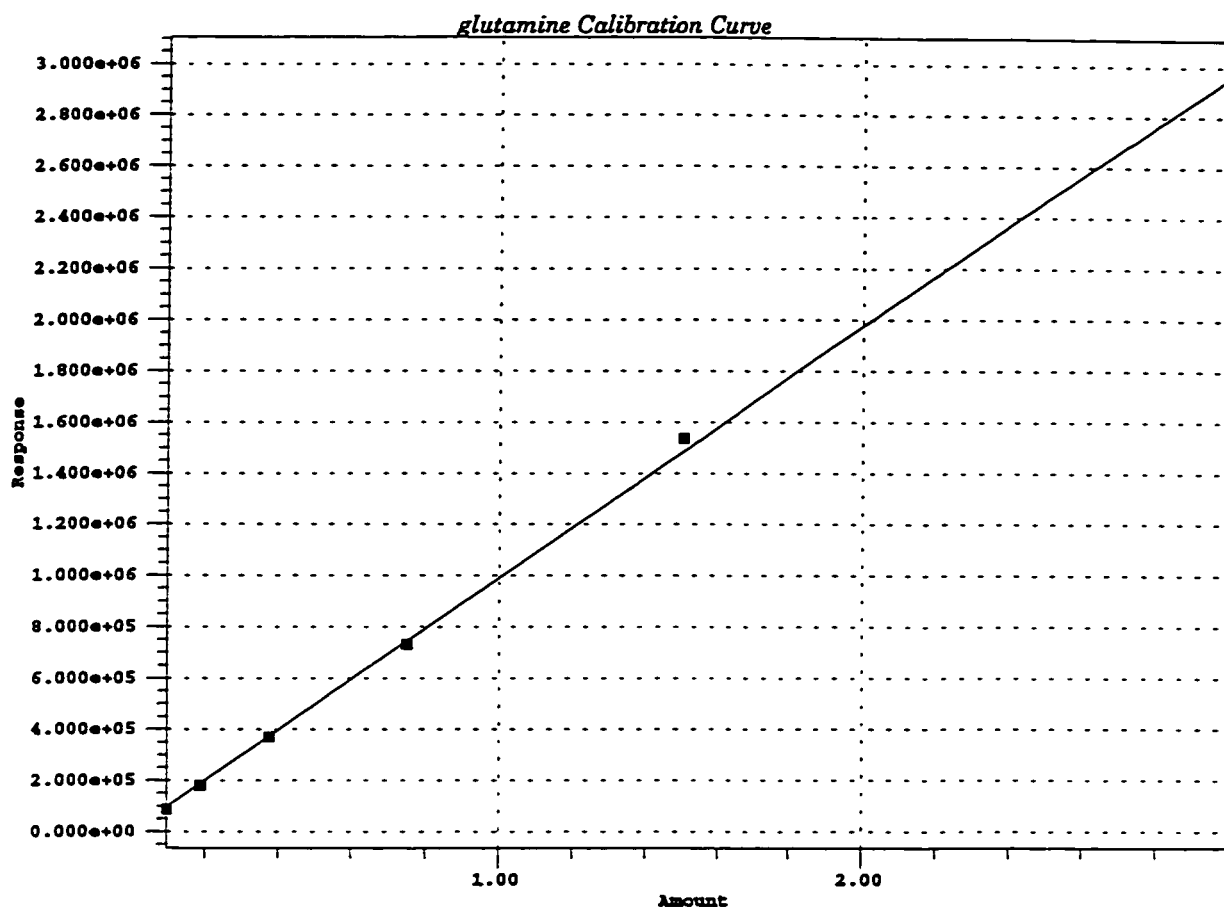
asparagine Calibration Information

Processing Method	roshni_29nov96	System	FLUORESCENCE_OPA
Channel	SATIN	Date	02-DEC-96
Type	LC	Name	asparagine
Retention Time	8.739 min	Order	1
A	21682.355633	B	928087.779345
C	0.000000	D	0.000000
E	0.000000	F	0.000000
R	0.999898	R ²	0.999795
Standard Error	16505.927327		

asparagine Point Table

#	Amount	Response	Calc. Amount	% Deviation	Manual	Ignore?
1	0.093750	111514.000000	0.096792	3.245	No	No
2	0.187500	188311.000000	0.179540	-4.245	No	No
3	0.375000	370307.898563	0.375639	0.170	No	No
4	0.750000	704410.000000	0.735628	-1.916	No	No
5	1.500000	1441166.000000	1.529471	1.965	No	No
6	3.000000	2795903.681988	2.989180	-0.361	No	No

Table 'asparagine Average Table' contains no data.



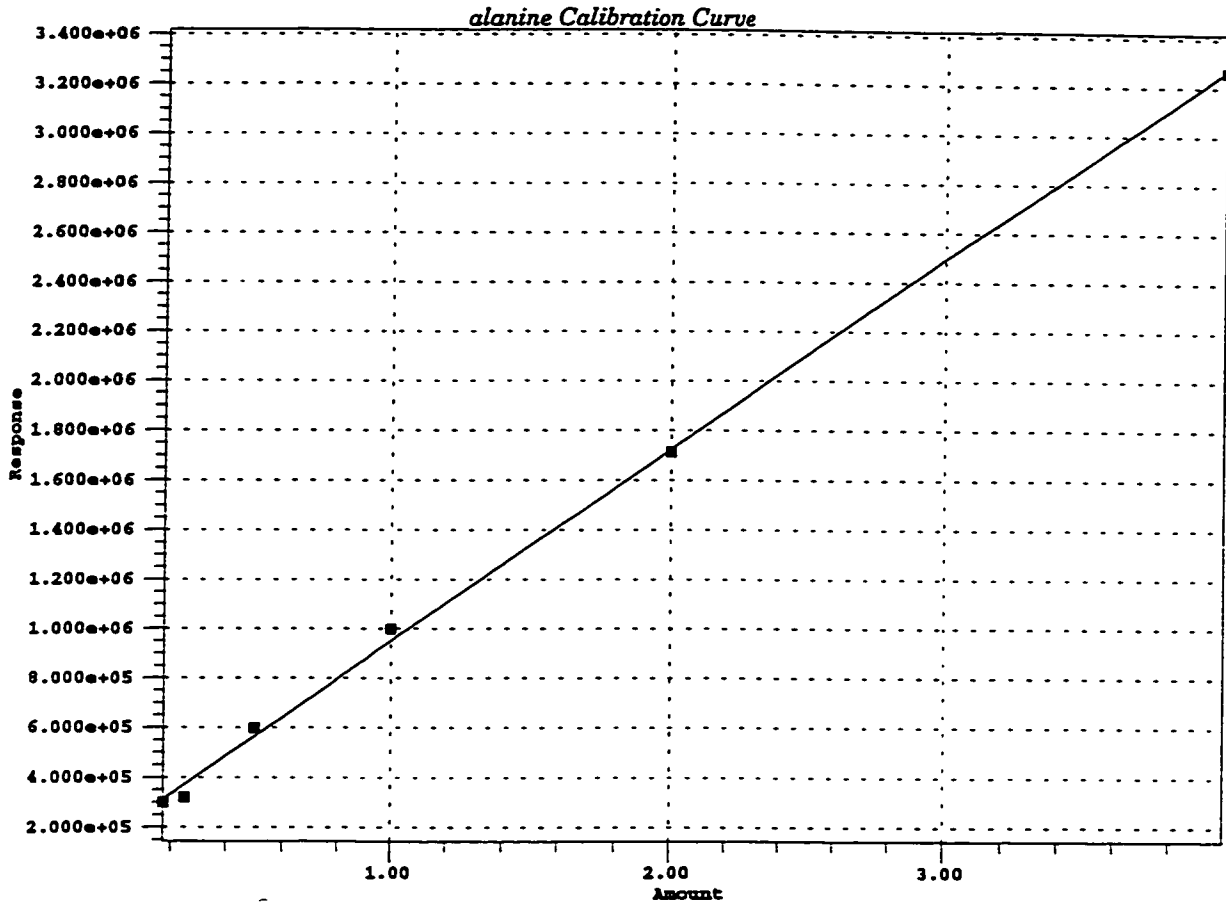
glutamine Calibration Information

Processing Method	roshni_29nov96	System	FLUORESCENCE_OPA
Channel	SATIN	Date	02-DEC-96
Type	LC	Name	glutamine
Retention Time	12.665 min	Order	1
A	2657.444395	B	986531.484373
C	0.000000	D	0.000000
E	0.000000	F	0.000000
R	0.999695	R ²	0.999390
Standard Error	30292.076526		

glutamine Point Table

#	Amount	Response	Calc. Amount	% Deviation	Manual	Ignore?
1	0.093750	86395.514856	0.084881	-9.460	No	No
2	0.187500	179412.000000	0.179168	-4.444	No	No
3	0.375000	370691.922613	0.373059	-0.518	No	No
4	0.750000	730690.716205	0.737973	-1.604	No	No
5	1.500000	1535968.000000	1.554244	3.616	No	No
6	3.000000	2939488.092276	2.976925	-0.769	No	No

Table 'glutamine Average Table' contains no data.



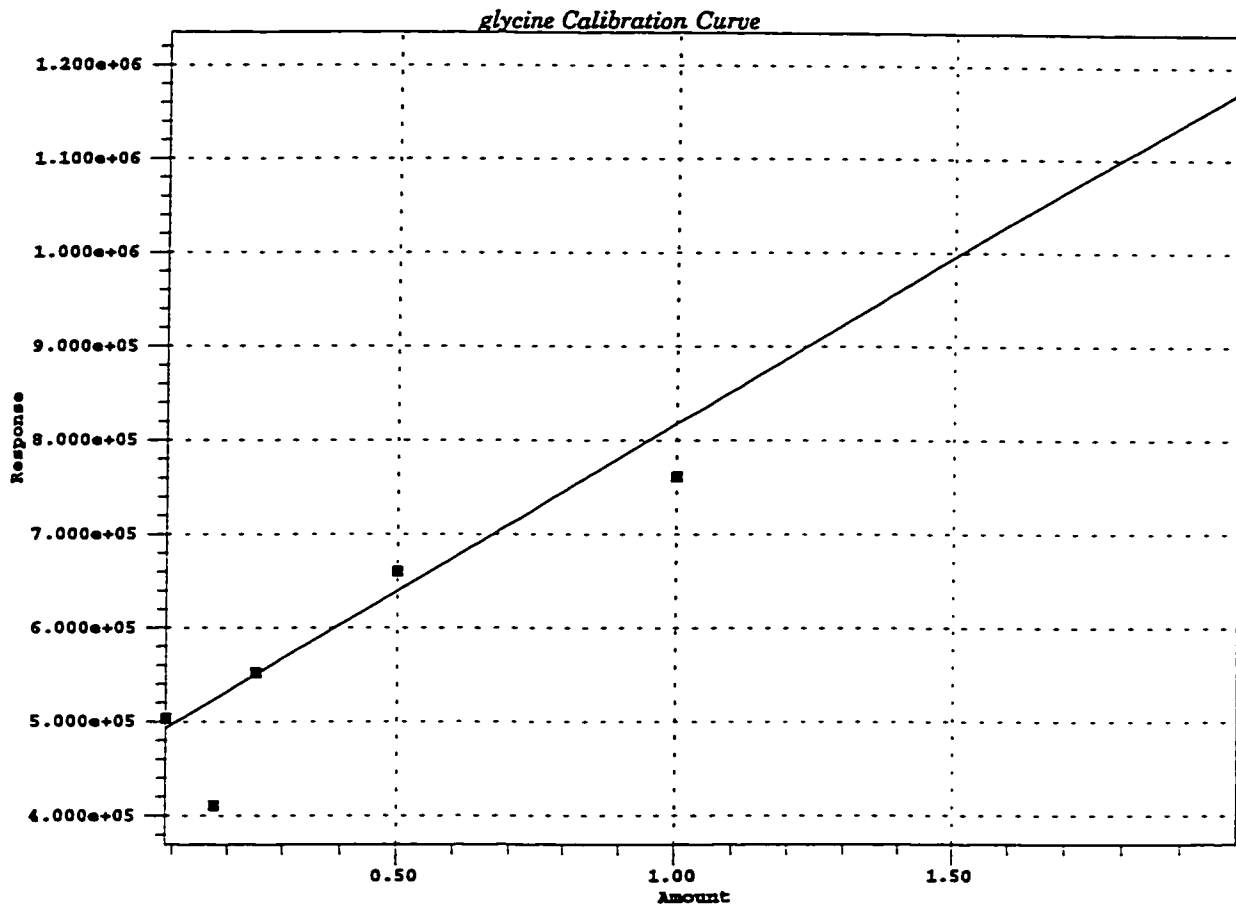
alanine Calibration Information

Processing Method	roshni_29nov96	System	FLUORESCENCE_OPA
Channel	SATIN	Date	02-DEC-96
Type	LC	Name	alanine
Retention Time	25.000 min	Order	1
A	177107.914061	B	773169.858021
C	0.000000	D	0.000000
E	0.000000	F	0.000000
R	0.999513	R^2	0.999027
Standard Error	39791.408255		

alanine Point Table

#	Amount	Response	Calc. Amount	% Deviation	Manual	Ignore?
1	0.175000	300149.784014	0.159140	-9.063	No	No
2	0.250000	319279.919543	0.183882	-26.447	No	No
3	0.500000	596499.905621	0.542432	8.486	No	No
4	1.000000	998559.000000	1.062446	6.245	No	No
5	2.000000	1712917.000000	1.986380	-0.681	No	No
6	4.000000	3262613.000000	3.990721	-0.232	No	No

Table 'alanine Average Table' contains no data.



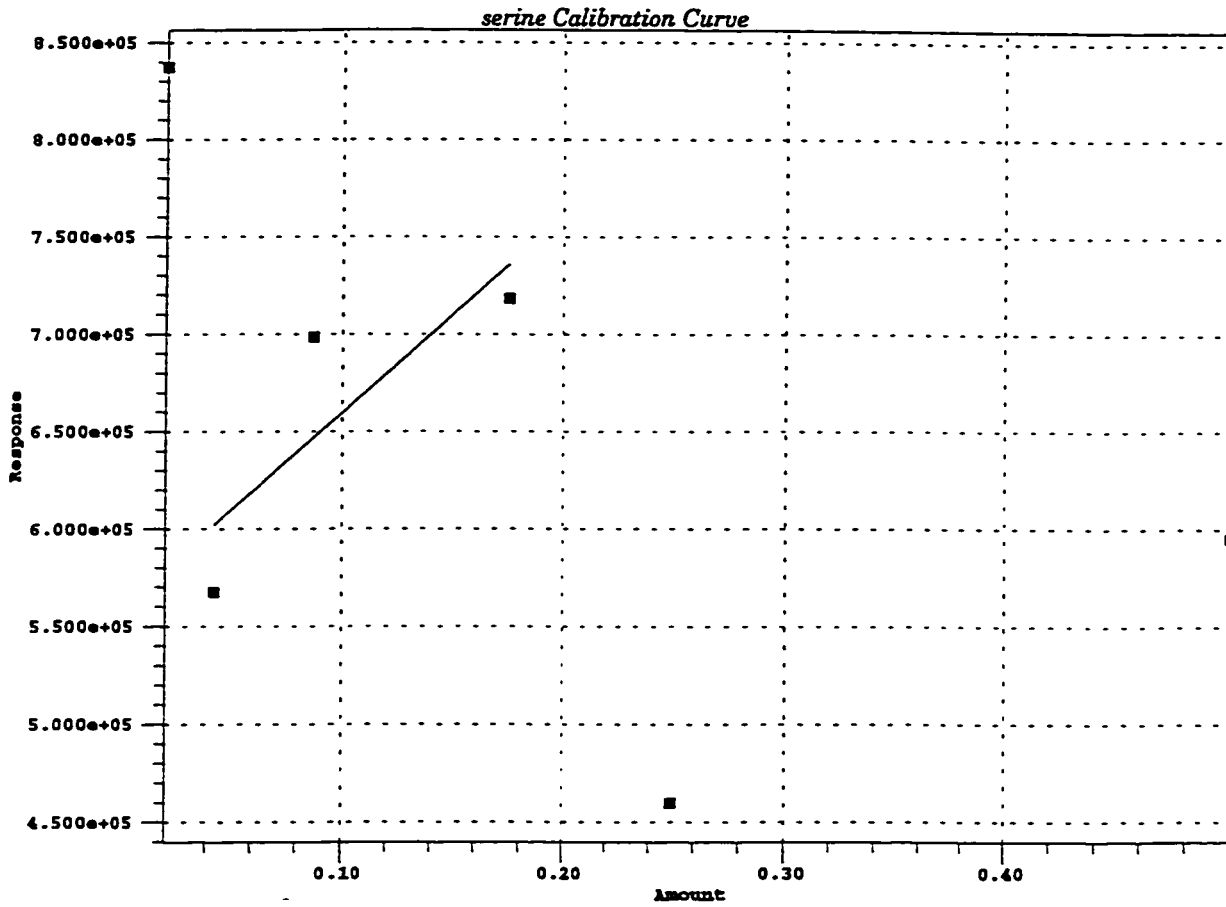
glycine Calibration Information

Processing Method	roshni_29nov96	System	FLUORESCENCE_OPA
Channel	SATIN	Date	02-DEC-96
Type	LC	Name	glycine
Retention Time	16.856 min	Order	1
A	461262.522289	B	356195.413112
C	0.000000	D	0.000000
E	0.000000	F	0.000000
R	0.993075	R ²	0.986199
Standard Error	37490.798845		

glycine Point Table

#	Amount	Response	Calc. Amount	% Deviation	Manual	Ignore?
1	0.087500	503664.434177	0.119041	36.047	No	No
2	0.175000	410692.497573			No	Yes
3	0.250000	552627.207109	0.256502	2.601	No	No
4	0.500000	659868.004895	0.557575	11.515	No	No
5	1.000000	761156.985805	0.841938	-15.806	No	No
6	2.000000	1195895.877277	2.062445	3.122	No	No

Table 'glycine Average Table' contains no data.



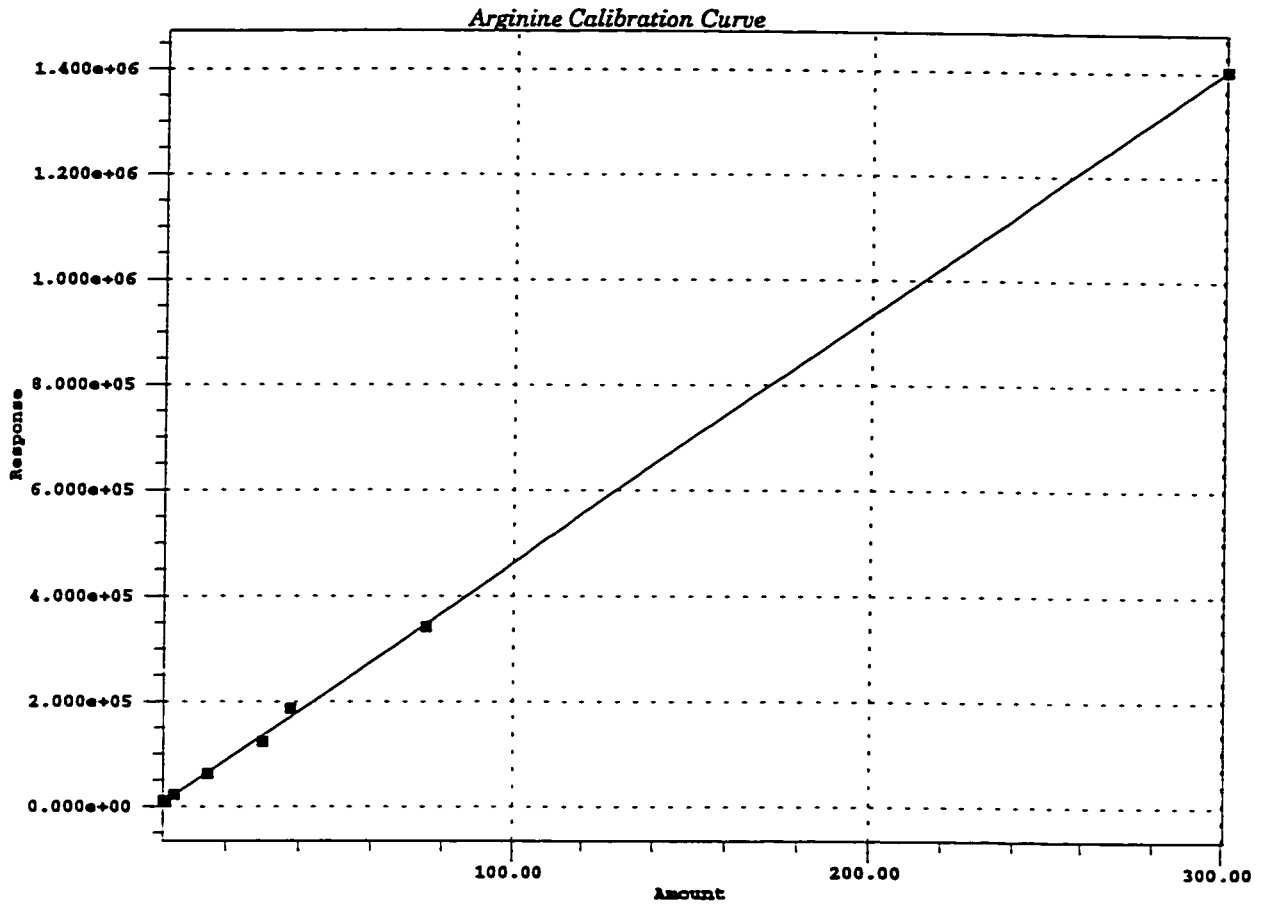
serine Calibration Information

Processing Method	roshni_29nov96	System	FLUORESCENCE_OPA
Channel	SATIN	Date	02-DEC-96
Type	LC	Name	serine
Retention Time	11.109 min	Order	1
A	557775.239390	B	1015756.366449
C	0.000000	D	0.000000
E	0.000000	F	0.000000
R	0.828489	R ²	0.686393
Standard Error	64889.906604		

serine Point Table

#	Amount	Response	Calc. Amount	% Deviation	Manual	Ignore?
1	0.021875	837436.218688			No	Yes
2	0.043750	567529.466369	0.009603	-78.050	No	No
3	0.087500	698681.592534	0.138721	58.538	No	No
4	0.175000	718190.046492	0.157926	-9.756	No	No
5	0.250000	459613.000000			No	Yes
6	0.500000	595158.000000			No	Yes

Table 'serine Average Table' contains no data.



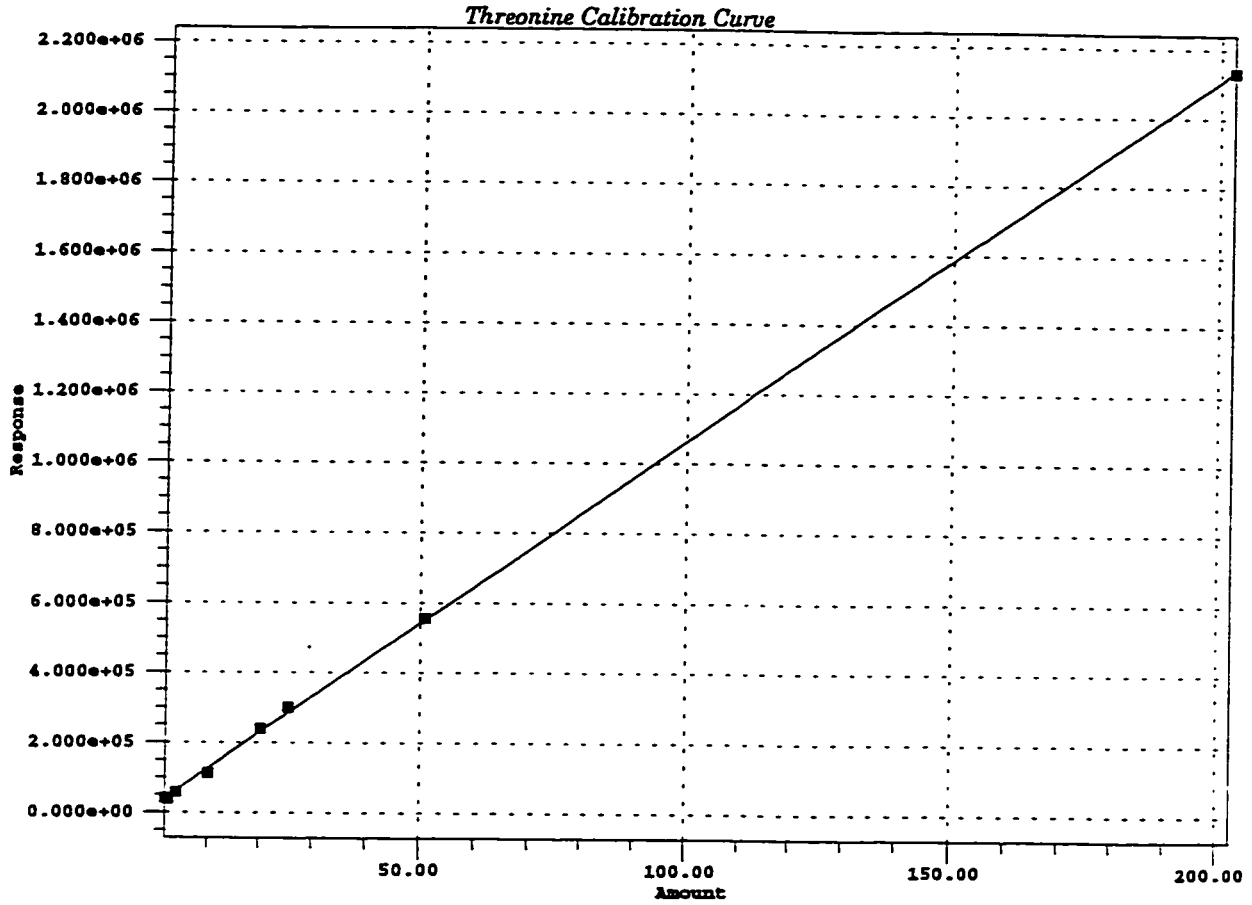
Arginine Calibration Information

Processing Method	OPA_Mar22	System	FLUORESCENCE_OPA
Channel	SATIN	Date	02-APR-96
Type	LC	Name	Arginine
Retention Time	19.314 min	Order	1
A	-6269.776804	B	4691.096519
C	0.000000	D	0.000000
E	0.000000	F	0.000000
R	0.999856	R ²	0.999713
Standard Error	8644.863356		

Arginine Point Table

#	Amount	Response	Calc. Amount	% Deviation	Manual	Ignore?
1	0.0173	11206.802090	3.725478	23.770	Yes	No
2	0.0216	9433.881312	3.347545	-10.970	Yes	No
3	0.0345	22165.294833	6.061498	0.857	Yes	No
4	0.0863	61885.101112	14.528560	-3.336	Yes	No
5	0.1726	122966.838846	27.549341	-8.352	Yes	No
6	0.2157	186474.079625	41.087165	9.333	Yes	No
7	0.4314	341986.367713	74.237685	-1.214	Yes	No
8	0.7256	1404168.100000	300.662728	0.021	Yes	No

Table 'Arginine Average Table' contains no data.



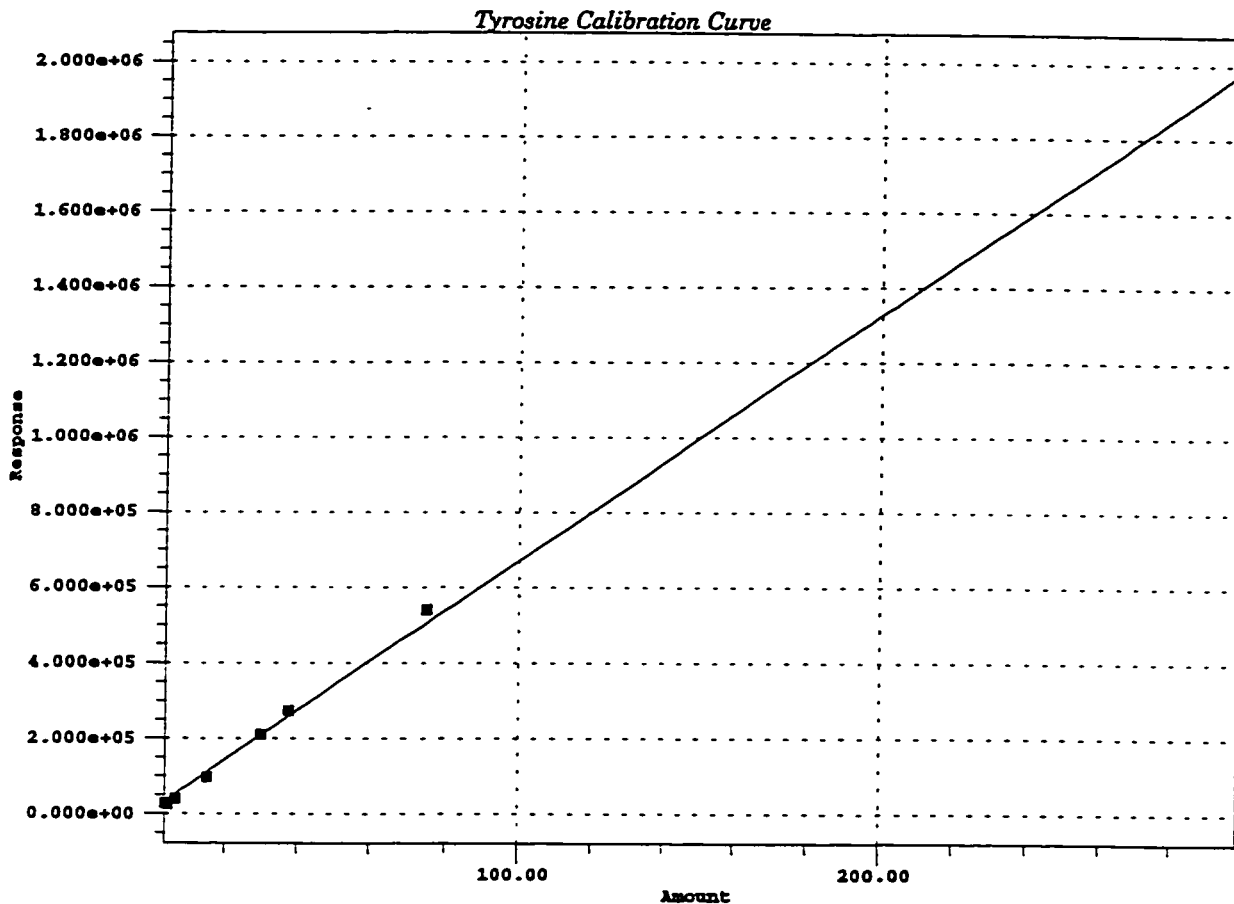
Threonine Calibration Information

Processing Method	OPA_Mar22	System	FLUORESCENCE_OPA
Channel	SATIN	Date	02-APR-96
Type	LC	Name	Threonine
Retention Time	21.818 min	Order	1
A	19797.667131	B	10431.469624
C	0.000000	D	0.000000
E	0.000000	F	0.000000
R	0.999907	R^2	0.999814
Standard Error	10428.910961		

Threonine Point Table

#	Amount	Response	Calc. Amount	% Deviation	Manual	Ignore?
1	0.0171	40184.125114	1.954323	-3.728	Yes	No
2	0.0213	38910.687052	1.832246	-27.864	Yes	No
3	0.03409	56825.224544	3.549601	-12.571	Yes	No
4	0.0851	111746.283269	8.814541	-13.072	Yes	No
5	0.1703	240149.156411	21.123724	4.160	Yes	No
6	0.2129	300006.433150	26.861869	5.964	Yes	No
7	0.4257	554945.121076	51.301252	1.186	Yes	No
8	1.7028	2131778.500000	202.462444	-0.166	Yes	No

Table 'Threonine Average Table' contains no data.



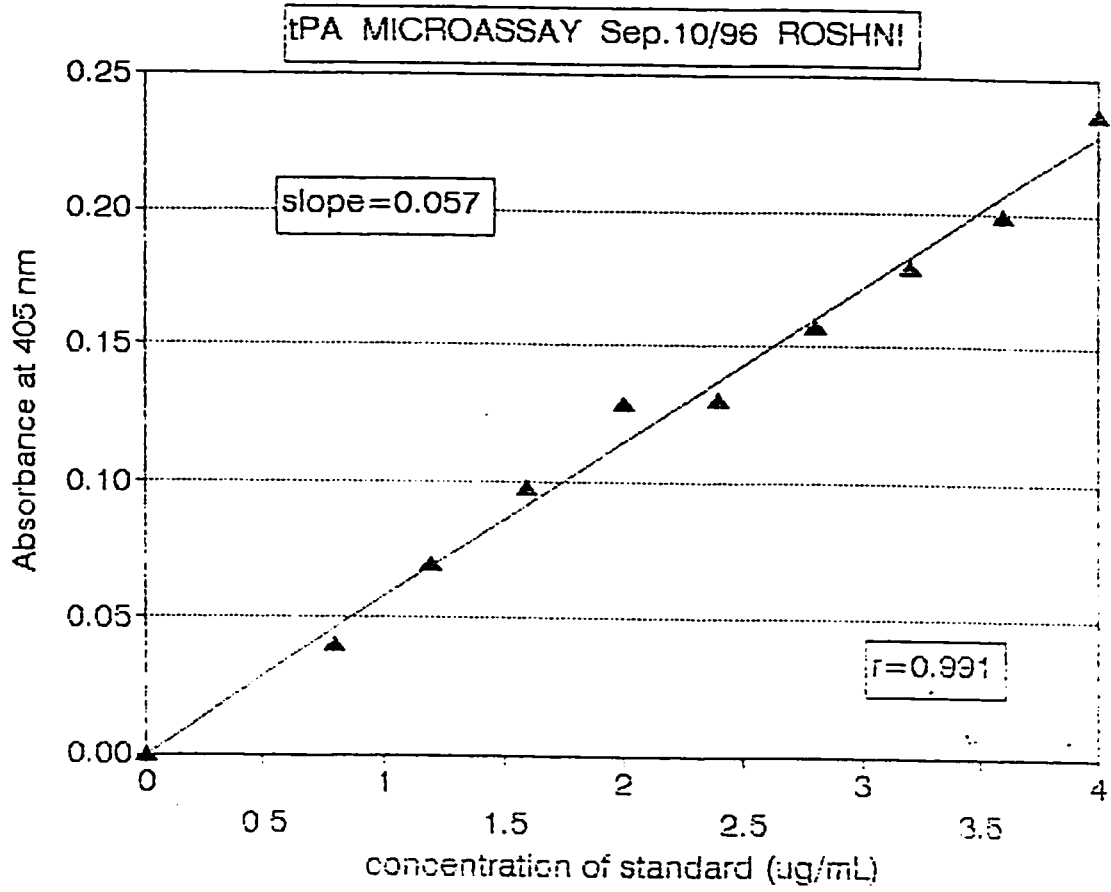
Tyrosine Calibration Information

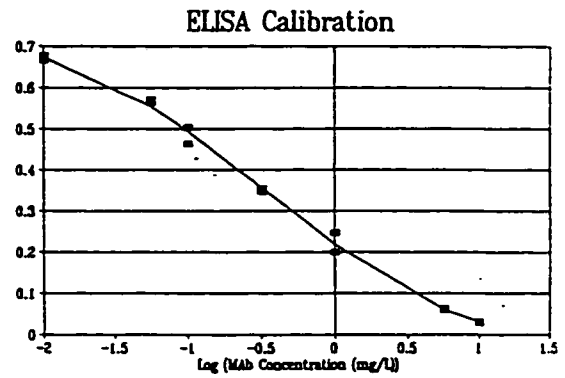
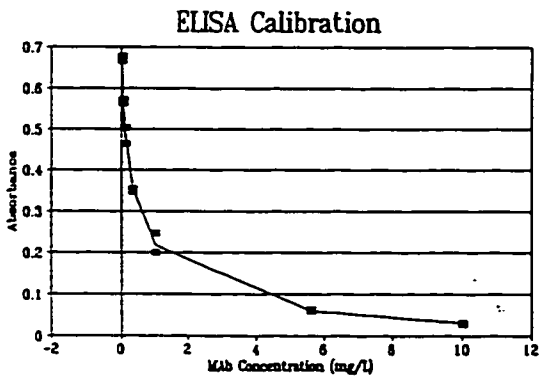
Processing Method	OPA_Mar22	System	FLUORESCENCE_OPA
Channel	SATIN	Date	02-APR-96
Type	LC	Name	Tyrosine
Retention Time	28.326 min	Order	1
A	12242.857527	B	6572.106187
C	0.000000	D	0.000000
E	0.000000	F	0.000000
R	0.999660	R^2	0.999320
Standard Error	18557.593728		

Tyrosine Point Table

#	Amount $\mu\text{g/L}$	Response	Calc. Amount	% Deviation	Manual	Ignore?
1	0.01652	28293.000000	2.442161	-18.322	Yes	No
2	0.0206	24914.000000	1.928019	-48.449	Yes	No
3	0.0331	39290.000000	4.115445	-31.295	Yes	No
4	0.0826	96915.157025	12.883587	-13.937	Yes	No
5	0.1652	210203.260000	30.121303	0.606	Yes	No
6	0.2066	272703.268293	39.631193	5.881	Yes	No
7	0.4131	539756.714286	80.265571	7.235	Yes	No
8	1.6523	1970222.615385	297.922721	-0.493	Yes	No

Table 'Tyrosine Average Table' contains no data.





ELISA Mab ASSAY Ver. 5-VII-90 GLH

ELISA Calibration Error Analysis

$$\text{Absorb} = A + B(\log \text{ Conc}) + C(\log^2 \text{ Conc}) + D(\log^3 \text{ Conc})$$

Regression Output:

Constant	0.219181
Std Err of Y Est	0.014714
R Squared	0.996498
No. of Observations	28
Degrees of Freedom	24
X Coefficient(s)	-0.26191 0.043646 0.030525
Std Err of Coef.	0.005684 0.007551 0.004286

Coef. for Cubic Soln.

A1	1.429856
A2	-8.58019
Q	3.08723
A1/3	0.476619
-2*Q^5	-3.5141

List of Symbols

A	specific biosynthetic energy rate (moles ATP/cell)
ALA	alanine concentration
A phase	apoptosis phase cells
AS	aggregate suspension
ATCC	American Type Culture Collection
B	specific maintenance energy rate (moles ATP/cell/time)
BSA	bovine serum albumin
c	cells
c-h	cell-hours (unit of measure)
CH	population cell-hours
CHvol	volumetric cell-hours (c-h/volume)
CHO	Chinese Hamster Ovary
CHO1-5 ₅₀₀	a recombinant Chinese Hamster Ovary cell line expressing tissue plasminogen activator
CIP	clean in place
<i>dhfr</i>	dihydrofolate reductase gene
DHFR	dihydrofolate reductase
DMSO	dimethyl sulfoxide
DS	dispersed suspension
ed	early decline phase
ELISA	enzyme-linked immunosorbent assay
e-tPA	extracellular tissue plasminogen activator
f ₁	fraction of glutamine completely oxidized
f ₂	fraction of glucose completely oxidized
f ₃	fraction of lactate consumed for serine synthesis
f ₄	fraction of alanine consumed for serine synthesis
f ₅	G1 fraction of the viable population
FBS	fetal bovine serum
F-MTX	fluorescein-methotrexate

f_g	growth or cycling fraction of the viable population
f_{G1}	G1 fraction of the viable population
FH ₂	dihydrofolate
FH ₄	tetrahydrofolate
f_v	fractional viability
FS	forward light scatter
G0	concentration of cells in G0 phase
G1	concentration of cells in G1 phase
G1CH	G1 phase cell-hours
G0 phase	quiescent phase cells (associated with G1 phase)
G1 phase	Gap 1 phase of cell cycle
G2 phase	Gap 2 phase of cell cycle
GLC	glucose concentration
GLN	glutamine concentration
G _s	substrate preference index
GLY	glycine concentration
h-tPA	human tissue plasminogen activator
IgG	immunoglobulin G
IgG ₁	immunoglobulin G ₁
ITES	insulin, transferrin, ethanolamine, and selenium
i-tPA	intracellular tissue plasminogen activator
k_d	specific death rate (time ⁻¹)
k_{GLN}	glutamine chemical degradation rate (time ⁻¹)
k_l	specific rate of cell lysis (time ⁻¹)
k_{tPA}	specific tPA degradation rate
LAC	lactate concentration
ld	late decline phase
LDH	lactate dehydrogenase
m	maintenance coefficient (substrate/cell/time)
M4-1	hybridoma cell line
MAb	monoclonal antibody
mATP	maintenance energy requirement (mol ATP/cell/time)
M phase	mitosis phase of cell cycle
mRNA	messenger RNA
MS	microcarrier attached suspension

MTX	methotrexate
$N^5, N^{10} CH_2 FH_4$	methylene tetrahydrofolate
NH_3	ammonia concentration
PBS	phosphate buffered saline
P_{max} or $[P]_{max}$	maximum product concentration
P_{vol} or dP/dt	volumetric productivity
qALA	specific alanine consumption rate
qAMM	specific ammonia consumption rate
q_{con}	specific consumption rate
qGLC	specific glucose consumption rate
qGLN	specific glutamine consumption rate
qGLY	specific glycine consumption rate
qLAC	specific lactate consumption rate
q_P	specific protein productivity
q_S	specific substrate consumption rate
qSER	specific serine consumption rate
q_{tPA}	specific tPA productivity
R	restriction point of cell cycle
R2	quiescent phase cells (associated with G2 phase of cell cycle)
rCHO	recombinant Chinese Hamster Ovary
rDNA	recombinant DNA
rpm	rotations per minute
s	substrate concentration
SER	serine concentration
S phase	DNA synthesis phase of cell cycle
SS	side light scatter
tPA	tissue plasminogen activator gene
tPA	tissue plasminogen activator
VI	viability index
X	cell concentration
X_d	dead cell concentration
X_l	lysed cell concentration
X_v	viable cell concentration
X_T	total cell concentration
Y	yield

Y_{ATP}	yield of cells on ATP
$Y_{AMM, GLN}$	yield of ammonia on glutamine
$Y_{ALA, GLN}$	yield of alanine on glutamine
$Y_{LAC, GLC}$	yield of lactate on glucose
Y_S	yield of cells on substrate
$Y_{X, S}$	yield of cells on substrate
α	growth association factor of productivity (Product/cell)
β	non-growth association factor of productivity (Protein/cell/time)
μ	specific growth rate (time ⁻¹)
%V	percent viability

REFERENCES

Abu JA & Bekairi AM (1987) Plasma prolactin, insulin and amino acid levels in hyperprolactinaemic patients: pre- and post-treatment with bromocriptine. *Med. sci. Res.* 15: 639-640.

Adamson SR, Behie LA, Gaucher GM & Lesser BH (1987) Metabolism of hybridoma cells in suspension culture: Evaluation of three commercially available media. in *Commercial Production of Monoclonal Antibodies. A guide to Scale Up*. Ed. SS Seaver. Marcel Dekker Inc. New York 17-33.

Aggeler J, Kapp LN, Tseng SCG & Werb Z (1982) Regulation of protein secretion in Chinese Hamster Ovary cells by cell cycle position and cell density. *Exp. Cell Res.* 139: 275-283.

Al-Rubeai M, Emery AN, Chalder S, & Jan DC (1992) Specific monoclonal antibody productivity and the cell cycle - comparisons of batch, continuous and perfusion cultures. *Cytotechnology* 9: 85-97.

Andersen DC & Goochee CF (1995) The effect of ammonia on the O-linked glycosylation of granulocyte colony-stimulating factor produced by Chinese Hamster Ovary cells. *Biotech. Bioeng.* 47: 96-105.

Ashman K & Bosserhoff A (1985) Amino acid analysis by high performance liquid chromatography. *Modern Methods Protein Chemistry* 2: 155-171.

Assaraf YG, Seamer LC & Schimke RT (1989) Characterization by flow cytometry of fluorescein-methotrexate transport in Chinese Hamster Ovary cells. *Cytometry* 10: 50-55.

- Avgerinos GC, Drapeau D, Socolow JS, Hsiao K & Broeze RJ (1990) Spin filter perfusion system for high density cell culture: Production of recombinant urinary type plasminogen activator in CHO cells. *Bio/Technology* 8: 54-58.
- Bailey JE & Ollis DF (1986) *Biochemical Engineering Fundamentals* 2nd. ed. McGraw Hill Book Co. New York
- Baines AD, Drangova R & Ho P (1988) Neural stimulation of gluconeogenesis in isolated pyruvate-perfused rat kidneys. *Can. J. Physiol. Pharmacol.* 66: 106-111.
- Banik GG, Todd PW & Kompala DS (1996) Foreign protein expression from Sphase specific promoters in continuous cultures of recombinant CHO cells. *Cytotechnology* 22: 179-184.
- Barford JP, Phillips PJ, Marquis CP & Harbour C (1996) Biosynthesis of protein products by animal cells. Are growth and non-growth associated concepts valid or useful? *Cytotechnology* 21: 133-148.
- Barford JP, Phillips PJ & Harbour C (1992) Simulation of animal cell metabolism *Cytotechnology* 10: 63-74.
- Barngrover D, Thomas J & Thilly WG (1985) High density mammalian cell growth in Leibovitz bicarbonate-free medium: Effects of fructose and galactose on culture biochemistry. *J. Cell Sci.* 78: 173-189.
- Barritt GJ (ed.) (1992) *Communication within Animal Cells*. Oxford Science Publications New York.
- Baserga R (1976) *Multiplication and Division in Mammalian Cells* Marcel Dekker Inc., USA.
- Baserga R (1985) *The Biology of Cell Reproduction*. Harvard University Press, Cambridge, Massachusetts.
- Batt BC & Kompala DS (1989) A structured kinetic modelling framework for the dynamics of hybridoma growth and monoclonal antibody production in continuous suspension cultures. *Biotech. Bioeng.* 43: 515-531.

Bedows E, Huth JR & Ruddon RW (1992) Kinetics of folding and assembly of the human chorionic gonadotropin beta subunit in transfected Chinese hamster ovary cells. *J. Biol. Chem.* 267: 8880-8886.

Berne FD, Panais B, Merlet N, Cauchi B & Legube B (1994) Total dissolved amino acid analysis in natural and drinking waters. *Environ. Technol.* 15: 901-916.

Berry JM, Huebner E & Butler M. (1996) The crystal violet nuclei staining technique leads to anomalous results in monitoring mammalian cell cultures. *Cytotechnology* 21: 73-80.

Bibila TA & Flickinger MC (1992a) Use of a structured kinetic model of antibody synthesis and secretion for optimization of antibody production systems: I. S-S analysis. *Biotech. Bioeng.* 39: 251-261.

Bibila TA & Flickinger MC (1992b) Use of a structured kinetic model of antibody synthesis and secretion for optimization of antibody production systems: II. Transient analysis. *Biotech. Bioeng.* 39: 262-272.

Borys M.C. & Papoutsakis E.T. (1992) Formation of bridges and large cellular clumps in CHO-cell microcarrier cultures: Effects of agitation, dimethyl sulfoxide and calf serum. *Cytotechnology* 8: 237-248.

Borys MC, Linzer DIH & Papoutsakis ET (1994) Ammonia affects the glycosylation patterns of recombinant mouse placental lactogen-I by Chinese hamster ovary cells in a pH-dependent manner. *Biotech. Bioeng.* 43: 505-514.

Bosch F, Rodriguez-Gil JE, Hatzoglou M, Gomez-Foix AM & Hanson RW (1992) Lithium inhibits hepatic gluconeogenesis and phosphoenolpyruvate carboxykinase gene expression. *J. Biol. Chem.* 267: 2888-2893.

Bosworth JM, Brimfield AA, Naylor JA, & Hunter Jr KW (1983) Measurement of monoclonal antibody concentrations in hybridoma cultures: Comparison of competitive inhibition and antigen capture enzyme immunoassays. *J. Immunol. Method.* 62: 331-336.

Bradford M (1976) A rapid and sensitive method for the quantitation of microgram quantities of protein using the principle of protein-dye binding. *Anal. Biochem.* 72: 248-253.

Buck LT, Brill RW & Hochachka PW (1992) Gluconeogenesis in hepatocytes isolated from the skipjack tuna (*Katsuwonus pelamis*). *Can. J. Zool. Rev. Can. Zool.* 70: 1254-1257.

Bushell ME, Bell SL, Scott MF, Snell K, Spier RE, Wardell JN, and Sanders PG (1993) A three-phase pattern in growth, monoclonal antibody production, and metabolite exchange in hybridoma bioreactor culture. *Biotech. Bioeng.* 42: 133-139.

Butler M (1991) *Animal Cell Technology: Principles and Products* Open University Press New York

Butler M (1996) *Animal Cell Culture and Technology: The Basics* IRL Press. New York

Butler, M (1986) Serum-free media. In: Thilly, WG (ed.) *Mammalian Cell Technology* (pp. 91-108). Butterworths Publishers, United States.

Cartwright T (1994) *Animal Cells as Bioreactors*. Cambridge University Press, Cambridge, England.

Chaplen FWR, Fahl WE & Douglas CC (1996) Effect of endogenous methylglyoxal on Chinese hamster ovary cells grown in culture. *Cytotechnology* 22: 33-42.

Cheung E. & Juliano R.L. (1984) CHO cell aggregation induced by fibronectin-coated beads: Differences between Wild-type and Adhesion-variant cells. *Exp. Cell Res.* 152: 127-133.

Chevalot I., Visvikis A., Nabet P., Engasser J.-M. & Marc A. (1994) Production of a membrane-bound protein, the human gamma-glutamyl transferase, by CHO cells cultivated on microcarriers, in aggregates and in suspension. *Cytotechnology* 16: 121-129.

Crouch C.F, Fowler HW & Spier RE (1985) The adhesion of animal cells to surfaces: The measurement of critical surface shear stress permitting attachment or causing detachment. *J. Chem. Tech. Biotechnol.* 35B: 273-281.

- Croughan MS & Wang DIC (1990) Reversible removal and hydrodynamic phenomena in CHO microcarrier cultures. *Biotech. Bioeng.* 36: 316-319.
- Dalili M & Ollis DF (1989) Transient kinetics of hybridoma growth and monoclonal antibody production in serum-limited cultures. *Biotech. Bioeng.* 33: 984-990.
- Dalili M & Ollis DF (1990) A flow/cytometric analysis of hybridoma growth and monoclonal antibody production. *Biotech. Bioeng.* 36: 64-73.
- Darzynkiewicz Z (1994) Simultaneous analysis of cellular RNA and DNA content. *Methods Cell Bio.* 41: 401-420.
- Darzynkiewicz A & Hoffmann MK (1994) CD4 engagement induces Fas antigen-dependent apoptosis of T cells in vivo. *Eur. J. Immunol.* 24: 1549-1552.
- de la Broise D, Noiseux M, Lemieux R & Massie B (1991) Long-term perfusion culture of hybridoma: a grow or die cell cycle system. *Biotech. Bioeng.* 38: 781-787.
- Denhardt DT, Edwards DR & Parfett CLJ (1986) Gene expression during the mammalian cell cycle. *Biochim. Biophys. ACTA* 865: 83-125.
- de Tremblay M, Perrier M, Chavarie C & Archambault J (1992) Optimization of fed-batch culture of hybridoma cells using dynamic programming: single and multi feed cases. *Bioprocess Eng.* 7: 229-234.
- Dileepan KN & Wagle SR (1985) Somatostatin: A metabolic regulator. *Life Sci.* 37: 2335-2343.
- Donato L, Des-Rosiers C, Montgomery JA, David F, Garneau M & Brunengraber H (1993) Rates of gluconeogenesis and citric acid cycle in perfused livers, assessed from the mass spectrometric assay of the C-13 labeling pattern of glutamate. *J. Biol. Chem.* 268: 4170-4180.

Dutton RL (1992) Initial and environmental culture conditions for monoclonal antibody production. M.A.Sc. thesis. University of Waterloo. Waterloo, Canada.

Dutton RL, Scharer JM & Moo-Young M (1998) Descriptive parameter evaluation in mammalian cell culture. *Cytotechnology* 26: 139-152.

Dutton RL, Scharer JM & Moo-Young M (1998a) Hybridoma growth and productivity: Effects of conditioned medium and of inoculum size. *Cytotechnology* (in press)

Dyring C (1997) Increased production of recombinant hIGFBP-1 in PEG induced autofusion of Chinese hamster ovary (CHO) cells. *Cytotechnology* 24: 183-191.

Feder JN, Assaraf YG, Seamer LC & Schimke RT (1989) The pattern of dihydrofolate reductase expression through the cell cycle in rodent and human cultured cells. *J. Biol. Chem.* 264: 20583-20590.

Flickinger, MC, Goebel, NK, Bibila, T & Boyce-Jacino, S (1992) Evidence for posttranslational stimulation of monoclonal antibody secretion by L-glutamine during slow hybridoma growth. *J. Biotechnol.* 22: 201-226.

Foa C, Soler M, Fraterno M, Passerel M, Lavergne JL, Martin JM & Bongrand P (1994) Electron microscopical analysis of cell-cell and cell-substrate interactions: Use of image analysis, x-ray microanalysis and EFTEM in *Studying Cell Adhesion* eds: Bongrand P, Claesson PM & Curtis ASG Springer-Verlag New York Pp 119-141.

Fox SI (ed.) (1993) *Human Physiology 4th ed.* Wm.C. Brown Pub. Iowa

Fotedar R, Diederich L & Fotedar A (1996) Apoptosis and the cell cycle. *Prog Cell Cycle Res.* 2: 147-163.

Frame, KK & Hu, W-S (1991a) Kinetic study of hybridoma cell growth in continuous culture. I. A model for non-producing cells. *Biotech. Bioeng.* 37: 55-64.

Frame, KK & Hu, W-S (1991b) Kinetic study of hybridoma cell growth in continuous culture. II. Behavior of producers and comparison to nonproducers. *Biotech. Bioeng.* 38: 1020-1028.

Franek, F (1995) Starvation-induced programmed death of hybridoma cells: Prevention by amino acid mixtures. *Biotech. Bioeng.* 45: 86-90.

Freedman RB, Greenall C, Jenkins N & Tuite MF (1995) Protein folding in the secretory pathway of animal cells. *Cytotechnology* 18: 77-82.

Gaertner, JG & Dhurjati, P (1993a) Fractional factorial study of hybridoma behavior. 1. Kinetics of growth and antibody production. *Biotechnol. Prog.* 9: 298-308.

Gaertner, JG & Dhurjati, P (1993b) Fractional factorial study of hybridoma behavior. 2. Kinetics of nutrient uptake and waste production. *Biotechnol. Prog.* 9: 309-316.

Garcia CK, Goldstein JL, Pathak RK, Anderson RGW & Brown MS (1994) Molecular characterization of a membrane transporter for lactate, pyruvate, and other monocarboxylates: Implications for the Cori cycle. *Cell* 76: 865-873.

Glacken MW, Adema E & Sinskey AJ (1988) Mathematical descriptions of hybridoma culture kinetics: I. Initial metabolic rates. *Biotech. Bioeng.* 32: 491-506.

Glacken MW, Fleischaker RJ & Sinskey AJ (1986) Reduction of waste product excretion via nutrient control: Possible strategies for maximizing product and cell yields on serum in cultures of mammalian cells. *Biotech. Bioeng.* 28: 1376-1389.

Glacken MW, Fleischaker RJ & Sinskey AJ (1983) Large-scale production of mammalian cells and their products: Engineering principles and barriers to scale-up. *Biochem. Eng. III* 413: 355-372.

Goergen, JL, Marc, A & Engasser, JM (1992) Comparison of specific rates of hybridoma growth and metabolism in batch and continuous cultures. *Cytotechnology* 10: 147-155.

Goldman SS (1988) Gluconeogenesis in the amphibian retina: Lactate is preferred to glutamate as the gluconeogenic precursor. *Biochem. J.* 254: 359-365.

Griffiths JB (1987) Serum and growth factors in cell culture media - An introductory review. *Develop. Biol. Stand.* 66: 155-160.

Grinnel, F. (1980) Fibroblast receptor for cell-substratum adhesion: Studies on the interaction of baby hamster kidney cells with latex beads coated by cold insoluble globulin (plasma fibronectin). *J. Cell Biol.* 86: 104-112.

Gu MB, Todd P & Kompala DS (1993) Foreign gene expression (β -galactosidase) during the cell cycle phases in recombinant CHO cells. *Biotech. Bioeng.* 42: 1113-1123.

Gu MB, Todd P & Kompala DS (1996) Metabolic burden in recombinant CHO cells: effect of *dhfr* gene amplification and *lacZ* expression. *Cytotechnology* 18: 159-166.

Hansen HA & Emborg C (1994) Extra- and intracellular amino acid concentrations in continuous Chinese hamster ovary cell culture. *Appl. Microbiol. Biotechnol.* 41: 560-564.

Hanson RW & Mehlman MA (1976) *Gluconeogenesis: Its Regulation in Mammalian Species* John Wiley and Sons New York.

Hayflick L & Moorhead PS (1961) The serial cultivation of human diploid cell strains *Exp. Cel Res.* 25: 585-594.

Hayter PM, Curling EMA, Gould ML, Baines AJ, Jenkins N, Salmon I, Strange PG & Bull AT (1993) The effect of the dilution rate on CHO cell physiology and recombinant interferon- γ production of glucose-limited chemostat culture. *Biotech. Bioeng.* 42: 1077-1085.

Hayter PM, Curling EMA, Baines AJ, Jenkins N, Salmon I, Strange PG, Tong JM & Bull AT (1992) Glucose-limited chemostat culture of Chinese Hamster Ovary cells producing recombinant human interferon- γ . *Biotech. Bioeng.* 39: 327-335.

Hayter PM, Kirkby NF & Spier RE (1992) Relationship between hybridoma growth and monoclonal antibody production. *Enzyme Microb. Technol.* 14: 454-461.

Hayward GL, Dutton RL, Zhang Z, Scharer JM & Moo-Young M (1998) Thickness shear mode acoustic assay for plasminogen activators. *Anal. Commun.* 35: 25-27.

Hayward, GL, Scharer, JM, Moo Young, M & Bols, N (1991) Photometric ELISA calibration for antibody assay. *Biotechnol. Tech.* 5: 35-38.

Hudokova A, Horakova K & Perenyi T (1992) The relation between the synergistic effect of cytostatics and metabolism of V 79B cells in vitro. *Cell Biochem. Funct.* 10: 109-113.

Hunt SMN, Pak SCO, Bridges MW, Gray PP & Sleigh MJ (1997) Chinese hamster ovary cells produce sufficient recombinant insulin-like growth factor I to support growth in serum-free medium. *Cytotechnology* 24: 55-64.

Jans AWH, Winkel C, Buitenhuis L & Lugtenburg J (1989) C-n.m.r. study of citrate metabolism in rabbit renal proximal-tubule cells. *Biochem. J.* 257: 425-429.

- Jenkins N & Hovey A (1993) Temperature control of growth and productivity in mutant Chinese Hamster Ovary cells synthesizing a recombinant protein. *Biotech. Bioeng.* 42: 1029-1036.
- Jeong Y-H & Wang SS (1995) Role of glutamine in hybridoma cell culture: Effects on cell growth, antibody production, and cell metabolism. *Enzyme Microb. Technol.* 17: 47-55.
- Johnson, LF (1984) Expression of dihydrofolate reductase and thymidylate synthase genes in mammalian cells. in: *Recombinant DNA and Cell Proliferation* eds: Stein, GS & Stein, JL Academic Press Inc. USA Pp 26-46.
- Jungas RL, Mitchell LH & Brosnan JT (1992) Quantitative analysis of amino acid oxidation and related gluconeogenesis in humans. *Physiological Reviews* 72:419-448.
- Kaufman RJ, Bertino JR & Schimke RT (1978) Quantitation of dihydrofolate reductase in individual parental and methotrexate-resistant murine cells. *J. Biol. Chem.* 254: 5852-5860.
- Keen RE & Spain JD (1992) *Computer Simulation in Biology: A BASIC Introduction* Wiley-Liss New York.
- Kempken R, Buntmeyer H & Lehmann J (1991) The medium cycle bioreactor (MCB): Monoclonal antibody production in a new economic production system. *Cytotechnology.* 7: 63-74.
- Kennard, M.L. & Piret, J.M. (1995) Membrane anchored protein production from spheroid, porous, and solid microcarrier Chinese Hamster Ovary cell cultures. *Biotech. Bioeng.* 47: 550-556.
- Kier LD, Wagner LM, Wilson TV, Li AP, Short RD & Kennedy GL Jr. (1995) Cytotoxicity of ethylene oxide/propylene oxide copolymers in cultured mammalian cells. *Drug Chem. Toxicol.* 18: 29-41.
- Kilburn DG, Lilly MD & Webb FC (1969) The energetics of mammalian cell growth *J. Cell Sci.* 4: 645-654.

Kim JH, Bae SW, Hong HJ & Lee GM (1996) Decreased chimeric antibody productivity of KR12H-1 transfectoma during long-term culture results from decreased antibody gene copy number. *Biotech. Bioeng.* 51: 479-487.

Kim B.-S., Choi Y.H., Choi C.Y. & Kim B.G. (1992) Mammalian cell cultivation on serum-coated microcarriers. *Biotechnol. Tech.* 6: 347-352.

Kim YH, Iida T, Fujita T, Terada S, Kitayama A, Ueda H, Prochownik EV & Suzuki E (1998) Establishment of an apoptosis-resistant and growth-controllable cell line by transfecting with inducible antisense *c-Jun* gene. *Biotech. Bioeng.* 58: 65-72.

Kohler G & Milstein C (1975) Continuous cultures of fused cells secreting antibody of predefined specificity. *Nature* 256: 495-497

Konstantinov KB, Tsai Y-S, Moles D & Matanguihan R (1996) Control of long-term perfusion Chinese hamster ovary cell culture by glucose auxostat. *Biotechnol. Prog.* 12: 100-109.

Konstantopoulos, N & Clark, S (1996) Reduced cell attachment and phosphorylation of focal adhesion kinase associated with expression of a mutant insulin receptor. *J. Biol. Chem.* 256 : 28960-28968.

Kromenaker SJ & Srien F (1994) Cell cycle kinetics of the accumulation of heavy and light chain immunoglobulin proteins in a mouse hybridoma cell line. *Cytotechnology.* 14: 205-218.

Kubbies M, Goller B & Giese G (1996) High-resolution cell cycle analysis of cell cycle-regulated gene expression. in *FlowCytometry Applications in Cell Culture* eds.: Al-Rubeai M & Emery AN Marcel Dekker Inc., New York Pp 63-83.

Kubbies M & Stockinger H (1990) Cell cycle-dependent DHFR and t-PA production in cotransfected, MTX-amplified CHO cells revealed by dual-laser flow cytometry. *Exp. Cell Res.* 188: 267-271.

Kunas KT & Papoutsakis ET (1989) Increasing serum concentrations decrease cell death and allow growth of hybridoma cells at higher agitation rates. *Biotech. Lett.* 10: 625-628.

Kurano N, Leist C, Messi F, Gandor C, Kurano S & Fiechter A. (1990) Growth kinetics of Chinese hamster ovary cells in a compact loop bioreactor. 3. Selection and characterization of an anchorage-independent subline and medium improvement. *J. Biotechnol.* 16: 245-258.

Lakhotia S & Papoutsakis ET (1992) Agitation induced cell injury in microcarrier cultures. Protective effect of viscosity is agitation intensity dependent: Experiments and modeling. *Biotech. Bioeng.* 39: 95-107.

Lao M-S, Toth D, Danell G & Schalla C (1996) degradative activities in a recombinant chinese hamster ovary cell culture. *Cytotechnology* 22: 43-52.

Laufenburger D & Cozens C (1989) Regulation of mammalian cell growth by autocrine growth factors: Analysis of consequences for inoculum cell density effects. *Biotech. Bioeng.* 33: 1365-1378.

Laufenburger D & Cozens C (1989) Regulation of mammalian cell growth by autocrine growth factors: Analysis of consequences for inoculum cell density effects. *Biotech. Bioeng.* 33: 1365-1378.

Lauris V, Crettaz M & Kahn CR (1986) Coordinate roles of insulin and glucose on the growth of hepatoma cells in culture. *Endocrinology* 118: 2519-2524.

Lee GM, Kaminski MA & Palsson BO (1992) Observations consistent with autocrine stimulation of hybridoma cell growth and implications for large-scale antibody production. *Biotech. Lett.* 14: 257-262.

Lee GM, Huard TK & Palsson BO (1989) Effect of serum concentration on hybridoma cell growth and monoclonal antibody production at various initial cell densities. *Hybridoma* 8: 369-375.

Leelavatharamas V, Emery AN & Al-Rubeai M (1994) Growth and interferon- γ production in batch culture of CHO cells. *Cytotechnology* 15: 65-71.

Lehninger AL (1982) *Principles of Biochemistry* Worth Publishers Inc. New York.

Lehninger AL, Nelson DL & Cox MM (1993) *Principles of Biochemistry 2nd ed.* Worth Publishers Inc. New York.

Leno, M, Merten, O-W & Hache, J (1992) Kinetic analysis of hybridoma growth and monoclonal antibody production in semicontinuous culture. *Biotech. Bioeng.* 39: 595-606.

Lin AA, Kimura R & Miller WM (1993) Production of tPA in recombinant CHO cells under oxygen-limited conditions. *Biotech. Bioeng.* 42: 339-350

Lin AA & Miller WM (1992) CHO cell responses to low oxygen: Regulation of oxygen consumption and sensitization to oxidative stress. *Biotech. Bioeng.* 40: 505-516

Lloyd, D, Poole, RK & Edwards, SW (1982) *The Cell Division Cycle. Temporal Organization and Control of Cellular Growth and Reproduction.* Academic Press, London, England

Luan, YT, Mutharasan, R & Magee, WE (1987) Strategies to extend longevity of hybridomas in culture and promote yield of monoclonal antibodies. *Biotechnol. Lett.* 9: 691-696.

Lucka, L, Cichocka, I, Baumler, K, Bechler, K & Reuther, W. (1995) A short isoform of carcinoembryonic-antigen-related rat liver cell-cell adhesion molecule (C-CAM/gp110) mediates intercellular adhesion.

Mariani BD, Slate DL & Schimke RT (1981) S phase-specific synthesis of dihydrofolate reductase in Chinese hamster ovary cells. *Proc. Natl. Acad. Sci. USA* 78: 4985-4989.

Marquis CP Barford JP & Harbour C (1996) Amino acid metabolism during batch culture of a murine hybridoma, AFP-27 *Cytotechnology* 21: 111-120.

Marquis CP, Barford JP, Harbour C & Fletcher A (1996) Carbohydrate and amino acid metabolism during batch culture of a human lymphoblastoid cell line, BTSN6 *Cytotechnology* 21: 121-132.

Martens, DE, de Gooijer, CD, van der Velden-de Groot, CAM, Beuvery, EC & Tramper, J (1993) Effect of dilution rate on growth, productivity, cell cycle and size, and shear sensitivity of a hybridoma cell in a continuous culture. *Biotech. Bioeng.* 41: 429-439.

Martens DE, Sipkema EM, De-Gooijer CD, Beuvery EC & Tramper J (1995) A combined cell-cycle and metabolic model for the growth of hybridoma cells in steady-state continuous culture. *Biotech. Bioeng.* 48: 49-65.

Martin BM (1994) *Tissue Culture Techniques: An Introduction* Birkhauser Boston.

Mastrangelo AJ & Betenbaugh MJ (1995) Implications and applications of apoptosis in cell culture. *Curr. Op. Biotechnol.* 6: 198-202.

Matherly LH, Schuetz JD, Westin E & Goldman ID (1989) A method for the synchronization of cultured cells with aphidicolin: Application to the large-scale synchronization of L1210 cells and the study of the cell cycle regulation of thymidylate synthase and dihydrofolate reductase. *Anal. Biochem.* 182: 338-345.

Matsumura M & Nayve Jr. FRP (1995) Effects of ammonium ion removal on growth and MAb production of hybridoma cells. *Cytotechnology* 18: 35-50.

McKinney KL, Dilwith R & Belfort G (1991) Manipulation of heterogeneous hybridoma cultures for overproduction of monoclonal antibodies. *Biotechnol. Prog.* 7: 445-454.

McQueen A & Bailey JE (1990) Effect of ammonium ion and extracellular pH on hybridoma cell metabolism and antibody production. *Biotech. Bioeng.* 35: 1067-1077.

- McQuiddy, P & Lilien, J (1974) Sialic acid and cell aggregation in *Cell Aggregation and Adhesion* eds: Seeds NW *et al.* MSS Information Corp. New York Pp 136-145.
- Meilhoc E, Wittrup KD & Bailey JE (1989) Application of flow cytometric measurement of surface IgG in kinetic analysis of monoclonal antibody synthesis and secretion by murine hybridoma cells. *J. Immunol. Methods* 121: 167-174.
- Mercille, S & Massie, B (1994) Induction of apoptosis in nutrient-deprived cultures of hybridoma and myeloma cells. *Biotech. Bioeng.* 44: 1140-1154.
- Merten, O-W (1988) Batch production and growth kinetics of hybridomas. *Cytotechnology* 1: 113-121.
- Merten O-W, Reiter S, Himmler G, Scheirer W & Katinger H (1985) Production kinetics of monoclonal antibodies. *Develop. Biol. Standard.* 60: 219-227.
- Michalik M & Bryla J (1987) Inhibitory effect of gentamicin on gluconeogenesis from pyruvate, propionate, and lactate in isolated rabbit kidney-cortex tubules. *Biochem. Med. Metab. Biol.* 38: 36-43.
- Miller, WM, Blanch, HW & Wilke, CR (1988) A kinetic analysis of hybridoma growth and metabolism in batch and continuous suspension culture: Effect of nutrient concentration, dilution rate, and pH. *Biotech. Bioeng.* 32: 947-965.
- Miller WM, Wilke CR & Blanch HW (1989) Transient responses of hybridoma cells to nutrient additions in continuous culture: 1. Glucose pulse and step changes. *Biotech. Bioeng.* 33: 477-486.
- Milner AE, Wang H & Gregory CD (1996) Analysis of apoptosis by flow cytometry in: *Flow Cytometry Applications in Cell Culture* Al-Rubeai M & Emery AN (eds.) Marcel Dekker Inc. New York Pp. 193-209.
- Moore A, Donahue CJ, Hooley J, Stocks DL, Bauer KD & Mather JP (1995) Apoptosis in CHO cell batch cultures: examination by flow cytometry. *Cytotechnology* 17: 1-11.

Moore A, Mercer J, Dutina G, Donahue CJ, Bauer KD, Mather JP, Etcheverry T & Ryll T (1997) Effects of temperature shift on cell cycle, apoptosis and nucleotide pools in CHO cell batch cultures. *Cytotechnology* 23: 47-54.

Moreira, JL, Santana, PC, Feliciano, AS, Cruz, PE, Racher, AJ, Griffiths, JB & Carrondo, MJT. (1995) Effect of viscosity upon hydrodynamically controlled natural aggregates of animal cells grown in stirred vessels. *Biotechnol. Prog.* 11: 575-583.

Moule SK & McGivan JF (1988) Epidermal-growth-factor stimulation of gluconeogenesis in isolated rat hepatocytes involves the inactivation of pyruvate kinase. *Biochem. J.* 255: 361-364.

Murray A & Hunt T (1993) *The Cell Cycle: An Introduction* Oxford University Press, New York.

Nikolai, TJ & Hu, W-S. (1992) Cultivation of mammalian cells on macroporous microcarriers. *Enzyme Microb. Technol.* 14: 203-208.

O'Connor KC & Papoutsakis ET (1992) Agitation effects on microcarrier and suspension CHO cells. *Biotechnol. Tech.* 6: 323-328.

Ogata M, Wakita K-I, Kimura K, Marumoto Y, Oh-i K & Shimizu S. (1993) High-level expression of recombinant human soluble thrombomodulin in serum-free medium by CHO-K1 cells. *Appl. Microbiol. Biotechnol.* 38: 520-525.

Ogata M, Marumoto Y, Oh-I K, Shimizu S & Katoh S. (1994) Continuous culture of CHO-K1 cells producing thrombomodulin and estimation of culture conditions. *J. Ferment. Bioeng.* 77: 46-51.

Ozturk SS & Palsson BO (1990a) Effect of initial cell density on hybridoma growth, metabolism, and monoclonal antibody production. *J. Biotechnol.* 16: 259-278.

Ozturk SS, Riley MR & Palsson BO (1992) Effects of ammonia and lactate on hybridoma growth, metabolism, and antibody production. *Biotech. Bioeng.* 39: 418-431.

Ozturk SS & Palsson BO (1990b) Chemical decomposition of glutamine in cell culture media: Effect of media type, pH, and serum concentration. *Biotechnol. Prog.* 6: 121-128.

Ozturk SS & Palsson BO (1991) Physiological changes during the adaptation of hybridoma cells to low serum and serum-free media. *Biotech. Bioeng.* 37: 35-46.

Packer, L (1990) Retinoids and cell adhesion. *Meth. Enzym.* 190: 81-91.

Papoutsakis ET (1992) Media additives for protecting freely suspended animal cells against agitation and aeration damage. *Trends Biotech.* 9: 346-354.

Papoutsakis ET (1991) Fluid-mechanical damage of animal cells in bioreactors. *Trends Biotech.* 9: 427-439.

Park SY & Lee GM (1995) Enhancement of monoclonal antibody production by immobilized hybridoma cell culture with hyperosmolar medium. *Biotech. Bioeng.* 48: 699-705.

Park, SH & Ryu, DDY (1994) Cell cycle kinetics and monoclonal antibody productivity of hybridoma cells during perfusion culture. *Biotech. Bioeng.* 44: 361-367.

Peshwa, MV, Kyung, Y-S, McClure, DB & Hu, W-S (1993) Cultivation of mammalian cells as aggregates in bioreactors: Effect of calcium concentration on spatial distribution of viability. *Biotech. Bioeng.* 41: 179-187.

Phillips HA, Scharer JM, Bols NC & Moo-Young M (1992) Design and performance of a trickle-bed bioreactor with immobilized hybridoma cells. *Cytotechnology* 9: 29-40.

Phillips HA (1991) Evaluation of hybridoma culture systems for the production of monoclonal antibodies. Ph.D. Thesis University of Waterloo. Waterloo, Ontario, Canada.

Phillips, HJ (1973) Dye exclusion tests for cell viability. In: Kruse Jr, PF & Patterson Jr. MK (eds.) *Tissue Culture: Methods and Applications*. (pp. 406-408) Academic Press, New York.

Pilo B & Mehta PC (1993) Neural and endocrine regulation of gluconeogenesis in the kidney of blue rock pigeon, *Columba livia*: A review. *Proc. Zool. Soc. - Calcutta* 46: 1-5.

Pirt SJ (1975) *Principles of Microbe and Cell Cultivation* Blackwell Scientific Publications London

Portner R & Schafer T (1996) Modelling hybridoma cell growth and metabolism - a comparison of selected models and data. *J. Biotech.* 49: 119-135.

Ramirez OT & Mutharasan R (1990) Cell cycle- and growth phase-dependent variations in size distribution, antibody productivity, and oxygen demand in hybridoma cultures. *Biotech. Bioeng.* 36: 839-848.

Rein A & Rubin H (1968) Effects of local cell concentrations upon the growth of chick embryo cells in tissue culture. *Exp. Cell Res.* 49: 666-678.

Renner WA, Jordan M, Eppenberger HM & Leist C. (1993) Cell-cell adhesion and aggregation: Influence on the growth behavior of CHO cells. *Biotech. Bioeng.* 41: 188-193.

Reuveny S, Valez D, Macmillan JD & Miller L (1986) Factors affecting cell growth and monoclonal antibody production in stirred reactors. *J. Immunol. Methods* 86: 53-59.

Riese U, Lutkemeyer D, Heidemann R, Buntemeyer H & Lehmann J (1994) Re-use of spent cell culture medium in pilot scale and rapid preparative purification with membrane chromatography. *J. Biotechnol.* 34: 247-257.

Rogers SA & Hammerman MR (1989) Mannose 6-phosphate potentiates insulin-like growth factor II-stimulated inositol trisphosphate production in proximal tubular basolateral membranes. *J. Biol. Chem.* 264: 4273-4276.

Rosa JL, Bartrons R & Tauler A (1992) Gene expression of regulatory enzymes of glycolysis/gluconeogenesis in regenerating rat liver. *Biochem. J.* 287: 113-116.

Rouf SA, Moo-Young M & Chisti Y (1996) Tissue-type plasminogen activator: Characteristics, applications and production technology. *Biotechnol. Adv.* 14: 239-266.

Ruaan, R-C, Tsai, G-J and Tsao GT (1993) Surface area and anchorage-dependent growth of chinese hamster ovary cells. *Biotechnol. Prog.* 9: 362-365.

Rubeai M & Emery AN (1990) Mechanisms and kinetics of monoclonal antibody synthesis and secretion in synchronous hybridoma cell cultures. *J. Biotechnol.* 16: 67-86.

Rubin H. (1966) A substance in conditioned medium which enhances the growth of small numbers of chick embryo cells. *Exp. Cell Res.* 41: 138-148.

Salmon SE & Sartorelli (1985) *Cancer Chemotherapy* Chapman and Hall London

Sanfeliu A, Cairo JJ, Casas C, Sola C & Godia F (1996) Analysis of nutritional factors and physical conditions affecting growth and monoclonal antibody production of the hybridoma KB-26.5 cell line. *Biotechnol. Prog.* 12: 209-216.

Schaeffer WI (1990) Terminology associated with cell, tissue and organ culture, molecular biology and molecular genetics. *In Vitro Cell. Dev. Biol.* 26: 97-101.

Schlaeger EJ & Shumpp B (1989) Studies on mammalian cell growth in suspension culture. in *Advances in Animal cell Biology and Technology for Bioprocesses*. Spier RE, Griffiths JB, Stephenne J & Crooy PJ (eds.) Pp. 386-397.

Schneider M, Marison IW & von Stockar U (1996) The importance of ammonia in mammalian cell culture. *J. Biotechnol.* 46 161-185.

Scott FM, de Serrano VS & Catellino FJ (1987) Appearance of plasminogen activator activity during a synchronous cycle of a rat adenocarcinoma cell line, PA-III. *Exp.Cell Res.* 169: 39-46.

Seewoster T & Lehmann J (1997) Cell size distribution as a parameter for the predetermination of exponential growth during repeated batch cultivation of CHO cells. *Biotech. Bioeng.* 55: 793-797.

Shiba, Y, Ohshima, T & Sato, M. (1998) Growth and morphology of anchorage-dependent animal cells in a liquid/liquid interface system. *Biotech. Bioeng.* 57: 583-589.

Shirai Y, Hashimoto K & Takamatsu H (1992) Growth kinetics of hybridoma cells in high density culture. *J. Ferment. Bioeng.* 73: 159-165.

Shirai, Y, Hashimoto, K, Aoki, T & Yoshimi, T (1994) Change in metabolic pathways in hybridoma growth and monoclonal antibody production. *J. Ferment. Bioeng.* 78: 315-320.

Singh, RP, Al-Rubeai, M, Gregory, CD & Emery, AN (1994) Cell death in bioreactors: A role for apoptosis. *Biotech. Bioeng.* 44: 720-726.

Smith CA & Wood EJ (1996) *Cell Biology* 2nd. ed. Chapman and Hall London

Smith JA & Martin L (1973) Do cells cycle? *Proc. Natl. Acad. Sci. USA* 70: 1263-1267.

Spier RE, Griffiths JB & MacDonald C (1992) *Animal Cell Technology: Developments, Processes & Products* Butterworth-Heinemann

- Suzuki E & Ollis DF (1990) Enhanced antibody production at slowed growth rates: Experimental demonstration and a simple structured model. *Biotechnol. Prog.* 6: 231-236.
- Suzuki E, Terada S, Ueda H, Fujita T, Komatsu T, Takayam S & Reed JC (1997) Establishing apoptosis resistant cell lines for improving protein productivity of cell culture. *Cytotechnology* 23: 55-59.
- Takahashi K, Terada S, Ueda H, Makishima F & Suzuki E (1994) Growth rate suppression of cultured mammalian cells enhances protein productivity. *Cytotechnology* 15: 57-64.
- Takazawa Y, Tokashiki M, Murakami H, Yamada K & Omura H (1988) High-density culture of mouse-human hybridoma in serum-free defined medium. *Biotech. Bioeng.* 31: 168-172.
- Takeichi M (1974) Changes in the properties of cell-substrate adhesion during cultivation of chicken fibroblasts *in vitro* in a serum-free medium. in: *Cell Aggregation and Adhesion* MSS Information Corp. New York Pp. 147-155
- Terada S, Itoh Y, Ueda H & Suzuki E (1997) Characterization and fed-batch culture of hybridoma overexpressing apoptosis suppressing gene bcl-2 *Cytotechnology* 24: 135-141.
- Tokiwa T, Kano J, Kodama M & Matsumura T. (1997) Multilayer rat hepatocyte aggregates formed on expanded polytetrafluoroethylene surface. *Cytotechnology* 25: 137-144.
- Tolbert WR, Hitt MM & Feder J. (1980) Cell aggregate suspension culture for large-scale production of biomolecules. *In Vitro* 16: 486-490.
- Tziampazis, E & Sambanis, A (1994) Modeling of cell culture processes. *Cytotechnology* 14: 191-204.
- van Erp R, Adorf M, van Sommeren APG, Schonherr OT & Gribnau TCJ (1991a) Monitoring of the production of monoclonal antibodies by hybridomas. Part I: Long-term cultivation in hollow fibre bioreactors using serum-free medium. *J. Biotechnol.* 20: 235-248.

van Erp R, Adorf M, van Sommeren APG, Schonherr OT & Gribnau TCJ (1991b) Monitoring of the production of monoclonal antibodies by hybridomas. Part I: Characterization and purification of acid proteases present in cell culture supernatant. *J. Biotechnol.* 20: 249-262.

Varani, J, Josephs, S & Hillegas WJ (1996) Human diploid fibroblast growth on polystyrene microcarriers in aggregates. *Cytotechnology* 22: 111-117.

Venkat RV & Chalmers JJ (1996) Characterization of agitation environments in 250 mL spinner vessel, 3 L, and 20 L reactor vessels used for animal cell microcarrier culture. *Cytotechnology* 22: 95-102.

Verheijen JH & Wijngaards G (1983) Large-scale production of extrinsic (tissue-type) plasminogen activator from human melanoma cells. *Adv. Biotechnol. Process.* 2: 97-110.

Wagner A, Marc A & Engasser JM (1992) The use of lactate dehydrogenase (LDH) release kinetics for the evaluation of death and growth of mammalian cells in perfusion reactors. *Biotech. Bioeng.* 39: 320-326.

Watson JD, Gilman M, Witkowski J & Zoller M (1992) *Recombinant DNA* 2nd. ed. Scientific American Books. New York.

Watson, E, Shar, B, Leiderman, L, Hsu, Y-R, Karkare, S, Lu, HS & Lin F-K. (1994) Comparison of N-linked oligosaccharides of recombinant human tissue kallikrein produced by Chinese Hamster Ovary cells on microcarrier beads and in serum-free suspension culture. *Biotechnol. Prog.* 10: 39-44.

Wiechetek M, Garwacki S, Karlik W, Lewicki J & Souffrant W (1993) Effect of nitrite on ureagenesis and carbohydrate metabolism in isolated rat hepatocytes. *Arch. Environ. Contam. Toxicol.* 24: 375-380.

Wierzba, A, Reichl, U, Turner, RFB, Warren, RAJ & Kilburn, DG (1995) Adhesion of mammalian cells to a recombinant attachment factor, CBD/RGD, analyzed by image analysis. *Biotech. Bioeng.* 46: 185-193.

Williams PD, Buening MK, Gries CL, Hanasono GK, Laska DA, Tamura RN & Heim RA (1990) Comparative toxicity of oral cephalosporin antibiotics in the rabbit and in a rabbit kidney cell line (LLC-RK-1). *Toxicol. -In-Vitro* 4: 207-210.

Winterbourne, DJ, Thomas, S & Hermon-Taylor, J (1993) Suppression of anchorage-independent growth after gene transfection. *Cytotechnology* 68: 251-257.

Wohlpert D, Kirwan D & Gainer J (1990) Effects of cell density and glucose and glutamine levels on the respiration rates of hybridoma cells. *Biotech. Bioeng.* 36: 630-636.

Wu J (1996) Insights into protective effects of medium additives on animal cells under fluid stresses: the hydrophobic interactions. *Cytotechnology* 23: 103-109.

Xie, L & Wang, DIC (1996) High cell density and high monoclonal antibody production through medium design and rational control in a bioreactor. *Biotech. Bioeng.* 51: 725-729.

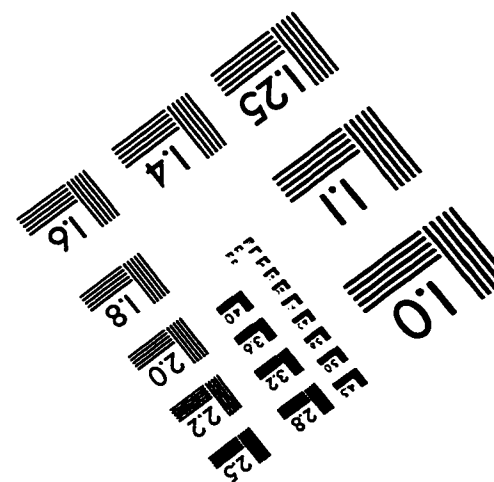
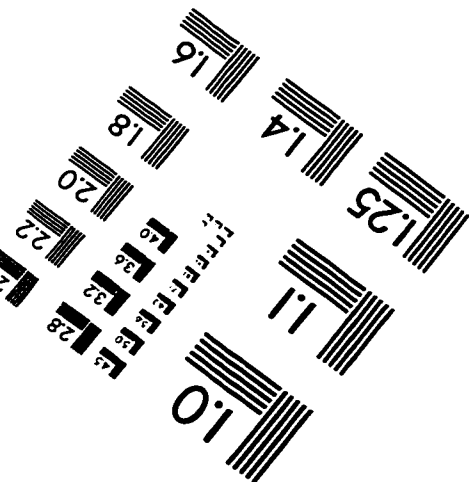
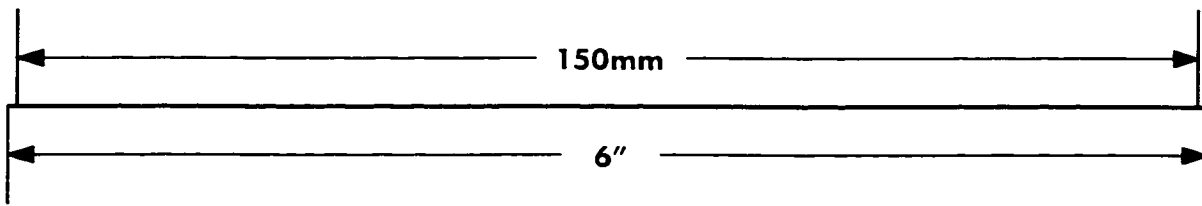
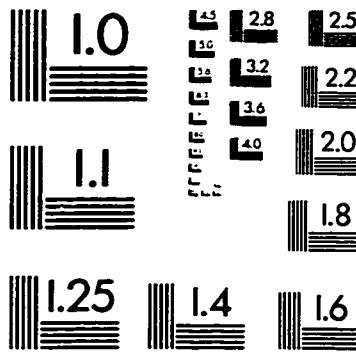
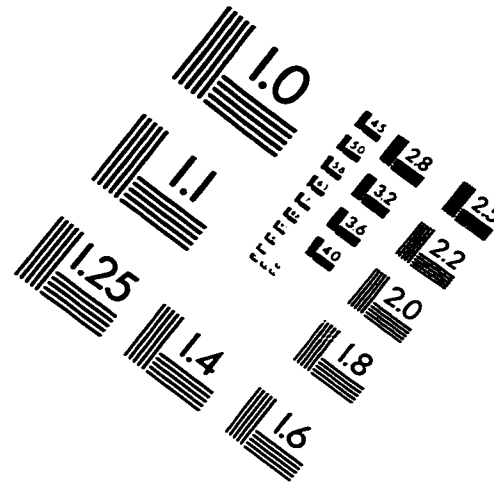
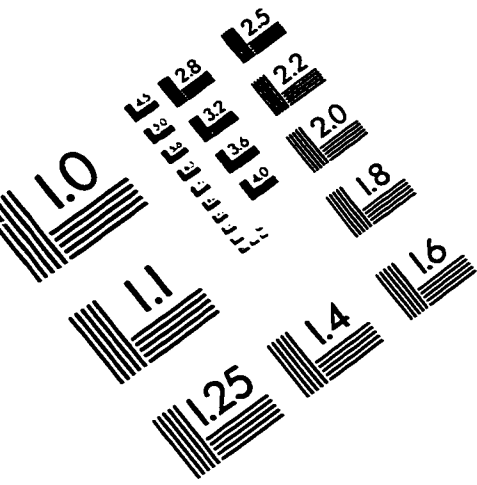
Xie, L & Wang, DIC (1994a) Stoichiometric analysis of animal cell growth and its application in medium design. *Biotech. Bioeng.* 43: 1164-1174.

Xie, L & Wang, DIC (1994b) Applications of improved stoichiometric model in medium design and fed-batch cultivation of animal cells in bioreactor. *Cytotechnology* 15: 17-29.

Yanagawa N, Nagami GT, Jo O, Uemasu Z & Kurokawa K (1983) Absence of regulatory role of both cytosolic NAD and gluconeogenesis activity on phosphate transport in renal proximal tubules. *Miner. Electrolyte Metab.* 9: 182.

Zhou W, Rehm J, Europa A & Hu W-S (1997) Alteration of mammalian cell metabolism by dynamic nutrient feeding. *Cytotechnology* 24: 99-108.

IMAGE EVALUATION TEST TARGET (QA-3)



APPLIED IMAGE, Inc
 1653 East Main Street
 Rochester, NY 14609 USA
 Phone: 716/482-0300
 Fax: 716/288-5989

© 1993, Applied Image, Inc., All Rights Reserved